GRADUATE COURSE IN PHYSICS
UNIVERSITY OF PISA

The School of Graduate Studies in Basic Sciences "GALILEO GALILEI"

PhD Thesis:

Absorption of an ultrashort intense laser pulse as a few degrees of freedom Hamiltonian system.

Candidate: Andrea Cintio

Supervisor: Prof. Fulvio Cornolti

Contents

List of Figures

1. Introduction

A new interest in the problem of interaction of electromagnetic radiation with matter came out after the development of the laser techniques[1] that enable to generate laser pulses with intensity exceeding $10^{16} - 10^{17}\ W/cm^2$ and durations of nearly $10\ fs$ [2] (ultrashort pulses). About the "laser-solid interaction" problem it is meant some physical issues which regards the interaction of ultrashort, high intensity laser pulses with solid targets, either metallic or dielectric.

The typical magnitude of the binding field experienced by a valence electron is $E_H = 5.1\ 10^9\ V/cm$[3]. Comparing the electric field amplitude E_l of the laser [4] with E_H we conclude that the former exceeds the latter as long as the laser intensity is greater than $3-4\ 10^{16}\ W/cm^2$. Therefore when a laser, with wavelength λ_l, hits a solid or dielectric target we expect that a dense plasma, with electron density n_e, is produced after a fast ionization; at the surface of a solid target an "overdense" plasma [5], whose thickness is of the order of the "skin depth" $c/\omega_p \ll \lambda$, is created.

In a naive, "linear" view, [6] it is expected that a largely supercritical plasma should reflect most of the impinging laser light; this is because n_e is large enough for the refractive index to be imaginary. Actually just in the earliest experiments very high coefficients of energy absorption were observed. This is due to a variety of "non-linear" effects through which a considerable part of the radiation energy is left in the plasma and converted into kinetic energy of electrons and ions or into plasma wave excitations and electromagnetic modes.

A distinguished matter is the high-power laser interaction with atomic and metallic clustered media. The peculiar feature with clusters is that properties of solids (high dielectric polarizaton effects) mix up with the behavior of systems with overall, low density which are freely penetrated (optical properties are not changed by clusters of dimensions much smaller than the laser wavelength).

In the complicated scenario of laser-matter interaction the absorption of energy takes place in various forms that ask to consider different physical effects. The dynamics involved in the interaction

[1] An important step forward was taken through the Chirped-Pulses-Amplification (CPA) technique in 1985.

[2] The space length of a pulse is nearly $3-4\ \mu m$; $1\ fs = 10^{-15}\ s$

[3] $E_H \equiv e^2/r_B^2$ is the unit of the electric field in the atomic units system (e is the electron charge and r_B is the Bohr radius)

[4] In order to give some qualitative evaluations it is helpful the following expression:

$$E_l = 2.7\ 10^{10}\ I_{18}^{0.5}\ \frac{V}{cm} \tag{1}$$

where I_{18} is the laser intensity in units of $10^{18}\ W/cm^2$.

[5] For a plasma with electron density n_e it is introduced the quantity (m_e is the electron mass)

$$\omega_p^2 = \frac{4\pi\, n_e\, e^2}{m_e}\ ;$$

ω_p called electron "plasma frequency".

For a given laser frequency $\omega_l = 2\pi c/\lambda_l$ a plasma is called "overdense" whenever $n_e > n_c(\omega_l)$ where

$$n_c(\omega_l) = \frac{m_e\, \omega_l^2}{4\pi\, e^2}$$

is called "critical density". Otherwise the plasma is called "underdense".

[6] For a cold plasma and a non-relativistic field amplitude a linear oscillator model is introduced that allows the refractive index to be written

$$n = \sqrt{1-\omega_p^2/\omega_l^2} = \sqrt{1-n_e/n_c}$$

of intense laser with matter can be understood on the basis of elementary processes: the motion of the single electron [7] in the electromagnetic field and its collisions with atoms, and then, the dynamics of charged particles due to collective fields that just the same particles lead to. The fluid description in terms of averaged quantities (density, flow velocity, temperature) is helpful to study phenomena. But for very intense laser fields in some plasma regions the validity of the description comes to be questionable owing to high mobility of charges under irradiation.

Depending on the nature of the actors of the interaction, the absorption processes are collected in three classes:

- "collisional" processes: the electromagnetic energy is left to particles through their coulomb scattering between point charges (it is also called inverse bremsstrahlung);
- "collective-kinetic" processes: the single particle gets resonant interaction with collective excitations ("modes"), of either the plasma or the electromagnetic field: examples are the Brunel's effect, charged particle acceleration, Landau damping;
- "collective" processes: the interaction is between modes ("mode conversion").

When collective (both "pure" collective and kinetic) absorption takes place, electromagnetic energy is converted into plasmons, phonons or particles are accelerated or heated.

Collisional absorption of energy (and heating) occurs via collisions of freed electrons with ions [8]; thus the electron-ion collision frequency ν_{ei} is the only one relevant parameter in the collisional absortion.

For establishing whether collisions play a role for the absorption of energy we must compare ν_{ei} with the laser frequency. The ion-electron collision frequency scales as $(I_{18}\ \lambda_\mu^2)^{-3/2}$ ([9]). For the problem of laser-matter interaction in which we are interested, the collision effects negligibly contribute to the energy absorption. In fact, in plasmas created irradiating solid targets or clusters by short ($\lesssim 1\,ps$) laser pulses of high irradiance ($I\ \lambda_l^2 \gtrsim\ 10^{16}\ W/cm^2\ \mu m^2$) the frequency ν_{ei} is considerably less than the laser frequency [10].

In laser-solid interaction, among the collisionless effects we have distinguished the "mode conversion" mechanisms: the incident laser wave excites some normal modes of the overdense plasma or an electromagnetic wave. The basic processes which take place can be a linear resonant coupling and a "nonlinear" decay of one mode to many modes (e.g. the "surface wave absorption") ; "weak" kinetic effects can occur together with the mode structures. The modes which play a role can be electromagnetic (photons), electrostatic (plasmons) and acoustic (phonons). It is important to keep in mind that

[7] The coherent oscillatory velocity of the electrons is $v_q = (eE_l)/m_e\,\omega_l$; it is called "quiver" velocity. It is helpful to note that $v_q \sim (I_{18}\ \lambda_\mu^2)^{0.5}$

[8] From the Poynting theorem the electron-electron collisions do not contribute to the absortion of energy; in fact, in the non-relativistic regime, they do not change the total electron momentum, i.e. the mean electron current.

[9] The electron ion frequency is given by

$$\nu_{ei} \propto \frac{n_i Z^2 e^4}{m_e^{1/2}\ v^3}\ \log\Lambda$$

n_i and Z are the ion density and the ion charge respectively; the "Coulomb logarithm" $\log\Lambda$ is nearly 10. The parameter v is an electron "typical" velocity; for intensities large enough $v \simeq v_q$, namely it depends on the intensity ($v \propto I_{18}^{1/2}$).

[10] Theoretical studies [19, 107] suggest that for a laser intensity large enough so that the electron mean free path is longer than the skin depth ($\simeq\ c/\omega_p$) the collisionless (collective) absorption mechanisms become dominant.

in order for a mode conversion to be effective it is necessary that the pulse duration is comparable to the time for the development of the hydrodynamics [11]; this is necessary for as the linear resonant coupling to take place as the "coherence length in the medium" [12] is large enough so that the interference effects are still appreciable. A laser pulse width of the order of one ps can be considered long enough so that the hydrodynamics expansions sets in. Consequently "smooth" density profiles can be formed; their typical "density scale length" $L \equiv n_e/\mathrm{grad}\, n_e$ is larger than λ_l. It is enlightening to introduce a scale law. After it is determined an estimate d of the width of the resonance, we get $d \propto L^{1/3}$, where the density scale length is characteristic of the hydrodynamics [13]. Therefore whenever L is large enough anharmonic effects in the electron motions near the critical point can be ignored in the first approximation, i.e. the non-linear coupling between the modes can be treated perturbatively. Usually the fluid description is a good approximation in this approach.

Coupling effects in regions large with respect to the laser wavelength.
The effects of collisionless absorption, that require space scales due to the hydrodynamics expansion, can be divided in the following way:

- "linear resonance absorption": the laser interacts with an inhomogeneous, overdense plasma. All essential aspects of the mode conversion can be studied in a "plane layered medium approximation" with initial density $n_0(x)$ (x is the relevant coordinate of the plasma plane geometry); at oblique incidence of the laser ($\theta \neq 0$ is the angle between the direction of the wave incidence and the density gradient) the electric field "linearly" forces the electrons of the critical layer ($n_0 = n_c$) to coherently oscillate along the density gradient and produces an electron plasma wave with $\omega_p = \omega_l$. The resonance absorption was first discussed in [82] but it was proposed as a mechanism for the collisionless absorption only later [93, 45].
  The process can be described using a plane, "electrostatic" model ("capacitor" model) [14]. If one assume a "moderate" density gradient then the model can be linearized; it is straightforward to show that the local density oscillation at the critical density experiences a linear resonance.
  For a more fundamental approach the Maxwell's equations in an inhomogeneous medium should be considered; under some simplifying assumptions [15] they can be written in the form of a wave equation (Piliya's equation, see [89]) for the electromagnetic field component E_x, which drives the electrons to oscillate along the density gradient. Actually E_x determines a "coherent" charge separation since the Piliya's equation is equivalent to the equation of a resonant driven plasma wave (see [80], pag. 153).

- mode conversion: the incident laser wave ("pump wave") excites one or more normal modes of

[11] There is an exception to this condition. An ultrashort laser pulse that impinges on a solid target, with steep density gradients, can experience a mode conversion to "surface waves", namely electromagnetic modes generated at the plasma-vacuum interface [34, 76].

[12] If the spectral linewidth of the source and the central wavelength are $\Delta\lambda$ and λ_0, the "coherence length in a medium" of reflactive index r is approximately $\lambda_0^2/(r\,\Delta\lambda)$

[13] We can consider the "conversion rate" for a steady state resonance absorption: $A \equiv S_{es}/S_{em}$, where S_{es} and S_{em} are the electrostatic and electromagnetic flux densities, respectively. It is found $A \propto L$

[14] The model is defined by the Poisson, continuity and Euler equations. A harmonic driver E_d, with frequency ω, acts upon a plane layered plasma with initial density $n_0(x)$. Assuming a "moderate" density gradient ($n/|\partial_x n| \gg \mathrm{v}_x/\omega$) both the continuity and Euler equations can be linearized; so one deals with a linear model. The amplitude $\delta n_e = (n_e - n_0)$ of the local density oscillation, at the frequency ω, is singular at $n_0 = n_c$ ($\delta n_e = \frac{1}{4\pi e}\,\frac{grad\, n_0 \cdot (E+E_d)}{n_0 - n_c}$, E is the electric field). In a linear theory, this fact is to say that at the "critical" layer (where $\omega = \omega_p$) a linear resonance occurs. It is straightforward to notice that the condition for the resonant excitation is $grad\, n_0 \cdot E_d \neq 0$; thus the laser has to be obliquely incident and have a "p-polarization" (E_d must oscillate in the plane of incidence, i.e. the plane defined by the laser wavevector and the density gradient.

[15] Among the assumptions the most important is the linearity of j (as noted above, for oscillation amplitudes small compared to λ_l the local ω_p is defined and higher driver harmonics do not have to be considered; hence $j \simeq e\, n_0\, \mathrm{v}_e$).

the plasma. The pump wave and the wave reflected from the "weak" electron density inhomogeneities constructively interfere. If the amplitude modulation and the normal plasma density have the same periodicity then the ponderomotive force, resulting from the total electric field, leads to an amplification of the electron density modulation and, in turn, to an increase of the reflection and the ponderomotive coupling; this process leads to an unstable growth the electron density fluctuation and to stimulated scattering of the pump wave. This mechanism underlies various "decay" processes from the pump mode to some modes which can be electromagnetic, electrostatic, and acoustic; e.g. we have the Brillouin instability, the Raman instability, two plasmon decay, etc. .

- when the laser intensity becomes sufficiently high some "weak" kinetic effects have to be added to the mode conversion which excites a plasma wave. Vlasov simulations show that even up to intensities of order $10^{16}\ W/cm^2$ the linear fluid theory still predicts the correct energy absorption value [10]. When the driver strength exceeds the linear limit, the Langmuir wave, excited to large amplitude, can experience a damping and then can break [16] The damping occurs since the wave potential becomes sufficiently large so that bunches of particles are captured [17] ("trapping") and, after, get accelerated.

We should keep in mind that the laser pulse, which we deal with, has a length of few femtoseconds ($\lesssim$ 10 fs); hence the time scale of the laser is too small in order that the hydrodynamics allows a solid target or a cluster to expand, namely the necessary condition for a mode conversion cannot happen. Therefore we expect that absorption with a mode interaction is not effective. In particular, since the plasma frequency is tipically much larger than the laser frequency ($\omega_p \gg \omega$), a linear resonance condition cannot be fulfilled because the scale time is too short to allow the charge density to sufficiently decrease. For this to occur it is necessary the driver is at least one picosecond long. Moreover we know that the effects of collisions are significant only during the first few cycles, when the collisions lead to ionizations on the target surface and in the cluster. So the scenario, we deal with, refers to the collisionless interaction of an ultrashort laser with an overdense plasma where steep spatial gradients of both the plasma density and the "macroscopic" fields exist; experiments and computer simulations have proved that an efficient collisionless absorption produces heating and fast electrons in the multi keV - several Mev range. Furthermore a considerable absorption is also observed under normal incidence. It is necessary to find an explanation for this "unexpected" absorption.

An insight into a possible key mechanism leading to collisionless energy absorption is provided by the "cycle-averaged Poynting theorem". This theorem describes the the "stationary" coupling between an estended medium and an electromagnetic radiation. It should be notice that from the simulations it can be seen that, in the interaction between a laser and a solid target, already after only $3-4$ cycles [18] all physical quantities turn into an essentially steady state. The Poynting theorem states that the averaged absorbed power is given by the time average of $(-j \cdot E)$, j is the density current and E is the sum of the induced and the driver fields. This general result stresses to focus on the following aspect which should be a key aspect of the absorption mechanism: each physical effect that produces irrevesible absorption has to lead to a suitable "dephasing" between j and E. In particular it is known that a resonance is always associated to a dephasing. In general, analytical treatments to determine the phase shift between j and E are not available; any quantitave analysis of the laser-matter interaction makes it necessary to use computer simulations (particle-in-cell (PIC), Vlasov, and molecular dynam-

[16] "Wavebreaking" is the loss of periodicity with respect to at least one "macroscopic" quantity (e.g. the electron density n_e, the electric field E) [80].

[17] The first particles which are trapped are those with speed close to the phase velocity of the electron wave.

[18] In a few cycles of the light wave the target surface is ionized through the field ionization and collisions.

ics methods). Therefore, for obtaining some explanations of the kinetic absorption, we need to find out some mechanisms that lead to an "adiabaticity-breaking" which provides a dephasing (microscopic disturbances (collisions) and linear resonances cannot be invoked).

A particle in a plasma experiences the driver fields and the "collective" fields generated by the plasma. Thus the crucial point is the ratio between the time (or spatial) scales of these two agents. It has been noticed that there are some small regions where the macroscopic, induced fields have steep gradients and so, we expect, these regions ($\sim L$) are shorter than the typical scale-lengths of the particle dynamics ($\sim \mathrm{v}_q/\omega_l$). In particular we consider the electrons which cross the small laser penetration depth $\delta_s \ll \lambda_l$ [19] in a fraction of the laser period; in analogy with a collision event, a dephasing between the particle motion and the driving fields can result. This is a condition because irreversible absorption of energy can occur; there is a conversion from a ordered wave energy into a particle kinetic form (which can be a random thermal motion and a particle coherent acceleration). Of course, these effects cannot be appropriately described by the hydrodynamics approach. Therefore it makes clear that a model offers, at least on the qualitative level, a correct physical scenario into irreversibility whenever it gives an important role to the induced fields.

No general picture of absorption is available. Various models, which all refer to the mechanism of dephasing, have been considered, They contribute with wide overlappings among them and possible transitions from an effect to the other. We collect these mechanisms in the class of "collective-kinetic" processes; a short review of some of these effects is given here below.

Dephasing processes

"$j \wedge B$-heating" effect The idea on the basis of $j \wedge B$ heating is the relevance given to the electron motion along the laser beam direction [66]. In particolar it is the mechanism which has been proposed for explaining the absorption at normal incidence: the component of the Lorentz force, that oscillates with a frequency twice the laser one [80, 101, 77], although generally nonresonant, accelerate some electrons which, therefore, move in the steep interface. This shows up as a train of high energy electrons separated by a distance of half of a laser wavelength. The crucial issue is that $j \wedge B$ is a "reversible" driver unless electrons undergo collisions in microscopic or macroscopic fields or resonate in a potential. The $j \wedge B$ heating is thought of to be connected with possible non-adiabaticities of the electron crossings at the vacuum plasma interface.

"Brunel" effect In the Brunel effect, that is introduced in [13], it is first recognized the significance of the plasma (collective) field E_{in} for the energy absorption. The effect is described through a one dimensional capacitor model. A harmonic electrostatic field E_d, with frequency ω, is normal to a plane geometry plasma of electrons that is "highly" overdense; the ions, with density $n_0 \gg n_c$, are assumed to be fixed. When a steady state is reached, a layer of electrons is extracted from the plasma surface and pushed into the vacuum by the driver and nearly half a driver period later is forced back to the target. The electron layer enters the bulk and is just a little slowed down since inside the target the driver is screened, except for the evanescent field in the thin skin depth δ_s ($\ll c/\omega$). Let us consider the l-th layer; by assuming the absence of wavebreaking [20] the plasma field on the layer, $E_{in}(l)$, is constant in time and can be computed [21] After each driver cycle a certain number of electrons

[19] The penetration depth equals approximately the classical skin layer thickness c/ω_p

[20] In [13] it is supposed that the trajectories of the plasma layers (i.e. the fluid elements) do not intersect (exclusion of wavebreaking effects): this hypothesis is difficult to motivate since it implies that resonances are forbidden.

[21] According to the Poisson's law, for the l-th layer

$$E_{in}(l) = 4\pi\, q(x_1(t), x_l(t))$$

is pushed into the bulk; their kinetic energy is irreversibly absorbed by the plasma from the laser. In order to explain this fact the physical relevant point is that the electrons move in the space charge field E_{in}. it produces the phase shift of the electron motion with respect to E, that is the necessary condition for the absorption, according to the Poynting theorem.

"Vacuum heating" [83] In the issue of the collisionless absorption, with the expression "vacuum heating" one usually refers to the fact, shown by PIC simulation studies, that a cloud of "hot" electrons is formed in the vacuum; in fact some electrons do not return to the plasma within a cycle and turn around in the vacuum region [53, 95]. In general one identifies the vacuum heating as the phenomenon, observed in simulations, of electrons that enter the vacuum side acquire a velocity of the order of the vacuum oscillation velocity and enter the plasma region. In [80]) it is claimed that the models of vacuum heating, which can be found in literature, do not provide any well defined physical effect for the heating. The relevant issues are to understand where the absorption takes place (vacuum or skin layer) and to investigate the dynamics of the electron reflection in the vacuum as a function of the relative phase between the injection instant and the laser wave. For addressing such issues a test particle model is considered in [8]. Through the model the vacuum heating result to differ from the Brunel effect since, in particular, the electron cloud in front of the target is confined by the ponderomotive force rather than by space charges.

"Anomalous skin" effect [38, 40] We notice that the efficiency of the mechanisms, described just above, depends on the conditions: (i) by neglecting the "$j \wedge B$" force (that becomes more and more important with growing intensities) the incidence has to be oblique and with a p-polarization so that the force excerted by the laser pulse has a longitudinal component; (ii) for "pure" step profiles ($n/|\mathrm{grad} n| < 0.01\lambda_l$) few electrons are pulled out from the plasma and vacuum heating appears to be negligible [83]; (iii) the same holds for large plasma densities ($n_c \ll n_0$) since the large back-holding force does not allow electrons to enter the vacuum. Even in the absence of the $j \wedge B$ heating, one can still find a non-negligible absorption with normal incidence to a plasma with a step-like density profile, whenever a plasma is "warm". In this case the explanation focuses on the electrons which, owing to their thermal motion, cross the skin layer in a time shorter than the laser period. This is the so called "anomalous skin effect" [108].

Low-dimensional Hamiltonian model.
It should be evident that in each non-resonant mechanism, we have reviewed, the attention is drawn on some processes which seem to work in specific circumstances. One wish to introduce a physical effect which can be assumed as a "paradigmatic", unifying principle able to describe the collisionless energy conversion in overdense targets and in clusters from ultrashort laser pulses. In this purpose a very different approach is considered [25, 87] defined by the following criteria:

- adopt a "Hamiltonian" dynamics in order to explicitly suppress any purely collisional (i.e. dissipative) effect;
- consider a system with few relevant degrees of freedom whose dynamics is defined by a "collective" potential (of the plasma).

Furthermore the PIC simulations show that electrons are excited well beyond the quiver energy, during only $1-2$ laser periods. It is concluded that in a Hamiltonian model with few degrees of freedom, the

where the total electronic charge between the first layer and the l-th one $q(x_1(t), x_l(t)) = q_{1l}$ is independent on t since the layers do not overtake each other. Moreover, each layer which is pulled out mantains a zero field $E = E_d + E_{in}$ in the bulk; hence if x_0 is a point in the bulk through which the l-th layer passes at t_l then $E_{in}(l) = -E_d(t_l)$.

physical effect that causes a finite phase shift in j and promptly accelerates electrons up to velocities exceeding the quiver velocity can only be a resonance [87]. As it has been said before, the acceleration takes places before the plasma can rarefy, namely before ω_p can shift down to meet ω_l. Therefore the non-linear resonance is the paradigmatic physical effect of the coupling between an overdense plasma, with steep density gradients, and an ultrashort laser pulse; a driven anharmonic oscillator is the model that describes the coupling. This approach is known as the "non-linear-resonance absorption" [86, 85, 25, 69, 68].

It is interesting to notice that the anharmonic resonance is an efficient mechanism which leads to a breaking of the dynamics of a fluid. If the laser intensity is sufficiently high a fluid element (electron layer), initially nonresonant ($\omega_p \gg \omega_l$), that moves in the local space charge potential, can be driven into resonance and then start to move oppositely to the next layer ("resonant wavebreaking").

Th reduction of the many particles problem to a Hamiltonian problem with few degrees of freedom obviously looses many aspects of the real interactions and sometimes raises questions about the reliability of the results. On the other side it enables to discuss the problem of the energy absorption, by applying the methods introduced to study the non-linear oscillations of Hamiltonian systems and allows to straightforwardly develop a geometric point of view and to refer to methods of the analysis. Moreover through this approach the notion of resonance is discussed as one of the fundamental concepts of the Hamiltonian theory, irrespective of the specific problem of the energy absorption, which is the essential reason because the anharmonic oscillator model is considered. And so, at least for small field ampltudes, we can obtain a rigorous analysis on the basis of general results of the perturbation theory, as the Kolmogorov-Arnold-Moser (KAM) theorem [63, 5, 6, 79] and the methods of the Nekhoroshev theorem [81].

We are given insight into some non-perturbative properties of the dynamics of one dimensional driven oscillators when this dynamics is addressed as a scattering problem. In a typical scattering event a free particle comes in from infinity, enters an interaction region and moves there for a finite time. After a while it leaves the interaction region and goes off to infinity, as a free particle again. If the system is governed by a Hamiltonian function the interaction region is described by a potential that vanishes fast enough out of the interaction region. A one-dimensional oscillator, that is periodically driven, can be described as a scattering of a particle by a one-dimensional oscillating potential well, even if the driver does not vanish asymptotically. Since a time dependent system in one dimension can be formulated as a time independent Hamiltonian system with two degrees of freedom, a driven oscillator can be regarded as a scattering process with a time independent Hamiltonian.

In the classical description of collisions one follows the phase space trajectories and calculates the dependence of the variables, which characterize the free particle motion after the scattering on some variables which specify the "incoming" channel. A function which describes this dependence is referred to as "scattering function". Appropriate output and input variables should become constant asymptotically so they serve to label the initial and final states.

The study of chaotic dynamics in Hamiltonian systems is straightforward on cases where the motion is bounded to a "finite" volume in phase space. The basic mechanism which brings chaos into the dynamics of simple deterministic systems is the "stretching and folding" mechanism [75, 54]. Whereas the stretching occurs along the unstable directions [22], the folding is a consequence of the phase volume preservation since the dynamics is confined to a "finite" volume of phase space.

[22] The Lyapunov exponent determines its average magnitude.

The proposition that chaos occurs also in scattering, where phase space and the relevant dynamics are unbounded, needs some explanation. Generally one would argue that because of the "finite" interaction time there cannot be scattering chaos. A trajectory stays in the interaction region for a finite time only, and although the trajectory may be arbitrarily complicated during this time, it eventually has to be smoothly connected to an outgoing trajectory. But there are situations in which a scattering function may contain a set of "singularities"; near any of the singularities, an arbitrary small change in the input variable can cause a large change in the output variable; this feature is reminiscent of chaos in bound systems. Actually a scattering process is called "chaotic" whenever the scattering function is singular on a "fractal" set. For its explanation it is assumed in the phase space the existence of a "hyperbolic" invariant set Λ [7] consisting of an uncountable infinity of periodic and aperiodic orbits [58, 59]. In other terms, the origin of the fractal set of singularities is assumed to be a chaotic motion on a invariant bound set. This is the crucial reason because a scattering process is called "chaotic".

In other words, in order to prove that the irregularity of a scattering function is just the distinct fingerprint of a form of bound chaos one needs to construct a family of solutions of the system whose investigation may carry out by the methods of "symbolic dynamics" [100, 3]. The first step is to construct a cross-section in the sense of Poincaré and the corrisponding mapping D. Then one constructs an invariant set of D, with a fairly complicated structure, on which the action of D is topologically isomorphic to a "topological Markov chain" [12]. Going back from the mapping D to the phase flow one obtains the family of trajectories of the invariant set Λ; the standard devices of symbolic dynamics now permit the determination of solutions of the scattering system with extremely varied behavior. In general, it is a difficult task to find a symbolic dynamics for a scattering system [88, 29, 103] Concerning the problem of the driven oscillator in [1, 2] for a rather large class of potentials it is proved the existence of a hyperbolic invariant set Λ, on which the dynamics of a appropriate discrete map ("return map") is described in terms of a symbolic dynamics which involves an "infinite" number of symbols [28]; the last result is expected since at every step of the self-similar structure of the scattering data, the scattering map is continuous in an infinity of components. We remark that in [2] is provided a symbolic dynamics for the restricted "three-body" problem [97]; it is known that a direct application of the Smale's theorem [99] to this problem is not possible.

Chapter 1

Mulser and nonlinear resonance.

1. Introduction.

The nonlinear resonance has been proposed as a *key* mechanism to understand collisionless energy absorption in solid density plasmas, cluster media, dusty plasmas in the coupling with an intense, ultrashort laser.

The eigenfrequency of electron oscillations in ionized, ordinary matter (which is of the order of the plasma frequency ω_p) is higher than the typical frequency of a driving field; hence the light absorption cannot be caused by a linear resonance. The way out of this argument is to take account of the property of anharmonic oscillators to have an oscillation period dependence on the oscillation amplitude. In the literature ([25, 87, 68, 69]) numerical studies suggest that, in various physical systems, the coupling of radiation to matter can be described by means of an "appropriate" nonlinear oscillator with few degrees of freedom, driven by a periodic force. The light absorption corresponds to the sudden jump in energy which is undergone by the oscillator when its "effective" period matches the period of the driver. The restoring force is given by the space charge potential that describes the "collective" screening effects of the microscopic Coulomb interactions. Therefore we expect that any bounded motion in the collective potential has an effective frequency which decreases with the amplitude, i.e., at fixed driver period, the system can "enter" into the resonance when it is excited to an amplitude large enough. The amount of energy absorbed depends on the length of the time during which the resonance occurs.

In this thesis we focus on the issue of the nonlinear resonance for a rather extended class of driven oscillators with one degree of freedom. The issue is faced through a complete, fairly mathematical approach in the "small" driver regime (where a KAM-like analysis is available) and by means of a numerical study for driver amplitudes "large enough", corresponding to the regime which papers [86, 85, 25, 69, 87] are devoted to. Our aim is to obtain some remarks helpful to the worth of explaining of the anharmonic resonance mechanism for the laser matter interaction problem. In particular, in the next chapter we will discuss whether there are some cases in which the resonance $1:1$ [1] does not produce any "significant" absorption and, on the other hand, a significant absorption can occur even when the period of the driver is "close" to a rational multiple of the effective period of the system.

[1] such that there is a bounded orbit whose unperturbed period equals the driver period

In the Mulser's papers the nonlinear resonance that provides absorption always takes place at the motion with the period of the driver. Moreover we attempt to realize whether the main point of the nonlinear resonance mechanism is just a "remnant" of a resonance in the KAM regime. In this chapter we describe the oscillator models that are introduced in the papers above in order to show that the anharmonic resonance can represent the leading physical mechanism of collisionless absorption in solid targets and clusters from intense ultrashort laser pulses.

2. Energy absorption of laser in matter.

A very efficient absorption of energy occurs when sub-picosecond [2] intense laser pulses of wavelength λ [3] hit matter. Both experiments and simulations have shown up to 70% absorption in solid targets and even more in the interaction with clustered matter. We assume that relativistic effects are negligible; therefore we deal with a laser whose typical intensity I is in the range $10^{16} - 10^{18}\ W/cm^2$ ("moderate intensity range") [4]. The important point to note is that the collisions cannot be taken into account in order to explain this fact; actually the laser light is intense enough so that accelerated particles experience important collision effects throughout periods longer than the period which allows the absorption to occur, i.e. $\nu \ll \omega_p$, the collision frequency is much less than the plasma frequency [5].

An insight into the collisionless absorption in overdense matter [6] and clusters can be provided by the Poynting's theorem [11] which describes a generic process of energy transfer from an electromagnetic field to the matter, independently on the particular absorption mechanism [65, 80]. The theorem expresses the conservation of energy and, in a general form, is given by

$$\frac{\partial u}{\partial t} + \mathrm{div}\, S = - j E \ , \tag{1.1}$$

where u is the field energy density and S is the "Poynting vector". The Poynting theorem can be interpreted in the sense that at each point the rate of energy density is due to both the energy flow, expressed by the Poynting's vector divergence, and the power supplied by the electric field onto the unit volume of matter [7]. We notice that the matter can be assumed "frozen": the matter varies on the

[2] A laser pulse with duration of few tens of femtoseconds is called "ultrashort".

[3] The wavelength λ of the light of a typical high power laser is of the order of one micrometer.

[4] The electric field is given by $E_0 = 2.7\ 10^{10}\ \sqrt{I_{18}}\ V/cm$, when the intensity of the radiation is $I_{18}\ 10^{18}\ W/cm^2$. Hence in our case the field amplitude takes values around $10^8 - 10^9\ V/cm$ and it is sufficiently large in order to ionize atoms.

[5] The interactions of charges are long range and the Coulomb cross section allows to estimate their effects on motions. In particular, the mean free path is obtained: $l \backsim \mathrm{v}_{th}^4/n$, where n is the density of the charged particle species and v_{th} is its thermal velocity; hence the collisional frequency $\nu \backsim n/\mathrm{v}_{th}^3$.
The laser electric field makes the particles to accelerate up to velocities v_{th} (we may estimate $v_{th} \approx E_0\ \lambda$) which are large enough such that

$$\frac{l}{\lambda_D} \backsim (T\ n^{-\frac{1}{3}})^{\frac{3}{2}} \gg 1$$

T ($\backsim v_{th}^2$) is the charge temperature and $\lambda_D = \mathrm{v}_{th}/\omega_p \backsim (T/n)^{1/2}$ is the Debye screening length. It follows that $l/\mathrm{v}_{th} \gg \lambda_D/\mathrm{v}_{th}$ or $\nu \ll \omega_p$. The plasma frequency $\omega_p = 4\pi\ n$ (both the mass and the charge of the electron are set equal to 1) reflects the fact that electrons in a plasma are exposed to their own space charge fields; it is an eigenfrequency of the local oscillations of the electron density.

[6] Let ω is the pulsation of the laser, the parameter $n_c \equiv \omega^2/(4\pi)$ is called the "critical density". A system with a charged species with density n is "overdense" when $n > n_c$. The interaction of an intense laser with solids and liquids gives rise to highly overdense plasmas of solid electron density.

[7] The term $j\ E$ is the sum of two contributions representing the resistive dissipation of energy (called "Joule's heat") and the mechanical work respectively.

time scales of the hydrodynamics which are much longer than the time scales of the energy absorption from an ultrashort pulse. Furthermore in respect of the electromagnetic fields only after few laser cycles ($3-4$ cycles) a substantially steady state is reached [8]. Therefore it follows that the integral $\int_0^\tau dt\ \partial u/\partial t \simeq 0$, where τ denotes the laser period; hence the averaging over τ of (1.1) provides

$$\langle \text{div}\, S \rangle \simeq -\langle j\, E \rangle \tag{1.2}$$

i.e. in order for the absorption occurs the phase difference between j and E has to be so that the second side of (1.2) is not zero. In particular when the driver field is $E \sim \cos(\omega t)$, we can write

$$\langle j \cdot E \rangle \sim \langle \cos(\omega t)\ \sin(\omega t + \phi) \rangle \sim \sin\phi \tag{1.3}$$

The condition for a net absorption, irrespective of the mechanism involved in the energy transfer, requires a deviation of the dephasing ϕ from $\phi = 0$. This condition is fulfilled either (1) if or time or spatial nonadiabaticities are present or (2) a resonance coupling of the electromagnetic field with some motion of the system takes place.

The nonadiabaticities include as particular cases the "collisional excitations":

- the Coulomb collisions, whose effects are negligible for intense laser pulses;
- each absorption phenomena when the exciting pulse length is shorter than a fraction of the period of a system motion [25], i.e. the excitation frequency spectrum is higher than the "inner" frequencies of the system. It has been already noted that a short laser pulse is long enough so that this kind of nonadiabaticities cannot be taken into account for the absorption.

Other forms of nonadiabaticities can take place in the interaction of ultrashort laser pulses with solid plasmas. In fact, for a sufficiently short laser pulse, the hydrodynamic motion of the heated target is negligible and hence the high density plasma, that is created, still has density gradients almost sharp. These give rise to nonadiabaticities when the electrons move through the vacuum-plasma interface.

In overdense plasmas with steep density gradients, collisionless absorption can be described according to models in which the irreversible energy conversion gives rise to ("periodic") jets of electrons which move perpendicularly to the vacuum-plasma interface, driven by the laser fields either under oblique incidence (Brunel mechanism) [13] or for normal incidence through the Lorentz force ("$j \wedge B$ heating") [66]. It is important to notice that the electron motion takes place in collective fields induced by the laser. In [66], by means of one-dimensional PIC simulations, an energy conversion of approximately 10% is found at $I\,\lambda^2 = 10^{18}\ \text{W cm}^{-2}\ \mu\text{m}^2$ [9].

On the other hand, also in the absence of any induced, longitudinal motion of the electrons, one still finds up to 16% absorption at normal incidence and $I\,\lambda^2 = 10^{18}\ \text{W cm}^{-2}\ \mu\text{m}^2$. At the sharp boundary of a highly overdense plasma the tunnelling laser field falls off in a thin skin layer. An electron moving at thermal speed oscillates in the layer in less than one laser cycle; therefore it "collides" with the laser and space charge fields and gains energy which is not given back to the laser field ("anomalous skin absorption").

[8] In particular in a solid target the absorption takes place in a small layer with a thickness of the order of one micrometer. Therefore we can expect that after few wavelengths a steady state is reached.

[9] For $I\,\lambda^2 = 10^{17}\ \text{W cm}^{-2}\ \mu\text{m}^2$ an absorption of 1.3% is observed.

The mechanism of the resonance is connected to the coupling of the laser field with a system that moves in a potential with a "collective" nature, i.e. many charges are exposed to their own space charge fields [10] which give rise to restoring forces that are smooth on space scales of the order of the oscillation amplitude (v_q/ω), where v_q is the quiver velocity [11].

The typical densities n's of plasmas formed from solid targets and clusters are so large that the strength of (electric) restoring forces gives eigenfrequencies (of the order of the plasma frequency ω_p) that are typically ten times higher than the frequency of the laser. Far away from the condition $\omega = \omega_p$, the energy absorption, connected to the coupling of the laser fields to the mode ω_p, becomes negligible just after the laser pulse is longer than one cycle; in fact it is saved less than 1 % of the maximum oscillatory energy absorbed during the pulse [12] [25]. On the other hand an ultrashort pulse is not sufficiently long to cause an hydrodynamic expansion that creates the conditions for a mode-mode coupling to be efficient. In particular the linear resonance coupling with the laser electric field E_d and the Lorentz force ("$v \wedge B_d$" resonance) can be taken into account only if the density profile is smooth enough [13]. Moreover E_d have to be coupled with a motion along the density gradient and hence it is required that $E_d \cdot gradn \neq 0$. The Lorentz force resonance [14], which occurs even if the previous condition drops, gives rise to oscillations at twice the driver frequency. However only the non-oscillating term (ponderomotive force) is present whenever the driver polarization is circular [35].

In the interaction of an ultrashort, intense laser pulse with a solid density plasma, the absortion of energy brought about by the mechanisms above is only a little part of what is expected: some experiments [37, 39, 51] and simulations [83, 49, 36] showed that an absorption is possible up to $70 - 80\%$. On the other hand, owing to the relevant time scales that are too short, the resonant linear couplings with respect to the matter cannot play any role. We have already remarked that in a solid plasma the electrons spend the most part of their motion in smooth space charge fields; therefore we expect that the nonadiabaticities can contribute to the energy gain but the resonance should play a major role. After the significant step forward due to Brunel, for more than two decades searching for the physical nature of collisionless absorption was not successful. Only recently a real breakthrough in understanding has been achieved [87].

Mulser et al. suggest the non-linear resonance as the explanation of the dephasing for the collisionless absorption when the linear resonance cannot occur. They consider an interaction model based on nonlinear forced oscillators, with few degrees of freedom. The free oscillation period depends on the amplitude; in oscillator models built from Coulomb systems the period of a bounded motion increases as the excitation level is increased At a fixed driver period (greater than the eigenperiod around the equilibrium point) the system may enter into resonance when excited to large amplitude. In this way the system can exchange a significant amount of energy with the driver. Actually if the amplitudes around the resonance are not reached then only a negligible energy is transferred from a laser pulse. Whereas if the resonance zone is crossed the oscillator stores energy which is not given back when the oscillator runs out of the resonance and after the driver is over. In fact, when a nonlinear resonance is crossed, the phase of j with respect to the driver field shifts by π and the driven oscillator

[10] In a first stage of irradiation single atoms are ionized by laser fields which are later replaced by collective fields.

[11] Possible fluctuations of a field of collective origin can have spatial extentions larger than a Debye length λ_D. Therefore the field fluctuations of "collisional" character can contribute to the heating but their effects are small.

[12] Given a system eigenfrequency ω_p, the larger the difference of ω_p from the laser frequency the faster the decreasing of the energy gain is with increasing duration of the pulse ("adiabatic effect").

[13] i.e. $(v_q/\omega) \ll n/|gradn| \equiv L$, n is the electron density, L is called density scale length. In [67] the absorption dependence on L is investigated and it is shown that the resonance absorption is negligible as soon as $L \simeq 0.1\lambda$, λ is the field wavelength.

[14] The effect is linear in respect of the plasma and nonlinear regarding the laser.

undergoes an irreversible absorption. The model is conceptually simple and robust, i.e. it works under all conditions as soon as certain level of laser intensity is reached.

In this approach the role of the collective fields generated by the plasma is crucial. In fact the resonance mechanism, which provides the necessary phase shift, is related to the motion in the plasma fields. The Brunel effect suggests an explanation of the collisionless absorption, which makes clear the function of the space charge field E_{in}, induced under oblique incidence or by the Lorentz force [13, 14]. Among the electrons that E_{in} pushes back after they are pulled out into the vacuum , the electrons, whose motion in the vacuum region is nearly synchronized to the laser period, are pushed into the target where the electrons are free and, hence, do not give back their energy to the laser. The energy which is irreversibly absorbed by the plasma in each cycle is a balance between the energy of the electrons that enter the plasma and the energy of the "cold" electrons that are pulled out into the vacuum, during one laser period. The absorbed energy per electron is, on average, of the order of the quiver one. Of course the Brunel effect represents a "non-adiabatic" absorption since the interaction lasts nearly half a laser period; thus the energy absorbed by an individual electron depends on the initial conditions, i.e. on the phase difference between the injection momentum of the electron and the laser field at the vacuum-target interface.

Mulser et al. devoted various papers to the application of the nonlinear resonance idea and considered models of heating of both overdense matter [87] and clusters [69, 68, 85, 86]. Moreover in [25] it is investigated how a harmonic oscillator with frequency ω_0 behaves under an external driver $a(t)\ \cos(\omega t)$ as the time duration of $a(t)$ is varied from many $2\pi/\omega$ to be istantaneous.

3. Nonlinear resonance and the collisionless absorption in overdense plasmas.

The interaction of sub-ps pulses with solid plasmas has been addressed. Various effects have been made responsible for the collisionless absorption. However some of them (mode-mode coupling) are intrinsically ineffective since they are incompatible with the time scales of the dynamics induced by an ultrashort pulse. The other effects (collective-kinetic effects) are insufficient since they supply absorption efficiencies that are approximately an order of magnitude lower than those observed in experiments and simulations. The model of the anharmonic resonance is a step forward in identifying a correct physics scenario.

There are some crucial facts that can be pointed out after an analysis of the simulations:

i) there is an irreversible conversion of energy;

ii) there is a prompt generation, during a few laser cycles, of fast electrons with energy many times larger than the quiver energy;

iii) in a plasma with electron density $n_0 > n_c$, n_c is the critical density, the absorption occurs before the density profile is significantly modified; therefore the typical eigenfrequency of the plasma remains different from the laser frequency.

In [87] the previous features are regarded to be sufficiently convincing to conclude that the nonlinear

resonance is the leading physical absorption mechanism in sub-ps laser pulse - overdense plasma interaction. In fact one can notice that

i) the irreversibility of the energy conversion is accomplished since a resonance causes the adiabaticity of the dynamics to be broken. The absorption is marked by a finite phase shift in j.

ii) A resonance is probably the only effect through which electrons can be accelerated to velocities much larger than the typical velocities of the "free" oscillation motion during only $1-2$ cycles.

iii) The period of the electron motion in the "anharmonic" plasma potential can meet the laser period; the coupling takes place through a resonance even though it cannot be linear.

Can the resonance mechanism explain why the absorption efficiency is so high? In order to address this question in [87] the authors study the dynamics of a statistically meaningful number of test electrons [15] in a PIC simulation [16] where, in a one dimensional geometry, a laser beam of $I = 10^{17}$ W/cm^2 and half width of 26 fs hits a plane target with the plasma density $n_0 = 80\,n_c$. All test particles which enter the laser field are accelerated. For each of them the momentum $p_x(t)$, along the normal $\hat{x}$ to the target, undergoes a strong increasing (up to many times the quiver momentum) and a phase shift with respect to the electric field at the particle position $x(t)$; these features make evident that a resonance is the acceleration process. Moreover the resonances experienced by the various particles look similar to each other. These observations lead to conclude that the mechanism of resonance is fit for the high absorption efficiency that is measured [17].

In [87] a semplified $n-$bodies model is introduced to describe, in a self-consistent way, the interaction of a laser pulse with a cold, solid plasma. The interaction region is thought as divided into a large number N of electron layers (of index l) of thickness d, oriented parallel to the surface. Each layer represents an oscillator in which the electron fluid oscillates against the attracting background of ion N layers (index n), that are assumed to be fixed, under the action of a driver f. The related Hamiltonian has the known form (electron mass $m_e = 1$)

$$H = \sum_{l}^{N} \left(\frac{p_l^2}{2} + \frac{1}{2} \sum_{l' \neq l}^{N} V(x_l - x_{l'}) - \sum_{n}^{N} V(x_l - a_n) - f(x_l, t)\, x_l \right) \tag{1.4}$$

where x_k and a_n are the positions of the k-th electron layer and the n-th ion layer respectively and the interaction potential

$$V(x) = \frac{1}{2}\,(\omega_p\, d)^2\, \left(\frac{1}{4} + \left(\frac{x}{d}\right)^2\right)^{1/2} \quad , \tag{1.5}$$

ω_p is the plasma frequency. The explanatory power of the model is examined by numerically solving its dynamics. The driver

$$f(x,t) = f_0(x)\, g(t)\, \cos t \quad , \tag{1.6}$$

calculated on the $l-$th electron layer, is assumed to be exponentially evanescent, $f_0(x_l) = f_0\, e^{-l\eta x_l}$, since it takes into account of the screening caused by the layers in front of the k-th one; $g(t)$ is the pulse shape. A Hamiltonian model like (1.4) is helpful in interpreting PIC simulations.

[15] The test particle approximation consists of visualising single particle trajectories in prescribed electric and magnetic fields to provide a qualitative understanding of the kinetic properties of a system.

[16] The code that is used is introduced in [37]; it is electromagnetic and includes the dynamics of the ions, the temperature and the return current.

[17] Particles in the target interior, which do not experience the laser field, can be heated whenever they interact with some plasmons excited by the fast particles accelerated by a resonance.

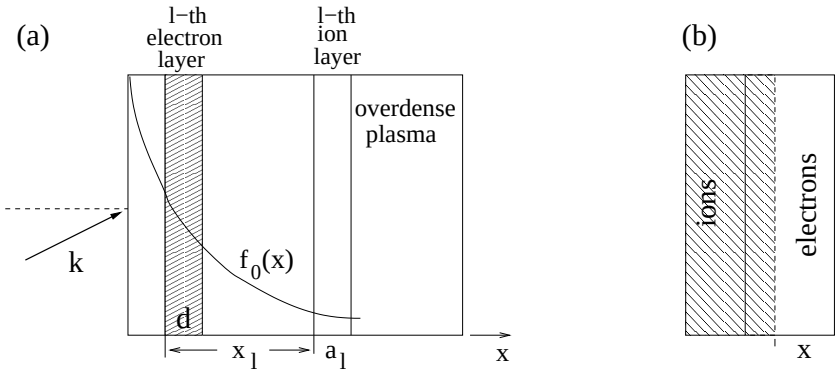

Figure 1.1: (a) A laser beam of wavevector k hits an overdense target that is cut into layers of thickness d; f_0 describes the screening of the laser in the matter. (b) The displacement x of an electron layer with respect to its neutralizing ion layer.

From (1.5) we notice that for $f_0 = 0$ and small layer displacement ($x \ll d$) the layers oscillate at ω_p. Whenever f_0 is large enough some layer is driven into a resonance and hence it moves oppositely to the layers which do not experience any resonance; therefore it can cross some of the adjacent nonresonant layers (resonant breaking of wave). This exchange of place between of layers produce nonadiabaticities; in fact, in a fraction of the laser period, the layer can reach a region where it experiences a restoring force and a driving force that are different from what it experienced before the crossing. This mechanism contributes to the irreversibility; however it can take place only if a resonance comes first. Therefore a resonance is the crucial mechanism of absorption. A signature of the occurrence of resonance is that the layers can gain energies exceeding their quiver energy U_p: layer energy spectra, that are determined in simulations, show typical plateaux between $1U_p$ and a cut off, whose value depends on the particular model that is considered (cut off values between 10 and 20 U_p are measured).

Other properties that characterizes an anharmonic resonance are

- the existence of a threshold in the laser amplitude for starting the resonant absorption;
- in the resonance zone the oscillator undergoes a phase shift, i.e. there is a smooth transition through $-\pi/2$ of the phase φ of the oscillator velocity v with respect to the driver E.

In a n-bodies model, like that in (1.4), one is not able to analytically calculate realistic thresholds. On the other hand, in order for a resonant absorption to take place the "crossing" of the resonance should last at least one laser period; in fact we already know that there is absorption whenever the cycle average of $\mathrm{v}E \sim jE$ is nonvanishing and hence if there are too rapid fluctuations no energy gain can be found [87]. In a n-bodies model the restoring force upon a given oscillator depends on the motion of all the other layers; this is of course a condition that can inhibit resonance crossings long enough. Fig. 1.2 shows the resonance dynamics of a layer ($l = 32$) of a system (1.4) with $N = 120$ [87]: only some particular transitions (see I and II in part (c)) of the phase φ through $-\pi/2$ are connected to absorptions (see part (b); the absorbed energy is equal to some units of U_p). Other transitions do not give rise to any significant gain of energy (see, in particular, 1 and 2 in (c)): they are related to oscillations that are fast with respect to the laser period.

The model (1.4) is a step forward to a simplification that identifies the relevant dynamics of the

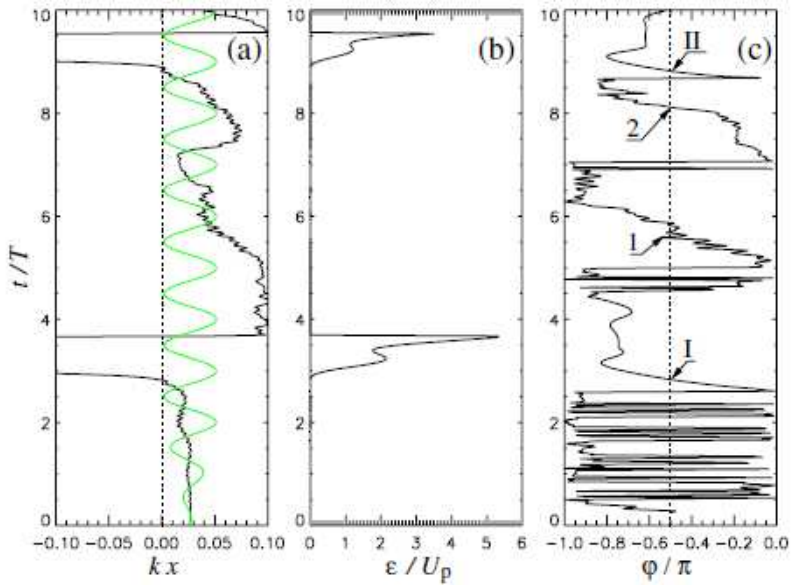

Figure 1.2: The dynamics at the resonance of a layer of the *n*-layers model (1.4). Part (a) shows the layer position (in units of k^{-1}, k is the driving laser wavelength) and the driver. Part (b) the absorbed energy (in units of the quiver energy). Part (c) the phase difference φ between v and the driving laser field. Borrowed from [87].

collective effects in the laser matter interaction; moreover an advantage of the model lies in its Hamiltonian structure. However the *n*-bodies nature of (1.4) is not substantial to make evident the contribution of the anharmonic resonance mechanism to the understanding of the physics of the collisionless absorption. Furthermore it makes the properties of the "collective" resonance dynamics difficult to be clearly identified. Therefore it is well founded to further semplify and consider models of individual oscillators in fixed potentials.

Thus a system (1.4) is considered where all layers are "frozen" except for one. In equation (1.4) N and a_1 are set equal to 1 and 0 respectively. In [87] the corresponding equation of motion

$$\ddot{\zeta} + V'(\zeta) = f(t) \tag{1.7}$$

is numerically integrated; V is defined by (1.5) and the driver is chosen

$$f(t) = f_0 \sin^2(t/(2n)) \cos t \tag{1.8}$$

For $f_0 = 0$ any motion is bounded. The relative period T [18] is a function of the oscillation amplitude x_0. For $x_0 \gg 1$ the free period

$$T(x_0) = 4\sqrt{2}\,\omega_p^{-1}\, x_0^{1/2} \tag{1.9}$$

increases with the oscillation amplitude; therefore the solution of

$$T(x_0) = 2\pi \tag{1.10}$$

exists and is the amplitude x_r corresponding to the *principal* resonance.

[18]
$$T = \int ds\, (2\,(V(x_0) - V(s)))^{-1/2}$$
the integration is along an orbit with amplitude x_0 and ds is the line element.

If f_0 is such that $x_0 < x_r$ the resonance is not crossed and the oscillator is not excited (fig.1.3 (a)).

On the other hand increasing f_0 the oscillator reaches the resonance and irreversibily gains much more energy than before (fig.1.3 (b)).

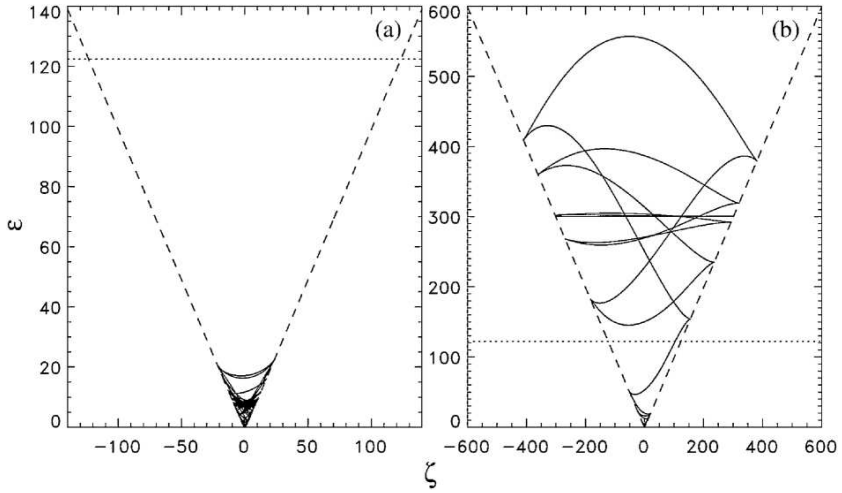

Figure 1.3: The crossing of the nonlinear resonance. Mechanical energy ε of the oscillator (1.7) driven by f, n=20, $\omega_p = 10$. (a) $f_0 = 0.921$; (b) $f_0 = 0.923$ - Borrowed from [87]

4. Interaction of lasers with clusters.

Atomic and metallic cluster turned out to be very efficient absorbers when they interact with a high power laser (whose wavelength usually belongs to the interval $800 - 1100nm$). In experiments with rare gas clusters [102] almost all the laser energy is absorbed. The absorption brings the electron energies up to several keV. Electrons leave net positive charge behind that expands and converts electron energy into ion energy of about 100 keV, and ions with MeV energies were found.

The scenario of the interaction is marked by a development through some steps. In a first stage the external electrons are removed from their "parent" atoms fields (inner ionization). At this stage the plasma heating is due to ion - electron collisions; however 1 keV electron energies cannot result from it beacause of the dependence of the collisions frequency on both the electron temperature ($\sim T^{-3/2}$) and the laser intensity ($\sim I^{-3/2}$). After, the ionization goes on in the cluster (collective) field ("outer ionization"). At this stage experiments show a strong increase of the laser - cluster coupling; the polarization field sums up to the laser one ("ionization ignition") [16]: the ionization is up to a charge state too high to be a result of the laser field alone.

We know that according to the Poynting's theorem (1.1) a dephasing is a prerequisite for absorption. The condition under which the phase difference between j and E changes is the occurrence of either collisions or resonances. From the point of view of the energy balance between electromagnetic fields and matter, the ionization process can be modelled as a collisional absorption characterized by an effective "collisional" frequency ν_I ([19]) [84]: the inner ionization gives a $\nu_I \neq 0$ as long as the process goes on. As the plasma is fully ionized ν_I goes to zero and the ionization absorption stops. Collisional absortion in the laser cluster interaction is dominant only for wavelengths shorter than 800 nm [23, 17, 18]. Thus in our case it should be considered to yield a minor contribution [23, 41].

[19] $\overline{J\,E} = \frac{\varepsilon_0\,\omega_p^2}{2}\,\frac{\nu_I}{\omega^2-\nu_I^2}\,E\,E^*$, E is a harmonic field with frequency ω

Nonadiabatic effects due to the finite size of the cluster ("collisions with the cluster boundary") are not the necessary condition for the absorption: when the electromagntic field is circularly polarized it is strongly suppressed ([20]) but the absorption results to be unchanged [68].

For ionized clusters a collective oscillation motion takes place; $\omega_{Mie}(t) = \sqrt{(4\pi\rho(t))/3}$[21], $\rho(t)$ is the ion density, is the typical oscillation frequency ("Mie frequency"). Before the ions expand, the density $\rho(t)$ is such that ω_{Mie} is much larger than the usual value ω of the driver frequency. Since the expansion occurs on the time scales of the hydrodynamics, the ion cluster needs to spend a few handred femtoseconds so that ω_{Mie} sufficiently decreases and hence the linear resonance condition $\omega_{Mie}(t) = \omega$ is fulfilled. Therefore the linear resonance cannot occur for short driver pulses. In this case the idea of nonlinear resonance appears to be the only one helpful for understanding the efficient absorption.

At high laser intensities, in spite of the many body nature of the interactions, collective oscillations $r(t)$ can be identified. Since the motion takes place in an anharmornic potential, the effective frequency ω_{eff} depends on its excursion amplitude a: $\omega_{eff}(a)$. The oscillator undergoes a nonlinear resonance just after $|r(t)| \geq a$, provided that $\omega_{eff}(a) = \omega$.

The dramatic increase of absorption when some nonlinear resonance is verified is quite general and can be observed not only for collective degrees of freedom but also for individual particles. In [68] it is perfomed a three-dimensional PIC simulation. It is studied the motion of each PIC electron that moves under the action of (1.8), $n = 8$, in the field E_{sc} of the own space charges. From the equation of motion of the i-th PIC electron it is obtained the effective oscillator frequency of the motion r_i of the electron i

$$\omega_{eff}^2 = \frac{E_{sc}(r_i)\, r_i}{|r_i|^2} \ ;$$

it depends on the position of all particles $j \neq i$.

Figure (1.4) shows the dynamics of the PIC electrons: the effective frequency squared (scaled to the driver frequency) is plotted vs their energy $E_{tot} = \dot{r}_i^2/2 + \Phi(r_i)$, r_i the position of the $i-th$ PIC particle. The quantities are measured at certain times (t=2.5, 3, 3.5, 4 driver cycles). When E_{tot} becomes positive the corresponding electron is considered to be ionized and then ω_{eff} goes to zero. The simulation starts when the cluster is at the neutral configuration, i.e. $\omega_{eff} = 0$ for every electron. Under the driver action the cluster becomes polarized and at the early times ω_{eff}/ω increases beyond the unity Fig.1.4 shows that electrons come to be ionized when they undergo the nonlinear resonance; in fact they come to $E_{tot} > 0$ when they pass close to the point $((\omega_{eff}/\omega)^2, E_{tot}/U_p) = (1,0)$.

As well for almost all the electrons the ionization takes place at the same distance from the origin. In fig. 1.4 the particle radial position is displayed by a color-code; at the resonance the radial position is $r \simeq 2$. These considerations strenghten the idea of the "collective" nature of the fields; hence the effective frequency is a well-founded concept. The nonlinear resonance is a robust phenomenon that is insensitive to the cluster and laser parameters.

In [85] it is described a model for a cluster. Both electrons and ions are modeled by rigid and homogeneously charged spheres: the negatively one oscillates against the field of the second positive sphere. The system is driven by the laser. The model enables us to get the physical essence of collisionless absorption of radiation by the electrons of the cluster:

- it is sufficient to reduce the analysis to a one dimensional problem; in this way what is irrelevant for the item is traken off;
- it displays the nonlinear resonance that is able to provide a natural and intrinsic characterization of the irreversible absorption.

[20] electrons mainly go around the boundary rather than crossing it

[21] $m_e = e = 4\pi\varepsilon_0 = 1$

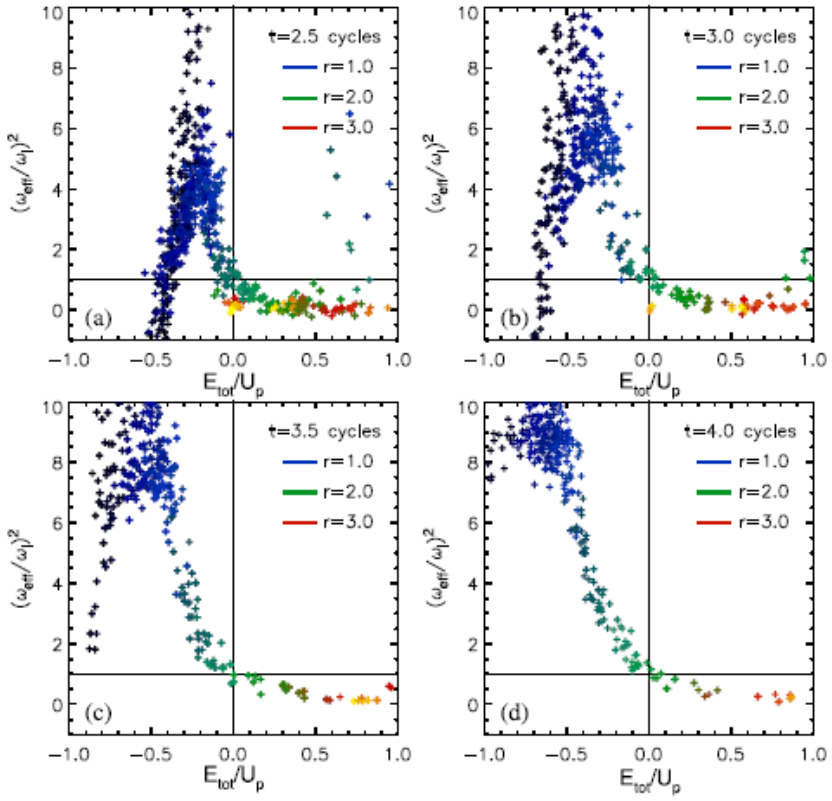

Figure 1.4: The preionized cluster is 40 times overcritical ($(\omega_{Mie}/\omega)^2 = 40/3$, the laser intensity is $I = 2.5\,10^{16}\ W/cm^2$ - Borrowed from [69]

We consider a simple version of model ([85] gives a detailed discussion about it), i.e. the rigid oscillator driven by a harmonic electric field. We make the following assumptions:

- we consider the electromagnetic field weak enough in order both ions and electrons to be nonrelativistic;
- we set the magnetic field $B = 0$ and so the electric field E is oscillating along x axis and is non propagating (dipole approximation):
- the spheres have the same radius R and opposite charges $q_i = -q_e = n_e\, e$.

$$E(t) = E_0 \begin{cases} \sin(\omega t/n)\ \sin(\omega\, t) & 0 \le \omega t \le n\pi \\ 0 & otherwise \end{cases}$$

- we only consider solutions with zero angular momentum.

Under these assumptions the equation of motion is

$$\frac{d^2}{d\tau^2}\xi + \frac{d}{d\xi}V(\xi) \;=\; \frac{1}{\omega^2\, R}\, E(\tau) \tag{1.11}$$

where the reduced mass is $\simeq 1$, $\omega t = \tau$, $\xi = x/R$ and

$$V(\xi) = \omega_{Mie}^2 \begin{cases} \frac{1}{2}\,\xi^2 \;-\; \frac{3}{16}\,|\xi|^3 \;+\; \frac{1}{180}\,|\xi|^5 & 0 \le |\xi| \le 2 \\ \frac{6}{5} \;-\; \frac{1}{|\xi|} & |\xi| \ge 2 \end{cases} \tag{1.12}$$

(in atomic unities) and $\omega_{Mie}^2 = n_e^2/R$.
It is a driven oscillator with a single well potential. Close to $\xi = 0$ ($|\xi| \leq 2$) the interaction is polinomial (the charge is partially screened) and for $|\xi| \geq 2$, when the spheres are not overimposed, the interaction is Coulomb-like. The matching of the force at $|\xi| = 2$ is $\mathcal{C}^1$-smooth [22]. In comparison with an intense driver amplitude, the inner interaction is not negligible only for $|\xi|$ some unities from the origin.

A difference between (1.12) and (1.5) is that the former has a finite depth. Going on as for (1.5) we may formally write (1.12) as

$$V(\xi) \;=\; \frac{1}{2}\left(\frac{\omega_0(\xi_0)}{\omega}\right)^2 \xi^2$$

where

$$\omega_0(\xi_0)^{-1} = \frac{2}{\pi}\int_0^{\xi_0} \frac{d\xi}{(2\,(V(\xi_0) - V(\xi)))^{0.5}}$$

where ξ_0 is the oscillation amplitude of the bound motion with period $2\pi/\omega_0(\xi_0)$.
In [85] it is determined $\omega_0 \sim |\xi_0|^{-3/2}$ for $|\xi_0|$ large enough ($|\xi_0| \geq 2-3$), whereas $\omega_0 \sim \omega_{Mie} \ll \omega$ for $|\xi_0| \simeq 0$.
E_0 and ξ_0 increase together. It follows that it exists a threshold E_0^{res} for the laser field amplitude such that for $E_0 < E_0^{res}$ no resonance occurs and as the laser is switched off the oscillator comes back to its initial energy level. On the other hand when $E_0 > E_0^{res}$ the nonlinear resonance condition $\omega_0 = \omega$ is fulfilled and the most part of energy pumped into the oscillator is left over. Fig.1.5-left shows the abrupt transition of absorption at E_0^{res}. Fig.1.5-right displays the absorbed energy, the displacement as a function of time: the motion drastically changes when the nonlinear resonance is crossed.

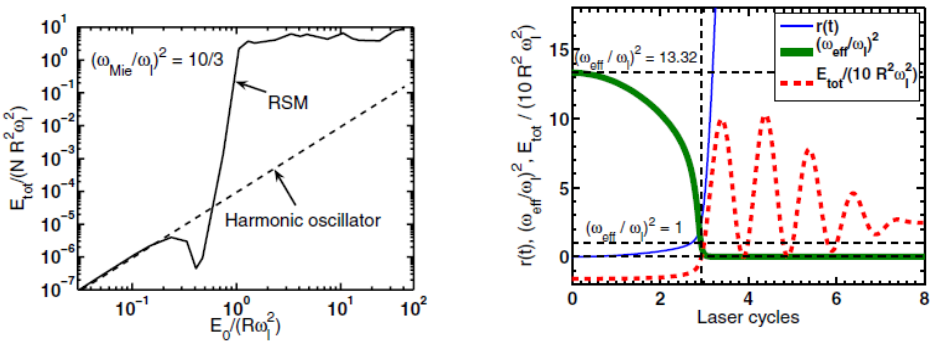

Figure 1.5: the preionized cluster is 10 times overcritical ($(\omega_{Mie}/\omega)^2 = 10/3$ - Borrowed from [68]

5. Beyond the Mulser analysis. The nonlinear resonance in the dynamical systems theory.

We have realized the explaining power of the nonlinear oscillator as a simple model of collective absorption. The discussion in the previous sections gives only few sketches on the numerical experiments and the physical bases to justify the model. For a fuller treatment we refer the reader to the references.

[22] V must be at least $\mathcal{C}^2$

We turn our attention to a different issue: how the absorption properties can be characterized when the model is thought of as a "dynamical system". On this matter a helpful way to illustrate the dynamics is by means of the Poincaré map P, i.e. the representation of the periodic traces of the phase portrait, whose computation is numerically performed. Accordingly, our analysis is mainly descriptive and focusses on "invariant" structures in the phase space section, defined by P. In particular, since we deal with an oscillator without damping, the possible invariant "objects", which we may meet, are

(i) the "fixed points" x_0's of P (x_0 is a fixed point of P if $Px_0 = x_0$), that can be elliptic and hyperbolic [23] (whenever a fixed point is at the infinity it is called parabolic),

(ii) the "closed" orbits about the elliptic points,

(iii) the trajectories connecting fixed points; they are called "heteroclinc" orbits or "separatrices" when they connect different fixed points. The last ones must be hyperbolic.

Other structures are not available.

We attempt to go on along the way traced by Mulser and al.
We think that, in order to investigate the properties relevant to the absorption issue, we do not need to consider the specific form of (1.5) and (1.12). On account of this we allow the freedom to choice any oscillator

$$\ddot{q} = -V'(q) + \varepsilon f(q,t) \tag{1.13}$$

where f is a "periodic" function of t (actually in the numerical study we will always consider a "harmonic" f). As well the potential V

i. is "regular enough". In particular, we will engage in a discussion on the resonance theory in a weakly perturbed nonlinear oscillator; there it is required the oscillator Hamiltonian to be analytic;

ii. has a stable equilibrium point [24] q^0, just to fix ideas, at $q^0 = 0$. For ε sufficiently small, through a straightforward application of the implicit function theorem [94], we expect that the Poincaré map P_ε of (1.13) has an elliptic point [25]

$$q^0_\varepsilon = q^0 + O(\varepsilon)$$

Therefore, for any ε small enough, there is a region around q^0_ε that is filled with a family $\{q^\alpha(t),\ \alpha \in A\}$ of (quasiperiodic) closed orbits, "except for a subset of A of zero measure".

We will see that a consequence of the assumption *ii*. is the following. Consider a motion, with initial conditions close enough to $(q^0_\varepsilon,\ 0)$; there exists a "threshold" ε_0, which actually can be rather large, such that,

a. whenever $\varepsilon < \varepsilon_0$, the motion remains close to a certain closed orbit $q^\alpha(t)$, and hence it is kept confined in a small phase space region around $(q^0_\varepsilon,\ 0)$.

[23] A fixed point is classified according to the value of "characteristic exponent" of the "linearization" of the map around it.

[24] i.e. the unperturbed Poincaré map P_0 has en elliptic fixed point.

[25] In fact the Jacobian $DP_0(q^0)$ does not contain 1 in its spectrum and hence $(I - DP_0(q^0))$ is invertible and hence there is a smooth curve of fixed points $(q^0_\varepsilon, \varepsilon)$ passing through $(q^0, 0)$.

b. While, for $\varepsilon > \varepsilon_0$, the motion can occur "faraway" from $(q^0_\varepsilon,\ 0)$, since it takes place in a domain where the closed orbits either are lost or, if they survive, have a topology different from that of $q^\alpha(t)$.

As concerns the energy absorption, the case *a*. corresponds to a forced oscillator motion along which only a "small" amount of energy is exchanged. Whereas in the case *b*. a "significant" amount of energy can be absorbed. We will devote the analysis described here to the last part of the next chapter.

It has been stated that the condition that the "effective" period of oscillation $T(a)$, a is the oscillation amplitude, is "nearly" equal to the driver period T_d is essential so that a significant absorption can take place. In the next chapter a numerical study will be performed by means of which some Poincaré maps are obtained. The study of these maps allows to conclude that the connection between the condition of "equality of the times" ($T(a) \simeq T_d$) and a large amount of absorption does not hold in general. Actually if a significant absorption is observed then one finds that the effective period $T(a)$ is such that $T(a) \simeq \alpha\, T_d$ for a certain $\alpha \in \mathbb{Q}$. In the next chapter we will realize that the dynamics close to a resonance depends on certain coefficients of the Fourier expansion (with respect to action-angle variables) of the perturbation. These coefficients determine the topology of the invariant structures around the resonance, i.e. how much the phase space is modified from the unperturbed situation. This is the same as to say that the Fourier coefficients determine the amount of energy absorption at a resonance. Therefore it can occur that the energy absorption when $T(a) \simeq T_d$ is less then the absorption at a resonance with $T(a) \simeq \alpha\, T_d$, $\alpha \neq 1$ and, in particular, it can be negligible.

In general, whatever small is the driver amplitude, the dynamics near a resonance gives rise to chaotic motions. However we should realize that for a driver small enough an when we deal with an oscillator with $1 + 1/2$ degrees of freedom the dynamics close to a resonance remains integrable for a very long time, that, in good approximation, can be assumed larger than any time scale that is relevant for the oscillator dynamics, and, in particular, for any absorption process. Therefore, for a small driver, the energy absorption should be thought distinct from the onset of chaos. This is a result of the perturbation theory; we will deal with this matter in chapter 3. On the other hand, as the driver amplitude increases, and the perturbation approach cannot be considered, chaotic dynamics and absorption can occur together. In particular, for a potential V which allows unbounded motions (see below case $V1$.) there are orbits which both are made asymptotically free, after an absorption of an enough amount of energy, and spend a certain phase of the motion in a bounded region where chaotic motions can occur. We will focus on this issue in chapter 4.

Another aspect which can be relevant in respect of the resonance absorption is the "asymptotic" behaviour of the potential. We can consider both

V1. potentials V that allow only bounded motions, i.e. such that

$$\lim_{q\to\pm\infty} V(q) = +\infty \quad ,$$

as for the model (1.5), and

V2. potentials V that have separatrices with critical points at $q = \pm\infty$ (parabolic points), i.e. such that

$$\lim_{q\to\pm\infty} V(q) = \max V \quad , \tag{1.14}$$

as for the model (1.12).

Concerning the nonlinear resonance absorption the asymptotic behavior is important in the sense that, if the driver frequency is lower than the oscillator eigenfrequency, which is the general case in the laser-dense matter interaction, then the energy absorption is inhibited whenever the effective period $T(a)$ decreases with the amplitude a. Therefore a potential V, where only bounded motions occurs (i.e. belonging to $V1$), allows significant resonant absorptions to take place on condition that V does not grow asymptotically faster than a parabula. The oscillator (1.7) is an instance of this fact. Of course whenever V belongs to the class $V2$ the resonant absorption can be always found.

In the case (1.14), an aspect that is worth highlighting is the following:

1. whenever parabolic points are present it is given a specific mechanism which causes chaotic motions around the separatrices connecting the points. Actually this mechanism is the same that leads to the onset of chaos in any resonance and is discussed in chapter 3. A crucial feature on the basis of the onset of the chaotic behavior at the separatrix is given by the following rough remarks.

   We consider the general form of a (one dimensional) oscillator affected by a periodic perturbation, with period $2\pi/\nu$:

   $$H = H_0(x, \dot{x}) + \varepsilon U(x, t)$$

   where $H_0(x, \dot{x}) = 1/2\dot{x}^2 + V(x)$.

   The unperturbed oscillator provides a separatrix $\mathcal{S}$ for $E = E_s$. We are going to qualitatively discuss the motion close to the unperturbed separatrix.
   The behaviour of the unperturbed velocity in the vicinity of the separatrix is the main point we have to take into account. It looks like a sequence of pulses (see fig. 1.6)

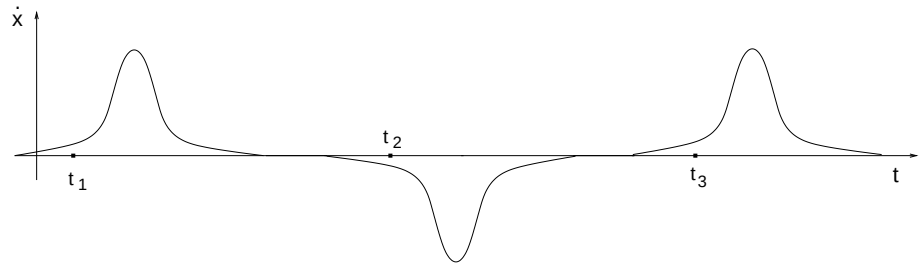

Figure 1.6: The unperturbed velocity close to the separatrix. There are shown some instants of $\mathcal{T}$ defining the map (1.15) .

   Consider an unperturbed motion with energy $E = H_0$. Let ω_0 be the proper frequency close to the equilibrium point and $\omega(E)$ the effective frequency of the chosen motion. We know $\omega(E) \to 0$ for $E \to E_s$. The oscillator spends much more time in the region where the restoring force is negligible (namely where $\dot{x}$ is nearly zero (see fig 1.6)) than in crossing the potential well (i.e. the width of a pulse in fig. 1.6). Hence we can write $2\pi/\omega(E) \gg 2\pi/\omega_0$.

   Let us consider the canonical pair (E, φ), $\varphi = \nu t + \varphi_0$ is an equivalent of the time variable. We measure (E, φ) at the instants $\mathcal{T} = \{t_n\}$ where $t_{n+1} = t_n + \pi/\omega'$, $\omega' = \omega(E(t_{n+1}))$. Each instant is chosen just before a velocity pulse (see fig 1.6). We may describe the perturbed motion through a map ("separatrix map")

   $$T: \begin{pmatrix} E(t_n) \\ \varphi(t_n) \end{pmatrix} \longrightarrow \begin{pmatrix} E(t_{n+1}) \\ \varphi(t_{n+1}) \end{pmatrix} = \begin{pmatrix} E(t_n) + \Delta E \\ \varphi(t_n) + \pi/\omega' \end{pmatrix} \tag{1.15}$$

$t_n \in \mathcal{T}$.
The value of the variation of energy is

$$\Delta E = \int_{t_n}^{t_{n+1}} dt' \ \{H_0, H\}_{pb} = \varepsilon \int_{t_n}^{t_{n+1}} dt' \ \{H_0, U\}_{pb} \tag{1.16}$$

where $\{\ldots\}_{pb}$ are the Poisson's brackets. It follows that the energy changes are negligible up to time interval $\Delta t \sim 1/\varepsilon$. Hence ΔE does not yield instability. However in the neighborhood of a separatrix even a small change in energy ($\Delta E \sim \varepsilon$) produces a large change of the oscillation period that results in a considerable change of φ. This is the essential of the "stochasticity" close to a separatrix.

2. the existence of the parabolic orbits causes that a function, which connects asymptotic quantities before the interaction region, defined by the potential, to analogous quantities after the interaction, displays peculiar, "hierarchical" structures which will be addressed in the chapter 4.

Chapter 2

The nonlinear resonance theory.

1. Formulation of the problem.

Making reference to the previous chapter, we are interested in the problem of the irreversible energy gain of an oscillator excited by a periodic driver. In this chapter we will partly face this issue through a descriptive analysis on the basis of some numerical data. The absorption of energy, viewed as a general problem of the laser-matter interaction, is related to the existence of a nonlinear resonance, when it is analyzed through the model of the oscillator. The phenomenon exists and is rather amplified when the fields are intense and, consequently, a perturbative method is not thought to be suited. However, even for small driver amplitude, a resonance, in a nonlinear oscillator, has various aspects that can be helpful for understanding the absorption in general: for instance, we mean the existence of different time scales and the fact that a resonance has a width in energy that gets an estimate of the amount of energy that can be absorbed.

So we focus our attention to the "resonance" problem of one degree of freedom, nonlinear oscillator, driven by a "weak" force and without damping. The resonance is one of the most important issue of the perturbative approach of a Hamiltonian oscillation theory. It is linked to fundamental results of the theory of Hamiltonian systems, i.e. the KAM theorem and the Nekhorossev's theorem. We will deal with this theoretical background. In this chapter we will introduce a typical approach to a resonance of the classical perturbation theory, namely we will refer to the method of canonical transformations. The forced oscillator is treated as a system with two degrees of freedom, with a Hamiltonian which is not explicitly time dependent. We consider a single canonical transformation that gives the Hamiltonian a "normal form", which defines the resonance and coincides with the pendulum Hamiltonian. The pendulum can give rise to a "secondary" resonance that is worked in a similar way as "primary" one, i.e. through a second canonical transformation, from the variables of the primary resonance, that produces a second normal form, and so on. In this way, it is defined a hierarchy of resonances.

The oscillations boundedness under a small perturbation is the first sign of the oscillator nonlinearity; this is not true for the linear oscillator. The smallness is due to the dependence on energy of the oscillation frequency. However, as we will show through the qualitative examination of some Poincaré maps, in general, the boundness of the oscillations does not take place when the driver is large enough. In fact we are definitely outside the domain of applicability of KAM theorem, which is

the mathematical statement of the boundness property. In this case a non negligible energy absorption can occur.

Anyway, there is an aspect that is shared by a small perturbation and a large driver. In fact in both cases the presence of a resonance modifies the structure of the phase space and causes non integrability. For a small driver the involved volume of the space is small with the perturbation; the non-linear stabilization is destroyed in the vicinity of destroyed separatrices of the resonance "pendulum". While, for a large driver, there are regions of phase space where the motion is not confined and that the system enters after it crosses the resonance. For a Hamiltonian system with at least three degrees of freedom the non integrability regions can result from the "interactions" of non-linear resonances; the interaction can be described by the "standard" map [15], i.e. the pendulum feels a periodic sequence of short "kick".

2. Basic definitions.

Integrable Hamiltonian system.

Let us consider a l-dimensional system $\mathcal{S}$ with a Hamiltonian H on a phase space $\mathcal{W}$.
In $\mathcal{W}$ we may consider a system of coordinates (I, φ) respect to which $\mathcal{W}$ appears as $\mathcal{U} \times \mathbb{T}^l$, $\mathcal{U} \subset \mathbb{R}^l$ is open, $\mathbb{T}^l$ is the l-dimensional torus. The motion is called 'quasi-periodic' when

$$(I, \varphi) \longrightarrow (I, \varphi + \omega(I)\, t) \quad ,$$

$\omega(\,\cdot\,)$ is analitic.

We say the system $\mathcal{S}$ is (canonically) 'integrable' if all motions in $\mathcal{W}$ are quasi-periodic and there exists a canonical map $\mathcal{G}:\ \mathcal{W} \to \mathcal{U} \times \mathbb{T}^l$ such that

$$H(\mathcal{G}^{-1}(I, \varphi)) = h(I) \tag{2.1}$$

h is an analitic function. The equation of motions in the coordinates (I, φ) are

$$\dot{I} = 0 \qquad\qquad \dot{\varphi} = \omega(I) \tag{2.2}$$

If a system is integrable then the phase space is 'foliated' into invariant tori, each torus is parametrized by $I \in \mathcal{U}$.

The mapping T.

Let φ_t be a flow in $\mathbb{R}^3$, arising from a periodic vector field $f(x, t)$, with period τ. The initial data $x_0 \in \mathbb{R}^3$ define an orbit $\varphi_t(x_0)$. Since f is periodic one can identify the surface $t = 0$ with the surface $t = \tau$. This defines a mapping T of the surface $\Sigma(t = 0)$ into itself:

$$T:\ x_0 \ \longrightarrow\ \varphi_\tau(x_0) \tag{2.3}$$

We note that $\varphi_{n\tau}(x_0) = T^n(x_0)$; hence the asymptotic properties of the flow is determined by the iterates T^n, $n \to \pm\infty$.

Let γ be a periodic orbit of φ_t. The intersection P of γ with Σ is a fixed point of T. We determine the differential DT of T at P; λ_1, λ_2 are the eigenvalues of DT. We assume T preserve the phase space volume. Therefore the product of the eigenvalues is equal to 1. Two cases can take place: (i) $\lambda_1,,\lambda_2$ are both real and $|\lambda_1| \leq 1 \leq |\lambda_2|$; (ii) λ_1 and λ_2 are complex conjugate and $|\lambda_1| = |\lambda_2| = 1$. In cases (i) and (ii) P is called hyperbolic and elliptic respectively.

3. Properties of the phase portraits of quasi-integrable systems. The nonlinear oscillator.

When the perturbation of an Hamiltonian system is sufficiently small it is expected that its phase portrait is kept topologically unchanged from the unpertubed case except for domain with a measure going to zero for the perturbation parameter going to zero.
We look into some features that mark the perturbed Poincaré sections near a resonance. We try to understand which terms in the Hamiltonian cause them. In order to make one step to get this purpose it is helpful to consider a driven harmonic oscillator; later on we are going to add nonlinearity effects on.

Let us consider

$$H = \frac{1}{2} p^2 + V(x) - \varepsilon\, x\, f(t) \tag{2.4}$$

where $x \in \mathbb{R}$. The potential $V(x)$ is a potential well with one critical, quadratic point and f is a periodic driver.

In order to show some properties in the phase portraits we choose the special case of a linear oscillator with a harmonic driver

$$V(x) = 1/2\ \omega_0^2\, x^2 \qquad f(t) = \cos(\nu t) \tag{2.5}$$

Actually the features hold for a generic, driven, one dimensional oscillator.

We write $\nu\, t$ as τ We move to the polar variables (I, ϕ) using the transformation equations of the linear oscillator

$$\begin{aligned} x &= (\frac{2I}{\omega_0})^{\frac{1}{2}}\ \sin\phi \\ \dot{x} &= (2I\ \omega_0)^{\frac{1}{2}}\ \cos\phi \end{aligned} \tag{2.6}$$

the transformed Hamiltonian of (2.4) in case (2.5)

$$H(I, \phi, \tau) = \omega_0\, I + \frac{\varepsilon}{2}\, (V(I, \phi + \tau) + V(I, \phi - \tau)) \tag{2.7}$$

where

$$V(I, \phi \pm \tau) = (2I/\omega_0)^{\frac{1}{2}}\ \sin(\phi \pm \tau)$$

Let $H_0 = \omega_0 I$ denote the unperturbed Hamiltonian.
It is straightforward to note that

$$H(I, \phi - \tau) = \omega_0\, I + \frac{\varepsilon}{2}\, V(I, \phi - \tau) \tag{2.8}$$

retains all the essential resonant behaviour of (2.4).
Let us introduce the canonical change of variables due to the time dependent generating function

$$F(I,\phi,\tau) = I\,(\phi-\tau)$$

and we obtain the "time independent" Hamiltonian

$$H(I,\varphi) = (\omega_0-\nu)\,I + \frac{\varepsilon}{2}\,V(I,\varphi) \tag{2.9}$$

We conclude that for studying the resonance for a driven harmonic oscillator with one degree of freedom we deal with a "one-dimensional" Hamiltonian system. Actually we will see that this feature holds for any driven oscillator with one degree of freedom.

Futhermore it is straightforward to show that *in a Poincaré section $t=\bar{t}$, the driver shifts the fixed point of oscillator (2.4) laterally along the x-axis.* We consider the equation of motion

$$\begin{aligned}\dot{x} &= p\\ \dot{p} &= -\partial_x(V(x)-\varepsilon\,x\,f(t))\end{aligned} \tag{2.10}$$

It follows that any fixed point must lie on the x axis ($p=0$) and it is a solution of

$$V'(x) = \varepsilon\,f(\bar{t})$$

and so the fixed point is shifted from the fixed point $x=x_0$, $V'(x_0)=0$, of the free oscillator by an amount that goes to zero as $\varepsilon\to 0$. The phase space portrait moves continuously with ε and develops around the new fixed point.

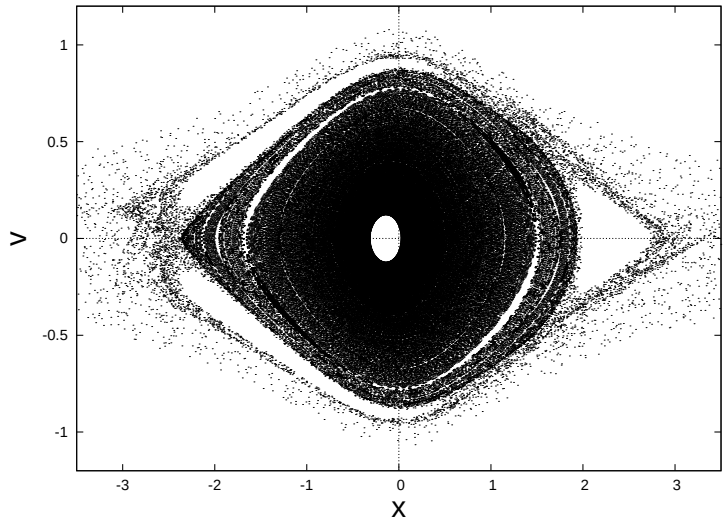

Figure 2.1: A tipical KAM pattern of the oscillator (2.4) with $V(x)=\beta^2\,\frac{6/5\,x^2}{12/5+x^2}$, $\beta=0.7$, that is shifted by a perturbation $f(t)=\varepsilon\,\cos(\nu t)$, $\nu=0.8$, with $\varepsilon=0.05$. Resonances can take place only for harmonics of the driver ($\beta<\nu$).

The displacement is unrelated to the resonance condition. On the other hand the 'driven solution', namely the solution of (2.4) that, as $\varepsilon\to 0$, approaches the solution $x=x_0$ of the free oscillator, depends on the resonance condition. In fact, let us consider, in particular, case (2.5) (where $x_0=0$); the driven solution is

$$x = \frac{\varepsilon}{2\,\omega_0\,(\omega_0-\nu)}\,\cos\tau + \frac{\varepsilon}{2\,\omega_0\,(\omega_0+\nu)}\,\cos\tau \tag{2.11}$$

A nonlinear oscillator is characterized by the properties:

- the "non-isochronicity", i.e. the dependence of the free oscillation frequency ω on the action I (or the energy);
- the "anharmonicity", i.e. the spectrum contains higher harmonics of the basic frequency $\omega(I)$.

Let us note that the shape of the oscillations has nothing to do with the non-linearity: there may exist a nonlinear but harmonic oscillator (the rotation motion of a pendulum) and a linear but anharmonic oscillator (an ultrarelativistic particle in a square potential with a constant frequency) [15].

In the case that nonlinear terms are added to H_0 in (2.4), i.e. ω_0 depends on I, it is worth pointing out some facts

- the phase portrait is shifted by the perturbation similarly to the linear case;
- non-linearity may introduce new equilibrium points besides to the linear equilibrium point;

As well, a resonance is forced to be stabilized by nonlinear terms in H; in fact there are orbits passing arbitrary close to it that are bounded. This property bring out a distinct difference between the linear and nonlinear cases.

4. A one-dimensional oscillator weakly driven.

We are interested in investigating the properties of a one dimensional ($x \in \mathbb{R}$) oscillator V, driven by a time dependent force f. We assume f is periodic and ν is its frequency. The equations of motion are given by (2.10). We deal with the nearly integrable problem, i.e. $\varepsilon > 0$ is a small parameter.

It is straightforward to show that a one dimensional system with a force that depends on time can be put into the form of a two dimensional hamiltonian system.
Let us consider the time as a new canonical coordinate t:

$$\begin{aligned} \dot{x} &= p \\ \dot{p} &= -\partial_x H \\ \dot{t} &= \partial_{p_t} H \\ \dot{p}_t &= -\partial_t H \end{aligned} \tag{2.12}$$

p_t is the momentum conjugated to t. The system is described by

$$H(x, p, t, p_t) = p^2/2 + V(x) - \varepsilon f(x,t) + \nu\, p_t \;=\; H_0(x, p, p_t) \;- \varepsilon f(x,t) \tag{2.13}$$

We allow the driver to depend on position; this extension does not imply any more difficulty and conceptual discrepancy. Of course it is $f(x,t) = x\, f(t)$ in the particular case of a driver that depends only on time.

If we change to the action-angle variables the nearly-integrable Hamiltonian comes to the form

$$\mathcal{H}(I_1,\, p_t, \varphi_1, t) = h(I_1) + \nu\, p_t + \varepsilon\, h_1(I_1, p_t, \varphi_1, t) \tag{2.14}$$

h is the Hamiltonian of the one dimensional oscillator in the action-angle coordinates (see 2.1) and h_1 is the perturbation. About the latter we shall give some specification later.

4.1 Action-angle variables.

In order to give an example, in which one is able to obtain closed form expressions for the integrals, we are going to calculate the action-angle variables for

$$V(x) = \beta^2 \frac{a x^2}{2a + x^2} \tag{2.15}$$

$a \in \mathbb{R}^+$ and $\beta \in \mathbb{R}$.

We will almost always refer to (4.1) in the simulations. The choice of this model is done keeping in mind that (4.1):

- has an unique elliptic point; this allows to make clear the characterization of the phase space structures that play a role in the resonance mechanism of absorption in laser absorption models as (1.7) and (1.12) of chapter 1;
- admits an analytic continuation into the complex plane; this property will be important in the fairly rigurous discussion of chapter 3 which is based on a perturbative approach to the resonance;
- is fit to reproduce properties that are observed in models of the interaction between a laser and "bounded" plasmas (as a cluster) and that concern the dynamics in unbounded domains of the phase space which is the issue faced in chapter 4.

In order to calculate the action-angle variables of we consider a trapped orbit with energy $0 \leq E_0 \leq E_\infty$, where $E_\infty \equiv \beta^2 a$ is the escape energy. The corresponding action is given by

$$J(E_0) = \frac{1}{2\pi} \oint dx\, p(x) \;=\; \frac{2}{\pi} \int_0^{x_m(E_0)} dx\, \sqrt{2\,(E_0 - V(x))}$$

where

$$p(x) = \pm \sqrt{2\,(E_0 - V(x))} \tag{2.16}$$

and $x_m(E_0)$ is the positive solution of the equation

$$E_0 = V(x_m)$$

It follows that

$$J(E_0) = \frac{2\sqrt{2}}{\pi} \int_0^{x_m(E_0)} dx\, \left(V(x_m(E_0)) - V(x)\right)^{\frac{1}{2}} = \frac{4}{\pi} (a\,E_0)^{\frac{1}{2}} \int_0^1 d\zeta\, \left(\frac{1-\zeta^2}{c+\zeta^2}\right)^{\frac{1}{2}} \qquad \zeta \equiv \frac{x}{x_m(E_0)}$$

where $c = c(E_0) = 2a/(x_m(E_0))^2$. The calculation of the integral is performed and finally we get

$$J(E_0) = \frac{4}{\pi\,\beta}\, E_\infty \left\{K\left(\left(\frac{E_0}{E_\infty}\right)^{\frac{1}{2}}\right) - E\left(\left(\frac{E_0}{E_\infty}\right)^{\frac{1}{2}}\right)\right\} \tag{2.17}$$

where K and E are the complete elliptic integral of the first kind and of the second one respectively [46].

Thus, the reversion of (2.17) gives us E_0 as a function of J; the unperturbed Hamiltonian can be written

$$H_0 = E_0(J) \tag{2.18}$$

The equations of motion assume the form

$$\begin{aligned} \dot{J} &= -\frac{\partial H_0}{\partial \theta} = 0 \\ \dot{\theta} &= \frac{\partial H_0}{\partial J} \equiv \Omega(J) = \frac{1}{\frac{\partial J}{\partial E_0}} \end{aligned} \tag{2.19}$$

Throught $8.123-2.$ and 4. of [46] we find

$$\Omega(J) = \frac{\pi\,\beta}{\sqrt{2}}\,(1-\frac{E_0(J)}{E_\infty})\;\frac{1}{E\big((\frac{E_0(J)}{E_\infty})^{\frac{1}{2}}\big)} \tag{2.20}$$

We observe that $\Omega(J)\to 0$ for $E_0\to E_\infty$. In (J,θ) variables, the dynamics is trivial: the action J is constant and

$$\theta(t) = \Omega(J)\,t\,+\,\theta_0 \tag{2.21}$$

Let $E_0 \le E_\infty$. From the equation $dx/dt = p(x)$, p is the momentum (2.16), we write the time increment as a function of the space one. Therefore we straightforwardly obtain the solution of the oscillator (4.1) with energy E_0 and $x(0)=0$:

$$t = \frac{x_m}{\sqrt{2\,c\,E_0}}\int_0^{\zeta(t)} d\zeta'\,\sqrt{\frac{c+\zeta'^2}{1-\zeta'^2}} \tag{2.22}$$

In order to check (2.22) we revert to it in the limits: $E_0\simeq 0$ ($c\gg 1$) and $1\ll E_0\le E_\infty$ ($c\ll 1$).

Let $E_0\simeq 0$. It is easy to verify that

$$t \sim \frac{x_m}{2E_0}\;\arcsin\zeta$$

and

$$\frac{x_m}{\sqrt{2E_0}} = \frac{1}{\beta\,\sqrt{\frac{c}{c+1}}} \overset{c\gg 1}{\longrightarrow} \frac{1}{\beta}$$

i.e. the motion is harmonic with period $2\pi/\beta$.

Let $E_0\simeq E_\infty$. We focus on the asymptotic behavior of the solution, i.e. on $|x|\simeq|x_m|\gg 1$. Let $t=t_0$ be a time such that $x(t_0)\simeq x_m$. In follows that (2.22) can be written

$$\begin{aligned} \sqrt{2\,c\,E_0}\;(t-t_0) \;&\simeq\; [(x_m^2-x(t_0)^2)^{\frac{1}{2}} - (x_m^2-x(t)^2)^{\frac{1}{2}}] \\ &= \sqrt{2}\,x_m\,[(1-\frac{1}{2}\frac{x(t_0)}{x_m}) - (1-\frac{1}{2}\frac{x(t)}{x_m})] = \frac{1}{\sqrt{2}}\,(x(t)-x(t_0)) \end{aligned}$$

where we took account that $c\ll 1$ and $(x_m-x(t_0))/x_m \simeq (x_m-x(t))/x_m \ll 1$. Therefore, as we expect, as long as the particle is faraway from the origin the motion is approximately free.

Since $V'(x)\in\mathcal{C}^1$ it follows that the solution (2.22) exists (and is unique) ; let it be denoted by

$$x(t,E_0) \,=\, x_m(E_0)\;\zeta(t) \tag{2.23}$$

Therefore, by substituting (2.18) and (2.21) in (2.23) we obtain the equation

$$x = x(J,\theta) \tag{2.24}$$

of a canonical transformation.

We notice that the perturbation $f(x,t) = x\ f(t)$, with a periodic f (t is an angle), written in the action-angle variables

$$h_1(J,\, p_t, \theta, t) = x(J,\theta)\ f(t)$$

is, in general, a Fourier series in the action-angle variables, even when f is harmonic.

5. A resonant one dimensional driven oscillator: an integrable problem.

In the previous sections we have introduced the essentials of the Hamiltonian theory helpful to study the dynamics in the region close to the resonance. Here we approach the problem of the resonance using the canonical transformation method of the Hamiltonian perturbation theory. We see that, in the nearly-integrable regime, a resonance of the system (2.14) gives rise to an integrable system except for terms that are small with respect to the perturbation parameter. Because of the dimensionality ($n = 2$) the resonance is simple and one can always find a second independent integral of motion that makes the leading term of the Hamiltonian integrable.

The problem can be stated as follow: for small ε we should find a family of canonical maps $\mathcal{G}_\varepsilon$, depending on ε, that are close to the identity and lead to a problem where the perturbation moves to an higher order with respect to ε (see appendix 2.).

We write again the Hamiltonian (2.14)

$$\mathcal{H}(I,\varphi) = h_0(I) + \varepsilon\, h_1(I,\varphi) \tag{2.25}$$

$I = (I_1,\, p_t)$, $\varphi = (\varphi_1, \nu t)$, and

$$h_0(I) = h(I_1) + \nu\ p_t$$

We suppose the perturbation h_1 in (2.14) is a Fourier polynomial

$$h_1(I,\varphi) = \sum_{|\mu|\le N} f_\mu(I)\ e^{i(\mu\varphi)} \tag{2.26}$$

where $\mu \in \mathbb{Z}^2$. Thus an assumption of the "Poincaré difficulty" (see appendix 2.3) is avoided; so the application of the "averaging principle" (see appendix 2.1) is not excluded. However in section 2. of chapter 3 we will consider a generic analytic h_1 (having a possibly full Fourier series); few analytical considerations are necessary to conclude that the "averaging principle" still holds but in a form that is weaker than that in the "Poincaré difficulty".

The problem is two dimensional, therefore the resonance is necessarily simple. In fact if there is a frequency $\omega(I) = \dot{\varphi}$ that satisfies two indipendent relations of resonance

$$\mu_1\ \omega(I) = \mu_2\ \omega(I) = 0 \qquad\qquad \mu_2 \neq k\,\mu_1$$

k is an integer, then $\omega(I) = 0$.
We suppose that exists a simple resonance, i.e. there is a "resonant manifold" $B = \{I^*\}$ such that $\omega(I^*)\,\mu = 0$, $\mu \in \{k\mu^* \in \mathbb{Z}^2\}$

Non resonant motion.
We consider the nonresonant motion, i.e. we assume the motion of actions occurs so that

$$\mu\,\omega(I) \gg \sqrt{\varepsilon} \tag{2.27}$$

We introduce the canonical transformation $(I', \varphi') = w_\varepsilon(I, \varphi)$, close to the identity,

$$I = I' - \varepsilon \frac{\partial}{\partial \varphi}\mathcal{F} \qquad \varphi' = \varphi - \varepsilon \frac{\partial}{\partial I'}\mathcal{F}$$

(see (17), appendix 2.2), whose generating function is (16), appendix 2.2. It produces a new Hamiltonian $H' = H \circ w_\varepsilon$:

$$\mathcal{H}'(I', \varphi') = h(I') + \varepsilon\,\langle h_1\rangle + \varepsilon^2\, f'(I', \varphi') \tag{2.28}$$

$\langle\cdot\rangle$ is the average in the angles. The Hamiltonian (2.28) is "more integrable" than H; the equation of motion of the action is pushed to ε^2: $\dot{I}' = O(\varepsilon^2)$.

We are going to calculate the explicit form of a canonical transformation that produces (2.28) If the transformation w_ε^{-1} is determined by a flow $\Phi^1_{\varepsilon\mathcal{F}}$, generated by the "Hamiltonian" $\varepsilon\,\mathcal{F}$ then the transformed Hamiltonian $H' = H \circ \Phi_{\varepsilon\,\mathcal{F}}$ can be expressed in the Lie series (see (18), appendix 2.2). The terms of first and second order in ε of the truncated expansion of H' can be easily calculated (see (19), appendix 2.2). They are

$$\begin{aligned} \langle h_1\rangle &= \{h, \mathcal{F}\} + h_1 \\ f' &= \{h_1, \mathcal{F}\} - \frac{1}{2}\{(h_1 - \langle h_1\rangle), \mathcal{F}\} + O(\varepsilon) = \frac{1}{2}\{(h_1 + \langle h_1\rangle), \mathcal{F}\} + O(\varepsilon) \end{aligned} \tag{2.29}$$

respectively. $\mathcal{F}$ is a solution of the basic equation of the perturbation theory (see (22) appendix 2.3); far from the resonance ($|I - I^*| \simeq O(1)$) the solution is (see (24) appendix 2.3)

$$\mathcal{F}(I, \varphi) = \sum_{0<|\mu|<N} \frac{f_\mu(I)}{i\,\mu\,\omega(I)}\, e^{i(\mu\varphi)} \tag{2.30}$$

Thus in the non resonant motion the canonical transformation permits to gain one order in ε; the Hamiltonian (2.28) is integrable (except for the $O(\varepsilon^2)$ remainder). The Hamiltonian (2.28) is called "first order normal form".

We should note that $f' \sim (\mu\ \omega(I))^{-2}$; in fact, in (2.29) the Poisson brackets give rise to derivatives of $\mathcal{F}$ with respect to the actions. Approaching the resonance $I = I^*$, when $\mu\ \omega(I) = O(\varepsilon^{1/2})$, $\varepsilon^2\ f'$, the perturbation of the new Hamiltonian (2.28), becomes as large as the perturbation of the original Hamiltonian H. The transformation of variables with "Hamiltonian" (2.30) is helpful provided that the motion does not occur in a neighborhood of the resonance where $\mu\ \omega(I) \lesssim O(\varepsilon^{1/2})$. This is the reason because, in the presence of only one resonance, the non resonant domain is characterized by (2.27).

The motion close to the resonance.
That is left to do is to investigate the motion inside the single resonance. Let $|I - I^*| \simeq \sqrt{\varepsilon}$; the new perturbation has norm $\varepsilon^2 \| f'\|^2 \sim \varepsilon$ and is as large as the original one.

We have to isolate the resonant term from the $\mathcal{H}'$ and study it separately, i.e. we deal with "the resonant normal form" (adapted to the resonance).

$$\mathcal{H}'(I', \varphi') = h'(I') + \varepsilon\, g(I', \varphi') \,+\, O(\varepsilon^2) \tag{2.31}$$

where

$$g(I', \varphi') \,=\, f_{\mu^*}(I')\, e^{i\mu^*\varphi'}\,,$$

$\mu^*\,\omega(I^*) = 0$. Let us consider $\mu_* \in \mathbb{Z}^2$ such that $\mu^*\,\mu_* = 0$. The linear combination

$$J \,=\, \mu_*\, I' \tag{2.32}$$

is a constant of motion; in fact, from the Hamilton equations it is straightforward to verify that $\dot{I}'$ is parallel to μ^*. Thus we conclude that inside a simple resonance the motion of J decouples and the system is essentially one dimensional. It follows that whenever we deal with a simple resonance the motion is integrable, except for terms of order $O(\varepsilon^2)$.

In the following section we will give another derivation of the one dimensional motion inside a simple resonance. Analogously to the present section, the method eliminates the resonant variables by a canonical transformation; the transformed Hamiltonian is pendulum-like. However there are some significant differences:

- the transformation, which is applied to a frame of reference that rotates with the resonance frequency, is not close to the identity;
- the method can be also applied to perturbations that are full Fourier series;
- the pendulum of a resonance can, in turn, experiences a resonance. The canonical transformation can be iterated so that, at each iteration, the variables of a certain resonance are transformed to the reference system rotating with the frequency of a resonance of the original resonance pendulum; the Hamiltonian in the transformed variables assumes again a pendulum-like form. Therefore this method allows to define, in a straightforward way, a "hyerarchy" of resonances.

The pendulum motion inside a single resonance consists of periodic action oscillations of amplitude $O(\varepsilon^{1/2})$ and period $O(1/\varepsilon^{1/2})$ around the constant J.

5.1 A primary resonance and higher order ones.

In this section we deal with the problem of the resonance in the perturbed oscillator (2.10). We study the dynamics near the resonance; we obtain a Hamiltonian that describes the generic motion of Hamiltonian systems near resonances. We are going to introduce a procedure that has been used in the accelerator dynamics (see [73]) and in the electron cyclotron resonance (see [96]); a similar technique is applied by Chirikov ([21]). The method consists in a canonical transformation to new coordinates that measure the slow oscillations of the variables about their values at the resonance which is an elliptic fixed point of the new phase plane.

Let us consider the two dimensional Hamiltonian (2.14) that we write in the form (2.25):

$$\mathcal{H}(I,\varphi) = h_0(I) + \varepsilon\, h_1(I,\varphi) \tag{2.33}$$

where h_1 is periodic in both φ's,

$$h_1(I,\varphi) = \sum_{\mu} \nu_\mu(I)\, e^{i\mu\varphi} \tag{2.34}$$

where $\mu \in \mathbb{Z}^2$.
A resonance exists and it is given by

$$a\,\omega_1 + b\nu = 0 \tag{2.35}$$

where $\omega_1(I_1) = \partial h_0/\partial I_1$. Here we assume (2.35) to be or a primary resonance or a secondary resonance caused by harmonic frequencies of an oscillating island generated by the primary resonance.

We choose the generating function

$$G = (a\varphi_1 + b\nu t)\, I_1' + \nu t\, I_2' \tag{2.36}$$

that gives the canonical transformation from I, φ to I', φ':

$$\begin{aligned} I_1' &= \frac{1}{a}\, I_1 \\ I_2' &= \frac{b}{a}\, I_1 + p_t \\ \varphi_1' &= a\varphi_1 + b\nu t \\ \varphi_2' &= \nu t \end{aligned} \tag{2.37}$$

In the new frame of reference

$$\dot{\varphi}_1' = a\dot{\varphi}_1 + b\nu \tag{2.38}$$

gives the rate of the slow deviation from the resonance.
We put (2.37) into (2.33) and we obtain

$$\mathcal{H}'(I',\varphi') = h_0'(I') + \varepsilon h_1'(I',\varphi') \tag{2.39}$$

where

$$h_1'(I',\varphi') = \sum_{\mu} \nu_\mu(I')\, e^{\frac{i}{a}(\mu_1\varphi_1' + (\mu_2 a - \mu_1 b)\varphi_2')} \tag{2.40}$$

We make the average over φ_2'; we come to the first order, transformed Hamiltonian:

$$\overline{\mathcal{H}'} = h_0'(I) + \varepsilon\,\overline{h_1'}(I',\varphi_1') \tag{2.41}$$

and

$$\overline{h_1'}(I',\varphi_1') = \sum_{n} \nu_{n\overline{\mu}}(I')\, e^{in\varphi_1'} \tag{2.42}$$

where $\overline{\mu} = (a, b)$. We assume $\mathrm{v}_{\mu} = \mathrm{v}_{-\mu}$, that is accomplished by a change $\varphi_1' \to \varphi_1' + const$. When I' is choosen near the resonance the averaging is well based; in fact we have $\dot{\varphi}_2' \gg \dot{\varphi}_1'$. The averaged Hamiltonian is independent of φ_2. The quantity

$$I_2' = \frac{b}{a} I_1 + p_t \tag{2.43}$$

is an invariant modified by the resonance. Only the resonances with low order $b \geq a$ can vary I_2'. In fact for $b \gg a$ I_2' is a multiple of the unmodified invariant I_1.

In (2.42) the coefficients $\mathrm{v}_{n\overline{\mu}}$ become rapidly negligible as n increases. Therefore we keep only the components $n = 0$, $n = \pm 1$:

$$\overline{\mathcal{H}'} = h_0'(I') \; + \; \varepsilon \, \mathrm{v}_{(0,0)}(I') \; + 2\varepsilon \, \mathrm{v}_{(a,b)}(I') \, \cos\varphi_1' \tag{2.44}$$

Since I_2' is a constant, the Hamiltonian (2.44) gives a one degree of freedom motion in $I_1' - \varphi_1'$ phase space.
The set of fixed points $\{(I_1^0, \varphi_1^0)\}$ is determined by

$$\frac{\partial \overline{\mathcal{H}'}}{\partial I_1'} = 0 \qquad\qquad \frac{\partial \overline{\mathcal{H}'}}{\partial \varphi_1'} = 0 \tag{2.45}$$

The conditions (2.45) are applied and we obtain ($\mathrm{v}_{(a,b)} = \mathrm{v}_{(-a,-b)}$)

$$\begin{aligned} \frac{\partial h_0'}{\partial I_1'} + \varepsilon \frac{\mathrm{v}_{(00)}}{\partial I_1'} + 2\varepsilon \frac{\mathrm{v}_{(a,b)}}{\partial I_1'} \, \cos\varphi_1' = 0 \\ \mathrm{v}_{(a,b)} \, \sin\varphi_1' = 0 \end{aligned} \tag{2.46}$$

We have two stationary point at $\varphi_1^0 = 0$ and $\varphi_1^0 = \pi$. As well at the resonance we note that

$$\frac{\partial h_0'}{\partial I_1'}(I^0) = \frac{h_0}{\partial I_1}(I^0) \, \frac{\partial I_1}{\partial I_1'} + \frac{h_0}{\partial I_2}(I^0) \, \frac{\partial I_2}{\partial I_1'} = \omega_1 \, a + \omega_2 \, b = 0 \tag{2.47}$$

where $I^0 = (I_1^0, I_2')$; hence the first equation of (2.46) is written

$$\frac{\mathrm{v}_{(0,0)}}{\partial I_1'} \pm 2 \, \frac{\mathrm{v}_{(a,b)}}{\partial I_1'} = 0 \tag{2.48}$$

where the plus sign and the minus one correspond respectively to $\varphi_1' = 0$ and $\varphi_1' = \pi$.

Fom the equations of motion of (2.44) we conclude that $\dot{I}_1' = O(\varepsilon \mathrm{v}_{(a,b)})$ and $\dot{\varphi}_1' = O(1)$. It follows that we can get an expansion of h_0' about a resonance I_1^0:

$$h_0'(I_1', I_2') = h_0'(I^0) + \frac{\partial h_0'}{\partial I_1'}(I^0) \, \delta I' \; + \; \frac{1}{2} \, \frac{\partial^2 h_0'}{\partial I_1'^2}(I^0) \, (\delta I')^2 \; + \; O((\delta I')^3) \tag{2.49}$$

where $\delta I' = (I' - I_1^0)$.
We may dismiss the first term, that is a constant, and from (2.47) the second term is zero. Finally we conclude that the motion near a resonance is determined by a pendulum-like Hamiltonian:

$$\delta H \; = \; \frac{1}{2} \, c \, (\delta I')^2 \; - \; u \, \cos\varphi_1' \tag{2.50}$$

The coefficient

$$c = \partial\omega_1(I^0)/\partial I_1' \tag{2.51}$$

is called nonlinearity parameter and

$$u = -2\,\varepsilon\,\mathrm{v}_{(a,b)}(I^0) \tag{2.52}$$

The Hamiltonian (2.50) provides an universal description of the dynamics of a Hamiltonian system close to a resonance.
If $c\,u > 0$ in the plane $I_1' - \varphi_1'$ there are both elliptic (at $\varphi_1' = 0$) and hyperbolic (at $\varphi_1' = \pm\pi$) fixed points. Futhermore the trajectories $\delta H = 0$ (sepratrices) divide the space into regions where trajectories possess different features.

When $\delta H < 0$ the phase of the oscillator varies between restrict limits (phase oscillations). The frequency of the small phase oscillations is

$$\omega_{ph} = (c\,u)^{1/2} \sim |\mathrm{v}_{(a,b)}(I^0)\,\varepsilon|^{1/2} \tag{2.53}$$

The frequency is small with respect to the frequency in the plane $I_2' - \varphi_2'$:

$$\omega_{ph} \ll \omega_2 = O(1) \tag{2.54}$$

As well the period of a bound motion becomes infinitely large as the separatrix is approached. The amplitude of the phase oscillations too is controlled by ε:

$$\delta I_1' = O(|\varepsilon\,\mathrm{v}_{(a,b)}(I^0)|^{1/2}) \tag{2.55}$$

We come to the important result that the topology of phase space is changed in the vicinity of a resonance; an unperturbed trajectory $I = I^0$ is substituted by a pendulum, complete with libration, separatrix and rotation motion.

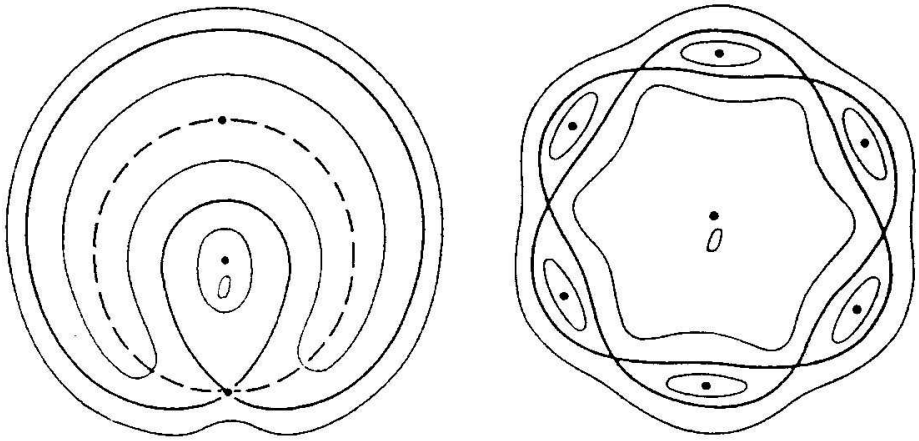

Figure 2.2: Motion near a primary resonance. The dashed line is the unperturded orbit with $I = I^0$. The thick line is the separatrix of the phase oscillation. Left: $a = 1$ $b = 1$. Right $a = 6$ $b = 1$

5.2 Higher order resonances

New resonances can occur between harmonics of ω_{ph} (see (2.53)), the phase oscillation in the plane $I_1' - \varphi_1'$, and the frequency ν of the driver. This is possible as ε, the amplitude of the driver, is not sufficiently small.
We consider a new Hamiltonian using the perturbation theory for the motion near the elliptic point of the primary resonance:

$$\mathcal{K} = K_0 + \varepsilon_1 k_1 \tag{2.56}$$

where K_0 and k_1 are constructed in the two items just below. k_1 takes into account the effect of a secondary resonance. Hamiltonian (2.56) has a form similar to (2.33): with ε_1 as a new ordering parameter. Therefore we may apply the method of section (5.1) to remove the secondary resonance.
Before using (2.56) we discuss how K_0 and k_1 are determined. We remove the prime from the notation of subsection 5.1.

- (*Hamiltonian (2.50): transformation to the action-angle* (J_1, θ_1))
  We use the perturbation theory for the motion near the elliptic point $(0, 0)$ of the primary resonance; the pendulum Hamiltonian (2.44) (in the variables $\delta I_1, \delta\varphi_1$, Hamitonian (2.50)) is transformed to an action-angle variables J_1, θ_1 of the unperturbed motion of the pendulum and we obtain the new Hamiltonian to first order (see appendix [**?**])

$$K_0(I_1, J_1, I_2) = h_0(I_1, I_2) + \omega_{ph} J_1 - \frac{\varepsilon}{16} c J_1^2 + O(\varepsilon^2) \tag{2.57}$$

  where c is defined in (2.51).
  In this approximation the average over φ_2 is valid; hence K_0 is independent on the angles, so that J_1 and I_2 are constants of motion.

- (*secondary resonance Hamiltonian: expansion about the elliptic point* $(I_1, I_2, \varphi_1, \varphi_2)$ *and transformation to the action-angle variables* (J_1, θ_1))
  In order to take into account the effects of the secondary resonace we reintroduce the part of Hamiltonian (2.40) that has been ignored in the average over θ_2, i.e. the Fourier expansion (2.40) except for the resonant term

$$\tilde{h}_1(I, \varphi) = h_1(I, \varphi) - \overline{h_1}(I_1, \varphi_1) = \sum_{\mu_2 a - \mu_1 b \neq 0} \nu_\mu(I)\, e^{\frac{i}{a}(\mu_1 \varphi_1 + (\mu_2 a - \mu_1 b)\varphi_2)} \tag{2.58}$$

  and we expand it about the elliptic point $(I_1, I_2, 0, \varphi_2)$ in the action-angle variables I_1, φ_1

$$\tilde{h}_1 = \sum_{\mu_2 a - \mu_1 b \neq 0} \nu_\mu(I_1 + \delta I_1, I_2)\, e^{\frac{i}{a}(\mu_1 \delta\varphi_1 + (\mu_2 a - \mu_1 b)\varphi_2)} \tag{2.59}$$

  where $\delta I_1, \delta\varphi_1$ describe the libration motion of the pendulum (2.50).

  We move to the action-angles variables J_1, θ_1 of the unperturbed pendulum motion and keep the lowest order for the motion $\delta I_1, \delta\varphi_1$. By the formula[1] that gives the

[1] The transformation equations from the action-angle variables (I, θ) to the variables p, q in the harmonic oscillator

$$H = \frac{c}{2} p^2 + \frac{u}{2} q^2$$

transformation from action-angle variables to the variable $\delta I_1'$ in the harmonic oscillator the transformed Hamiltonian of (2.59) is

$$k_1 = \sum_{\mu_2 a - \mu_1 b \neq 0} \nu_\mu(I_1, I_2)\, e^{\frac{i}{a}(\mu_2 a - \mu_1 b)\varphi_2}\, e^{\frac{i}{a}\,\mu_1\,(4c/u)^{1/4}\,J_1^{1/2}\,\sin\theta_1}. \tag{2.61}$$

c and u are defined in (2.51) and (2.52); δI_1 is neglected in the coefficient ν_μ since $\delta I_1 = O(\varepsilon^{1/2})$ (see (2.55)).
The second exponential is expanded:

$$k_1 = \sum_{\mu_2 a - \mu_1 b \neq 0,\ n} k_{\mu,n}(I_1, J_1, I_2)\, e^{i(n\theta_1 + \frac{1}{a}(\mu_2 a - \mu_1 b)\varphi_2} \tag{2.62}$$

and

$$k_{\mu,n}(I_1, J_1, I_2) = \nu_\mu(I_1, I_2)\, g_n(\mu_1/a\,(4c/u)^{1/4}\,J_1^{1/2}) \tag{2.63}$$

g_n is the Bessel function of order n.

Subsequently we write θ_2 for $\varphi_2 = \nu t$ and J_2 for $I_2 = p_t$.
We consider the Hamiltonian (2.56) explicitely showing the variables:

$$\mathcal{K} = K_0(J) + \varepsilon_1\, k_1(J, \theta) \tag{2.64}$$

where we set $J = (J_1, J_2)$ and $\theta = (\theta_1, \theta_2)$; we leave out the 'parameter' I_1.
Resonances of higher order between θ_1 and θ_2 can arise in k_1. It follows that the average over θ_2 in (2.64) is not zero.
We assume a resonance occurs:

$$a_1\,\omega_1 + b_1\,\nu = 0 \tag{2.65}$$

where $(a_1, b_1) \in \mathbb{Z}^2$

$$\omega_1 = \frac{\partial K_0}{\partial J_1} = \omega_{ph} = O(\varepsilon^{1/2}) \tag{2.66}$$

as established in (2.57) and

$$\nu = \frac{\partial K_0}{\partial J_2} \quad (= O(1))$$

To remove resonance (2.65) we proceed as in section (5.1).

We apply a canonical transformation from J, θ to (J', θ'), that eliminates the action J_2. We choose the generating function

$$G = (a_1\,\theta_1 + b_1\,\theta_2)\, J_1' + \theta_2\, J_2' \tag{2.67}$$

The new coordinates correspond to a rotating frame where

$$\theta_1' = a_1\,\theta_1 + b_1\,\theta_2 \tag{2.68}$$

---

are given by

$$\begin{aligned} q &= (4c/u)^{1/4}\, I^{1/2}\, \sin\theta \\ p &= (4u/c)^{1/4}\, I^{1/2}\, \cos\theta \end{aligned} \tag{2.60}$$

is the 'slow' variable. The average is taken over the 'fast' phase θ_2' $(= \nu t)$.
After the transformation the exponent in perturbation (2.64) comes to the form

$$i\frac{n}{a_1}\theta_1' + i(-n\frac{b_1}{a_1} + \mu_1\frac{b}{a} + \mu_2)\theta_2'$$

Averaging over θ_2' in the transformed Hamiltonian only the terms with

$$-nb_1 + \mu_1\frac{a_1 b}{a} + \mu_2 a_1 = 0 \tag{2.69}$$

survive. In (2.69) the second term is an integer; thus there are $k, l \in \mathbb{Z}$ such that

$$\mu_1 = ka \qquad n = la_1$$

By fixing n and μ_1 in (2.69), μ_2 is determined.
Finally, performing the average over θ_2' in the transformed Hamiltonian, (2.64) becomes

$$\overline{\mathcal{K}} = K_0(J(J')) + \varepsilon_1\,\overline{k}_1(J', \theta_1') \tag{2.70}$$

K_0 is the same as (2.57) with the old variables expressed as functions of the new actions.

$$\overline{k}_1(J', \theta_1') = \sum_{l,k}\overline{k}_{lk}(J')\,e^{il\theta_1'} \tag{2.71}$$

and

$$\overline{k}_{lb_1-2kb\neq 0}(J') = \nu_{ka,(lb_1-kb)}(J(J'))\,g_{la_1}(k\,(4c/u)^{1/4}\,J_1(J')^{1/2}) \tag{2.72}$$

The motion $J_1 - \theta_1'$ of Hamiltonian (2.70) is integrable. Because after averaging $\mathcal{K}$ does not depend on θ_2' the new (adiabatic) invariant corresponding to the secondary islands oscillations is

$$J_2' = \frac{a_1}{b_1}J_1 + J_2 \tag{2.73}$$

It is helpful to clear up an estimate of the strength of the secondary resonance.
We are interested in the harmonics for $l = 1$, $k = 1$; as well we choose $b_1 = 1$, i.e. from the resonance condition (2.65) we consider the resonance with the frequency of the driver ν. Since $\omega_{ph} = O(\varepsilon^{1/2})$ it follows that $a_1 = O(\varepsilon^{1/2})$.
Comparing (2.70) with (2.44) we may straight give the amplitude and the frequency of the oscillations in $J_1' - \theta_1'$; we have to replace ν_μ with (2.72) We take into account (2.55)

$$\delta J_1' = O(\varepsilon_1^{1/2}\,|\overline{k}_{11}(J')|^{1/2}) = O(\varepsilon_1^{1/2}\,|\nu_{11}(J')|^{1/2}\,|g_{a_1}(4c/u)^{1/4}\,J_1^{1/2}|^{1/2}) \tag{2.74}$$

and from (2.53) it is given

$$\delta\omega_1 \sim \omega_{ph}\,|g_{a_1}(4c/u)^{1/4}\,J_1^{1/2}|^{1/2} \tag{2.75}$$

We should focus on the amplitude of the perturbation that is proportional to $g_{a_1}((4c/u)^{1/4}\,J_1^{1/2}))$.
We note that (see 2.60)

$$(c/u)^{1/4}\,J_1^{1/2} \sim \delta I_1' = O(\varepsilon^{1/2})$$

the Bessel function can be expanded for small values of the argument

$$g_n((4c/u)^{1/4}\, J_1(J')^{1/2}) \sim \{(c/u)^{1/4}\, J_1^{1/2}\}^{a_1/2}\, (a_1!)^{-1} \sim (a_1!)^{-1}\, a_1^{-a_1/2} \tag{2.76}$$

We conclude that the ways the secondary and primary resonances depend on ε are very different. For small ε the strength of the primary resonance is related weakly on ε, as $\varepsilon^{1/2}$. On the other hand the amplitude and frequency of the secondary resonance depend strongly on $a_1 \sim \varepsilon^{1/2}$ as (2.76) involves. A secondary island becomes rapidly negligible with respect to a primary one for small ε and may be as important as a primary resonance for relatively large ε.

6. KAM theorem.

In this section we introduce some essentials of the KAM theory, a fundamental result of the Hamiltonian theory. Our aim is to supply the necessary "machinery" suited to a "descriptive" analysis of the phase space structures of a perturbed system. The KAM theorem provides a deep characterization of the invariant structures. Therefore it is an essential framework for any study that attempts to give a "geometric" characterization of the numerical results concerning the dynamics of perturbed oscillators.

The theorem is an understanding of the non-perturbative meaning of the perturbation theory. In particular, as seen in the previous sections, in a typical investigation of a perturbation theory the role of the neglected terms can be estimated for a "finite" time. The approach to the stability problem developed by the KAM theory is very different and it establishes stability results for an "infinite" time.

The crucial idea of the KAM theory is to consider invariant tori rather than trajectories; the invariant tori are important landmarks that organize the motions of the system. As well rather than stability of trajectories a perturbation of the tori is studied; notably many of the mechanisms of instability use as ingredients some invariant tori.

We know that an oscillator with $1 + 1/2$ degrees of freedom is a Hamiltonian system with two degrees of freedom (see (2.13)). Therefore we consider a system with an Hamiltonian $H(x_1, p_1, x_2, p_2)$. The Hamiltonian is constant on solution curves; hence, the Hamiltonian flow is essentially three dimensional and, for a given h, its manifold is $H = h$. We can construct a two dimensional cross section and define an associate Poincaré map to study the dynamics of the system. We are going to make more precise this remark.

We may express the couple of coordinates x_2, p_2 as angle-action variables through an invertible canonical change of coordinates

$$\begin{aligned} x_2 &= x_2(I, \theta) \\ p_2 &= p_2(I, \theta) \end{aligned} \tag{2.77}$$

under which the Hamiltonian becomes (we drop the subscripts)

$$H(x, p, I, \theta) = H(x_1, p_1, x_2(I, \theta), p_2(I, \theta)) \tag{2.78}$$

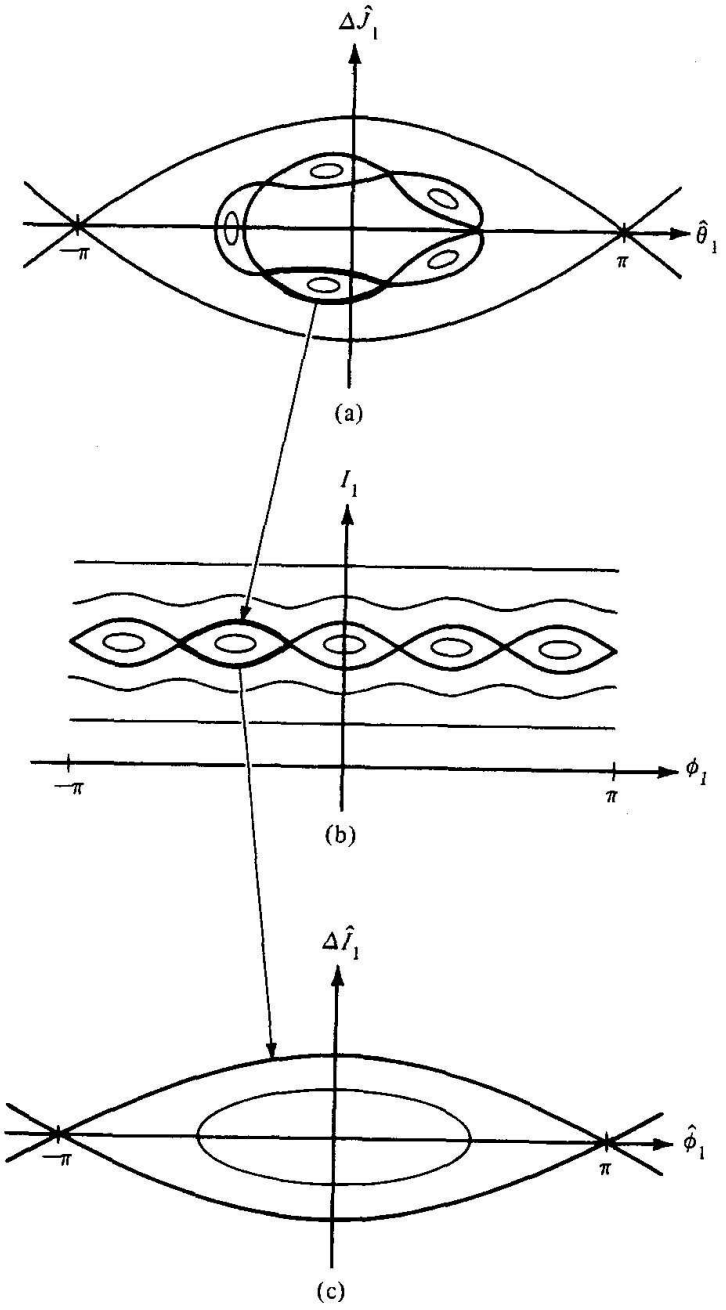

Figure 2.3: Motion near a secondary resonance. (a) The secondary islands in thre original coordinates which appears when $a_1 = 5$, $b_1 = -1$. (b) Transformation to action-angle coordinates of original, libration motion. The resonant value of the action is obtained from $5\,\omega_1(I_1) = \nu$. (c) Transformation to a rotating coordinate system associted with the secondary librations. It is obtained the phase space of a pendulum.

We assume that $\partial H/\partial I \neq 0$ in some region of the phase space. Therefore the (2.78) can be inverted and I can be expressed in terms of x, p and θ in the manifold $H = h$

$$I = -K(x, p, \theta, h) \tag{2.79}$$

As well since $\dot{\theta} = \partial H/\partial I \neq 0$ we can eliminate the explicit dependence on time and the equations of motion assume the form[2]

$$\begin{aligned} x' &= \frac{dx}{d\theta} = \frac{\partial K}{\partial p}(x, p, \theta; h) \\ p' &= \frac{dp}{d\theta} = -\frac{\partial K}{\partial x}(x, p, \theta; h) \end{aligned} \tag{2.80}$$

where $(x, p) \in D \subset \mathbb{R}^2$ and $\theta \in S^1 \equiv [0, 2\pi]$ and the assumption $\partial H/\partial I \neq 0$ is valid in $D \times S^1$. Finally, for any Hamiltonian system with two degrees of freedom, in a phase space domain where the "non-degeneracy condition" $\partial H/\partial I \neq 0$ holds, we can take a cross section

$$\Sigma_{\theta_0} = \{(x, p, \theta = \theta_0) \;\; (x, p) \in D \;\; \theta_0 \in S^1\}$$

and the solutions of (2.80) ($H = h$ is fixed) determine the Poincaré map

$$P_0 \; : \; \Sigma_{\theta_0} \longrightarrow \Sigma_{\theta_0} \tag{2.81}$$

The system with Hamitonian K is called "reduced Hamiltonian system" of the system with Hamiltonian H. We notice that in (2.13), for $\varepsilon \neq 0$, $H_0 = h$

$$I = p_t = (h - (p^2/2 + V(x)))\, \nu^{-1} \qquad \theta = \nu t \qquad \partial H_0/\partial p_t = \nu \neq 0$$

Consider a system with a Hamiltonian of the same form as (2.13) for $\varepsilon \neq 0$ ($\nu > 0$)

$$H^\varepsilon(x, p, \theta, I) = F(x, p) + \nu\, I + \varepsilon\, H^1(x, p, \theta, I) \tag{2.82}$$

where $F(x, p) = p^2/2 + V(x)$ and $H^1 = -f(x, \theta)$. The equation $H^\varepsilon = h$ can be trivially solved for I [3]

$$-I = K^\varepsilon(x, p, \theta; h) = \nu^{-1}\,(F(x, p) - h) - \varepsilon\,\nu^{-1}\, f(x, \theta) \equiv K^0(x, p; h) + \varepsilon\, K^1(x, \theta) \tag{2.83}$$

We know that the system F has a region of the phase plane that is filled with periodic orbits: each orbit α has an energy $F(x, p) = h_\alpha$ and a period which continuously depends on h_α. It follows that for any orbit α the system K^0 has a closed orbit, connected to α, which has an energy

$$K^0(x, p; h) = \nu^{-1}\,(h_\alpha - h) = k_\alpha$$

and a period T_α which varies continuously with k_α.

[2] We should take into account that

$$x' = \frac{\dot{x}}{\dot{\theta}} = \frac{\partial H/\partial p}{\partial H/\partial I} \qquad p' = \frac{\dot{p}}{\dot{\theta}} = -\frac{\partial H/\partial x}{\partial H/\partial I}$$

and differentiating (2.78), by means of (2.79),

$$\frac{\partial H}{\partial x} - \frac{\partial H}{\partial I}\,\frac{\partial K}{\partial x} = 0 \qquad \frac{\partial H}{\partial p} - \frac{\partial H}{\partial I}\,\frac{\partial K}{\partial p} = 0$$

[3] In a more general case where H^1 depends on I, "for small ε" the inverse function K of (2.79) can be computed as a power series in ε [48].

Since the system K^0 is integrable therefore each motion is quasiperiodic (see section 2.)[4] and exists a canonical transformation $(p, x) \to (J, \varphi)$ such that the Poincaré map, associated with K^0, can be written

$$P_0 : \ (J, \varphi) \quad \longrightarrow \quad (J, \varphi + 2\pi\, \lambda(J)) \tag{2.85}$$

where $\lambda(J) = T_\alpha/2\pi$, i.e. J parametrizes the continuous family of invariant closed curves of K^0 and, in the curve with period T_α (and action J), the trajectory of P_0

a. visits only a finite number of "periodic" points whenever $T_\alpha/2\pi \in \mathbb{Q}$,

b. otherwise the trajectory densely fill out the curve.

The orbits of *a*. are exceptional, that is they form a set of measure zero.

The perturbed system with Hamiltonian (2.83) defines a Poincaré map P_ε that can be written ("twist mapping")

$$(J, \varphi) \xrightarrow{P_\varepsilon} (J + \varepsilon\, f(J, \varphi, \varepsilon), \varphi + 2\pi\, \lambda(J) + \varepsilon\, g(J, \varphi, \varepsilon)) \tag{2.86}$$

where f and g are periodic with respect to φ; P_ε

i) preserves the volume of the phase space;

ii) does not preserve neither the energy nor the invariant curves of K^0.

A nice situation would be the existence of a canonical transformation

$$(J, \varphi) = \mathcal{C}_\varepsilon(J', \varphi', \varepsilon) \quad , \tag{2.87}$$

close to the identity, i.e.

$$|J' - J| = O(\varepsilon) \qquad\qquad |\varphi' - \varphi| = O(\varepsilon) \tag{2.88}$$

such that the transformed Poincaré map $P_\varepsilon \circ \mathcal{C}_\varepsilon$ has form (2.85). In this case each curve $J(t)$ would survive and would be a small, continuous deformation of an invariant closed curve $J'(t) = J'(0)$; as well, according to (2.88),

$$|J(t) - J(0)| = O(\varepsilon) \qquad \forall t \tag{2.89}$$

Unfortunately we can find counterexamples for which this situation is not verified; in particular, we will see in the next chapter that in the motion inside a resonance the transformation $\mathcal{C}_\varepsilon$ cannot be found.

Actually the KAM theorem [63, 5, 6, 79] asserts that the previous prospective is not far away from the truth. We state the theorem in the particular context of the two-dimensional mappings [104]:

[4] i.e. there exists a system of coordinates (J, φ) such that any motion can be written

$$(J, \varphi) \longrightarrow (J, \varphi + \lambda(J)\, \theta) \tag{2.84}$$

where $\theta = \nu t \ mod(2\pi)$.

Theorem 1 (KAM theorem) *Let $\mathcal{S}$ be the phase space domain where the maps are defined. If the Hamiltonian K^ε is*

- *analytic in a suitable complex domain [104],*
- $\lambda'(J) \neq 0$ *and*
- ε *is sufficiently small*

then there exist

- *a canonical transformation (2.87),*
- *a map $\mathcal{P}$ of the form (2.85) and*
- *a set $\mathcal{S}_\varepsilon \subset \mathcal{S}$ of large Lebesgue measure μ, i.e. $\mu(\mathcal{S} \setminus \mathcal{S}_\varepsilon) \to 0$ for $\varepsilon \to 0$,*

such that, except for the points in $\mathcal{S} \setminus \mathcal{S}_\varepsilon$,

$$P_\varepsilon \circ \mathcal{C}_\varepsilon = \mathcal{P} \tag{2.90}$$

For initial data in $\mathcal{C}_\varepsilon(\mathcal{S}_\varepsilon)$ the map P_ε behaves as if it were integrable. Therefore

- the set of closed, invariant curves of P_ε (i.e. the "tori" of the original perturbed system (2.82)) covers the domain $\mathcal{C}_\varepsilon(\mathcal{S}_\varepsilon)$ of positive measure whose complement set has a measure that tends to zero as $\varepsilon \to 0$;
- by taking into account of 2.89 each invariant curve of P_ε is close to an invariant curve of the unperturbed system;
- from numerical experiments it follows that the "more irrational" $\lambda(J)$ is the more robust the related closed curve J appears. In section 3. of chapter 3 we will consider what happens to the curves with rational $\lambda(J)$, i.e. the "resonant" tori.

The persistence of sets of invariant closed curves has consequences for the "stability" of motion; this aspect of the KAM theory has major relevance in our investigation on the resonant dynamics of oscillator (2.82), through two dimensional maps. The system (2.82) has two degrees of freedom; each energy manifold $H^\varepsilon = h$ is three-dimensional. The family of two dimensional tori $J' = cost$, which are preserved for $\varepsilon \neq 0$, can divide the energy manifold into disconnected, finite components We know that for initial data in $\mathcal{S}_\varepsilon$ the motion is stable, for all times (see (2.89)). On the other hand for initial data in $\mathcal{S} \setminus \mathcal{S}_\varepsilon$ the motion is trapped in a disconnected component since torus surfaces cannot be crossed; hence the perturbed solutions cannot wander arbitrarily far in phase space and still satisfies a condition of stability as (2.89).

7. Numerical results

We are interested in studying the changes of the phase space pattern of the oscillator

$$H = 1/2\dot{x}^2 + \omega_0^2 V(x) + \varepsilon f(t) = H_0 + \varepsilon f(t)$$

where

$$V(x) = \frac{6/5\, x^2}{12/5 + x^2} \tag{2.91}$$

and $f(t) = \sin(\nu t)$
Numerical investigations are performed as ε and ν are varied.
We calculate some Poincaré sections that allow us to follow the KAM surfaces when they change shape, size and are destroyed. Some possible resonances modify the topology of the phase space in places whose size and position depend on ε and ν. Since we deal with a periodic driver we may restrict the inspection in the region $[0,\ 2\pi/\nu] \times \mathbb{R}^2$. This is the same to set a plane Γ by fixing a time $0 \le t_0 \le 2\pi/\nu$ and to calculate the Poincaré map

$$P \ : \Gamma \longrightarrow \Gamma \qquad (p_n, x_n) \mapsto (p_{n+1}, x_{n+1}) \tag{2.92}$$

where $p_k = p(t_k)$ and $x_k = x(t_k)$ and

$$t_k = t_0 + k\, 2\pi/\nu \quad k \in \mathbb{Z} \tag{2.93}$$

We choose $t_0 = \pi/(2\nu)$, i.e. the time at which the fast oscillating component of the velocity[5] would be zero.
In order to obtain a Poincaré section we start from an uniform distribution of initial conditions and for each orbit we mark 200 iterations.
The mapping is effective to study the relevant features of the dynamics in the various regions of the phase spaces. We can observes the effects of resonances, the splitting of separatrices and the appearance of complicated structures that can give rise to irregular behavior. We consider the "effective" frequency $\omega_0(e) = (2\pi)/T(e)$ of a bound motion with energy $H_0 = e$ and period $T(e)$ of the unperturbed oscillator.
The function $\omega_0(e)$ is continuous and, in connection with potential (2.91), the function $\omega_0(e)$ is decreasing as e increases in $[0, 6/5\,\omega_0]$. As well it is straighforward to note that $\omega_0(e) \to \omega_0$ as $e \to 0$ and $\omega_0(e) \to 0$ as $e \to 6/5\,\omega_0$. We determine $\omega_0(e)$ for the unperturbed oscillator defined by (2.91).

We consider orbits that have a fixed initial position: $x(0) = 0$ and a set of initial velocity v_0. We introduce a multivalued map W that connects v_0 to the set of energy values $H_0(t_k)$ of the orbit

$$W : \ v_0 \longrightarrow H_0(t_k) \quad 0 \le k \le 200 \tag{2.94}$$

where the unperturbed energy values $H_0(t_k)$ are computed at a set of instants t_k defined by (2.93).

The numerical integration of the problem (2.91), for various values of ε and ν, determine Poincaré maps which display a typical pattern where

[5] i.e. the velocity of the driven solution in the linear approximation.

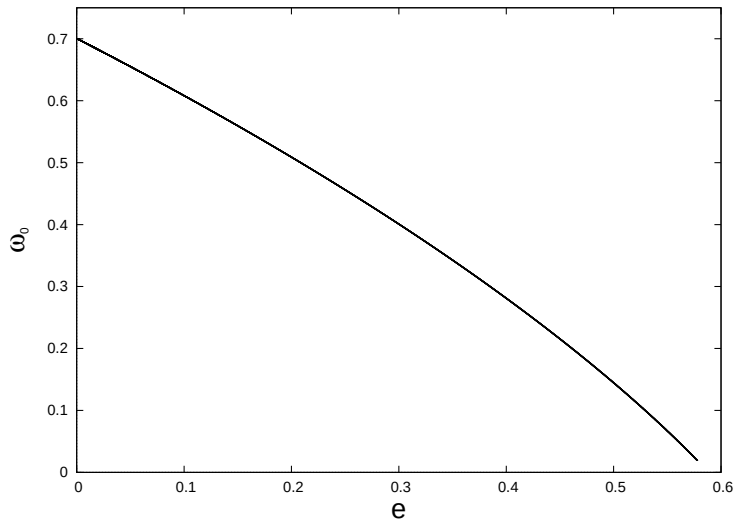

Figure 2.4: "Effective" frequency of the unperturbed oscillator 2.91

- a bounded area is filled with KAM curves that turn around an elliptic point ("KAM islands") (see figs. 2.5, 2.6 (a) and 2.8 (a))

and, outside the KAM area,

- some bound orbits remain close to invariant curves and their points are distributed over a strip surrounding the KAM area (see fig. 2.6 (a));
- some other orbits are more erratic and can leave away from their initial points (see fig. 2.7 (b));
- some orbits run away asymptotically, soon at the beginning, approaching the escape velocity (see fig. 2.8 (b) for $v_0 \in [1.4, 1.5]$, the potential depth is 0.588).

In addition, whenever a resonance takes place the topology of some regions of Γ is modified. It may happens that elliptic and hyperbolic fixed points are created; consequently new invariant curves wind around the first ones and new separatrices converge in the second ones. Otherwise a resonance involves the breaking of invariant structure outside a KAM pattern.

We may compare the behavior of W with facts and features of the structures in the Poincaré section

- We consider a motion on a KAM curve, with initial v_0 (see figs. 2.6 (b) and 2.8 (b)). If the motion is quasiperiodic then W makes v_0 to correspond to an interval of energy values. On the other hand this interval is splitted in many subintervals whenever the rotation number of the invariant curve is ”less irrational”. When the motion is periodic the energy interval becomes a discrete set of values; in particular the interval of energy degenerates to a point with relation to a fixed point (of course it is unlikely to observe a hyperbolic point.)

- Whenever a resonance occurs the energy interval of W varies discontinuously as v_0 crosses the resonance (see fig. 2.6 (b), resonance $2:5$ and fig. 2.8 (b), resonance $1:18$).

The function $\omega_0(e)$ allows to arrange an approximate resonance condition

$$m\omega(e) = n\nu \tag{2.95}$$

that provides, at least for small ε, a rough tool to establish the occurrence of a resonance and to determine the order of the resonance, i.e. the integers m, and n.
In fact every time the function W displays a discontinuity we may estimate the value of the energy e, at which the discontinuity occurs, and then determine $\omega(e)$ through fig. 2.4. By using (2.95) we estimate the pair m, n; in order to do this we also count the number of elliptic points, i.e. the number of islands, at the resonance.

We apply this procedure to some particular instance. Even though it is an approximate technique, the property related to the unperturbed system, i.e. the 'effective' frequency $\omega(e)$, is still reliable even for large driver amplitude.

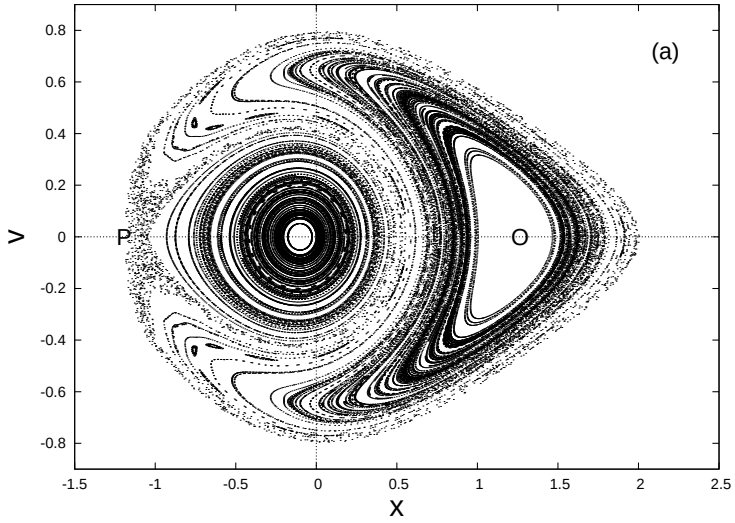

Figure 2.5: Primary resonance for $\varepsilon = 0.05$ and $\nu = 0.5$.

7.1 Absorption of energy for large laser field.

In chapter 1 we dealt with the problem of the interaction between a short, intense laser and a dense plasma. Numerical experiments show clear evidence for the role played by collective, resonant motions. It is observed that a large absorption of energy occurs whenever a condition of "sincronization" ("resonance" condition) is established between the period of the driver and the period of the oscillation motion of charges in collective, space charge fields. These

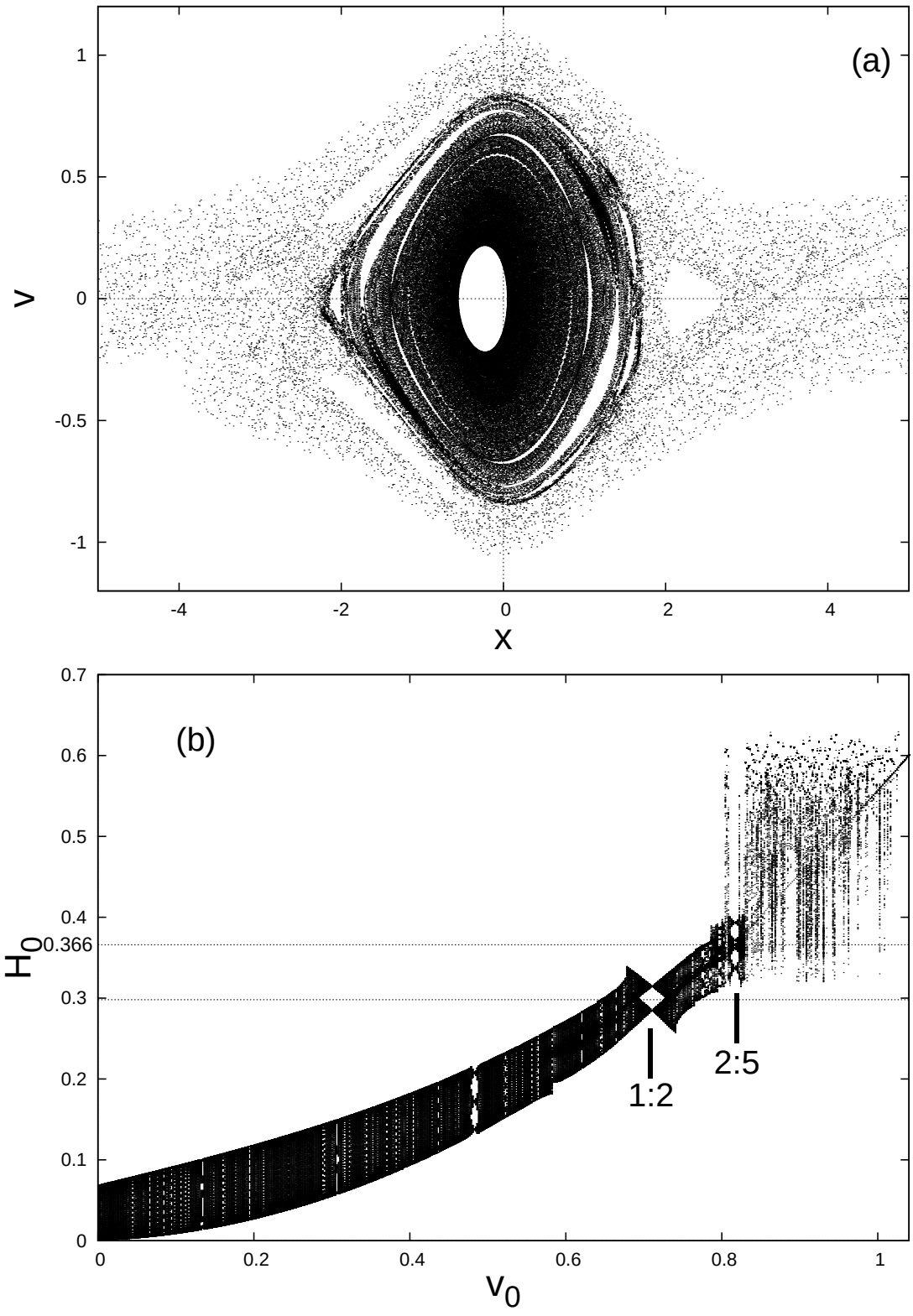

Figure 2.6: Primary resonance for $\varepsilon = 0.1$ and $\nu = 0.8$. (a) Poincaré map: note the two "pendulum-like" structures connected with the resonance $1:2$; (b) pattern of the map W.

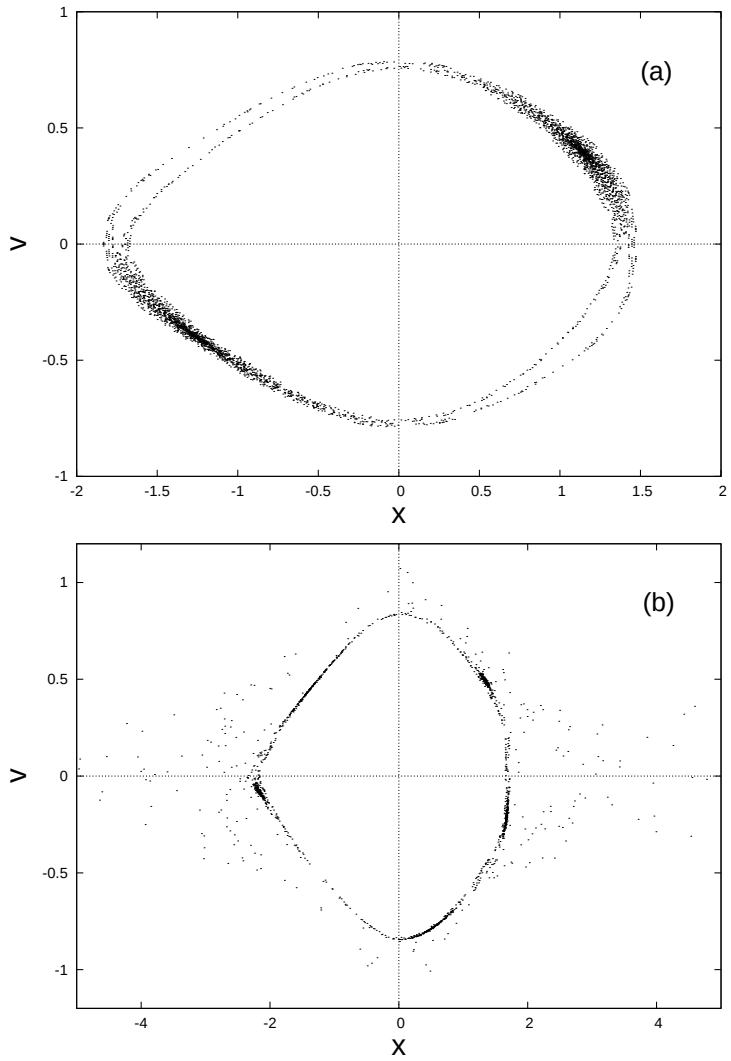

Figure 2.7: Primary resonance for $\varepsilon = 0.1$ and $\nu = 0.8$. Orbits in a neighborhood of the resonant curve $1:2$ (a) and the resonant curve $2:5$ (b)

observations motivate the choice of a driven, nonlinear oscillator with a low number $(1+1/2)$ of degrees of freedom as a model fit to describe the mechanism of coupling in both laser-cluster and laser-solid target interactions.

The "rigid spheres model" [85, 69]

$$\ddot{x} - \varepsilon\, e(t) = -\beta^2\, sgn(x) \begin{cases} x - 9/16\, x^2 + 1/32\, x^4 & |x| \leq 2 \\ x^{-2} & |x| > 2 \end{cases} \tag{2.96}$$

where $x \in \mathbb{R}^6$, describes the interaction of a cluster with a high intensity laser field, so it gives an account of the following effects:

(a) the initial configuration is the neutral cluster. By removing eletrons from their 'parents' ions (inner ionization), the fields create charge states so high that the restoring

[6] i.e. we consider solutions with zero angular momentum

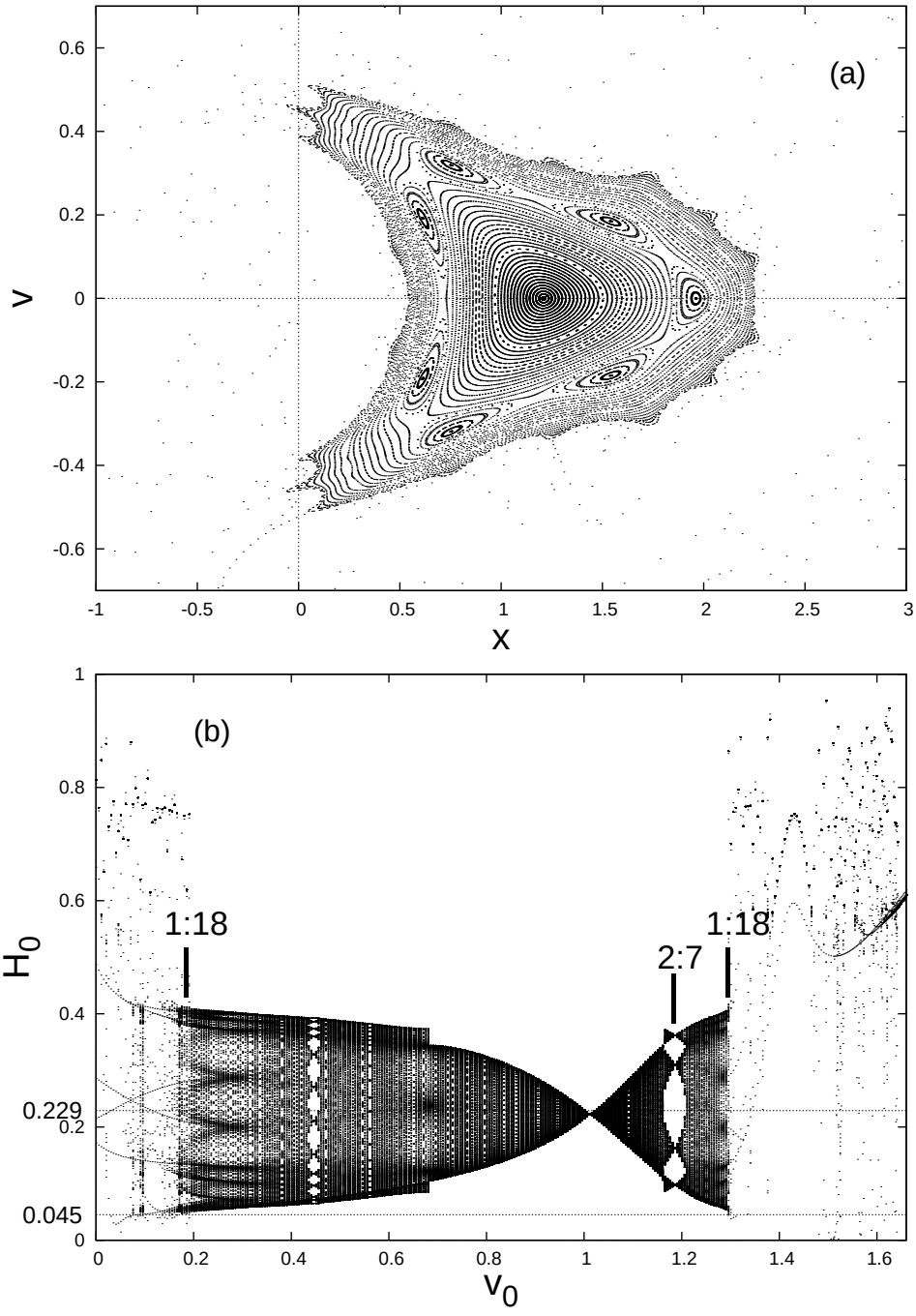

Figure 2.8: Primary resonance for $\varepsilon = 1$ and $\nu = 0.8$.

force has a frequency of small oscillations ω_{Mie} (Mie frequency) that exceeds the driver frequency (see fig. 1.5 of chapter 1).

(b) After the inner ionization the electrons are still bound to the cluster. As the laser amplitude increases the electrons absorb energy from the laser and may leave the cluster (outer ionization). The laser field, represented by $\varepsilon\, e(t)$ is large. Hence the motions, represented by equation (2.96), of the electron oscillations in the anharmonic potential

of the restoring force can become so large that the oscillation period approaches the laser period; that is the electrons that contribute to the outer ionization pass through a resonance.

On the other hand

$$\ddot{x} + \beta^2 x/(1+x^2)^{1/2} = \varepsilon\, e(t) \tag{2.97}$$

is the model of collisionless absorption on a stratified, overdense plasma [87]; it describes the resonance experienced by a single layer.
For the typical laser frequencies the small oscillations frequency β is larger than 1. Under a weak driver, the period $T(a) = \frac{2\pi}{\beta}\,(1+a^2)^{1/2}$ of the layer oscillation motion with amplitude $a \ll 1$ remains less than the driver period ($= 2\pi$), i.e. the motion follows in phase the applied driver $e(t)$. Under a strong driver, a becomes large and the period $T(a) \simeq (4/\beta)\, a^{1/2}$ increases and can meets the laser period.

Both models can be put into the canonical form with a Hamiltonian

$$H(\dot{x}, x, t) = \dot{x}^2/2 + \beta^2\, V(x) \; - \varepsilon\, x\, e(t) \tag{2.98}$$

where V is a potential well with only one critical point.

The perturbative analysis of the previous sections, describes the resonant motions of (2.96) and (2.97) only for drivers small enough. Actually it is not fit for explaining the amount of absorbed energy for the regime of driver amplitudes considered in the previous papers[7]. According to (2.55) we expect that the amplitude of the action oscillations, which is linked to the absorbed energy, to be $O(\varepsilon^{1/2})$. Whereas in [85, 69], as the charge crosses the resonance, the absorbed energy jumps from negligible values to $10^4 - 10^5$ times the ponderomotive potential[8]. In [87] it is measured that, crossing a resonance, the energy absorbed by a layer can be some tens times higher than the energy gained if the resonance does not occur[9].

We discuss some qualitative facts on the phase space pattern of (2.98) with a resonance and for large driver amplitude. Unlike the analysis provided in [85, 69] and [87] where the driver is a harmonic function times a function with finite length we use a harmonic driver; this is of no consequences to the mechanism of crossing of the resonance.
We perform some numerical computations on model (2.96); we choose the driver $e(t) = \sin(0.5t)$.

An important aspect is that for large strength driver the resonance works as a threshold. Whenever the motion takes place below the resonance it appears slightly deformed with respect to the near integrable case: its energy is not conserved but varies in a little interval close to the value for $\varepsilon = 0$. On the other hand the resonance can drastically modify the

[7] In these papers the anahrmonic resonances that are considered require that the driver has to produce large oscillations in strong restoring fields so that the effective period becomes equal to the driver one.

[8] the absorbed energy 'per electron' is order the ponderomotive potential $\varepsilon^2/(4\nu^2)$ (ν is the laser frequency), i.e. the time-averaged quiver energy of a free electron in the laser field.

[9] In [87] for $\beta = 10$ and $\varepsilon \simeq 0.92\,\beta^2$ it is observed that, near a resonance, increasing the driver strength by only 0.2% the absorbed energy increases by 43 times.

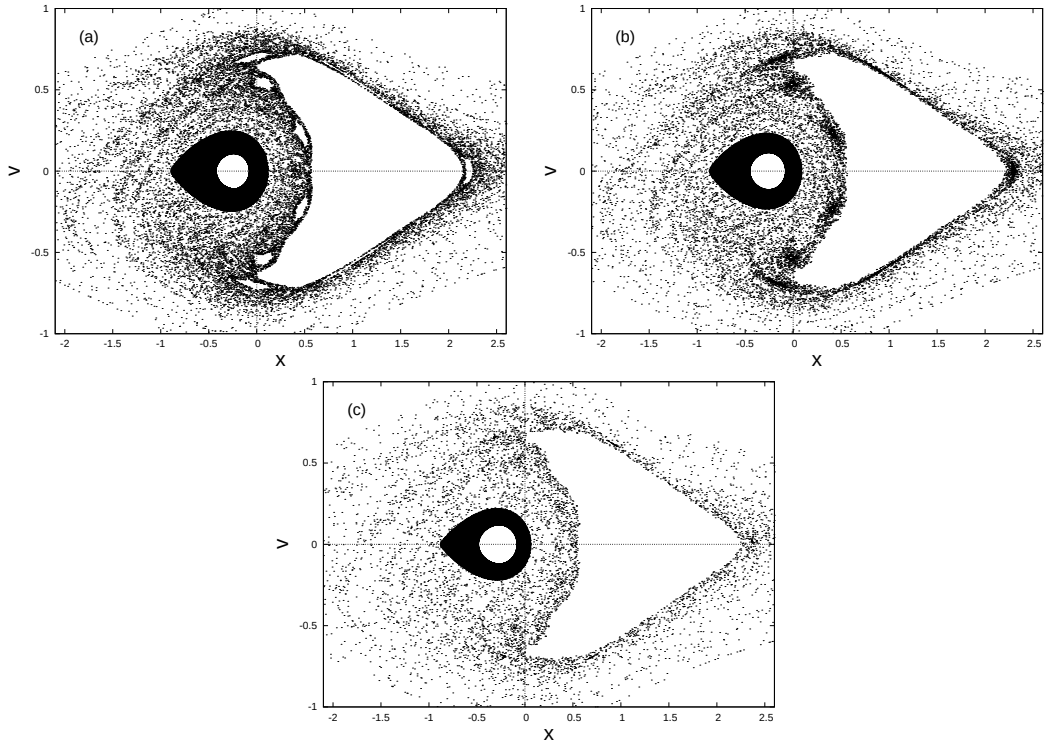

Figure 2.9: Primary resonance of system (2.97) for $e(t) = \sin(0.5t)$ and $\varepsilon = 0.11$ (a), $\varepsilon = 0.115$ (b), $\varepsilon = 0.12$ (c).

character of the motion when it is crossed.
In fact the resonance leaves almost unchanged a region of phase space where an elliptic center is surrounded by a continuous family of closed orbits (KAM structure) and modifies the topology of the phase space outside the KAM structure. An orbit that stays inside the unmodified area, i.e. does not cross the resonance, turns round the fixed point. It is not much changed with respect to the orbit with the same initial conditions in the near integrable pattern.
An orbit that crosses the resonance visits the part of phase space that is modified; the orbit can reach to a phase space region which can be far away from the bounded region where the orbit with the same initial conditions stays confined in the near integrable regime.
It is important to note that the orbits, which have an "effective period" nearly equal to the laser period, are not, in general, closed to a "resonant absorption", i.e. close to the borders of a KAM region or close to a region where the KAM structure is strongly modified: see for instance the resonance $2:5$ in fig. 2.6 and the resonance $1:18$ in fig. 2.8.

We analize the behavior of KAM structure of (2.98) when the driver amplitude ε is varied. The fixed point x_0 is a nondegenerate singular point[10]. In fact upon linearizing the Hamiltonian system (2.98) at the fixed point

$$\begin{pmatrix} x \\ \dot{x} \end{pmatrix} = Df(x_0) \begin{pmatrix} \delta x \\ \delta \dot{x} \end{pmatrix}$$

[10] A singular point of a vector field is said to be 'degenerate' if zero is an eigenvalue of the linearization of the field at that point

one finds that $trace(Df) = 0$ because the area phase is preserved.
For a small change of ε a nondegenerate singular point does not disappear (see theorem at pg 96 of [7]) and moves only slightly (in view of the implicit function theorem). Therefore we can always find an interval of ε values such that the qualitative structure of the phase portrait about the fixed point does not change.
For a small change of ε in the KAM pattern nearly all closed orbits are shifted by a small amount. They preserve their character of closed orbits encircling the elliptic center. Only orbits that are close to the boundary of the KAM area, i.e. that are 'the most resonant', experience a drastic change; from close orbits they become erratic, maybe, unbounded.
Fig. 2.9 displays the Poincaré patterns of the primary resonance $\omega(e) = 0.5$ of oscillator (2.96) with $e(t) = \sin(0.5t)$; there are fixed $\varepsilon = 0.11$, (a), $\varepsilon = 0.115$, (b), $\varepsilon = 0.12$ - (c)). The distinguishing features are the simultaneous presence of a KAM structure, the typical pattern due to the topological change caused by the resonance and the stochastic region that grows around them. The KAM structure is preserved by a small increase of perturbation strength (compare (a) and (b)) except for a thin strip of orbits near the border of the region. The KAM structure is progressively reduced; the plot (c) shows that the KAM structure derives from a partial breaking of the structures in (a) and (b).

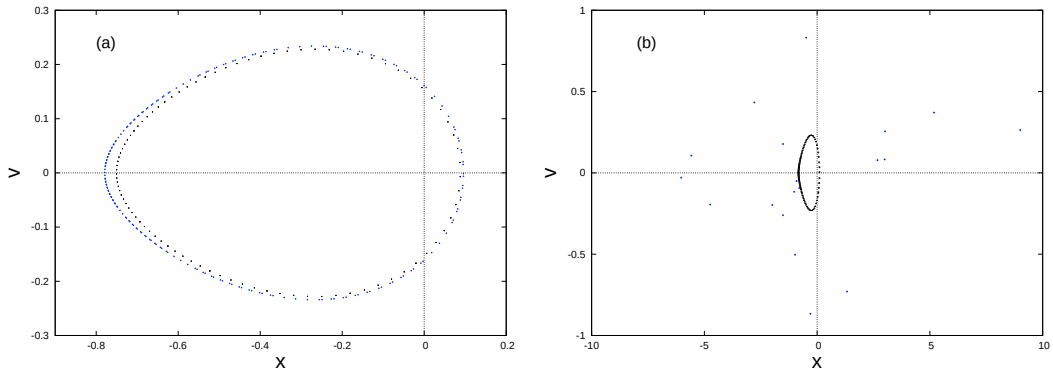

Figure 2.10: Orbits with initial conditions P_0 (black) and P_1 (blue) of system (2.97) for $e(t) = \sin(0.5t)$ and $\varepsilon = 0.11$ (a), $\varepsilon = 0.115$ (b).

We consider two close oscillators (2.96): one for $\varepsilon = 0.11$ and one for $\varepsilon = 0.115$.
As well we focus on pairs of orbits of each system with given initial conditions, that are close to each other; we choose $P_0 = (x(0) = -0.28, \dot{x}(0) = 0)$ and $P_1 = (x(0) = -0.29, \dot{x}(0) = 0)$. The two orbits for $\varepsilon = 0.11$ belong to the KAM region; they are closed and wind staying close to the boundary of the region (see fig. (a) of 2.10). The variations of the mechanical energy along the orbits are nearly identical.
On the other hand the corresponding orbits for $\varepsilon = 0.115$ have a character quite different (see fig. (b) of 2.10). That with initial conditions P_0 is closed and twistes on to a torus. The orbit with initial conditions P_1 crosses the resonance and runs out from the KAM area.

Through this geometric pattern we may understand the behavior of solutions of (2.96) and (2.97) as the driver amplitude is increased.
The initial conditions are chosen such that the orbit winds a torus. When ε is varied and the orbit still belongs to the KAM pattern the absorbed energy is quite little (see, for instance, (a) of 2.10). On the other hand, whenever ε varies so that the orbit, for the given initial

conditions, no longer adheres to a torus, i.e. it crosses the resonance, the absorbed energy is allowed to be large . The orbit leaves out from the KAM pattern and can reach to regions of phase space far away from it. The orbit can pass from the twisting to the stochastic motion through only a small change of the driver strength (compare the trajectory with initial conditions P_1 in (a) and (b) of (2.10)).

Chapter 3

Perturbative theory of a resonance. The onset of chaos.

1. Introduction.

In the previous chapter we have seen that near a resonance, by means of a suitable canonical transformation, close to the identity, any "weakly" perturbed oscillator, with one degree of freedom, essentially reduces to a pendulum (in general, near a resonance of order r a system with a convex, free Hamitonian reduces to a system of r coupled rotators, subject to a force that depends on only r angles). "Essentially" means that a "small remainder", in the transformed Hamiltonian, is disregarded. We know that the resonance "islands", produced by the perturbation, extend in general over a region of order $\varepsilon^{1/2}$, where ε is the size of the perturbation. The first basic question one would like to answer is how long this "stability" property can hold. To this end we should estimate the "remainder", i.e. on which time-scale its effects become important.

Actually in our case we "do not" need to make this estimate, at least, as regards the stability problem. In fact we know that, in the case of a system with two degrees of freedom, the KAM theorem solves this problem all over the phase space. Given the special, topological structure of the phase space, the "connected" components of the complement of the set where the Hamiltonian can be reduced to an integrable form, can be at most of order ε^a, $a > 0$. Therefore, even though the set, where the system behaves as if it were integrable, has an empty interior, the stability is always guaranteed. While, this is not true for the "integrability".

It is clear that the issue of the time scales is of interest concerning the integrability. What we may try to do is to adapt the ideas of the Nekhoroshev-like perturbation theory; they provide stability results in the whole phase space, for a time scale growing exponentially with ε ("exponential estimate"). They essentially consists in introducing new canonical variables, ε-closed to the original ones, such that in the transformed Hamiltonian the terms that can define "nonlocal" motions are "very" ("exponentially") small for small ε. Actually, it is straighforwardly noticed that, for a suitably transformed Hamiltonian with two degrees of freedom,

in place of the "unstable" terms there are ones that define "local" dynamics which nontrivially involve both of the degrees of freedom. Therefore these terms can produce chaotic dynamics; however, their effects are confined to strips, around the pendulum separatrices of a resonance, which have sizes exponentially small with ε, which is the same as to say that their effects become important in a region of order ε^a, on time scales exponentially long with $1/\varepsilon$.

2. From one resonance to the "geometry" of resonances in phase space. Geometric properties of the dynamics close to a resonance. The slow and fast variables and their time scales.

In the previous sections we have worked out some results about the motion close to a resonance in a system (2.25), with one and half degrees of freedom. A Poincaré theorem establishes the existence at the resonance of a sequence of fixed points that alternate between an elliptic point and a hyperbolic one. Moreover through a canonical transformation ε-near the identity we change to a frame of reference about an elliptic point; if one neglects terms of order higher than the first in ε, the new variables describe the motion of a pendulum. Meanwhile, heteroclinic intersections take place close to the hyperbolic points; they indicate the presence of irregular dynamics no matter how small ε is chosen.

The irregular dynamics depends on the neglected terms in the perturbative step that moves the perturbation to a higher order in ε. We know that the terms of the Hamiltonian that are distinguished by different orders in a small parameter correspond to distinct time scales in the dynamics. Therefore if the resonance is of order one, as it is our case, the "perturbed" motion remains integrable (one dimensional pendulum is integrable) over a period of time that can be very long (because of the smallness of the neglected terms), after which the dynamics can turn to a chaotic behaviour near the resonance.

If we forget about the $O(\varepsilon^2)$ term in (2.31) we conclude that close to a (single) resonance $\mathcal{L}$ of a system with one and half degrees of freedom, namely of the corresponding Hamiltonian system with two degrees of freedom,

- one degree of freedom is bounded in a domain of order $\varepsilon^{1/2}$;
- the action of the other degree of freedom is constant,

if we consider $t < 1/\varepsilon^2$.

Some analytical considerations are needed to produce longer confinement times; under general assumptions, through the method of canonical transformations, stability results (like the previous picture) are proven to hold even for exponentially long time scales (in term of $1/\varepsilon$), namely,

$$|I(t) - I(0)| < c\,\varepsilon^{b_2} \qquad for\ \ t < T_\infty(\varepsilon) \equiv e^{d\ (1/\varepsilon)^{b_1}} \tag{3.1}$$

c, d, b_1, b_2 being positive constants. Along these lines we can introduce a new time scale $T_\infty(\varepsilon) \gg 1/\varepsilon$, inside which the dynamics does not move the actions more than a power of ε.

Consider the nearly integrable system with two degrees of freedom

$$H(I,\varphi) = h(I) + \varepsilon\, f(I,\varphi) \qquad\qquad (I,\varphi) \in \mathcal{B} \times \mathbb{T}^2 \tag{3.2}$$

where $\mathcal{B}$ is a domain in $\mathbb{R}^2$ and $\mathbb{T}^2$ is the two dimensional torus. In order to study the dynamics close to the resonance $\mathcal{L}$, by means of the perturbation method we produce a canonical transformation that yields the Hamiltonian in the new variables the form

$$H(I,\varphi) = h(I) + \varepsilon\, g_{\mathcal{L}}(I,\varphi,\varepsilon) + R(I,\varphi,\varepsilon) \qquad\qquad \|R\| = O(T_R(\varepsilon)^{-1}) \tag{3.3}$$

where T_R sets the time scale in which the effects of the remainder R on the dynamics can be neglected. In order to accomplish the task stated in (3.1) we need to produce a canonical transformation such that $T_R(\varepsilon) \equiv T_\infty(\varepsilon) = O(e^{d\ (1/\varepsilon)^{b_1}})$. The main result of this chapter is to show the existence of a canonical transformation that, close to a resonance, leads Hamiltonian (3.2) to the form (3.3) so that (3.1) is given. This construction is roughly adapted from [42, 44] where we are given a complete proof of Nekhoroshev theorem [81], that guarantees that (3.1) holds for a nearly integrable Hamiltonian system under both a smoothness condition (the analyticity of the Hamiltonian) and a geometric (the "steepness") condition.

2.1 Infinitely many Fourier components. The ultraviolet cut off.

We now proceed to an extension of the previous results and admit f in (3.2) to have a full Fourier expansion

$$f(I,\varphi) = \sum_{\nu \in \mathbb{Z}^2} f_\nu(I)\, e^{i\nu\varphi}$$

We reach the conclusion that only a finite number of components of f are relevant in the dynamics of the action whenever we determine a time scale. This is a consequence of the analycity of f in appropriate domains.

In this system, we know, all resonances are simple. Let

$$\mathcal{L} = \{\lambda\,\nu, \lambda \in \mathbb{Z}\}$$

be a one dimensional subspace of $\mathbb{Z}^2$. We determine $\mathcal{L}$ by giving a base $\{\nu\}$. Of course a base is defined up to a moltiplication by an integer. Each base is specified by $|\nu|$; we denote by $w(\mathcal{L})$ the minimal modulus among the bases of $\mathcal{L}$.

For any $B \subset \mathcal{B}$ and any couple of positive parameters ρ and σ, we introduce a neighborhood of the real domain $B \times \mathbb{T}^2$ in the complex space $\mathbb{C}^2 \times \mathbb{C}^2$ of the actions and the angles:

$$D_{(\rho,\sigma)}(B) \equiv B_\rho \times S_\sigma \tag{3.4}$$

where

$$B_\rho = \{I' \in \mathbb{C}^2\ dist(I',\, B) \le \rho\} \tag{3.5}$$

and

$$S_\sigma = \{\varphi \in \mathbb{C}^2 \mid |\mathrm{Im}\,\varphi_i| \le \sigma,\ i = 1, 2\} \tag{3.6}$$

in which

$$dist(I, \mathcal{B}) = \inf_{I' \in \mathcal{B}} \max_{i=1,2} \{|I'_i - I_i|\}$$

The sets (3.5) and (3.6) are displayed in fig. 3.1.

For a function $u : B \times \mathbb{T}^2 \to \mathbb{C}^q$, with analytic extension to $\mathcal{D} = D_{(\rho,\sigma)}(B)$, we introduce the supremum norm[1]

$$\|u\|_{\mathcal{D}} = \sup_{(I,\varphi) \in D_{(\rho,\sigma)}(B)} sup_{j=1,\dots,q} |u_j(I, \varphi)|$$

Moreover, for any $B \subset \mathcal{B}$ we denote by $B^{-\delta}$ the set of points $P \in B$ such that a δ-neighborhood of P is contained in B.

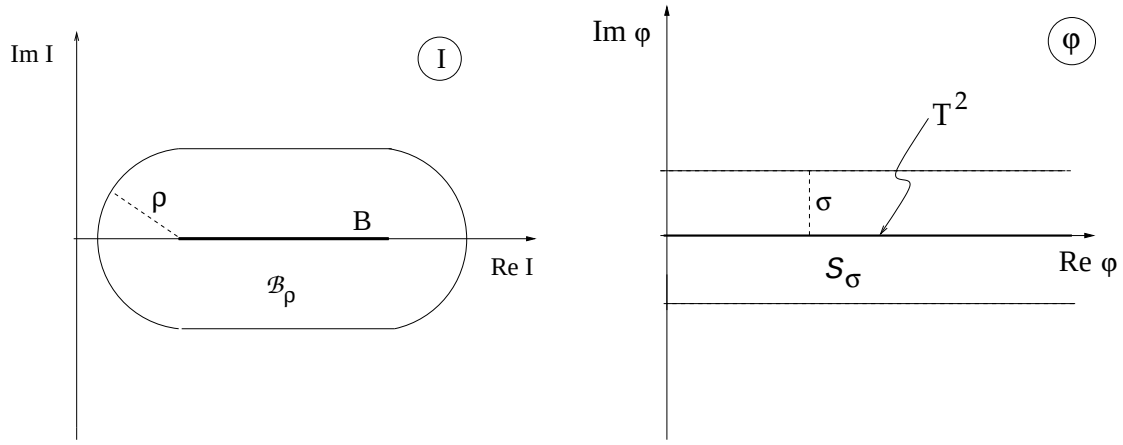

Figure 3.1: The domains $\mathcal{B}_\rho$ (left) and $\mathcal{S}_\sigma$ (right).

We assume that

(A) the Hamiltonian H is analytic in the complex neighborhood $D_{(\rho,\sigma)}(\mathcal{B})$ of the real domain $\mathcal{B} \times \mathbb{T}^2$

The analytic estension to a complex domain allows to estimate the derivatives using the Cauchy inequalities[2], that we also call "dimensional estimates".

[1] We may also consider the "Fourier norm"

$$\|u\| = \sup_{I \in B_\rho} \sum_{\nu \in \mathbb{Z}^2} |u_\nu(I)|\, e^{\sigma\,|\nu|}$$

i.e. the supremum in I of the sum of the sup-norms in φ of the Fourier components.

[2] For a function f analytic in a disk $\mathcal{C}_a(z)$, centered at z, with radius a, a basic Cauchy inequalities is

$$|f'(z)| \le \frac{1}{a}\, sup_{\zeta \in \mathcal{C}_a(z)} |f(\zeta)|$$

The perturbation theory, precisely the method of canonical transformation, runs into problem in dealing with data too close to a resonant surface. We should realize that a resonance affects the system only on a certain time scale. As we wish to construct a canonical transformation to the variables whose dynamics is described by (3.1), we disregard resonances whose corresponding time scale is beyond $T_\infty(\varepsilon)$.

A heuristic argument suggests that a resonance of order one, $\Sigma_{\{\nu\}}$, has an associated time scale $e^{\xi\,|\nu|}$, where $\xi > 0$ depends on how regular, in the φ variable, is the analytic function $f(I,\varphi)$. In fact ξ measures the size of the strip of the holomorphy domain of f with respect to the angles. The reason for the above estimate is very simple: the ν-th component of the function $\varepsilon\, f$ (whose presence leads to the necessity of dividing by $\omega(I)\,\nu$ in perturbation theory) has size $O(\varepsilon\, e^{-\xi\,|\nu|})$. It follows that one can neglect it for times shorter than $O(\varepsilon^{-1}\, e^{\xi\,|\nu|})$. Since we are trying to reach a time scale of order $e^{d\,(1/\varepsilon)^{b_1}}$ we can neglect all resonances $\mathcal{L}$ for which

$$w(\mathcal{L}) > \varepsilon^{-\tau} \equiv N(\varepsilon) \tag{3.7}$$

where $\tau > 0$ is a parameter to be optimally adjusted.

We may introduce the "ultraviolet cut-off"

$$N = N(\varepsilon) \tag{3.8}$$

and write f as the sum

$$f = f^{\le N} + f^{>N} \tag{3.9}$$

of the "infrared" part

$$f^{\le N}(I,\varphi) = \sum_{|\nu|\le N} f_\nu(I)\, e^{i\nu\varphi}$$

and the "ultraviolet" part $f^{>N} = f - f^{\le N}$.

We can proceed similarly as in section 5.. For each $\mathcal{L}$ we produce a canonical transformation $(I,\varphi) = \Phi_{\varepsilon\,\chi}(I',\varphi')$ with

$$\chi(I,\varphi) = \sum_{\nu\notin\mathcal{L}}^{|\nu|\le N} \frac{f_\nu(I,\varphi)}{i\,\omega(I)\,\nu}$$

such that the the resonant normal form is

$$\begin{aligned} H'\circ w_{\Phi_{\varepsilon\,\chi}} &= h + \varepsilon\, g + r(\varepsilon) \\ r(\varepsilon) &= \varepsilon^2\, f' + \varepsilon\, \tilde f^{>N} + O(\varepsilon^3) \end{aligned} \tag{3.10}$$

where

$$g(I',\varphi') = f_\nu^{\le N}(I')\, e^{\nu\varphi'} \qquad\qquad \nu\in\mathcal{L}$$

is the projection of $f^{\le N}$ onto the resonance $\mathcal{L}$,

$$f' = \{f^{\le N},\chi\} + \frac{1}{2}\,\{\{h,\chi\},\chi\}$$

and

$$\tilde f^{>N} = f^{>N}\circ\Phi_{\varepsilon\chi}$$

The perturbation f is assumed holomorphic in $\mathcal{D}_{(\rho,\sigma)}$, and hence in the strip $|Im\varphi_j| < \sigma$, $j = 1, 2$. The term $\varepsilon\ \tilde{f}^{>N}$ is negligible in $r(\varepsilon)$, since the ultraviolet part decreases exponentially with small ε:

$$\| f^{>N} \|_{\rho/2} < C\ e^{-\sigma/\varepsilon^{\tau}}\ , \tag{3.11}$$

C is positive. In fact on account of the choice (3.8) of the cut off the evaluation (3.11) is a consequence of (29) of appendix 5.

Hence the motions described by the infrared part agree with the ones of the complete Hamiltonian up to a time of the order $e^{\rho_\varphi\ N(\varepsilon)}$; in particular the mechanism of confinement of the actions in resonant regions of size as in (3.1) does not need to consider the ultraviolet part. Even in the case of a generic analytic f we can proceed exactly as before: the Fourier polynomial is the infrared part with $N = N(\varepsilon)$. We are left to consider only a finite number of resonances $\omega(I)\ \nu$.

This result is not in conflict with the averaging principle. Actually $N \to \infty$ as $\varepsilon \to 0$ and then some new resonances come to afflict any normal form generated by a finite number of Fourier components.

2.2 "Geometry of resonances" .

We are going to give a description of the arrangement of resonances in the phase space $\mathcal{B} \times \mathbb{T}^2$, $\mathcal{B} \subset \mathbb{R}^2$.

Let $\mathcal{L}$ be a one dimensional subspace of $\mathbb{Z}^2$. The "resonance line" associated with $\mathcal{L}$ is the set

$$\Sigma_{\mathcal{L}} = \{I \in \mathcal{B},\ \omega(I)\,\nu = 0 \text{ for all } \nu \in \mathcal{L}\}\ \ ^{3}$$

As well $\Sigma_{\{0\}} = \mathcal{B}$ and $\Sigma_{\mathbb{Z}^2} = \{I\,|\,\omega(I) = 0\}$. We note that in our case $\Sigma_{\mathbb{Z}^2} = \emptyset$ since a generic frequency vector is $\omega(I) = (\omega_1(I),\ u)$, u is the driver frequency.

On the base of the previous paragraph, for any ε one has to take care of the infrared part $f^{\leq N}$, with $N = N(\varepsilon)$, and then of a finite set of resonance lines which forms a web in $\mathcal{B}$.

We introduce a covering of the action space $\mathcal{B}$ by sets in which the frequency $\omega = \partial h/\partial I$ has well-defined resonance properties.

Let $\mathcal{L} \subset \mathbb{Z}^2$ be generated by $\{\nu\}$, such that $w(\mathcal{L}) \leq N$.

It is given a sequence

$$\lambda_i = \ c_{\lambda}^{(i)}\ \varepsilon^{\sigma_i} \qquad\qquad 0 \leq \sigma_i \leq 1/2 \tag{3.12}$$

$i = 1, 2, 3$. We suppose $0 < \lambda_0 < \lambda_1 < \lambda_2$; furthermore

$$\lambda_{i+1} \to 0 \qquad \frac{\lambda_i}{\lambda_{i+1}} \to 0 \tag{3.13}$$

[3]For each subspace $\mathcal{L}$ of dimension $d = 1$ $\Sigma_{\mathcal{L}}$ is a manifold of codimension d (a line in $\mathbb{R}^2$).

for $\varepsilon \to 0$. We define the "resonance block" of the resonance $\mathcal{L}$ of dimension r, $r = 0, 1, 2$

$$B_{\mathcal{L}}^{\sigma,N}(\varepsilon) = \{I \in \mathcal{B} \; \|\omega_{\mathcal{L}}(I)\| \leq \lambda_r, \; |\omega(I)\,\nu| > \lambda_{r+1} \text{ for all } \nu \notin \mathcal{L}, \; |\nu| \leq N\} \tag{3.14}$$

where $\omega_{\mathcal{L}}$ is the orthogonal component of ω onto $\Sigma_{\mathcal{L}}$. A convenient measure of $\omega_{\mathcal{L}}(I)$ is

$$\|\omega_{\mathcal{L}}(I)\| = \inf_{\nu} |\omega(I)\,\nu|$$

where the infimum is over all $\nu \in \mathcal{L}$, $|\nu| < N$. In $B_{\mathcal{L}}^{\sigma,N}$ the divisors $\omega\,\nu$, for $\nu \in \mathcal{L}$, are small.

For $r = 0$

$$B_{\{0\}}^{\sigma,N}(\varepsilon) = \{I \in \mathcal{B} \;\; |\omega(I)\,\nu| > \lambda_1 \text{ for all } \nu \neq 0\}$$

is the "noresonance block". On the other hand if $r = 2$

$$B_{\mathbb{Z}^2}^{\sigma,N}(\varepsilon) = \{I \in \mathcal{B} \; \|\omega_{\mathbb{Z}^2}(I)\| \leq \lambda_2\}$$

i.e. it is a neighborhood of $\omega = 0$.

The blocks for all resonances $\mathcal{L}$'s provide a covering of $\mathcal{B}$ (but not a partition). From a given dimension of $\mathcal{L}$ on, the blocks can be empty.

Since $\lambda_{i+1} > \lambda_i$, any two resonance blocks $B_{\mathcal{L}}$ and $B_{\mathcal{L}'}$, relative to different resonances of dimension one, do not overlap and stay well separated. Blocks of different dimensionality can overlap: there is a small intersection between $B_{\{0\}}^{\sigma,N}$ and $B_{\mathbb{Z}^2}^{\sigma,N}$, but this will be irrelevant later on[4] In the case with two degrees of freedom, for any resonance $\mathcal{L}$ of dimension one the block $B_{\mathcal{L}}^{\sigma,N}$ is a layer around the resonance line $\Sigma_{\mathcal{L}}$. If a neighborhood of $\omega = 0$ is excluded, if a point P does not belong to any block of order one then P belongs to the noresonance block. Therefore a motion that enters or leaves a block of order one coming from or arriving at a noresonance block (see fig. 3.2).

If ε is lowered then the cut-off N increases and the set of resonance lines becomes more dense; according to (3.13) the resonance blocks become thinner and thinner the closer ε is to zero.

Finally, for a given $\varepsilon > 0$, if

$$0 < \tau \ll \sigma_i \; < 1/2$$

$i = 0, 1, 2$, then the points of the most part of $\mathcal{B}$ belong to the noresonance block and the most of the remaining points are in the resonance block with $r = 1$, etc. . In fact the estimate of the volume V_r of the phase space filled by blocks of order r is [5]

$$V_r \leq C\,\varepsilon^{(\sigma-2\tau)r}\,Vol(\mathcal{B})$$

[4]Except for this small overlapping to $I \in \mathcal{B}$ we can uniquely associate the corresponding "leading resonance" $\mathcal{L}$ such that $I \in B_{\mathcal{L}}^{\sigma,N}(\varepsilon)$.

[5]A block $B_{\mathcal{L}}^{\sigma,N}$ of order r is a "tube" with r dimensions of order ε^{σ} and $(2-r)$ dimensions of order R, the linear dimension of $\mathcal{B}$; thus has a volume $O(R^{2-r}\,\varepsilon^{r\sigma})$. The number of resonances $\mathcal{L}$ of order r such that $w(\mathcal{L}) < N$ is the number of r-ples with $|\nu_i| < N$ i.e. it is estimated by $\begin{pmatrix} N^2 \\ r \end{pmatrix} \sim O(N^{2r})$. Since $N = \varepsilon^{-\tau}$ we conclude that

$$V_r \leq O(N^{2r} R^{2-r}\,\varepsilon^{r\sigma}) \leq C\,\varepsilon^{(\sigma-2\tau)r}$$

The arrangement of the resonance lines (the lines) and the resonance zones (the stripes around the lines), that is displayed in the action space by the system we are studying, i.e. a one-dimensional forced oscillator described by the two-dimensional Hamiltonian (2.14)), is shown in figure 3.2.

We recover the unperturbed Hamiltonian

$$h(I) = h_0(I_1) + u\, I_2 \tag{3.15}$$

where I_2 is the action conjugated to the angle $\varphi_2 = ut$, u is the driver frequency.

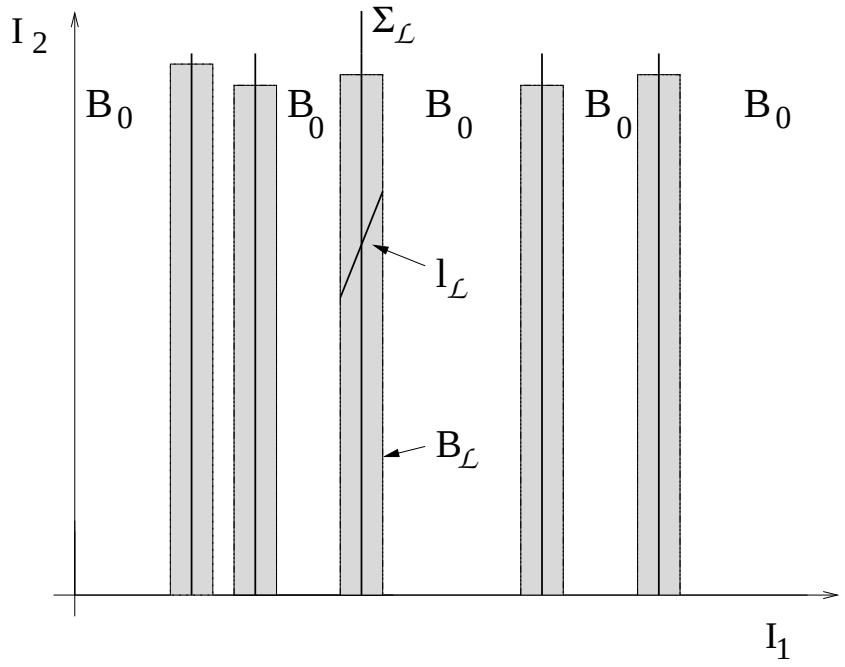

Figure 3.2: Geometry of resonances. For any one dimensional resonance $\mathcal{L}$ there are displayed the resonance line $\Sigma_{\mathcal{L}}$, the resonance block $B_{\mathcal{L}}$ (the layer around the resonance line), and the line of fast drift $l_{\mathcal{L}}$; the noresonance block B_0.

The set of resonance lines is the same as that of vertical lines $I_1 = I(\alpha)$, in which $I(\alpha)$ is the solution of the equation

$$h_0'(I(\alpha)) \;+\; \alpha\, u \;=\; 0$$

for each $\alpha \in \mathbb{Q}$, $\alpha = \nu_2/\nu_1$ and $|\nu_1| + |\nu_2| < N$.

From this geometric arrangement it may be concluded that we cannot expect to see any chaotic phenomena before a time scale $T_\infty(\varepsilon)$ by randomly sampling the initial data far away from the origin. We will discuss on this matter in detail.

After we describe a covering of the phase space by suitable sets related to the arrangement of resonances, we now try to understand how the dynamics moves the actions in this construction.

2.3 The "line of fast drift".

We focus on a resonance $\mathcal{L}$. The essential condition to determine the canonical transformation to the normal form (3.3) ($R = O(\varepsilon^2)$ after the first perturbative step) is that the motion takes place "far enough from other resonances". The geometrical construction is helpful to apply the condition. In particular we expect that whenever the initial datum I_0 belongs to $B_{\mathcal{L}}^{\sigma,N}(\varepsilon)$ the motion "essentially" results to be confined in the block. Indeed this is what happens.

If the condition of absence of other resonances holds then the motion inside the resonance will obey the resonant normal form (3.3), in which all Fourier components of the perturbation but that of $\mathcal{L}$ is eliminated *up to* $T_R(\varepsilon)$ *time scale* (see in section 5.).

In (3.3) we drop the $O(T_R(\varepsilon)^{-1})$ remainder and study how the normal part

$$h_\varepsilon(I,\varphi) = h(I) + \varepsilon\, g_{\mathcal{L}}(I,\varphi,\varepsilon) \tag{3.16}$$

moves the actions. Close to the resonance $\mathcal{L} = \{\nu\}$, the Hamilton equation can be written

$$\dot{I} = \varepsilon\, a_\nu(I,\varphi,\varepsilon)\, \nu \qquad\qquad a_\nu(I,\varphi,\varepsilon) = i\, g_{\mathcal{L}}(I,\varepsilon)\, e^{i\nu\,\varphi} \tag{3.17}$$

Since h_ε depends only on one combinations of angles, it follows that (3.16) admits one combination of actions which is an integral of motion (see (2.32)) so that the action is confined to move in a line $l_\lambda(I_0)$, the line through the initial datum I_0 and parallel to the resonance $\mathcal{L}$. The manifold $l_\lambda(I_0)$ is called "line of fast drift".

If a motion, transversal to $l_{\mathcal{L}}(I(0))$, takes place it is produced by the remainder R in (3.3). Considering again the complete Hamiltonian $h_\varepsilon + R$ we assume that the deviation from $l_{\mathcal{L}}(I(0))$, produced up to a time $T_R(\varepsilon)$, is d. In order to determine d we need an estimate for R, i.e. it depends on the performed normalization (3.3). We will give some hints on the analytic facts regarding the construction of a normal form with a remainder exponentially decreasing with the ultraviolet cut off N. Only after we will say on the estimate of d. In any case it is small and the motion $I(t)$ is essentially "aligned" along $l_{\mathcal{L}}(I(0))$ up to times of order $T_R(\varepsilon)$. The parameter d is used in the geometrical construction together with the parameters λ_i's and the cut off N.

The meaning of the parameter d suggests to apply the geometric construction of the section 2.2 to the action space $\mathcal{B}^{-2d}$ [6], where $\mathcal{B}$ is the space in which is defined the Hamiltonian (3.2).

For any point I in a block $B_{\mathcal{L}}$ [7] let us denote by $l_{\mathcal{L}}(I) + d$ the cylinder with radius d and axis $l_{\mathcal{L}}(I)$, the line through I, parallel to the resonance $\mathcal{L}$. We also call "cylinder" the intersection

$$C_{\mathcal{L}}^d(I) = (l_{\mathcal{L}}(I) + d) \cap B_{\mathcal{L}} \tag{3.18}$$

Given a resonance $\mathcal{L}$, in order to use the geometric construction, we crucially needs that for any initially datum $I(0) \in B_{\mathcal{L}}$, the normal form adapted to $\mathcal{L}$ is valid in the region visited

[6] Any $I \in \mathcal{B}^{-2d}$ has a $2d$-neighborhood contained in the definition domain of (3.2)

[7] We abbreviate $B_{\mathcal{L}}^{\sigma,N}(\varepsilon)$ to $B_{\mathcal{L}}$

along the motion. Actually (3.3) should be valid not only inside $B_{\mathcal{L}}$ but also in an "extended" region, i.e. the region that can be reached by starting in $B_{\mathcal{L}}$ and moving along $l_{\mathcal{L}}(I(0))$ until the normal form is valid. To make this notion more precise it is introduced the "extended block"

$$B^{ext}_{\mathcal{L}d} = \cup_{I\in B_{\mathcal{L}}} C^d_{\mathcal{L}}(I) \tag{3.19}$$

In order to assure that the normal form adapted to $\mathcal{L}$ can be used all over $B^{ext}_{\mathcal{L}d}$, we require the following "non overlapping condition" to hold: take the parameters λ_i, $i = 1,2,3$, defined in section 2.2,

$$|\omega(I)\ \nu| \geq \lambda_r \tag{3.20}$$

for all $I \in B^{ext}_{\mathcal{L}d}$, $\nu \notin \mathcal{L}$, $|\nu| \leq N$. The condition (3.20) just amounts to state that there is not any intersection between $B^{ext}_{\mathcal{L}d}$ and each block $B_{\mathcal{L}'}$, with $\mathcal{L}'$ of the same dimension as $\mathcal{L}$.

According to the property of d a motion $I(t)$, starting at I, is forced to remain inside $C^d_{\mathcal{L}}(I)$ up to $T_R(\varepsilon)$, otherwise it can leave (or enter) $B_{\mathcal{L}}$ at $\tau < T_R(\varepsilon)$ ($\tau > -T_R(\varepsilon)$) only moving through the "bases" of the cylinder.

Furthermore we know that the following crucial property holds (see section 2.2): a motion that crosses a basis of a cylinder of a block of order r comes from or enters a block of order $r' < r$. It follows that a motion $I(t)$ is constrained to remain inside the nonresonance block $B_{\{0\}}$ if $I(t)$ starts in $B_{\{0\}}$.

In our simple system it is easy to explicit the consequences that can be drawn from the non overlapping condition (see [42], "geometric lemma", for more details). In particular, consider a motion $I(t)$ generated by the Hamiltonian (3.2), with $I(0)$ that belongs to a block $B_{\mathcal{L}}$ of a resonance of order one[8], i.e. $I(0) \in B^{ext}_{\mathcal{L}d}$. We see that for $t \leq T_R(\varepsilon)$, T_R connected to the normal form (3.3) adapted to $\mathcal{L}$, only the following cases can occur:

- the motion $I(t)$ is confined to the cylinder $C^d_{\mathcal{L}}(I(0))$, namely the motion takes place only within the block $B_{\mathcal{L}}$;
- $I(0)$ is so close to a basis of $C^d_{\mathcal{L}}(I(0))$ that it leaves $B_{\mathcal{L}}$ through the basis and comes to the non-resonance block; from now on $I(t)$ is constrained to take place in the cylinder $C^d_{\{0\}}(I(t'))$[9], where t' is a time after the crossing of the basis ($I(t') \in B_{\{0\}}$). Indeed if the non-overlapping condition holds for $t < O(T_R)$ then whenever $I(t)$ enters a non-resonance block we can use the form (3.16) in which $g_{\mathcal{L}}$ is φ-indipendent and thus $I = \text{const}$, namely the point will no longer move before a time $O(T_R)$.

Already we have said that whenever the motion starts in the nonresonance block ($I(0) \in B_{\{0\}}$), it is confined there.

Let us consider

$$\mathcal{A}_{\mathcal{L}}(I) = l_{\mathcal{L}}(I) \cap B_{\mathcal{L}}\ ,$$

[8] We ignore the uninteresting neighborhood of $\omega = 0$

[9] $C^d_{\{0\}}(I(t')) = (l_{\mathcal{L}}(I(0)+d) \cap B_{\{0\}})$

to be the axis of the cylinder.

From the previous observations, the following, crucial property can be concluded. Up to $T_R(\varepsilon)$, for any initial datum $I(0) \in B_{\mathcal{L}}$,

$$|I(t) - I(0)| \leq \text{diam}\mathcal{A}_{\mathcal{L}}(I(0)) + d \tag{3.21}$$

where diam is the diameter of a set. That is to say that $\text{diam}\mathcal{A}_{\mathcal{L}}(I(0))$ gives an estimate of the motion along $l_{\mathcal{L}}(I(0))$.

It is clear that a property that allows to estimate $\text{diam}\mathcal{A}_{\mathcal{L}}(I(0))$, i.e. that can warrant the confinement of the motion "in" $l_{\mathcal{L}}(I_0)$, is geometric in nature.

The "quasi-convexity" property.

The following geometric assumption on the unperturbed energy h is the base of a simple mechanism of confinement.

We denote by h' the frequency vector and h'' the matrix of the second derivatives. The energy $h : \mathcal{B} \to \mathbb{R}$ is said to be "quasi-convex" in $\mathcal{B}$ if for any $I \in \mathcal{B}$, the trivial solution ($\zeta = 0$) is the only one solution of the equations

$$h'(I)\,\zeta = 0 \qquad\qquad h''(I)\,\zeta \cdot \zeta = 0 \tag{3.22}$$

We come back to our system (2.14). The unperturbed Hamiltonian (3.15) is not (strictly) convex [10] since the unperturbed system is isoenergetically non-degenerate.

However, by taking account of (3.15), the equations (3.22) become

$$\begin{aligned} h'(I_1)\,\zeta_1 + u\,\zeta_2 &= 0 \\ h''(I_1)\,\zeta_1^2 &= 0 \end{aligned} \tag{3.23}$$

Since the system is anisochronous ($h''(I) \neq 0$) the equations (3.23) have the unique solution $\zeta = 0$. Therefore the quasi-convexity holds for the system.

An important fact can be shown (see appendix 3.): if the quasi-convexity is verified then the line of fast drift $l_{\mathcal{L}}$ and the resonance line $\Sigma_{\mathcal{L}}$ are transversal. The figure 3.3 displays the geometry of the manifolds close to the resonance I^*. The transversality is the geometric condition which implies that the motion is "constrained" along $l_{\mathcal{L}}$. This is not sufficient to conclude about the confinement of the motion. To this end we need an argument based on the energy.

[10] The function h is said to be convex in $\mathcal{B} \subset \mathbb{R}^2$ if for a suitable $m > 0$

$$m\,\|\mathrm{v}\|^2 \leq \frac{\partial h}{\partial I \partial I}(I)\,\mathrm{v} \cdot \mathrm{v}$$

for all $\mathrm{v} \in \mathbb{R}^2$, for all $I \in \mathcal{B}$

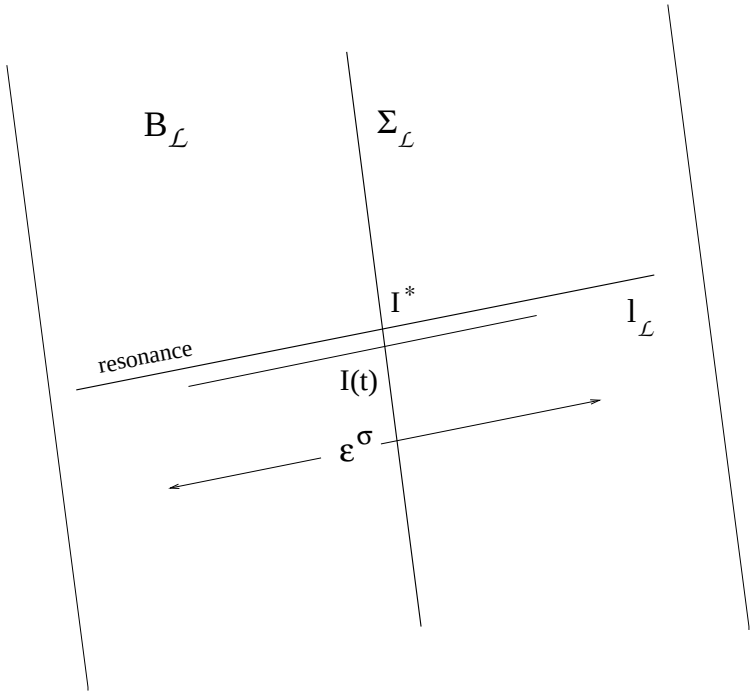

Figure 3.3: The geometry of manifolds near a resonance I^*. If the free Hamiltonian h in (3.16) is quasi-convex then the resonance line $\Sigma_{\mathcal{L}}$ and the line of fast drift $l_{\mathcal{L}}$ are transversal each other. The normal form (3.16) moves the action $I(t)$ along the $l_{\mathcal{L}}$; the energy conservation implies that motion is bounded by the diameter of $B_{\mathcal{L}} \cap l_{\mathcal{L}}$ ($\sim O(\varepsilon^{\sigma})$).

Through the quasi-convexity the energy conservation implies the confinement.

We know that near a resonance I^*, up to a time order $T_R(\varepsilon)$, as long as the transversal motion d is neglected, the dynamics of the action is determined by the Hamiltonian (3.16), i.e.

$$h_\varepsilon = h + \varepsilon\, g_{\mathcal{L}} \quad ,$$

It is easily shown that if h is quasi-convex then there is a consequence for the dynamics induced by h in $l_{\mathcal{L}}$: the *restriction of h to $l_{\mathcal{L}}$* has a quadratic estremum in I^*, the unique intersection point between $l_{\mathcal{L}}$ and $\Sigma_{\mathcal{L}}$. In fact, for $\zeta \in l_{\mathcal{L}}$, by definition we have $h'(I^*)\ \zeta = 0$ and hence

$$h(I^* + \zeta) = h(I^*) + h''(I^*)\zeta \cdot \zeta + O(\|\zeta\|^3) \quad ; \tag{3.24}$$

moreover the second term of (3.24) has a definite sign.

If R is negligible then the Hamiltonian (3.16) is conserved, thus h is almost conserved, except for a quantity of order ε. It follows that, the motion $I(t), I(0) \in l_{\mathcal{L}}$, occurs near a level line of $h = c$ by an energy that is $O(\varepsilon)$. Since $|h(I(0)) - h(I^*)| = O(\varepsilon)$ it follows that also $|c - h(I^*)| = O(\varepsilon)$ and thus

$$|h(I(t)) - h(I^*)| = O(\varepsilon) \tag{3.25}$$

as long as (3.3) holds. If h is quasi-convex and the quadratic term in (3.24) is positive then I^* is an elliptic point. From this it follows that $\|I(t) - I(0)\| \lesssim O(\varepsilon^{\sigma})$, $\sigma < 1/2$ since (3.25) holds. Therefore, using the definition (3.14) , $\|I(t) - I(0)\|$ is bounded by the diameter of $B_{\mathcal{L}}^{\sigma,N}(\varepsilon) \cap l_{\mathcal{L}}$.

In brief: whenever h is quasi-convex and the quadratic form part of (3.3) can be used, the energy conservation and the elliptic structure due to h prevent the system from escaping.

The estimate of the diameter of $\mathcal{A}_{\mathcal{L}}(I(0))$ relies on the transversality of $\Sigma_{\mathcal{L}}$ and $l_{\mathcal{L}}(I(0))$. Indeed, whenever the transversality occurs the diameter is, up to a factor, the width of the block (the argument of the conservation of energy yields an estimate of the width of the block ($\lambda_r \sim O(\varepsilon^{\sigma})$)). Otherwise diam$\mathcal{A}_{\mathcal{L}}(I(0))$ could be the whole "length" of the block, that, in general, is not small with ε.

In the case of the forced oscillator, the quadratic term of the Hamiltonian (3.15), which is quasi-convex, is given by $h_0''(I_1)\ \zeta_1^2$. Consequently the mechanism of confinement takes place whenever $h_0'' > 0$.

We remark that if I^* is an hyperbolic estremum the mechanism of confinement, based on the energy conservation, fails. In fact an escaping motion takes place, close to a energy level of h and conserving the energy. In this case the Hamiltonian that moves the action is $O(1)$.

2.4 From one perturbative step to many ones. Exponential estimates.

The basic idea of the perturbation theory is to transform a given Hamiltonian

$$H(I,\varphi) = h(I) + \varepsilon\ f(I,\varphi)$$

to an approximate normal form, that, in the non-resonance case, is given by

$$H'(I,\varphi) = h(I) + \varepsilon\, g(I)\ +\ R(I,\varphi,\varepsilon)$$

in which the angles have been eliminated up to a remainder R, that is "smaller" than $O(\varepsilon)$. In doing the transformation one can meet the small divisors $\omega(I)\ \nu$, which vanish in a dense subset of the domain A of h. We have already noticed that for an analytic Hamiltonian we should take care of a finite number of small divisors, namely those with $|\nu| \leq N$, N is larger, as ε is smaller (see (3.8)). In the non-resonance case $\omega(I)\ \nu \geq \alpha$ holds for $|\nu| \leq N$ and $I \in A$; therefore small divisors do not take place and it is got a description by an approximate normal form. On the other hand, even in a resonance layer (see (3.14)) of $\mathcal{L} \subset \mathbb{Z}^2$ it is possible to give a suitable normalization. In fact, if it exists a certain domain such that, for I in it, $|\omega(I)\ \nu| \geq \alpha$ for $|\nu| \leq N$ and $\nu \notin \mathcal{L}$ then in the corresponding region of the phase space we can put the Hamiltonian into the normal form adapted to $\mathcal{L}$ (see (3.3) and the footnote (11)):

$$H'_{\mathcal{L}}(I,\varphi) = h(I) + \varepsilon\, g_{\mathcal{L}}(I,\varphi)\ +\ R(I,\varphi,\varepsilon) \tag{3.26}$$

where [11]

$$g_{\mathcal{L}}(I,\varphi) = g_{\nu}(I)\ e^{i\nu\ \varphi}\ . \tag{3.27}$$

R is small with respect to ε.

[11] At the first perturbative step

$$g_{\mathcal{L}\ \nu} = f_{\nu} \qquad\qquad \nu \in \mathcal{L}$$

f is the infrared part of the perturbation. In particular, if $\mathcal{L} = \{0\}$ then (3.26) reduces to the non-resonance case.

In this section we provide a trace describing how to perform a normalization such that the remainder is exponentially decreasing with N, i.e. when ε goes to zero. The basic idea is to produce, for each resonance $\mathcal{L}$, a canonical transformation that is defined by a sequence of a finite number of elementary steps like (3.10). Some estimates on some functions and derivatives, together with a condition of non-resonance, allow to verify the existence and the number of the steps. The estimates are performed on the analytic estensions of the functions in neighborhoods of the type (3.4) of real domains which are close to the resonance.

The starting Hamiltonian

$$H(I,\varphi) = h(I) \,+\, \varepsilon\, f(I,\varphi) \tag{3.28}$$

is extended to an analytic function in a neighborhood $\mathcal{D} = D_{(\rho,\sigma)}(A)$ of the type (3.4) of $A \times \mathbb{T}^2$. On both the "free part" and the "interaction part" we will impose a condition that determines their size.

For a suitable $M > 0$ we assume

$$\left\| \frac{\partial^2 h}{\partial I \partial I} \nu \right\|_{\mathcal{D}} \leq\, M\, \|\nu\| \quad \text{for all } \nu \in \mathbb{C}^2 \tag{3.29}$$

Given any resonance $\mathcal{L}$, $B \subset \mathcal{B}$ is a set such that for all $I \in B$ the nonresonance relation

$$|\omega(I)\,\nu|^{-1} \leq C_0\, \varepsilon^{-\alpha} \quad \text{for all } \nu \notin \mathcal{L} \quad |\nu| \leq \varepsilon^{-\tau} \ , \tag{3.30}$$

$C_0 > 0$ is large enough and $\alpha > 0$, is satisfied.

To be able to make dimensional estimates of the derivatives, one works in the set

$$\mathcal{B} = D_{(\tilde{\rho},\sigma)}(B)$$

for $\tilde{\rho} = O(\varepsilon^{(\alpha+\tau)})$. Indeed, concerning to the actions, the set is characterized by the condition $dist(I,\, B) \leq \tilde{\rho}$, hence in $D_{(\tilde{\rho},\sigma)}(B)$ and for $I_0 \in B$

$$|\omega(I)\,\nu| > |\omega(I_0)\,\nu| - |(\omega(I_0) - \omega(I))\,\nu| > C_0^{-1}\, \varepsilon^{\alpha} - M\, N\, \tilde{\rho} = C_1\, \varepsilon^{\alpha} \tag{3.31}$$

for all $\nu \notin \mathcal{L}$ and $|\nu| < N = e^{-\tau}$. C_1 is a constant and we used (3.30) and (3.29).

With reference to $\mathcal{L}$ we consider the decomposition of the perturbation f in (3.28)

$$f(I,\varphi) \;=\; g_{\mathcal{L}}(I,\varphi) \,+\, R(I,\varphi) \tag{3.32}$$

where $g_{\mathcal{L}}$ is known and

$$R(I,\varphi) = \sum_{\nu \notin \mathcal{L}} r_\nu(I)\; e^{i\nu\,\varphi} \tag{3.33}$$

Without loss of generality we assume

$$\|h\|_{\mathcal{B}} \leq E \qquad\qquad \|f\|_{\mathcal{B}} \leq E \tag{3.34}$$

i.e. the order of the sizes of h and f is E.

As well we introduce the positive number η

$$\|R\|_{\mathcal{B}} \leq \eta \;\; E \tag{3.35}$$

Furthermore, for $N = \varepsilon^{-\tau}$, we consider the "ultraviolet part" $R^{>N}$ of R, that is defined by the part of the sum (3.33) for $|\nu| > N$. Similarly the "infrared part" $R^{<N} = R - R^{>N}$ is given.

The single canonical transformation.

We have to determine a suitable canonical transformation $\Phi_{\varepsilon\,\chi}$, namely its generating function χ. In order to do this we need the following observation.

Applying (19) of appendix 2.2 for $g = H$, the transformed Hamiltonian

$$H' = H \circ \Phi_{\varepsilon\,\chi}$$

can be decomposed as follows

$$H' = h + \varepsilon\, g_{\mathcal{L}} + R^{<N} + \varepsilon\,\{h, \chi\} + \tilde{R} \tag{3.36}$$

where

$$\tilde{R} = R^{>N} + \varepsilon\,\{f, \chi\} + H' - H - \varepsilon\,\{H, \chi\} \tag{3.37}$$

This decomposition is justified on the basis of the remarks in section 2.1: the ultraviolet part R is moved to the "remainder" since, we have observed, it is exponentially small with respect to N.

We consider the solution χ of the equation

$$R^{<N} + \varepsilon\,\{h, \chi\} = 0 \tag{3.38}$$

in the complex domain $\mathcal{B}$. The solution is found to be

$$\chi(I, \varphi) = \sum_{|\nu| \leq N} x_\nu(I)\; e^{i\varphi\,\nu} \qquad\qquad \varepsilon\, x_\nu(I) = -i\,\frac{r_\nu(I)}{\omega(I)\;\nu} \tag{3.39}$$

$\omega = \partial h / \partial I$.

Given the positive parameters $\delta \leq \tilde{\rho}$ and $\xi \leq \sigma$, we have to check that (3.39) is the generating function of a canonical transformation

$$\Phi_{\varepsilon\chi} = (\Phi^I_{\varepsilon\chi},\, \Phi^\varphi_{\varepsilon\chi}) :\; \mathcal{B}' \longrightarrow\; \mathcal{B} \tag{3.40}$$

where $\mathcal{B}' = D_{(\tilde{\rho}-\delta,\,\sigma-\xi)}(B')$, B' is compact and $B^{-\delta} \subset B' \subset B^{-\delta/2}$. A condition that is sufficient to establish the feature involves estimates of the complex derivatives of χ (see lemma (7..1) appendix 7.): we should verify that

$$\varepsilon \left\| \frac{\partial \chi}{\partial I} \right\|_{\mathcal{B}_{\frac{1}{2},\frac{1}{2}}} \leq\; a_1\, \xi \qquad\qquad \varepsilon \left\| \frac{\partial \chi}{\partial \varphi} \right\|_{\mathcal{B}_{\frac{1}{2},\frac{1}{2}}} \leq\; a_2\, \delta \tag{3.41}$$

where $\mathcal{B}_{1/2,1/2} = D_{(\tilde{\rho}-\delta/2,\sigma-\xi/2)}(B^{-\delta/2})$, $a_1 \leq 1/2$, $a_2 \leq 1/2$. If we assume the following "smallness condition" on η:

$$\varepsilon^{-\alpha}\,\eta\,E \;<\; C_1\,\xi^3\,\delta \;, \tag{3.42}$$

where C_1 is a positive constant, the inequalities (3.41) are verified via the following two items, in which a sequence of elementary estimates are performed in progressively reduced domains:

a. the condition of non-resonance (3.31), which holds in $\mathcal{B}$, allows to estimate $\omega\,\nu$ and since (3.33) is analytic in $\mathcal{B}$ we can estimate the coefficient r_ν using (28) of appendix 5. [12] for $g = R$. Thus we can apply the lemma of appendix 6. and in the reduced domain $\mathcal{B}_{0,\frac{1}{2}} = D_{(\tilde{\rho},\sigma-\xi/2)}(B)$ (31) of the lemma yields the following estimate of (3.39):

$$\varepsilon\,\|\chi\|_{\mathcal{B}_{0,\frac{1}{2}}} \leq C_2\,\xi^{-2}\,\varepsilon^{-\alpha}\,\eta\,E \tag{3.43}$$

where C_2 is a positive constant.

b. through Cauchy estimates, the derivatives of χ can be estimated in terms of $\|\chi\|_{\mathcal{B}_{0,1/2}}$, in the reduced domain $\mathcal{B}_{1/2,1/2}$ (see (32) in appendix 6.).

Finally we conclude that

$$\varepsilon\,\left\|\frac{\partial\chi}{\partial I}\right\|_{\mathcal{B}_{\frac{1}{2},\frac{1}{2}}} \leq C_2\;\xi^{-2}\,\delta^{-1}\;\varepsilon^{-\alpha}\,\eta\,E$$

$$\varepsilon\,\left\|\frac{\partial\chi}{\partial\varphi}\right\|_{\mathcal{B}_{\frac{1}{2},\frac{1}{2}}} \leq C_2\;\xi^{-3}\;\varepsilon^{-\alpha}\,\eta\,E$$

The condition (3.41) is satisfied on condition that η is chosen small enough, as it is required by the smallness condition (3.42). Therefore it is established that the canonical transformation (3.40) is defined and analytic in $\mathcal{B}'$. Moreover the condition (3.41) determine the size of the "Hamilton equations" with Hamiltonian $\varepsilon\,\chi$; it follows that $\Phi_{\varepsilon\,\chi}$, which is the time-one map of the flow with Hamiltonian $\varepsilon\,\chi$, is near the identity $I = (I^I,\, I^\varphi)$ (δ and ξ are arbitrary and can be chosen small as desired). In particular (3.40) satisfies

$$\|\Phi^I_{\varepsilon\,\chi} \;-\; I^I\|_{\mathcal{B}'} \leq \frac{\delta}{2} \tag{3.44}$$

The transformed Hamiltonian $H' = H \circ \Phi_{\varepsilon\,\chi}$ is an analytic function in $\mathcal{B}'$ (since H is analytic in $\mathcal{B}$) and takes a form

$$H' = h + \varepsilon\,g'_{\mathcal{L}} + R' \tag{3.45}$$

where the "interaction part" is decomposed analogously to (3.32), i.e.

$$\varepsilon\,g'_{\mathcal{L}} = \varepsilon\,g_{\mathcal{L}} + \tilde{R}_{\mathcal{L}} \qquad\qquad R' = \tilde{R} - \tilde{R}_{\mathcal{L}}$$

and $\tilde{R}_{\mathcal{L}}$ is the Fourier harmonics of $\tilde{R}$ which belongs to $\mathcal{L}$.

[12] that is an application of Cauchy's inequalities (see [43])

Estimates of the terms of the transformed Hamiltonian.

In a typical step the imput is a Hamiltonian of the form (3.28) and the output is (3.45), a Hamiltonian of the same form. Taking into account the decomposition (3.36) we can yield estimates of the terms of (3.45) for the given estimates (3.34) and (3.35) of the terms of (3.36).

In order to face this matter we mainly refer to the holomorphy of the functions: the decreasing property of the coefficients of the analytic Fourier series, the dimensional estimates of the derivatives (see appendix 4.) which involves a reduction of the sizes of the analytic domains. As a result of these estimates the parameters that determine the reduction enter the inequalities. Moreover the values of the constant parameters result from the count of the numbers of terms in the sums.

It is straighforward to estimate H':

$$\|H'\|_{\mathcal{B}'} \leq \|H\|_{\mathcal{B}} \leq E \tag{3.46}$$

We next turn to estimating R' and $\varepsilon\, g'_{\mathcal{L}} + R'$, the remainder and the interaction part after a single step, respectively:

$$\|R'\|_{\mathcal{B}'} \leq \|\tilde{R} - \tilde{R}_{\mathcal{L}}\|_{\mathcal{B}'} \leq 2\, \|\tilde{R}\|_{\mathcal{B}'} \tag{3.47}$$

and

$$\|\varepsilon\, g'_{\mathcal{L}} + R'\|_{\mathcal{B}'} = \|\varepsilon\, g_{\mathcal{L}} + \tilde{R}\|_{\mathcal{B}'} \leq \varepsilon\, \|f\|_{\mathcal{B}'} + \|\tilde{R}\|_{\mathcal{B}'} \tag{3.48}$$

since $\tilde{R}_{\mathcal{L}}$ and $g_{\mathcal{L}}$ are the averages of $\tilde{R}$ and f over certain combinations of angles, respectively.

We are going to focus on $\tilde{R}$. By recalling (3.37) we have

$$\|\tilde{R}\|_{\mathcal{B}'} \leq \|R^{>N}\|_{\mathcal{B}'} + \varepsilon\, \|\{f, \chi\}\|_{\mathcal{B}'} + \frac{\varepsilon^2}{2}\, \|\{\{H, \chi\}, \chi\}\|_{\mathcal{B}'} \tag{3.49}$$

where for the last term we use (19) of the appendix 2.2.

We are left with the task of estimating

- $\|R^{>N}\|_{\mathcal{B}'}$, that is the "ultraviolet part" of R, which is analytic in $\mathcal{B}$. Since $\mathcal{B}' \subset \mathcal{B}_{0,1}$, from (29) of the appendix 5. we have

$$\|R^{>N}\|_{\mathcal{B}'} \leq\ \|R^{>N}\|_{\mathcal{B}_{0,1}} \leq C_3\, \xi^{-2}\, e^{-\frac{1}{2}\xi\, N}\, \|R\|_{\mathcal{B}_{0,0}} \leq C_3\, \xi^{-2}\, e^{-\frac{1}{2}\xi\, N}\, \eta\, E\ \equiv \eta_a\, E \tag{3.50}$$

  C_3 is a constant;

- the sup-norms of the Poisson brackets $\{f, \chi\}$ and $\{\{H, \chi\}, \chi\}$. The simple and double brackets involve the generating function (3.39) and a function analytic in $\mathcal{B}_{0,0}$, namely f and H respectively. The estimates of the derivatives, required to estimate the Poisson brackets, are expressed in terms of the norms of the function and the parameters that give the sizes of the reductions of the complex domains. The last ones are connected to the dimensional estimates of the derivatives.

Some details are given in appendix 8., where taking into account (36) for $g = \varepsilon\ f$ and (37) for $g = H$ one gets

$$\begin{aligned}\varepsilon\,\|\{f,\chi\}\|_{\mathcal{B}'} \;+\; & \frac{1}{2}\|\{\{H,\chi\},\chi\}\|_{\mathcal{B}'} \\ & \leq C_4\,\delta^{-1}\,\xi^{-1}\;\|\chi\|_{\mathcal{B}_{0,\frac{1}{2}}}\;\varepsilon\,\|f\|_{\mathcal{B}_{0,0}} \;+\; C_5\,\delta^{-2}\,\xi^{-2}\;\|\chi\|^2_{\mathcal{B}_{0,\frac{1}{2}}}\;\|H\|_{\mathcal{B}_{0,0}} \qquad (3.51)\\ & \leq\; \eta_b\,E\end{aligned}$$

since $\mathcal{B}'$ is a subset of $\mathcal{B}_{0,\frac{1}{2}}$. If we choose ε small enough such that $E\ \delta^{-1}\ \varepsilon^{-\alpha} > 1$, $\xi < 1$ (ξ is free and can be chosen small as desired) and

$$\eta < c\,\varepsilon \quad , \qquad (3.52)$$

$c > 0$, in virtue of (3.43) one gets

$$\begin{aligned}C_4\,\delta^{-1}\,\xi^{-1}\;\|\chi\|_{\mathcal{B}_{0,\frac{1}{2}}}\,\varepsilon + C_5\,\delta^{-2}\,\xi^{-2}\;\|\chi\|^2_{\mathcal{B}_{0,\frac{1}{2}}} & \\ \leq C_6\;\xi^{-6}\,(E\;\delta^{-1}\,\varepsilon^{-\alpha})^2\,\eta\varepsilon\;\equiv\eta_b & \end{aligned}$$

where η_b is assigned according to (3.34).

In virtue of (3.47), (3.50) and (3.51) we are able to conclude that

$$\|R'\|_{\mathcal{B}'} \leq\; \eta'\,E \qquad (3.53)$$

where

$$\eta' = \eta_a \;+\; \eta_b \;= C_3\,\xi^{-2}\,e^{-\frac{1}{2}\xi\,N}\,\eta \;+\; C_6\;\xi^{-6}\,(E\;\delta^{-1}\,\varepsilon^{-\alpha})^2\,\varepsilon\,\eta \qquad (3.54)$$

Similarly, according to (3.48) and taking account of (3.34) and the estimate of $\tilde{R}$ one finds

$$\|\varepsilon\,g'_{\mathcal{L}} + R'\|_{\mathcal{B}'} \leq (\varepsilon + \eta')\,E \;\equiv\; \varepsilon'\,E \qquad (3.55)$$

Iterative perturbation scheme. Exponentially small remainders.

In the previous section we saw that if we are give an Hamiltonian $H_0 = h + \varepsilon\,f_0 = h + \varepsilon g^0_{\mathcal{L}} + R_0$, defined in a domain $D_0 = D_{\rho_0,\sigma_0}(B)$[13], there exists a canonical transformation $\psi_0 = \Phi_{\varepsilon\chi}$ such that the new Hamiltonian $H_1 = H_0 \circ \psi_0 = h + \varepsilon\,g^1_{\mathcal{L}} + R_1$ is defined in a suitable domain $D_1 = D_{\rho_1,\sigma_1}(B_1)$, where $\rho_1 = \rho_0 - \delta_0$, $\sigma_1 = \sigma_0 - \xi_0$ and $B_0^{-\delta_0} \subset B_1 \subset B_0^{-\delta_0/2}$, i.e. D_1 is reduced, with respect to D_0, by a thin strip.

We have also seen that if $\|R_0\| \leq \eta_0\,E$, where the parameter $\eta_0 \leq c\,\varepsilon$, then $\|R_1\| \leq \eta_1\,E$; η_0 and η_1, which stay for η and η' of the previous section, respectively, are connected by (3.54). The idea one want to develop is to arrange a (finite) sequence of canonical transformations defined in such a way that the remainder of the final normal form is exponentially small as the ultraviolet part $R^{>N}$ of the perturbation.

[13] $\rho_0 = O(\varepsilon^\alpha)$. B is such that the property (3.30) holds

More explicitly we can introduce r perturbative steps and hence, for any $0 \leq l \leq r$, it is given the transformed Hamiltonian $H_l = h + \varepsilon g^l_{\mathcal{L}} + R_l$, defined in $D_l = D_{\rho_l,\sigma_l}(B_l)$, $\rho_l = \rho - \sum_l \delta_l$ and $\sigma_l = \sigma - \sum_l \xi_l$, with $\|\varepsilon g^l_{\mathcal{L}} + R_l\| \leq \varepsilon_l E$ and $\|R_l\| \leq \eta_l E$. It is shown (see [42]) that the sequence of arbitrary parameters δ_l and ξ_l, $l = 0, 1, \ldots, r$, can be chosen so that

a. there are given $\sum_l^r \delta_l < \rho$ and $\sum_l^r \xi_l < \sigma$. Since at each step the domain is reduced by a strip measured by δ_l, ξ_l, after r steps the extension of D_0 gets reduced by a certain factor;

b. in the formula that determines η_l, $l = 1, \ldots, r$, [14]

$$\eta_{l+1} = C_3\, \xi_l^{-2}\, e^{-\frac{1}{2}\xi_l\, N}\, \eta_l + C_6\, \xi_l^{-6}\, (E\, \delta_l^{-1}\, \varepsilon_0^{-\alpha})^2\, \varepsilon_l\, \eta_l = \Lambda(\delta_l, \xi_l, \varepsilon_l)\, \eta_l \qquad (3.56)$$

(let us note that $\varepsilon_l = \varepsilon(\delta_{l-1}, \xi_{l-1})$ see (3.55)), for all l the factor Λ satifies the inequality

$$|\Lambda(\delta_l, \xi_l, \varepsilon_l)| < e^{-1} \qquad (3.57)$$

We note that Λ contains two large factors: one ($\varepsilon^{-\alpha}$) is due to small divisors, the other is due to the Cauchy estimates of the Poisson brackets (the negative powers of ξ and δ).

We know that η_l gives the size of the remainder after r steps. In virtue of (3.57) and (3.52)

$$\|R_r\|_{D_r} \leq \eta_r\, E \leq C_7\, e^{-r}\, \varepsilon\, E \qquad (3.58)$$

($\varepsilon = \varepsilon_0$). We are able to construct a canonical transformation $\psi = \psi_r \circ \ldots \circ \psi_0$ that provides a normalization H_r with a remainder that is exponentially as small as the ultraviolet part $R^{>N}$, namely, since we set the ultraviolet cut-off $N = \varepsilon^{-\tau}$ (see (3.8)), the remainder is exponentially decreasing with $1/\varepsilon$, as it is stated in (3.3). In fact, whenever we choose a sequence of transformations ψ_l such that both *a*. and *b*. features hold, from (3.58) we conclude that ψ is produced by $r \simeq N^a$ perturbative steps[15].

Moreover we note that through the property *a*. the transformation ψ satisfies (3.44),

$$\|\psi^I - I^I\|_{\mathcal{B}_1} \leq \frac{1}{2} \sum_l^{N^a} \delta_l \leq \frac{\delta}{2}\ , \qquad (3.59)$$

i.e. it can be chosen arbitrarily close to the identity since δ and ξ are free.

Let us summarize our results on the analytic part.

$\mathcal{L}$ is a resonance and B is the subset of action space $\mathcal{B}$ such that (3.30) holds. A Hamiltonian (3.28) is analitic in a suitable complex domain $D = D_{\rho,\sigma}(B)$, $\rho = O(\varepsilon^{(\alpha+\tau)})$, ε small enough. There exists a canonical transformation $\psi : D' \longrightarrow D$, $D' = D_{\rho-\delta\,\sigma/2}(B')$, $B^{-\delta} \subset$

[14] i.e. the recursive application of (3.54)

[15] In [42] the calcolations are performed for $a = 1/4$.

$B' \subset B$, which satisfies (3.59) such that in the new coordinates the Hamiltonian (3.28) takes the form

$$H'(I,\varphi) = h(I) + \varepsilon\, g_{\mathcal{L}\,\nu}(I,\varphi,\varepsilon) + R(I,\varphi,\varepsilon) \tag{3.60}$$

$$\|R\| \leq O(e^{-cN(\varepsilon)}) \tag{3.61}$$

where $c > 0$, $N(\varepsilon) = \varepsilon^{-\tau}$ and

$$g_{\mathcal{L}\,\nu}(I,\varphi,\varepsilon) = g_{\mathcal{L}}(I,\varepsilon)\; e^{i\nu\varphi}$$
$$g_{\mathcal{L}\,\nu}(I,\varphi,0) = f_\nu(I)$$

f_ν is the Fourier component of f. The time scale connected to the normal form (3.60) is $T_\infty(\varepsilon) = O(e^{cN(\varepsilon)})$

The analytic part and the geometric framework.

We are interested in understanding how the analytic construction, from which the normalization (3.60), is connected to the geometric description of the resonances.

For a given resonance $\mathcal{L}$, $\dim\mathcal{L} = i$ [16], we apply the analitic construction choosing as basic set Λ one of the extended block $B^{ext}_{\mathcal{L}\,d}$ (see (3.19)) related to $\mathcal{L}$. We assume that (3.28) is analytic in $D = D_{2\delta\,\sigma}(\Lambda^{-\delta})$.

Let $I(0) \in B_{\mathcal{L}}$ be the initial datum. As long as the motion $(I(t),\varphi(t))$ of the Hamiltonian (3.28) is such that $I(t) \in B^{ext}_{\mathcal{L}\,d}$ we can use the analytic construction with $C_0 = c^i_\lambda$ and $\alpha = \sigma_i$ (see (3.30) and (3.12)). Therefore it is given a canonical transformation ψ, that provides the normalization (3.60).

We next we give some sketchs on how the transversal motion d and the motion along $l_{\mathcal{L}}(I(0))$ can be estimated.

We focus on the motion $I'(t) = \psi^{p\,-1}(I(t))$ which is the solution of the Hamilton equation $\dot{I}' = -\partial H'/\partial\varphi'$, with the Hamiltonian (3.60). The term $\partial g_{\mathcal{L}}/\partial\varphi'$ is proportional to $\nu \in \mathcal{L}$ and consequently

$$\begin{aligned} I'(t) &= I'(0) - \int_0^t dt' \left[\varepsilon\,\frac{\partial g_{\mathcal{L}}}{\partial\varphi'}(I'(t'),\varphi'(t'),\varepsilon) + \frac{\partial R}{\partial\varphi'}(I'(t'),\varphi'(t'),\varepsilon)\right] \\ &= I'_{\mathcal{L}}(t) - \int_0^t dt'\,\frac{\partial R}{\partial\varphi'}(I'(t'),\varphi'(t'),\varepsilon) \end{aligned}$$

with $I'_{\mathcal{L}}(t) \in l_{\mathcal{L}}(I'(0))$. It follows that

$$\|I'(t) - I'_{\mathcal{L}}(t)\| \leq |t| \left\|\frac{\partial R}{\partial\varphi'}\right\|$$

[16] In our case $i = 1,2$

It is assumed $d = O(\varepsilon^{(\alpha+\tau)})$; it is set $\delta = d/2$ as well. The derivative can be estimated through a Cauchy inequality applied to the domain D and taking account of the estimate (3.61). Finally it results that for $|t| < T_\infty(\varepsilon)$

$$\|I'(t) - I'_{\mathcal{L}}(t)\| \leq O(\varepsilon^{(\alpha+\tau)}) \quad ([17]) \tag{3.63}$$

It is straightforward to determine the transversal motion

$$\begin{aligned} d =& \text{dist}(I(t), l_{\mathcal{L}}(I(0))) \\ &\leq \|I(t) - I'(t)\| + \|I'(t) - I'_{\mathcal{L}}(t)\| + \text{dist}(I'_{\mathcal{L}}(t), l_{\mathcal{L}}(I(0))) \\ &\leq O(\varepsilon^{(\alpha+\tau)}) \end{aligned} \tag{3.64}$$

since from (3.59) both $\|I(t) - I'(t)\|$ and $\text{dist}(I'_{\mathcal{L}}(t), l_{\mathcal{L}}(I(0))) = \|I'_{\mathcal{L}}(0) - I_{\mathcal{L}}(0)\|$ are less than $\delta/2 < d$.

We are left to determine an estimate of the motion along the line of fast drift. We make more quantitative the notes of section (2.3). The Hamiltonian we should take into account is (3.16), i.e. from (3.60) we exclude the remainder R which determines only a transversal motion if $|t|$ is bounded by $T_\infty(\varepsilon)$. A control on $\|I'(t) - I'(0)\|$ is achieved by the conservation of energy, combined with the convexity property

$$m \, \|\mathrm{v}\|^2 \, \leq \, \frac{\partial^2 h}{\partial I \, \partial I}(I)\mathrm{v}\,\mathrm{v} \quad \text{for all } \mathrm{v} \in \mathbb{R}^2 \text{ and } I \in \mathcal{B}$$

for a suitable $m > 0$. The latter is a stronger condition than (3.23) that does not hold for the hamiltonian translation of a one and half degrees of freedom systems.

We expand around $I'(0)$ the 'kinetic energy'

$$h(I'(t)) = h(I'(0)) \, + \, \omega(I'(0)) \, (I'(t) - I'(0)) \, + \, \frac{1}{2} \, h''(\tilde{I}(t)) \, (I'(t) - I'(0)) \, (I'(t) - I'(0))$$

where $h'' = \partial^2 h / \partial I \partial I$ and $\tilde{I}(t)$ belongs to the segment joining $I'(t)$ and $I'(0)$ [18]. From the convexity property of h

$$\frac{1}{2} \, m \, \|I'(t) - I'(0)\|^2 \leq |h(I'(t)) - h(I'(0))| + |\omega(I'(0)) \, (I'(t) - I'(0))| \tag{3.65}$$

Let us denote $\zeta = (I'(t) - I'(0))$. From the conservation of energy ($h_\varepsilon = \text{cost}$)

$$\begin{aligned} |h(I'(t)) - h(I'(0))| \leq& \varepsilon \, |g_{\mathcal{L}}(I'(t), \varphi'(t), \varepsilon) - g_{\mathcal{L}}(I'(t), \varphi'(t), \varepsilon)| \\ &\leq C_6 \, (c\,\delta + \zeta) \, \varepsilon = \, C_6 \, (O(\varepsilon^{(\alpha+\tau)}) + \zeta) \, \varepsilon \end{aligned} \tag{3.66}$$

C_6, and c are positive constants [19].

[17] See [42], where it is taken

$$\alpha + \tau = 1/4 \tag{3.63}$$

[18] $\mathcal{B}$ is convex and hence $\tilde{I}(t)$ belongs to it

[19] See [44] equation (7.9) of the 'analytic lemma'.

The last term of (3.65) can be estimated by means of geometric properties. We neglect a small neighborhood of $\omega = 0$; then we can assume $\mathcal{L}$ to be one dimensional. As $I(0) \in B_{\mathcal{L}}$ it follows that, for $\nu \in \mathcal{L}$, we have

$$\begin{aligned} |\omega(I'(0))\,\nu| \leq & |\omega(I(0))\,\nu| + |h''(\tilde{I}(0))\,(I'(0) - I(0))\,\nu| \\ \leq & c_\lambda^{(1)}\,\varepsilon^{\sigma_1} \;+\; MN\,\delta \leq C_7\,\varepsilon^{\alpha} \end{aligned} \tag{3.67}$$

according to (3.8), (3.29), (3.14), (3.59), recalling that it is set $\sigma_1 = \alpha$ and using the mean value theorem.

Denote $\omega_\perp$ the orthogonal projection of $\omega(I'(0))$ to $\mathcal{L}$; in virtue of (3.67) we can write[20]

$$|\omega_\perp| \leq C_7\,\varepsilon^{\alpha}$$

and thus

$$|\omega(I'(0))\,(I'(t) - I'(0))| \;=\; |\omega_\perp|\,\zeta \leq C_7\,\varepsilon^{\alpha}\,\zeta \tag{3.68}$$

In virtue of (3.67) and (3.68) we can rewrite (3.65) as

$$\frac{1}{2}\,m\,\zeta^2 \;\leq C_9\,\varepsilon^{\alpha}\,\zeta \;+\; C_8\,\varepsilon^{2\alpha+\tau} \equiv\; A_1\,\zeta + A_2 \tag{3.69}$$

$C_9 = C_6 + C_7$, since we assume $\alpha < 1$ (see (3.63)). We conclude that

$$\zeta \leq \frac{A_1}{m}\,\sqrt{1 + 2\,m A_2/A_1^2} = C_{10}\,\varepsilon^{\alpha} \tag{3.70}$$

where

$$\frac{A_2}{A_1^2} = \frac{C_9}{C_8^2}\,\frac{1}{N}$$

N is the ultraviolet cut off (3.8).

Finally, we take account of (3.59) for $\delta = d/2$ and thus (3.70) allows to estimate the motion along $l_{\mathcal{L}}(I(0))$ of the "old variables":

$$d_l \;\leq\; \|I'(0) - I(0)\| + \zeta + \|I'(t) - I(t)\| \leq C_{11}\,\varepsilon^{\alpha} \tag{3.71}$$

In general, for $\mathcal{L}$ with $\dim\mathcal{L} = i$, it is obtained (see [44])

$$d_l \leq C_{11}\,\varepsilon^{(\alpha - (i-1)\tau)} \tag{3.72}$$

Up to now we separately devoted ourself on different domains $B^{ext}_{\mathcal{L},\,d}$; for this reason the parameters $c_\lambda^{(i)}$, σ_i, $i = 0,1,2$, of the geometric construction are still free. A consistency problem arises when all the resonances relevant for $t \leq T_\infty(\varepsilon)$ are considered. It consists in determining a suitable covering of the action space $\mathcal{B}$ into resonance blocks so that the

[20] It is sufficient to note that

$$|\omega_\perp| \leq |\omega_\perp|\,|\nu| = |\omega_\perp \cdot \nu| = |\omega(I'(0)) \cdot \nu|$$

as $|\nu| \geq 1$. This is a trivial case of the "technical lemma 1" of [42].

analytic construction can be applied, and then all of the previous considerations are valid, for $t < T_\infty(\varepsilon)$.

More clearly, whenever $I(0) \in B_{\mathcal{L}}$, $\dim \mathcal{L} = i$, we require that $I(t) \in B^{ext}_{\mathcal{L}\,d}$ and the non-overlapping condition (3.20) holds, i.e. for all $\nu \notin \mathcal{L}$, $|\nu| \leq N = \varepsilon^{-\tau}$

$$|\omega(I(t))\,\nu| > c_\lambda^{(i)}\,\varepsilon^{\sigma_i} \tag{3.73}$$

for $t \leq T_\infty(\varepsilon)$, is satisfied.

On the other hand if $I(t) \in B^{ext}_{\mathcal{L}\,d}$ then $\|I(t) - I(0)\| \leq d + d_l = d_{\mathcal{L}}$, d and d_l are given by (3.64) and (3.72) respectively. Therefore, according to (3.14), for all $\nu \notin \mathcal{L}$, $|\nu| \leq N = \varepsilon^{-\tau}$ we can write

$$\begin{aligned} |\omega(I(t))\,\nu| &> |(\omega(I(0)) + \omega(I(t)) - \omega(I(0)))\,\nu| \\ &> |(\omega(I(0))\,\nu| - MN\,d_{\mathcal{L}} \\ &\geq c_\lambda^{(i+1)}\,\varepsilon^{\sigma_{i+1}} - MC_{11}\,\varepsilon^{(\sigma_i - i\tau)} \end{aligned} \tag{3.74}$$

that is handled in the same way as in (3.67).

The condition (3.73) is satisfied by $I(t) \in B^{ext}_{\mathcal{L}\,d}$, i.e. within a distance $d_{\mathcal{L}}$ from $I(0)$, as long as one has

$$c_\lambda^{(i+1)}\,\varepsilon^{\sigma_{i+1}} - MC_{11}\,\varepsilon^{(\sigma_i - i\tau)} > c_\lambda^{(i)}\,\varepsilon^{\sigma_i} \tag{3.75}$$

Examples of solutions of the "condition of consistency" (3.75) are given in both [42] and [44]. Each of them defines a particular geometric construction such that for any $\mathcal{L}$, if $I(0) \in B_{\mathcal{L}}$ then the analytic construction can be applied as long as $t < T_\infty(\varepsilon)$.

Theses notes on the consistency problem completes our elementary discussion on the main items of the proof of the claim in (3.1); there exists a canonical transformation to a normalization (3.60) through which we can be seen that the motions (3.64) and (3.72)), longitudinal and transversal to $l_{\mathcal{L}}$, are caused for $t < T_\infty(\varepsilon) = O(\|R\|^{-1})$, $\|R\|$ is the estimate (3.61).

3. The structure at a rational winding number.

The fixed points of the iterates of T_ε

The KAM theorem tells us that irrational surfaces retain their topology and are only slightly deformed from the unperturbed ones. The KAM theorem cannot be applied in a neighborhood of a rational surface. The following theorem (see Ref. [104]) gets an insight into the involved structure in a gap between two invariant, irrational surfaces.

We consider, in a Poincaré section, an invariant curve Γ of the mapping T. We suppose the angle corresponding to Γ is rational:

$$\lambda(I)/2\pi = m/n$$

i.e. T^n is the identity in Γ. Poincaré proved that this property of T is not preserved for a small perturbation: for ε small enough, T_ε^n, the n-fold iteration of the perturbed mapping T_ε, has an even multiple of n, i.e., $2,kn$ ($k = 1, 2, \ldots$) fixed points.
The theorem is easily proved.
Without loss of generality we assume $\lambda'(I) > 0$. There exist curves Γ^+, with action I^+, and Γ^-, with action I^-, that are invariant under T, and such that T^n maps Γ^+ counterclockwise and Γ^- clockwise; in fact $n\lambda(I^+) > m2\pi > n\lambda(I^-)$. This property of T^n is retained by T_ε^n. It follows that, for all angle α, between Γ^+ and Γ^- there exists a point P_ε such that

$$\alpha(T_\varepsilon^n(P_\varepsilon)) = \alpha(P_\varepsilon) + n2\pi$$

where $\alpha(x)$ is the angle coordinate of the point x. It follows that P_ε moves under T_ε^n along the radius.
The set of points P_ε's is a closed curve C_ε. This curve is not invariant under T_ε^n.

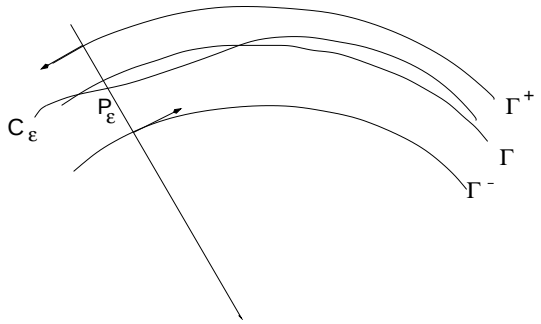

Figure 3.4: The T-invariant curves Γ^+ and Γ^- are rotated through angles λ's incommensurate with 2π. They are close to Γ whose points are fixed under T^n. For ε small enough, between Γ^+ and Γ^- there is a closed curve C_ε whose points move under T_ε^n along the radius, T_ε is the perturbed map.

However, since T_ε^n is area preserving, C_ε and $T_\varepsilon^n(C_\varepsilon)$ enclose an equal area. This is only possible if the two curves cross each other an even number of times: therefore there exist $2k$ crossings $x \in C_\varepsilon$ which are fixed points of T_ε^n (see fig. 3.5).
For ε small enough these points are elliptic or hyperbolic [21]; elliptic and hyperbolic fixed points alternate about the resonance curve. An explanation of this fact can be outlined using fig. 3.5. We examine the mapping in the neighborhood of the fixed points and there are two distinct types of behavior that alternates. Near some fixed points the radial transformation is connected to the winding one where $\lambda/(2\pi) \neq m/n$; thus the phase space tends to circle about the fixed point. In this circumstance the fixed point is elliptic. Near the other fixed points the successive transformations take the points further from the neighborhood of the fixed point. In this second case the fixed point is hyperbolic[22] Two fixed points $x \in C_\varepsilon$ can

[21] For $\varepsilon = 0$ the fixed points in Γ are parabolic, with eigenvalues $\lambda_1 = \lambda_2 = 1$. For ε small enough, the eigenvalues are close to the unperturbed ones: therefore $\lambda_1 \simeq 1 \simeq \lambda_2$, i.e. the occurrence of an hyperbolic point with reflection is excluded.

[22] In appendix 27 of [104] it is introduced the index

$$Ind = sign(dR/d\alpha\ d\lambda/dI)$$

where

$$R(\alpha) = I(T_\varepsilon^n(P)(\alpha)) - I(P(\alpha))$$

is the radial displacement of $P(\alpha) \in C_\varepsilon$ on the radius α, where $I(P)$ is the action coordinate of P. It readily seen that half of

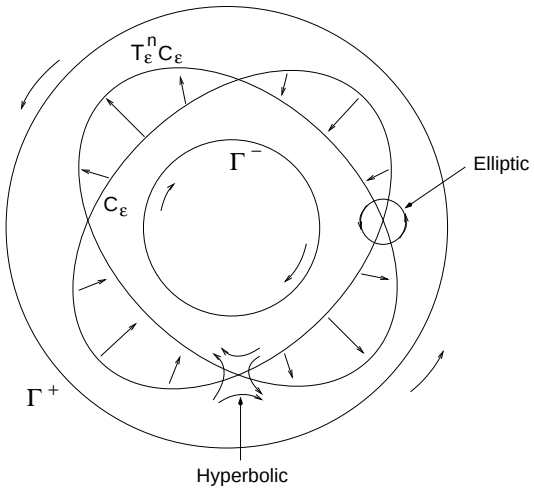

Figure 3.5: In a small perturbation the mapping T_ε^n retains some fixed points in a neighborhood of an invariant curve with a winding number $\lambda/(2\pi) = m/n$. The points of curve C_ε are radially mapped by T_ε^n; the intersections of C_ε and $T_\varepsilon^n C_\varepsilon$ are preserved fixed points. It is shown the circumstance $k = 1$ and $n = 2$.

belong to different orbits $\{T_\varepsilon^l x, 0 \leq l \leq (n-1)\}$. All points of an orbits are fixed points of T_ε^n; as well they are elliptic whenever x is elliptic. Let k be the number of elliptic points with different orbits; then there are kn elliptic points. This proves the existence of $2kn$ (elliptic and hyperbolic) fixed points of T_ε^n in a neighborhood of Γ.

The perturbed mapping in a neighborhood of an elliptic point.

In sections 5.1 and 5.2 we investigated the phase space in the neighborhood of an elliptic fixed point at a resonance.
By canonical transformations we examined both the primary resonance and, in the neighborhood of each of its elliptic points, the higher order resonances, i.e., fixed points which have motions similar to that of the primary resonance but on a finer scale. A secondary resonance rapidly becomes small as the order of the resonance increases. If the perturbation is small the most of the phase space is topologically similar to the corresponding, integrable problem. In the remaining, topologically modified space new closed curves fill the regions surrounding the elliptic points; these curves are invariant under T_ε^n. Therefore a perturbation does not change the stable character of the dynamics in a neighborhood of an elliptic point at a resonance.
In the pendulum-like pattern of a resonance hyperbolic points of T_ε^n are given. Stochastic motions can take place only in the neighborhood of the hyperbolic points where separatrices intersect each other and create an intertwined structure.

the fixed points have index $+1$ and the others have index -1 and the first ones separate the second ones. A point with index $+1$ is elliptic and one with index -1 is hyperbolic (see appendix 27 of [104]).

The perturbed mapping in a neighborhood of a hyperbolic point.

At the hyperbolic singularity p there are four curves of the separatrix passing to through the point : two trajectories $W^s(p)$ entering to and two trajectories $W^u(p)$ leaving the fixed point. At a resonance we may have a chain of kn hyperbolic points of T_ε^n.

In a integrable problem with a chain of hyperbolic points the separatrix smoothly joins a hyperbolic point to its nearest neighbors; a branch of separatrix is a W^s curve of a hyperbolic end point and a W^u curve of the other hyperbolic end point.
Let T be the time shift mapping of the integrable system. A separatrix is an invariant curve of T; the period is infinite on the separatrix trajectory.
When a point z lies in $W^s(p)$ the iterates $T^n z$ appraoch the hyperbolic point p as $n \to \infty$. Similarly when z lies on $W^u(p)$ $T^{-n}z$ is brought to the hyperbolic point as $n \to \infty$. In each case the approaching of the iterates of z to the hyperbolic point becomes increasingly slow as n increases.

The problem of the mapping in a neighborhood of a resonance corresponds to a near-integrable system. In this case the situation is more complicated. For semplicity of notation we write T instead of T_ε^n.
Two hyperbolic points of T are not smoothly joined by a separatrix and W^u and W^s do not close on themself. The W^u curve leaving one hyperbolic point p_1 transversely intersects the W^s curve entering the neighboring hyperbolic point p_2[23]. It is easy to see that, if there is one point $q \in W^u(p_1) \cap W^s(p_2)$, with $q \neq p_i$, $i = 1, 2$, then an infinity of points lie in $W^u(p_1) \cap W^s(p_2)$. In fact W^u and W^s are invariant sets of T; therefore $T^l(q) \in W^u(p_1) \cap W^s(p_2)$, $l \in \mathcal{Z}$.
The point q lies in $W^s(p_1) \cap W^u(p_2)$. As $W^s(p_1)$ approaches p_2 it intersects $W^u(p_2)$ at a set of points $\{q_i\}$ that accumulate against p_2, due to the slowdown of motion in the neighborhood of p_2. In addition, the areas enclosed by the intersections are conserved since they are mapped one to the other and T is determined by an Hamiltonian flow. Therefore $W^s(p_1)$ oscillates with an amplitude that increases as p_2 is approached (see fig. 3.6). Similarly the curve $W^s(p_2)$ arrives at p_1 oscillating just as wildly as what we have described above and so also for the other two branches. Thus in the neighborhood of the singular point p_2 $W^s(p_1)$ from below also oscillates in an erratic way and intersects $W^u(p_1)$ from above an infinite number of times.
The orbit $\{T^n(q)\}$ plays an important rôle in the global dynamics of the map T. The violent winding of the invariant curves W^u, W^s in the neighborhood of p_i leads to a sensitive dependence of orbits $\{T^n(x_0)\}$ on the initial condition x_0; the presence of homoclinic orbits tends to promote erratic behavior. The homoclinic points by themselves do not completely yield the complex region near a separatrix. The period of rotation goes to infinity at the separatrix. Thus in the neighborhood of the separatrix there an infinite number of secondary resonances. Each resonance has its own set of hyperbolic fixed points (that alternate with elliptic ones) with its own wild motion. Oscillating invariant curves at hyperbolic points of the secondary resonances intersect both each other and the first order separatrix trajectories. All of these trajectories fill densely regions of phase space bounded between KAM curves; only there an exceedingly complicated behavior can take place and stochasticity occurs, even under a

[23] It is known as the 'splitting' of the separatrix.

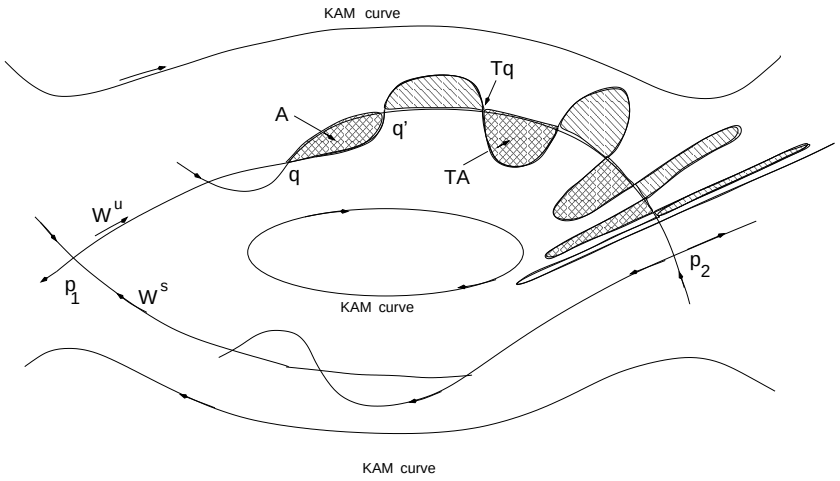

Figure 3.6: Pattern of the intersections between the invariant curve $W^u(p_1)$ and $W^s(p_2)$ in the neighborhood of the hyperbolic point p_2. Successive crossings are closer together and the oscillations become more wildly as p_2 is approached.

small perturbation.

4. Description of the dynamics inside a resonance: slow and fast variables.

In order to support these qualitative considerations on the mechanism that gives rise to non integrability at a resonance we introduce a more quantitive approach following [42].

We suppose that, in the coordinates (I', φ'), the Hamiltonian (3.2) has the form (3.60).

We consider a oscillator perturbed by a periodic force with frequency u. The unperturbed Hamiltonian $h(I_1', I_2')$ is (3.15). We focus on a resonance $(I_1^{0'}, I_2^{0'})$ of multiplicity one, i.e. there exists $(\nu_1, \nu_2) \in \mathcal{L} \subset \mathbb{Z}^2$, $\dim \mathcal{L} = 1$, such that

$$\nu_1 \, h_0'(I_1^{0'}) + \nu_2 \, u = 0$$

One can find a linear, "canonical" change of coordinates $\mathcal{C}_R$ (see [44], Sec. 9, lemmas 5, 6)

$$\mathcal{C}_R : \; (I', \varphi') \; \longrightarrow \; (\tilde{I}, \tilde{\varphi}) = (RI', \; R^{T^{-1}} \varphi')$$

where R is an integer matrix with determinant one, such that the frequency vector evaluated at $\tilde{I}_0 = R \, I_0'$ has the form

$$\frac{\partial h}{\partial \tilde{I}}(\tilde{I}_0) = (0, \omega) \qquad\qquad \omega \in \mathbb{R} \tag{3.76}$$

It is easy to show that (see appendix ?)

$$R = \begin{pmatrix} a & b \\ -\nu_2 & \nu_1 \end{pmatrix}$$

where $(a, b) \in \mathbb{Z}^2$ such that $\det R = 1$.

Consider the Hamiltonian (3.60), where h is given by (3.15). A motion that starts near the resonance $\tilde{I}_0 = (\tilde{I}_1^0, \tilde{I}_2^0)$, i.e. $h_0'(\tilde{I}_1^0) = 0$, can be written as

$$\begin{aligned} \tilde{I}_1(t) &= \tilde{I}_1^0 + \sqrt{\varepsilon}\, p_1(\sqrt{\varepsilon}\, t) & \tilde{\varphi}_1(t) &= \gamma_1(\sqrt{\varepsilon}\, t) \\ \tilde{I}_2(t) &= \tilde{I}_2^0 + \sqrt{\varepsilon}\, p_2(\sqrt{\varepsilon}\, t) & \tilde{\varphi}_2(t) &= \gamma_2(\sqrt{\varepsilon}\, t) \end{aligned} \tag{3.77}$$

This is the convenient way to study the motions from initial data close within ε^α, $\alpha < 1/2$, to the resonance. Substituting (3.77) into the Hamilton's equations

$$\begin{aligned} \varepsilon\, \dot{p}_1(\sqrt{\varepsilon}t) &= -\,\varepsilon\, \frac{\partial g_{\mathcal{L}}}{\partial \tilde{\varphi}_1}(\tilde{I}_1^0 + \sqrt{\varepsilon}\, p_1(\sqrt{\varepsilon}\, t),\, \tilde{I}_2^0 + \sqrt{\varepsilon}\, p_2(\sqrt{\varepsilon}\, t), \gamma_1(\sqrt{\varepsilon}\, t), \gamma_2(\sqrt{\varepsilon}\, t), \varepsilon) \,-\, \frac{\partial R}{\partial \tilde{\varphi}_1} \\ \varepsilon\, \dot{p}_2(\sqrt{\varepsilon}t) &= -\,\varepsilon\, \frac{\partial g_{\mathcal{L}}}{\partial \tilde{\varphi}_2}(\tilde{I}_1^0 + \sqrt{\varepsilon}\, p_1(\sqrt{\varepsilon}\, t),\, \tilde{I}_2^0 + \sqrt{\varepsilon}\, p_2(\sqrt{\varepsilon}\, t), \gamma_1(\sqrt{\varepsilon}\, t), \gamma_2(\sqrt{\varepsilon}\, t), \varepsilon) \,-\, \frac{\partial R}{\partial \tilde{\varphi}_2} \\ \sqrt{\varepsilon}\, \dot{\gamma}_1(\sqrt{\varepsilon}\, t) &= h_0'(\tilde{I}_1^0 + \sqrt{\varepsilon}\, p_1(\sqrt{\varepsilon}\, t)) \\ &\quad + \varepsilon \frac{\partial g_{\mathcal{L}}}{\partial \tilde{I}_1}(\tilde{I}_1^0 + \sqrt{\varepsilon}\, p_1(\sqrt{\varepsilon}\, t),\, \tilde{I}_2^0 + \sqrt{\varepsilon}\, p_2(\sqrt{\varepsilon}\, t), \gamma_1(\sqrt{\varepsilon}\, t), \gamma_2(\sqrt{\varepsilon}\, t), \varepsilon) \,+\, \frac{\partial R}{\partial \tilde{I}_1} \\ \sqrt{\varepsilon}\, \dot{\gamma}_2(\sqrt{\varepsilon}\, t) &= u + \varepsilon \frac{\partial g_{\mathcal{L}}}{\partial \tilde{I}_2}(\tilde{I}_1^0 + \sqrt{\varepsilon}\, p_1(\sqrt{\varepsilon}\, t),\, \tilde{I}_2^0 + \sqrt{\varepsilon}\, p_2(\sqrt{\varepsilon}\, t), \gamma_1(\sqrt{\varepsilon}\, t), \gamma_2(\sqrt{\varepsilon}\, t), \varepsilon) \,+\, \frac{\partial R}{\partial \tilde{I}_2} \end{aligned}$$

For ε small enough and denoting $\tau = \sqrt{\varepsilon}\, t$ they are written

$$\dot{p}_1(\tau) = -\,\frac{\partial g_{\mathcal{L}}}{\partial \tilde{\varphi}_1}(\tilde{I}_1^0 + \sqrt{\varepsilon}\, p_1(\tau),\, \tilde{I}_2^0 + \sqrt{\varepsilon}\, p_2(\tau), \gamma_1(\tau), \gamma_2(\tau), \varepsilon) \,-\, \frac{1}{\varepsilon}\, \frac{\partial R}{\partial \tilde{\varphi}_1} \tag{3.78}$$

$$\dot{p}_2(\tau) = -\,\frac{\partial g_{\mathcal{L}}}{\partial \tilde{\varphi}_2}(\tilde{I}_1^0 + \sqrt{\varepsilon}\, p_1(\tau),\, \tilde{I}_2^0 + \sqrt{\varepsilon}\, p_2(\tau), \gamma_1(\tau), \gamma_2(\tau), \varepsilon) \,-\, \frac{1}{\varepsilon}\, \frac{\partial R}{\partial \tilde{\varphi}_2} \tag{3.79}$$

$$\begin{aligned} \dot{\gamma}_1(\tau) &= h_0''(\tilde{I}_1^0)\, p_1(\tau) \\ &\quad + \sqrt{\varepsilon} \frac{\partial g_{\mathcal{L}}}{\partial \tilde{I}_1}(\tilde{I}_1^0 + \sqrt{\varepsilon}\, p_1(\tau),\, \tilde{I}_2^0 + \sqrt{\varepsilon}\, p_2(\tau), \gamma_1(\tau), \gamma_2(\tau), \varepsilon) + \frac{1}{\sqrt{\varepsilon}}\, \frac{\partial R}{\partial \tilde{I}_1} \end{aligned} \tag{3.80}$$

$$\begin{aligned} \dot{\gamma}_2(\tau) &= \frac{u}{\sqrt{\varepsilon}} \\ &\quad + \sqrt{\varepsilon} \frac{\partial g_{\mathcal{L}}}{\partial \tilde{I}_2}(\tilde{I}_1^0 + \sqrt{\varepsilon}\, p_1(\tau),\, \tilde{I}_2^0 + \sqrt{\varepsilon}\, p_2(\tau), \gamma_1(\tau), \gamma_2(\tau), \varepsilon) + \frac{1}{\sqrt{\varepsilon}}\, \frac{\partial R}{\partial \tilde{I}_2} \end{aligned} \tag{3.81}$$

where $\zeta > 0$. We notice that γ_2 rotates very faster than γ_1 (compare (3.80) and (3.81)). Therefore we are allowed to describe the motions of p_1, p_2 and γ_1, on time scales larger than $1/\sqrt{\varepsilon}$, considering the the solutions of the averages over the "fast angle" γ_2 of the equations of motion (3.78) - (3.81). Furthermore we study the motion up to time scales $O(e^{c\varepsilon^{-\zeta}})$, namely we neglect the remainders.

Accordingly, from the equation (3.79) we see that

$$\dot{p}_2(\tau) = -\,\overline{\frac{\partial g_{\mathcal{L}}}{\partial \tilde{\varphi}_2}}(\tilde{I}_1^0 + \sqrt{\varepsilon}\, p_1(\tau),\, \tilde{I}_2^0 + \sqrt{\varepsilon}\, p_2(\tau), \gamma_1(\tau), \gamma_2(\tau), \varepsilon) = 0 \tag{3.82}$$

where the overline denote the average over γ_2. Therefore for $1 < \tau < \varepsilon\, T_\infty(\varepsilon)$ the "fast" action $\tilde{I}_2$ results to be a constant parameter; it can appreciably move on times of order $T_\infty(\varepsilon)$.

Let us consider the initial datum $\tilde{I}_2(0) = \tilde{I}_2^0 + \sqrt{\varepsilon}\ p_2^0$. Thus the equations (3.78) and (3.80), averaged over γ_2, are the Hamilton's equations of the "slow variables" γ_1, p_1, relating to the "effective Hamiltonian"

$$H_{\tilde{I}_1^0\ \tilde{I}_2^0}(p_1,\gamma_1) = \frac{1}{2}\, h_0''(\tilde{I}_1^0)\ p_1^2 + \overline{g}_{\mathcal{L}}(\tilde{I}_1^0 + \sqrt{\varepsilon}\, p_1,\ \tilde{I}_2^0 + \sqrt{\varepsilon}\, p_2^0, \gamma_1, \varepsilon) \tag{3.83}$$

where $\overline{g}_{\mathcal{L}}$ is the average of $g_{\mathcal{L}}$ over γ_2. The Hamiltonian depends on both the parameters $\tilde{I}_1^0, \tilde{I}_2^0$ corresponding to the resonance we have considered [24].

The term $\overline{g}_{\mathcal{L}}$ in (3.83) can take a form in which a function, independent of ε, is separated:

$$\overline{g}_{\mathcal{L}}(\tilde{I}_1^0 + \sqrt{\varepsilon}\, p_1,\ \tilde{I}_2^0 + \sqrt{\varepsilon}\, p_2^0, \gamma_1, \varepsilon) = V^0_{\tilde{I}_1^0\ \tilde{I}_2^0}(\gamma_1) + \sqrt{\varepsilon}\, V^1_{\tilde{I}_1^0\ \tilde{I}_2^0}(p_1, p_2^0, \gamma_1, \varepsilon) \tag{3.84}$$

where

$$V^0_{\tilde{I}_1^0\ \tilde{I}_2^0}(\gamma_1) = \overline{g}_{\mathcal{L}}(\tilde{I}_1^0,\ \tilde{I}_2^0, \gamma_1, 0)$$

We have got a result that we have already obtained: within the approximation in which the "effective" Hamiltonian (3.83) is good, a simple resonance is an integrable system. It is essentially a pendulum with a potential $, V^0_{\tilde{I}_1^0\ \tilde{I}_2^0}(\gamma_1) + O(\varepsilon^{1/2})$. This is the only nontrivial possibility in our case (Hamiltonian system with two degrees of freedom) except for a neighborhood of $\omega = 0$ where a resonance of order two takes place and the motion is like the one of a really two degrees of freedom system.

We also take into account the degree of freedom of the "fast" variables γ_2, p_2 for $t < T_\infty(\varepsilon)$. The dynamics of γ_2 is determined by (3.81) while, according to (3.82), p_2 is "frozen". Therefore the "fast" evolution is driven by the Hamiltonian

$$\frac{p_2\, u}{\sqrt{\varepsilon}} \ +\ \sqrt{\varepsilon}\, V^1_{\tilde{I}_1^0\ \tilde{I}_2^0}(p_1, p_2, \gamma_1, \varepsilon) \tag{3.85}$$

We resume the remarks we have stated in this section. Let $\mathcal{L}$ be a resonance of order one and it is given $\tilde{I}_0 = (\tilde{I}_1^0, \tilde{I}_2^0) \in B_{\mathcal{L}}$ such that the condition (3.76) holds. A motion $(\tilde{I}(t), \tilde{\varphi}(t))$ with action initial data $(\tilde{I}_1(0), \tilde{I}_2^0) \in B_{\mathcal{L}}$ is described by the rescaled variables $p_1, p_2, \gamma_1, \gamma_2$, defined in (3.77), whose dynamics is governed by the Hamiltonian

$$\begin{aligned} \mathcal{H}_{\tilde{I}_1^0\ \tilde{I}_2^0}(p_1, p_2, \gamma_1, \gamma_2) = h_{fast}(p_2) \ +\ H^{eff}_{\tilde{I}_1^0\ \tilde{I}_2^0}(p_1, \gamma_1) \ +\ \sqrt{\varepsilon}\, V^1_{\tilde{I}_1^0\ \tilde{I}_2^0}(p_1, p_2, \gamma_1, \varepsilon) \\ +\ \frac{1}{\varepsilon}\, \tilde{R}(p_1, p_2, \gamma_1, \gamma_2, \varepsilon) \end{aligned} \tag{3.86}$$

$$\begin{aligned} h_{fast}(p_2) &= \frac{p_2\, u}{\sqrt{\varepsilon}} \\ H^{eff}_{\tilde{I}_1^0\ \tilde{I}_2^0}(p_1, \gamma_1) &= \frac{1}{2}\, h_0''(\tilde{I}_1^0)\ p_1^2 + V^0_{\tilde{I}_1^0\ \tilde{I}_2^0}(\gamma_1) \end{aligned}$$

[24] We know that the condition (3.76) is provided by $\omega_1(\tilde{I}_1^0) = 0$. In [44] it is shown that a function $\tilde{I}_1^0(\tilde{I}_2^0)$ is implicitly defined by $\omega_1(\tilde{I}_1^0(\tilde{I}_2^0), \tilde{I}_2^0) = 0$. Consequently the Hamiltonian (3.83) results to be dependent on only one parameter, However, in our case the existence of the function cannot be established as it is required the convexity property which is not yielded.

where we have removed all approximations and also considered the exponentially small coupling term ($\|R\| \leq O(e^{-c\varepsilon^{-\zeta}})$). Of course the variables $p_1, p_2, \gamma_1, \gamma_2$ are canonical as their motion is described by canonical equations with the Hamiltonian (3.86).

The method of characterizing the dynamics in terms of slow and fast variables is strongly connected to the geometric features of the dynamics close to a (one dimensional) resonance $\mathcal{L}$, for $t < T_\infty(\varepsilon)$, described above:

- the integrable dynamics of the "slow" degree of freedom corresponds to the motion along the "line of fast drift" $l_{\mathcal{L}}$. It is essentially defined by the Hamiltonian $H^{eff}_{\tilde{I}_1^0\,\tilde{I}_2^0}$ and hence it is bounded in a domain $O(1)$, i.e. it is $O(\varepsilon^{1/2})$ in the original coordinates $\tilde{I}$ ($\tilde{I}_i \sim \varepsilon^{1/2}\, p_i$);
- the dynamics of the "fast" variable p_2 is connected to the transversal motion, namely the motion along the resonance line $\Sigma_{\mathcal{L}}$. We know that p_2 is a constant of motion (see (3.82)); this is linked to the "essential" confinement of the motion in $l_{\mathcal{L}}$, since, we know, the transversal motion produces a small displacement ($d \sim O(\varepsilon^\sigma)$, $\sigma < 1/2$) in a very long time ($\sim T_\infty(\varepsilon)$), i.e. it is "extremely slow".

The functions V^0 and V^1 depend on h, f and their first two derivatives; in fact the γ_1 dependence of the first three terms in (3.86) follows by a Taylor expansion of $h + \varepsilon\, f$.

We stress that, though all these considerations require the condition (3.76) of the resonance, the example is generic since R, a transformation to canonical variables such that (3.76) is verified, can always be introduced.

The form of the Hamiltonian (3.86) implies far reaching consequences, particularly, for resonances of multiplicity at least two. A deeper discussion of this matter can be found in [44]. We devote the next section to some notes on the meaning of (3.86) regarding a resonance of order one.

4.1 Times scales near a resonance.

For the reason that the Hamiltonian is turned into the form (3.86) it is made evident the existence of three time scales of the perturbed dynamics inside a resonance (E is the parameter that gives the size of the energy (see (3.34))):

- $t < (\sqrt{\varepsilon}\, E)^{-1} \equiv T_{1/2}(\varepsilon)$ "the unperturbed time scale"; the dynamics is driven by h_{fast}.
- $T_{1/2}(\varepsilon) < t < E^{-1}\, e^{c\, \varepsilon^{-\zeta}} \equiv T_\infty(\varepsilon)$ "the perturbative regime"; in this time scale the relevant Hamiltonian is

$$h_{fast}(p_2) \;+\; H^{eff}_{\tilde{I}_1^0\,\tilde{I}_2^0}(p_1, \gamma_1) \;+\; \sqrt{\varepsilon}\, V^1_{\tilde{I}_1^0\,\tilde{I}_2^0}(p_1, p_2, \gamma_1, \varepsilon) \tag{3.87}$$

- $t > T_\infty(\varepsilon)$ "the strongly perturbed regime"; all terms of (3.86) play a role.

For each time scale we discuss the main features of the dynamics inside a resonance of the first order (many results can be extended to resonances of a greater order).

In the unperturbed regime the system is integrable; all variable are frozen except for the "fast" angle.

In the "perturbative regime", the fast momentum is still frozen and the fast angle has an angular speed of $O(1)$ $(= u)$. On the other hand the slow variables evolve as described by the one degree of freedom Hamiltonian $H^{eff} + \varepsilon^{1/2} V^1$. Hence, in the approximation connected to the time scale, the motion is always integrable, no matter how the potentials V^0 and V^1 are chosen [25], and takes place in a bounded domain of $O(1)$, i.e. it is $\tilde{I} \sim O(\varepsilon^{1/2})$ (a domain small with ε). Therefore for the whole perturbative regime chaotic motions cannot occur. Indeed the main point is that p_2 is a constant parameter and hence in the motion defined by (3.87) the "slow" dynamics is decoupled. Consequently the motion are local and regular.

In the "strongly perturbed regime" both the slow and the fast variables perform non-trivial motions; the actions can change as it is allowed by the conservation of the total energy. Therefore we deal with a irreducible dynamics with just two degrees of freedom. In this case, potential functions, producing chaotic motion, can be found (in the appendix A of [44] a Hamiltonian system with two degrees of freedom, containing homoclinic intersections, is explicitly constructed). Later on we will provide a heuristic explanation of how chaos can arise in systems with two degrees of freedom (Melnikov's method). It is important to note that the motions are still local: in the "strongly perturbed regime" we can find chaotic motions that evolve bounded, close to a first order resonance.

We notice that if the initial datum of motion is in a non-resonance block then the scaling (3.77) cannot be considered, i.e. the variables p's and γ's cannot be introduced. Therefore the perturbative regime disappears and the unperturbed scale extends up to $T_\infty(\varepsilon)$ [27].

Resume. For a Hamiltonian system with two degrees of fredoom, except a small neighborhood of $\omega = 0$, the phase space is either in a block of order one or in the non-resonance block; hence in such a case we cannot expect to see any chaotic phenomena before a time scale $T_\infty(\varepsilon)$. The chaotic motions are bounded near the resonances.

5. Homoclinic chaos in a resonance. Heuristic discussion.

The Hamiltonian (3.83) can be helpful to understand how chaotic motions occur near a resonance. Since we consider the dynamics for times larger than $T_\infty(\varepsilon)$ we should only require

[25] The situation is completely different for a resonance of order $r \geq 2$. Consider the system defined by H^{eff}: it is a system with at least two degrees of freedom. In this case we can always find potentials that produce chaotic motions [26]. V^0 is a function that can get any arbitrarly assigned form by suitably choosing f. Therefore whenever resonances of order $r \geq 2$ take place, chaotic motions can occur in the perturbative regime; with respect to the original coordinates they are local since take place inside the resonance. On account of the structural stability the same features are verified in the system $H^{eff} + \varepsilon^{1/2} V^1$

[27] Since most of the phase space consists of points in the non-resonance block there is a connection between this mechanism of stability and the KAM theorem.

that p_2 is not longer a constant parameter, as p_2 changes on this time scale.

Suppose, for definiteness, that

- the one dimensional motion of the slow variables p_1, γ_1 is described by the "pendulum Hamiltonian";
- the pendulum is driven by a harmonic force

$$f(t) = \varepsilon \cos(\omega t)$$

with ω that is "constant" and $\omega/(2\pi) \sim T_\infty(\varepsilon)^{-1}$.

The "fast" action

$$p_2 \approx \frac{\gamma_1}{u} f(t)$$

is conjugated to $\gamma_2 = u\, t$, $\omega/u \ll 1$ [28]. We notice that the time scale of f determines that of p_2; in fact since $\omega^{-1} \ll \dot{\gamma}_1^{-1}$ p_2 changes over the time scale $O(T_\infty(\varepsilon))$ of the period of f. Furthermore $\dot{p}_2(t) \simeq 0$ (see 3.89). Thus we are left to the equation of motion

$$\ddot{\gamma}_1 + \sin\gamma_1 = \varepsilon \cos(\omega t) \tag{3.91}$$

The model of forced pendulum permits to relate the problem of the onset of chaos at a resonance to the mechanism of "homoclinic intersection", i.e., as we have already notice above, chaotic motions at a resonance are an instance of the "homoclinic chaos"; by means of the "Melnikov's method" (see [106]) it is not difficult to give a quantitative support to the qualitative considerations, stated in the section above. The discussion is only heuristic; in fact, instead to consider the equation (3.97) with a constant $\omega = O(T_\infty(\varepsilon))$, strictly, one should face the difficult problem which consists in replacing ω with $\omega(\varepsilon) = c/T_\infty(\varepsilon)$, $c > 0$.

In the plane (q, v), $q = \gamma_1$ and $\mathrm{v} = p_1$, it is defined the Poincaré map P_ε corresponding to the section $\omega t = 0 \,(\mathrm{mod}\, 2\pi)$ at any fix energy E, i.e. any point of the plane (q, v) is mapped

[28] The Hamiltonian

$$H(p_1, p_2, \gamma_1, \gamma_2) = \frac{p_1^2}{2} - \cos\gamma_1 - \varepsilon\, \gamma_1 \cos(\frac{\omega}{u}\gamma_2) + p_2\, u$$

defines the forced pendulum-like dynamics for the variables $\gamma_1,\ p_1$, while the equations of motions for the "fast" variables are

$$\begin{aligned} \dot{\gamma}_2 &= u \\ \dot{p}_2 &= -\varepsilon\, \gamma_1\, \frac{\omega}{u} \sin(\frac{\omega}{u}\gamma_2) \end{aligned} \tag{3.88}$$

By the definition of "fast" speed $u \sim \varepsilon^{-1/2}$ we have $u^{-1} \ll T_{1/2}(\varepsilon)$ and hence

$$\dot{p}_2 \sim \gamma_1\, \frac{\omega}{u} \sim \frac{\gamma_1}{T_\infty(\varepsilon)}\, u^{-1} \sim \delta\gamma_1(u^{-1}) \simeq 0 \tag{3.89}$$

We integrate by part (3.88) and, by applying the mean theorem, we get

$$p_2 \sim \frac{\varepsilon}{u}\, \gamma_1 \cos(\omega t) - \frac{\varepsilon}{u} \int dt'\, \dot{\gamma}_1(t') \cos(\omega\, t') \simeq \frac{\varepsilon}{u}\, \gamma_1\, (\cos(\omega t) - \cos(\omega t^*)) \tag{3.90}$$

Therefore p_2 changes over a time scale ω^{-1} since it evolves following the "slowest" function $f(t)$.

into the point $P_\varepsilon(q, \mathrm{v})$ to which it evolves in the time $2\pi/\omega$. We know that for $\varepsilon = 0$ the map admits two hyperbolic points $z_0^\pm = (0, \pm\pi)$, connected by the separatrices

$$\xi_0^\pm(q) = \pm\sqrt{2\,(1+\cos q)}$$

The problem is defined except for a 2π-translation of the angle. Thus instead of the plane (q, v) we can use the representation of the cylinder where the q-axis is drawn as a circle. So the fixed points z_0^+ and z_0^- merge into one point z_0 The separatrices are both stable and unstable manifolds of z_0.

For small ε, P_ε has a fixed point z_ε close to z_0 (by the implicit function theorem). Unlike the $\varepsilon = 0$ case, the stable and unstable manifolds of z_ε, are no longer merged into each other and cross at a "homoclinic point" A_ε, with a nonzero angle α_ε. Let ξ_ε^s and ξ_ε^u denote the stable manifold and the unstable one, respectively.

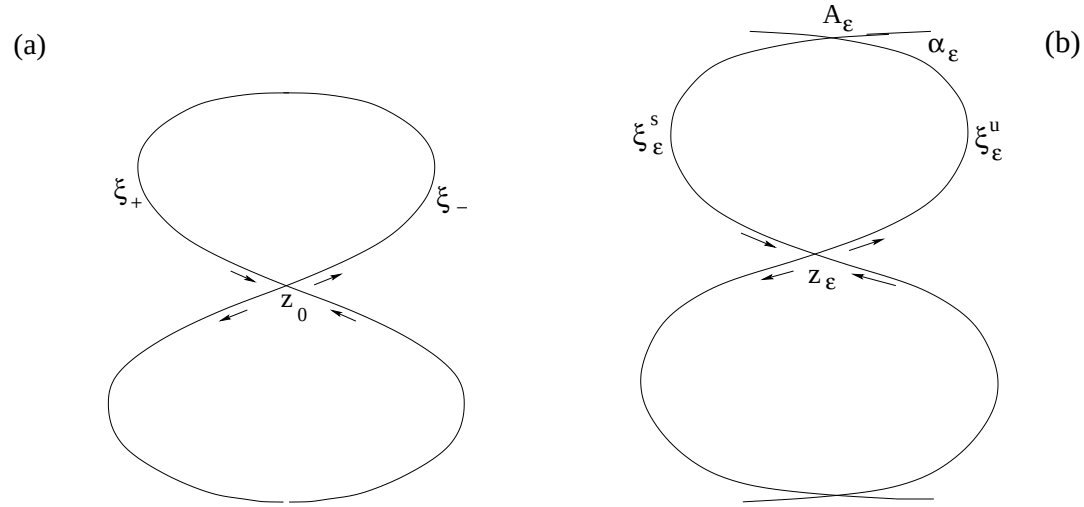

Figure 3.7: (a) Separatrix of the unperturbed pendulum: z_0 is the hyperbolic point and the stable ξ_+ and the unstable ξ_- manifolds merge into each other. (b) The "splitting" of the stable ξ_ε^s and unstable ξ_ε^u manifolds of z_ε for $\varepsilon \neq 0$; A_ε is a homoclinic point.

We already discussed in section 3. about the mechanism that leads to chaotic motions near the separatrix for $\varepsilon \neq 0$, owing to the transversal crossings between ξ_ε^s and ξ_ε^u [29]. We shall apply the Melnikov's method in order to prove the existence of one transversal, homoclinic point.

The first item to check is that $\lambda_0 = 1$ is not an eigenvalue of the Jacobian $dP_0(z_0)$ of the Poincaré map for $\varepsilon = 0$ at $z_0 = (\pi, 0)$. To this end we consider a motion on the separatrix of the unperturbed pendulum [30]

$$Q(t) = \pi - 4\arctan e^{-t} \tag{3.92}$$

corresponding to the initial datum $q(0) = 0$, $\dot q(0) = 2$. The "upper part" $(q, \xi_0^+(q))$ and the "lower part" $(q, \xi_0^-(q))$ of the separatrix are described by $(Q(t), \dot Q(t))$ and $(Q(t), -\dot Q(t))$,

[29] We know that if stable and unstable manifolds cross once they cross infinitely many times.

[30] whose equation is $\dot q = (2\,(1+\cos q))^{1/2}$

respectively. By definition, for $q = Q(t)$ we have $P_0(q, \xi_0^+(q)) = (q', \xi_0^+(q'))$ where $q' = Q(t + 2\pi/\omega)$.

We consider $|\pi - q| \ll 1$ hence it is $t \gg 1$ and then we can write $\arctan e^{-t} \simeq e^{-t}$. We notice that

- for the transformed point q' under the Poincaré map

$$q' - \pi \simeq (q - \pi)\, \lambda_0^- \tag{3.93}$$

  where $\lambda_0^- = e^{-2\pi/\omega}$; furthermore

- since $\xi_0^+(q) \simeq -(q - \pi)$ $(\xi_0^+(\pi) = 0)$ hence

$$\xi_0^+(q') \simeq -(q' - \pi) \simeq \xi_0^+(q)\ \lambda_0^- \tag{3.94}$$

We can conclude that λ_0^- is an eigenvalue of $dP_0(z_0)$ with eigenvector $\begin{pmatrix} \xi_0^+(q) \\ q - \pi \end{pmatrix}$. Finally as $dP_0(z_0)$ preserves the area (it is symplectic) the second eigenvalue is $\lambda_0^+ = e^{(2\pi/\omega)}$ [31]. We conclude that $dP_0(z_0)$ does not have any eigenvalue equal to one. This implies that z_ε is a hyporbolic fixed point of P_ε .

Now we shall focus on the invariant manifolds of $z_\varepsilon = (q_\varepsilon, \mathrm{v}_\varepsilon)$. They depend on ε in an analytic way [90]. The "upper part" of the stable manifold can be written

$$\xi_\varepsilon^s(q) = \xi_0^+(q) + \varepsilon\, \xi_1(q) + \varepsilon^2\, \xi_2(q) + \ldots \tag{3.95}$$

In order to determine the functions ξ_i, $i = 1, 2, \ldots$ we require

(a) the manifold $(q, \xi_\varepsilon^s(q))$ is invariant;

(b) since $(q, \xi_\varepsilon^s(q))$ is a stable manifold

$$\lim_n P_\varepsilon^n\, (q, \xi_\varepsilon^s(q)) = (q_\varepsilon,\ \mathrm{v}_\varepsilon) \tag{3.96}$$

In order to establish the condition (a) we demand that there exists a motion which is solution of the problem

$$\begin{aligned} \dot{q}(t) &= \mathrm{v}(t) \\ \dot{\mathrm{v}}(t) &= -\sin q + \varepsilon\, \cos \omega t \\ q(0) &= q^0 \\ \mathrm{v}(0) &= \xi_\varepsilon^s(q^0) \end{aligned} \tag{3.97}$$

[31] We can proceed as above and show that λ_0^+ is an eigenvalue of $dP_0(z_0)$ with eigenvector $\begin{pmatrix} \xi_0^-(q) \\ q - \pi \end{pmatrix}$. It is sufficient to notice that the motion with velocity $-\dot{Q}(t)$ requires the backward time translation of $Q(t)$.

i.e. it is a motion of the perturbed pendulum with initial data $\begin{pmatrix} q^0 \\ \xi^s_\varepsilon(q^0) \end{pmatrix}$.

The solution of the equation (3.97) is written in the form of the series

$$q(t) = q_0(t) + \varepsilon\, q_1(t) + \varepsilon^2\, q_2(t) + \dots \tag{3.98}$$

and the same is done for $\mathrm{v}(t)$

On substituting (3.98) to (3.97) we obtain the zero order (with respect to ε) equation

$$\begin{aligned} \dot{q}_0(t) &= \mathrm{v}_0(t) \\ \dot{\mathrm{v}}_0(t) &= -\sin q_0(t) \\ q_0(0) &= q^0 \\ \mathrm{v}_0(0) &= \xi_0^+(q^0) \end{aligned} \tag{3.99}$$

and the equation of order j, $j \geq 1$, as well

$$\begin{aligned} \dot{q}_j(t) &= \mathrm{v}_j(t) \\ \dot{\mathrm{v}}_j(t) &= -\cos q_0(t)\, q_j(t) + f_j(t) \\ q_j(0) &= 0 \\ \mathrm{v}_j(0) &= \xi_j(q^0) \end{aligned} \tag{3.100}$$

where $f_1(t) = \cos \omega t$ and f_j, $j \geq 2$, is a function of $q_0, q_1, \dots, q_{j-1}$. The ξ_j's are still unknown.

The solutions of (3.99) and the "linear" equations (3.100) can be written

$$\begin{aligned} j = 0 \qquad & q_0(t) = Q(t + t_q) \\ j \geq 1 \quad & \begin{pmatrix} q_j(t) \\ \mathrm{v}_j(t) \end{pmatrix} = W_0(t + t_q) \\ & \times \left(W_0(t_q)^{-1} \begin{pmatrix} 0 \\ \xi_j(q^0) \end{pmatrix} + \int_0^t d\tau\ W_0(\tau + t_q)^{-1} \begin{pmatrix} 0 \\ f_j(\tau) \end{pmatrix} \right) \end{aligned} \tag{3.101}$$

in which t_q is the time which the motion $Q(t)$ spends to arrive at q^0, namely the initial position of the solution of (3.97). W_0 is the Wronskian matrix, i.e the solution of

$$\dot{W}_0(t) = M_0(t)\, W_0(t) \qquad W_0(0) = \mathbb{I} \tag{3.102}$$

and

$$M_0(t) = \begin{pmatrix} 0 & 1 \\ -\cos Q(t) & 0 \end{pmatrix}$$

Some further explanation on how (3.101) is obtained is postponed to the appendix ?

The meaning of (3.101) is the following: when the functions ξ_j's, which define the stable manifold ξ^s_ε and are still unknown, are determined we can state that ξ^s_ε is invariant and, in particular, the motion (3.101) takes place on it.

The same considerations have to be made about the unstable manifold. In particular the manifold is defined by a series similar to (3.95)

$$\xi^u_\varepsilon(q) \;=\; \xi^+_0(q) + \varepsilon\,\tilde{\xi}_1(q) \;+\; \varepsilon^2\,\tilde{\xi}_2(q) \;+\; \ldots \quad , \tag{3.103}$$

we will focus on the unknown functions $\tilde{\xi}_j$'s later. Furthermore it is determined a motion $\tilde{q}(t)$ that is solution of the equation (3.97) with initial data $\begin{pmatrix} \tilde{q}^0 \\ \xi^u_\varepsilon(\tilde{q}^0) \end{pmatrix}$ and we obtain formulas similar to that found for $q(t)$.

We next wish to impose the condition (b). To this end we require that

$$\lim_{n\to+\infty} \begin{pmatrix} q_j(n2\pi/\omega) \\ \mathrm{v}_j(n2\pi/\omega) \end{pmatrix} = \begin{pmatrix} q_{\varepsilon j} \\ \mathrm{v}_{\varepsilon j} \end{pmatrix} \qquad , \tag{3.104}$$

namely the $\begin{pmatrix} q^0 \\ \xi^s_\varepsilon(q^0) \end{pmatrix}$ lays on the stable manifold of z_ε. The same condition as (3.104), for $n \to -\infty$, has to be satisfied by the motion $\tilde{q}(t)$ on the unstable manifold .

We focus on two items that will be used to obtain the main result of this section.

Regarding the first feature we need to consider the equation

$$\dot{y}(t) = M_0(t)\,y(t) \qquad\qquad y = \begin{pmatrix} \eta \\ \dot{\eta} \end{pmatrix} \tag{3.105}$$

which is, of course, tantamount to

$$\ddot{\eta}(t) + \cos Q(t)\,\eta(t) = 0 \tag{3.106}$$

We know that

$$\ddot{Q}(t) + \sin Q(t) = 0 \tag{3.107}$$

We straightforwardly conclude that $\eta = \dot{Q}$ is a solution of (3.106) [32] and hence $x = \begin{pmatrix} \dot{Q} \\ \ddot{Q} \end{pmatrix}$ is solution of (3.105). Moreover from (3.92) we get

$$\dot{Q}(t) = -2/\cosh t \tag{3.108}$$

According to (3.102) we notice that the columns y_1 and y_2 of the matrix W_0 are solutions of (3.105) with initial data $\begin{pmatrix} 1 \\ 0 \end{pmatrix}$ and $\begin{pmatrix} 0 \\ 1 \end{pmatrix}$, respectively. In view of (3.108) we can state that x is a linear combination of y_1 and y_2 such that

$$x(t) = \alpha\,y_1(t) \;+\; \beta\,y_2(t) \;\overset{t\to+\infty}{\longrightarrow}\; 0 \tag{3.109}$$

[32] Indeed this is a general property. In fact if $Q(t)$ satisfies $\ddot{Q} = -V'(Q)$ and if $Q \in L^2$ then the "Schrödinger operator"

$$-\frac{d^2}{dt^2} \;-\; V''(Q(t))$$

admits an eigenvalue $E = 0$.

The second item concerns the following formula that is obtained beginning from (3.109)[33]

$$(-\beta,\ \alpha)\ W_0(t+t_q)^{-1} = (-\ddot{Q}(t+t_q),\ \dot{Q}(t+t_q)) \tag{3.110}$$

So we have taken the necessary steps we need.

Assuming that α, β are chosen so that (3.109) holds, we multiply (3.101), for $j \geq 1$, to the left by (3.110), set $t = n\,2\pi/\omega$ and then let $n \to +\infty$. Taking into account of (3.104) we get

$$\begin{aligned} 0 =& (-\beta, \alpha)\ \left(W_0(t_q)^{-1} \begin{pmatrix} 0 \\ \xi_j(q^0) \end{pmatrix} + \int_0^{+\infty} d\tau\ W_0(\tau + t_q)^{-1} \begin{pmatrix} 0 \\ f_j(\tau) \end{pmatrix} \right) \\ =& \dot{Q}(t_q)\ \xi_j(q^0) + \int_0^{+\infty} d\tau\ \dot{Q}(\tau + t_q)\ f_j(\tau) \end{aligned}$$

where we still use (3.110). Since $\dot{Q}(t_q) \neq 0$ (from (3.108)) we can determine

$$\xi_j(q^0) = \int_0^{+\infty} d\tau\ \frac{\dot{Q}(\tau + t_q)}{\dot{Q}(t_q)}\ f_j(\tau) \tag{3.111}$$

We compute, in a similar way as above, the functions $\tilde{\xi}_j$'s regarding the unstable manifold of z_ε:

$$\tilde{\xi}_j(q^0) = \int_0^{-\infty} d\tau\ \frac{\dot{Q}(\tau + t_q)}{\dot{Q}(t_q)}\ f_j(\tau) \tag{3.112}$$

We limit the discussion to the first order in ε. We are able to write the condition that determines the position q^0 of any point where the stable and the unstable manifolds cross

$$\xi_1(q^0) = \tilde{\xi}_1(q^0) \tag{3.113}$$

and in such way that the crossing is transverse

$$\xi_1'(q^0) \neq \tilde{\xi}_1'(q^0) \tag{3.114}$$

where the derivatives, with respect to the argument, are computed at each solution of (3.113). We notice that the conditions which we have established for the pendulum are quite general. They are on the base of the most important technique used to compute the location of any homoclinic point [34], which is the essential element of the "homoclinic chaos". In fact through the standard "Smale-Birkhoff theorem" (see for instance [54], pg. $181 - 188$) we can state

[33] In fact it is sufficient to not that the linear combination (3.109) can be written

$$\begin{pmatrix} -\ddot{Q}(t) \\ \dot{Q}(t) \end{pmatrix} = L\ W_0(t)\ L^{-1} \begin{pmatrix} -\beta \\ \alpha \end{pmatrix}$$

where

$$L = \begin{pmatrix} 0 & -1 \\ 1 & 0 \end{pmatrix} \qquad L \begin{pmatrix} a_1 \\ a_2 \end{pmatrix} = \begin{pmatrix} -a_2 \\ a_1 \end{pmatrix}$$

Finally it is easy to check that $L\ W_0\ L^{-1} = (W_0^{-1})^t$

[34] The existence of a homoclinic point is guaranteed by the implicit function theorem.

that when the dynamics Φ has a hyperbolic fixed point , if there exists a transversal intersection between the positively and the negatively asymptotic sets of the fixed point then Φ has an invariant set on which it is equivalent the symbolic dynamics of the horseshoe. This is a sufficient condition because (homoclinic) chaos can occurs.

We apply (3.113) (3.114) to the the pendulum ($f_1(t) = \cos(\omega t)$)

$$\begin{aligned} \xi_1(q^0) - \tilde{\xi}_1(q^0) &= \int_{-\infty}^{+\infty} d\tau \ \frac{\dot{Q}(\tau + t_q)}{\dot{Q}(t_q)} \ \cos(\omega\tau) \\ &= \cos(\omega\, t_q) \ \frac{1}{\dot{Q}(t_q)} \ A \end{aligned} \tag{3.115}$$

where we use that $\dot{Q}$ is even and the integral

$$A = \int_{-\infty}^{+\infty} d\tau' \ \dot{Q}(\tau') \ \cos(\omega\,\tau')$$

is not zero [35]. Hence the condition (3.113) is satisfied only if

$$\omega\, t_q \ = \ (2k \ + \ 1)\ \frac{\pi}{2} \tag{3.116}$$

$k = 0, \pm 1, \ \pm 2, \ \ldots$.

The condition on the derivatives is applied where (3.116) holds

$$\begin{aligned} \xi_1'(q^0) - \tilde{\xi}_1'(q^0) \ &= \ - \ t_q' \ \left\{ \omega \ \sin(\omega\, t_q) \ \frac{1}{\dot{Q}(t_q)} \ + \ \cos(\omega\, t_p) \ \frac{\ddot{Q}(t_p)}{\dot{Q}(t_p)^2} \right\} \ A \\ &= \pm \ t_q' \ \frac{1}{\dot{Q}(t_q)} \ A\, \omega \ \neq \ 0 \end{aligned} \tag{3.117}$$

since $t_q' \neq 0$ whenever $t_q \neq 0$. We conclude that, to the first order in ε, all the crossings (3.116) are transversal.

Finally, we have found a mechanism to explain the onset of chaos in a resonance: we have seen that a resonance is essentially a perturbed pendulum, which, can experience chaos near the separatrix, no matter small the perturbation is.

35

$$\int_{-\infty}^{+\infty} d\tau \ \frac{\cos(\omega\,\tau)}{\cosh\tau} \ = \ \frac{\pi}{\cosh(\frac{\pi}{2}\,\omega)}$$

Chapter 4

Non perturbative regime. A potential scattering approach.

1. Introduction

In a scattering problem the system is characterized by having a localized region of configuration space ('interaction region') where the interaction is relevant, while elsewhere the interaction is absent. A particle is injected into the interaction region and experiences a scattering event; after each event it may escape from the interaction region forever ('scattered' trajectories) or eventually proceed to another scattering event. A map that links some initial parameter to some feature of the outgoing state is called a scattering function. There may exist 'trapped' trajectories, i.e. particles that wander for ever in the interaction region. In these circumstances the scattering function is not defined. A scattering process is called 'irregular' or 'chaotic' when a scattering function is singular on a fractal set of variable initial values (see Ref. [30]).

A condition for having chaotic scattering is the existence of an invariant set Λ of an infinite number of unstable, periodic and aperiodic orbits, localized in the interaction region. Whenever Λ contains a Cantor set, irregular scattering occurs. In fact the stable manifolds of orbits in Λ reach out into the asymptotic region by means of the Hamiltonian flow; an orbit started on one of the stable manifolds is captured in the interaction region for all the time, i.e. the final state is not defined. Hence there exists a fractal set of asymptotic in-variables (the initial conditions lie in the stable manifolds of orbits in Λ) where the scattering function is singular [58, 59]. The pattern of homoclinic/heteroclinc connections of invariant manifolds of Λ is called 'chaotic saddle'.

Therefore incoming parameters close to each other and close to the 'stable manifold' of the chaotic saddle can be mapped to very different outgoing parameters. They spend a long time in the vicinity of Λ and trace out the type of motion performed by the localized trajectories. Similarly outgoing parameters close to each other and close to the unstable manifold can come from very different incoming parameters. Λ acts as a "repeller" with global influence on the asymptotic region. Therefore the scattering function displays wild

fluctuations on all scales on each set containing initial conditions leading to trapped orbits. The origin of the fractal singularities of a scattering function is the chaotic motion in the invariant bound set; the irregularity of the motion in an unbound phase space is connected to a form of bound chaos.

Thus, the main issue in studying a problem of chaotic scattering is to determine the properties of the invariant set, in particular the topological pattern of the chaotic saddle and the character of the dynamics in it. In this regard it is hoped that an equivalent symbolic dynamics is found out to explain the behavior of a scattering function. The invariant set provides a fractal structure whose dimension, Lyapunov exponents and escape rate can be connected to the particular arrangement of the singularities in the scattering function or in the delay time function.

The chaotic (invariant) set shows a relatively simple structure when it is completely hyperbolic. In this case it consists of unstable periodic orbits (all of them are hyperbolic) and their homoclinic and heteroclinic connections only. As Smale shows [99], this is connected with the horseshoe construction. A system with n fixed points (periodic solutions) corresponds to a horseshoe with the same number of fixed points; one can obtain the horseshoe structure by plotting the invariant manifolds of any unstable periodic point. The invariant set may contain KAM tori and sets of marginal stability; in this case it is not completely hyperbolic and the horseshoe is not fully developed. We will present a system which differs from a standard Smale's horseshoe model:

- the configuration space is infinite, the interaction is long ranged and parabolic orbits exist; it follows that the invariant set is not compact and the system is described by a symbolic dynamics with an infinite number of symbols;

- in the phase space there are islands which consist of unbroken KAM surfaces.

Many physical scattering systems can be modeled in the following way. We consider a set S in the phase space. A driving force removes a fraction of points from S after each step of an iterative process: after the first step, it leaves a number of intervals in S, after the second step a set of new subintervals replaces each old interval. This process can be infinitely repeated. The structure of the set of points that are never removed is Cantor-like. This process is characteristic of systems with fully developed chaos.

In chaotic scattering the Smale's mechanism leads to an exponential decay of phase space ensembles: all phase space points are depleted except for the invariant set, which consists of all trapped orbits of the system. However the assignment of an exponential decay law to a chaotic dynamics is not general. When in the phase space some regular islands with KAM surfaces survive, the particle initialized in a chaotic region can spend a long time near the boundary of a regular region. In this case, the leaving away of the particles from the KAM region gives an algebraic decay [20, 61, 78].

The existence of KAM surfaces is not the only mechanism resulting in an algebraic decay. In the Ref. [52] the authors present a chaotic system that does not show any KAM structures and that decays according to a power law. The scaling is explained through a model of

random walk in phase space; the dynamics of symbolic strings is Markovian. Beeker et al. [9] observe an algebraic scaling of the scattering function. Nevertheless they claim that the KAM component effects are negligible for the parameter values they choose. Beeker et al. provide reasons for the scaling by means of a different mechanism than the stickiness of KAM tori. They consider the survival time of the temporarily bound orbits close to the parabolic orbit. If the system is described by a symbolic dynamics with infinite symbols, one can have a chaotic dynamics in a phase space without any regular region and, at the same time, a scaling with a power law.

When an external control parameter is varied, the invariant set changes its structure. In particular, if some non-hyperbolic components enlarge, then the stable and unstable bundles can be displaced one with respect to each other. For certain parameter values, intersections are destroyed and some localized orbits of the invariant set get lost, i.e. bifurcations take place. As a consequence, the invariant set may be no longer topologically equivalent to a complete Cantor set. Some relevant quantities (such as the escape rate and the topological entropy) have general features: as functions of the parameter they display plateaux, where no orbits disappear. There is also a set of parameter values where the quantities change indicating the presence of bifurcations. This set can have an involved structure; in fact for a class of systems the topological entropy exhibits a devil's staircase [72].

There is a wide variety of applications of the chaotic scattering in classical physics.

In celestial mechanics complicated motions can take place for close encounters, but, after, the particles separate, with the exception of a set of initial conditions of zero measure [88].

In many chemical reactions (in particular, in the case of a biatomic molecule interacting with an atom) small changes in the initial conditions lead to drastic differences in the final states so that a nonreactive trajectory may exist in the vicinity of a reactive one. Pollack et al. [91] emphasized the importance of unstable periodic orbits that, typically, provide a non-attracting, infinite set [62]. Skodje et al. [98] got a chaotic scattering approach to the matter.

In hydrodynamics the scattering among more than three ideal, linear vortices can bring to chaotic dynamics. Aref and Eckhardt et al. [31, 4] draw attention to the processes occurring in the interaction. Two couples of vortices that interact can either pass by each other or exchange their partners and then spend time moving along circular motion, until the next collision when they can either convert to the original couples or scatter away from each other. This capture state is unstable and exhibits all properties of chaotic scattering, and, in particular, it may be disrupted by a small change in the parameters.

There are many applications of the chaotic scattering to the classical scattering problem by a potential. The heart of all examples is the existence of unstable, bounded orbits that trap a set of orbits in the continuum of the scattering trajectories and lead to singularities in the scattering functions [32, 55, 56, 58]. A particular class of problems is connected with the internal dynamics of atomic systems or clusters interacting with an external electromagnetic field. Even if the motion is integrable in the field-free case, external driving generically destroys integrability and can lead to irregular dynamics, sensitive with respect to both initial conditions and parameters of the driver. This class of systems contains models

of one-dimensional oscillating potential wells.

In this chapter we deal with a representative of this class of systems: the model of 'rigid spheres' [85, 69]. It is introduced in connection with the problem of the energy absorption in clusters irradiated by intense electromagnetic fields; the model provides a basic mechanism of absorption. We focus on some features of the dynamics of the model. These features are understandable by means of a chaotic scattering approach.

In section 2, we introduce the model and we list the particular cases we consider in the numerical study. In section 3, we summarize the relevant numerical results about the scattering function and its structure of singularities; the geometry of the scattering function is dominated by the escape orbits while the singularities are caused by the captured orbits. We show that the scaling of the delay time function is algebraic. In section 4, following Alekseev [1, 2] and Ref. [28] we introduce a return map and we obtain a detailed description of the structure of the scattering function. In section 5, we give a different approach to the investigation of the structure of the scattering function. We construct the pattern of intersections of invariant manifolds of the two outermost fixed points. The singularities structure of the delay time function corresponds to the pattern in which the bundles of stable manifolds intersect the local segment of the unstable manifold. As Smale has shown, the homoclinic/heteroclinic bundle is connected with a horseshoe construction. We obtain that the horseshoe map is not completely developed due to the non-hyperbolic effects created by the surfaces of KAM islands and their secondary structures; they cause the algebraic behavior in the statistics of the delay time function. In section 6, we investigate the outgoing energy as a function of the driver amplitude for fixed initial conditions. We observe that this function displays behaviors similar to the scattering function. This is interpreted through some essential properties of the topology of the homoclinic/heteroclinic bundle. The discrepancies between the two functions depend on secondary aspects of the topology.

2. The problem

We study the scattering of a particle (mass m=1) by a one-dimensional potential well $V(x)$, $x \in \mathbb{R}$, driven by a homogeneous, time dependent force f.

The potential we consider is attractive, bell-shaped, symmetric, limited, with a single equilibrium point. The definite expression we treat is provided by the model of rigid spheres. It is a simple electrostatic system where a negatively charged sphere moves in the potential generated by a fixed, positively charged one. The potential is Coulomb-like when the spheres do not overpose; otherwise it is polynomial. Following Ref. [69] we assume

$$V_1(x) = \begin{cases} 1/2x^2 - 3/16\,|x|^3 + 1/160\,|x|^5 & |x| \leq 2 \\ -1/|x| + 6/5 & otherwise \end{cases} \tag{4.1}$$

V_1 is $\mathbb{C}^2$ for $x \in \mathbb{R}$.

For reference, we also perform simulations with a Lorentz-shaped potential V_2 character-

ized by general features similar to V_1 except for being $\mathbb{C}^\infty$.

$$V_2(x) \;=\; \frac{6/5\,x^2}{(12/5+x^2)} \tag{4.2}$$

We also test potentials of different shapes with the same general features: the results relevant for our discussion are essentially the same.

The system is driven by a homogeneous, time-dependent force f representing the effect of an applied oscillating electric field. We study two cases: $f = f_1$ (compact support) and $f = f_2$ (periodic).

$$f_1(t) \;=\; \begin{cases} e_0 \sin^2(\frac{\nu t}{n})\;\cos(\nu t) & 0 \le \nu t \le n\pi \\ 0 & otherwise \end{cases} \tag{4.3}$$

n in $\mathbb{N}^+$ $n >> 1$. The support of the envelope is one period of $\sin^2(\frac{\nu t}{n})$; in this way it is introduced a time scale n/ν . Therefore f_1 is defined by the amplitude e_0, the width of the envelope and the frequency ν of the co-sinusoidal factor.
The second form of f we study is purely sinusoidal

$$f_2(t) = e_0 \sin(\nu t) \tag{4.4}$$

We always assume $\nu > 1$.

The time-dependent Hamiltonian is given by

$$\begin{aligned} H(p,x,t) &= H_0(p,x) \;-\; e_0\; f(t)\, x \\ &=\; p^2/2 \;+\; U(x,t) \end{aligned} \tag{4.5}$$

where $H_0(p,\,x) = p^2/2 + \omega^2\, V(x)$, and, according to the case, $V = V_i$ and $f = f_i$, $i = 1,2$. In both cases the undriven oscillators are characterized by a linear angular velocity $\omega = 0.7$ and an escape solution x_h ('heteroclinic' orbit) with parabolic critical points, i.e. $|x_h(\pm\infty)| = \infty$ and $\dot{x}_h(\pm\infty) = 0$. The energy of the unperturbed escape orbit is $6/5\,\omega^2 = 0.588$.

The phenomenology we study concerns drivers with strength even many times the maximal oscillator force. Therefore it cannot be fully understood only through perturbative methods. However there are some perturbative treatments (in particular [54, 22, 24]) that show the important role of the escape orbit in the explanation of the irregular dynamics of the driven oscillators. Thus we concentrate on orbits in the phase space with energies not far from the escape energy of the free oscillator. In such situations, at fixed strength of the driver, in the phase space there are size-able regions of initial conditions characterized by unstable trajectories which appear to be so erratic that the system motions can be regarded as stochastic. Elsewhere, irregular motions are absent. In addition, if the strength of the driver is varied then stochastic regions move in the phase space.

The properties of the dynamics can be approached by studying the scattering functions, i.e. maps connecting the initial states to the final ones, after a time long enough such that the particle can move in the interaction region and possibly comes out of it. In order to determine the scattering functions, we are interested in asymptotic data. For the case $f = f_1$ we get the relevant quantities at $t \ge n\pi/\nu$. The driver should play the role of a transient. Actually, we

find that the main descriptive properties are developed, at least partially, before the end of the transient. In the case $f = f_2$ we simply take the data after many periods of f_2.

The maps we obtain display the irregular behavior of the dynamics: intervals of the initial state variables, where the map is sensitively depending on, alternate with intervals where the map is smooth.

The irregular behavior of the scattering functions can be analyzed through the approach of the irregular scattering theory. Actually the chaotic scattering theory deals with physical situations where the dynamics takes place in an infinite volume of the phase space, the interaction is confined to a finite region and there are some scattering functions which display wild fluctuations on all scales.

We briefly give an outline of the main results of the numerical calculations.

- For both the oscillators with the sinusoidal driver f_2 we determine two scattering functions. For a trajectory with initial velocity v_0 we get the energy H_0 and the number N_c of crossings through $x = 0$ after the particle has moved out from the interaction region. Then we plot H_0 and N_c as functions of v_0. Both of the maps display the same sequence of intervals of v_0 where the outgoing variable (H_0 or N_c) is smooth. Between these intervals there are gaps in which H_0 and N_c jump in an irregular way. Hence there is a correspondence between the number of crossings through the origin and the regular intervals for H_0.

- An analogous analysis is performed with the driver f_1. The patterns of the scattering functions are qualitatively similar to the previous ones.

- We initialize at $t = 0$ an ensemble of scattering orbits and we calculate the number $N(t)$ of orbits that are still inside the interaction region at the time t. We obtain an algebraic decay law.

- For the same ensemble the distribution of zeros $N(n)$ is determined. For the considered parameters of the simulation we again obtain a power law.

- We fix the initial conditions and we calculate H_0 and N_c as functions of the parameter e_0. The resultant plots show the same structures described for the previous scattering functions

Note

A resonance may be a rich source of highly complex motions (see Ref. [50]), as chaotic patterns and irreversibility in the transfer of energy between different oscillatory states. It takes place only if the system stays in one of those particular regions of the phase space in which the frequencies of some angular variables become nearly commensurate. We guess that the irregular motions of the systems we consider are due to a mechanism distinct from and more general than a resonance. Actually we avoid the resonance condition, since the driver frequency ν is larger than the highest 'effective' frequency of the free oscillator.

3. Numerical results.

We use the Runge-Kutta algorithm of fourth order to integrate the Hamilton's equations (4.5). In order to check our code, we solve the rigid spheres model and we compare with the same simulations in Ref. [69].

3.1 Scattering functions

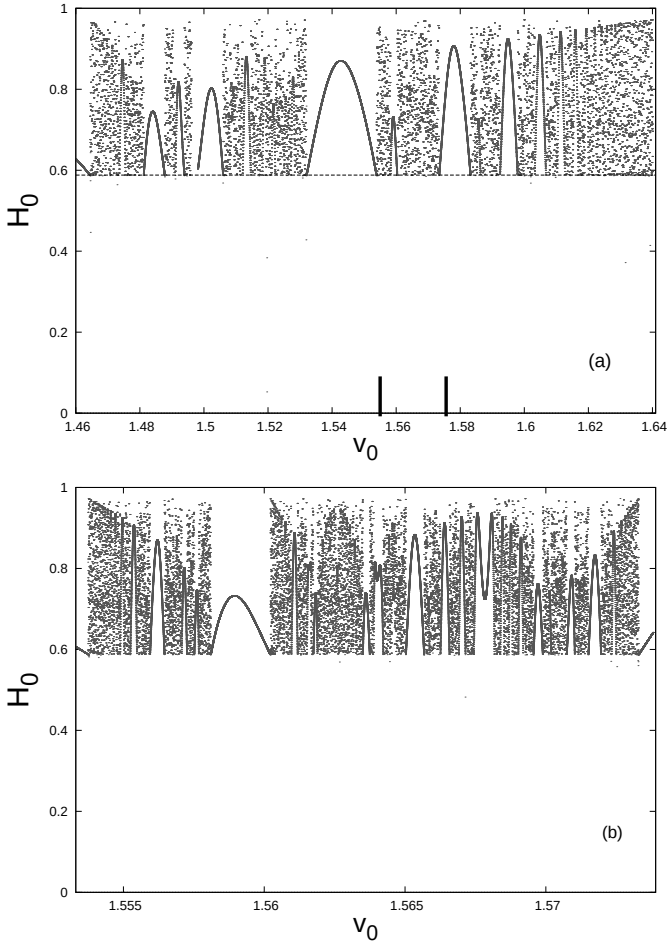

Figure 4.1: The map of the outgoing energy H_0 vs the initial velocity v_0 for $x(0) = 0$ with $e_0 = 1$ and $\nu = 0.8$. Plot (b) is a magnification of the marked interval of plot (a).

A scatterig function is a map connecting some variables that refer to states before the interaction to some other concerning states after it. Our choice of the variables of the mapping is partially different from that in Refs. [9] and [28].

When $f = f_1$ we obtain the map

$$S^1_{(x_0,e_0)} : \ (x(0) = 0,\ \mathrm{v}(0) = \mathrm{v}_0) \ \mapsto \ H_0(p(t^*), x(t^*))$$

$t^* > n\pi/\nu$, $n = 340$, i.e. it links the initial conditions $(0, v_0)$ of a trajectory to the energy H_0 of the trajectory at a time t^* after the driver f_1 is switched off. The driver amplitude e_0 is treated as a parameter. Analogous maps are obtained as functions of x_0 for a given v_0. When $f = f_2$ (periodic case) we consider the map

$$S^2_{(x_0,e_0)}: \ (x(0) = 0,\ v(0) = v_0) \ \mapsto \ H_0(p(t_k), x(t_k))$$

$\nu t_k = 2k\pi$, $k = 1, 2, \ldots$. It is a map from one value to many ones which connects the initial conditions $(0, v_0)$ to the energies H_0's taken at times t_k such that $t_{k+1} - t_k$ is one driver period.

In all the cases the dependence of H_0 on v_0 alternates between regular intervals, where $S^i_{(x_0,e_0)}$, $i = 1, 2$, shows a smooth behavior, and irregular intervals, where $S^i_{(x_0,e_0)}$ is much more sensitive. In the plot (a) of fig. 4.1 we present the results for the v_0 interval $[1.46, 1.64]$. Plot (b) of fig. 4.1 is an expansion of the irregular interval marked in the plot (a) (v_0 varies in $[1.5533 : 1.5739]$).

An orbit may be marked by the number N_c, the number of crossings of $x = 0$. Another scattering map we obtain is N_c as a function of v_0; it is displayed in the part (a) of fig. 4.2. We note the following features:

- N_c is constant in each interval where the scattering map is regular; N_c and the scattering map are singular at the same points (compare (a) of fig. 4.1 to (a) of fig. 4.2);
- each regular interval between two regular ones with the same N_c has a crossing number greater than N_c;
- in the region between two regular intervals with the same N_c, a sequence of $N_c + 1$ regular intervals accumulates as v_0 gets next to the boundaries of the region (see (b) and (c) of fig. 4.2).

These rules define the 'hierarchy' of the structure of the scattering function and of the delay time function.

A trajectory belonging to a regular interval spends a finite time in the interaction region since, we know, it experiences a finite number of zeros. When the trajectory leaves out the interaction region, only the driver has an effect on the particle and therefore the values of H_0 at times t_k, taken at the end of each driver period (see the definition of $S^2_{x_0,e_0}$), are almost constant, i.e. for v_0 in a regular interval the map $S^2_{x_0,e_0}$ is characterized by a 'fixed' point (see fig. 4.1).

The horizontal line in fig. 4.1 - (a) displays the energy h' of the unperturbed escape orbit (0.588 in our cases). From the plot we may state that if v_0 is in a regular interval then $H_0 \geq h'$ for all times large enough. An orbit belonging to a regular region is called hyperbolic and parabolic when $H_0 > h'$ and $H_0 = h'$, respectively.

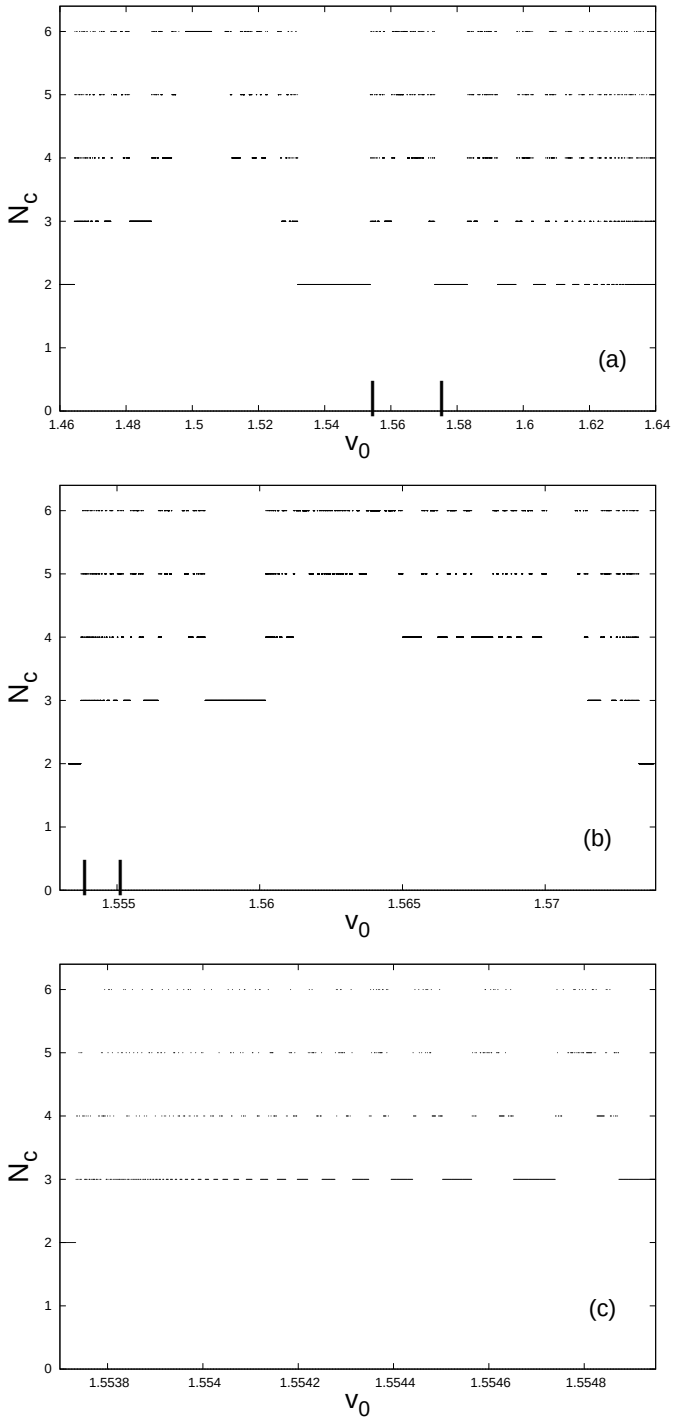

Figure 4.2: The number of zeros N_c of a trajectory with initial velocity v_0 ($x(0) = 0$); the marked interval of (a) is magnified in (b); the plot (c) shows a sequence of intervals with three zeros that accumulates to a two zeros interval as v_0 approaches the border of the two zeros interval.

We note that a magnification of an irregular interval between two regular intervals with N_c zeros gives a pattern qualitatively similar to the complete one; the irregular gap in (a) dissolves into a sequence of regular subintervals, with at least $N_c + 1$ zeros, separated by

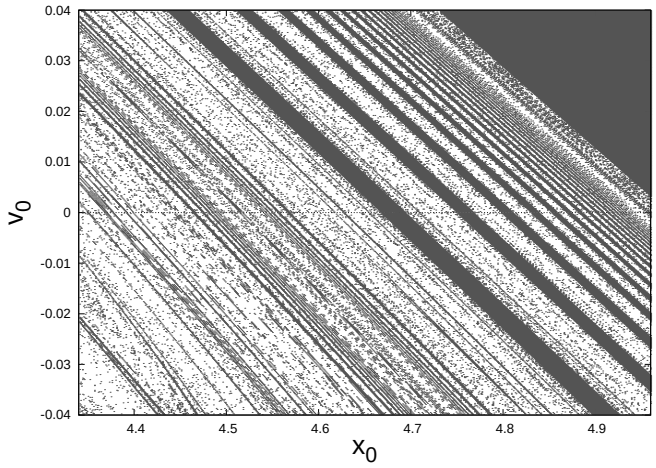

Figure 4.3: Distribution of initial conditions of nearest trajectories with the same number of crossings of the origin. We choose an ensemble of orbits with an uniform distribution of initial conditions and we mark an initial condition whenever its orbit experiences the same N_c as the orbits from the closest initial conditions.

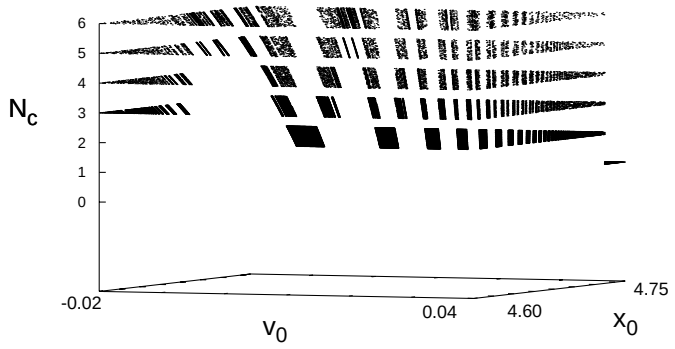

Figure 4.4: The plot shows N_c versus the initial conditions in the same numerical experiment as in fig. 4.3. Note the stripes arrangement of the structure and the hierarchy of stripes according to what described above. The N_c stripes accumulate going close to a $N_c - 1$ stripe.

irregular gaps. Whenever we continue in this way we find an intertwined structure of regular and irregular intervals; at each step the distribution of regular intervals, marked by the number of zeros, meets the three rules listed above.

From our numerical inspection we are driven to argue that $S^2_{(x_0,e_0)}$ should possess fractal features; the scattering function is continuous for all v_0 except a set $\mathcal{C}$ of singularities. $\mathcal{C}$ is the set of points after removing all the regular intervals with any number N_c of zeros. We guess the measure of $\mathcal{C}$ should be zero. In fact $\mathcal{C}$ appears to be determined in analogy to the hierarchical procedure of a Cantor set, by giving level by level the endpoints of cut out

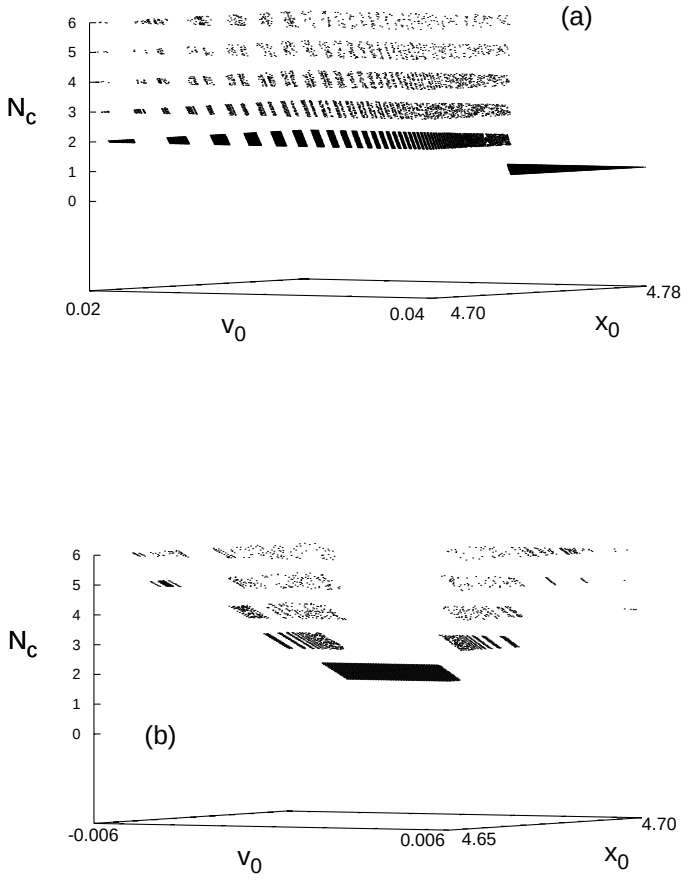

Figure 4.5: There are shown some details of fig. 4.4. In (a) there is a sequence of stripes $N_c = 2$ approaching the domain $N_c = 1$. (b) is an example of the structure with a sequence of $N_c + 1$ stripes accumulating against a N_c domain.

intervals.

Fig. 4.3 illustrates the distribution of the nearest trajectories which cross the origin the same number of times. Starting from a uniformly distributed ensemble of initial conditions, we mark a pair (x_0, v_0) of initial conditions only if its trajectory experiences the same number of zeros as the trajectories corresponding to the closest pairs. The plot shows a pattern organized as a sequence of stripes accumulating to a domain corresponding to parabolic and hyperbolic orbits with only one zero, i.e. to the set of initial conditions of orbits that escape after crossing once the origin. Each stripe in the figure is marked by a determined N_c.

Fig. 4.4 displays the distribution of the number of zeros N_c, with $1 \leq N_c \leq 6$, extracted from the fig. 4.3. We observe the hierarchical structure, ordered with respect to N_c and described above. In particular we point out that the pattern is arranged in sequences of stripes

that accumulate at the border of the domain with $N_c = 1$ (see (a) in fig. 4.5). In the hierarchy of the structure the level $N_c + 1$ is a sequence of stripes approaching the stripe N_c (see (b) in fig. 4.5) as well.

A similar hierarchy is observed by Eckelt at al. [28] for a class of oscillators characterized by attractive potentials. In order to explain the properties of the hierarchy, they use a map (return map) introduced by Alekseev [1]. We guess that the mechanism acting in our problem should be treatable in the same way by a suitable return map: we will come back to it in the next section. We also consider the non periodic case ($f = f_1$) and compute the

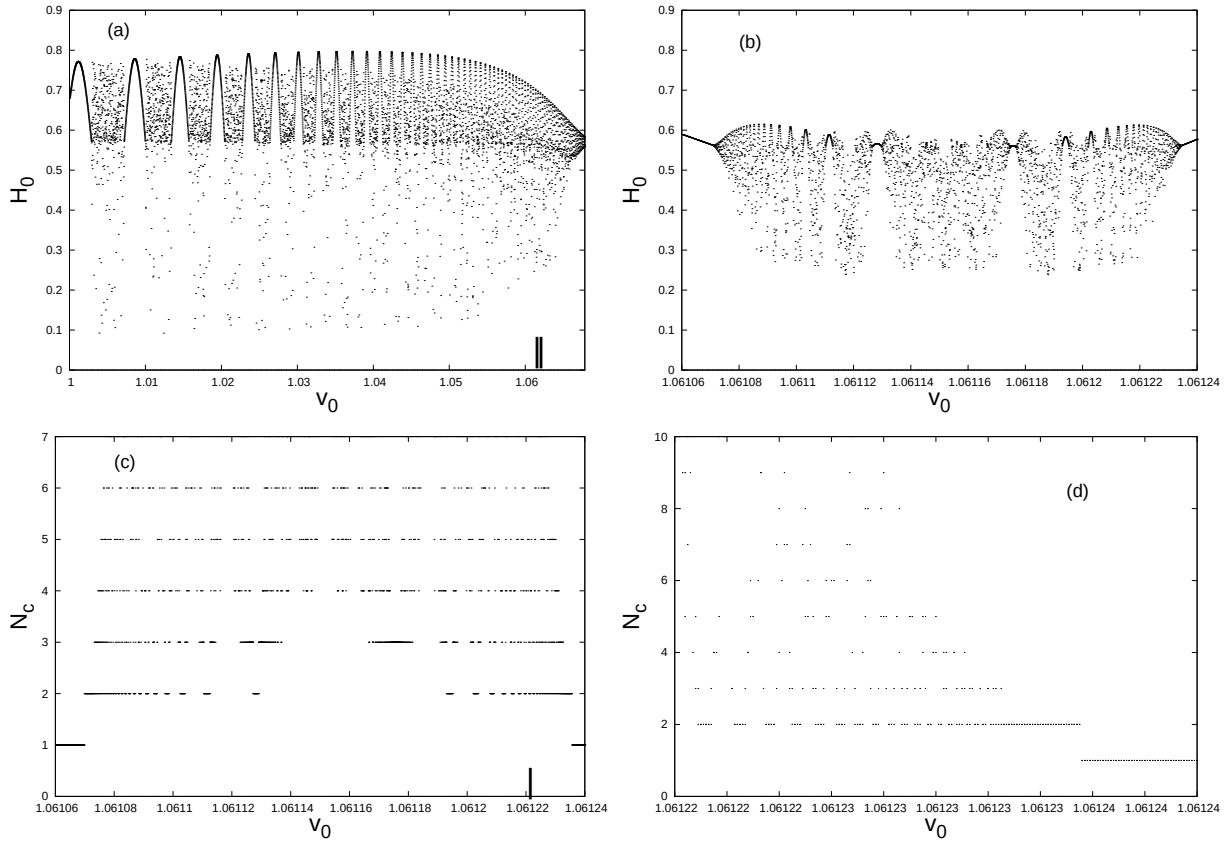

Figure 4.6: Scattering map and N_c function of the oscillator (4.2) with the driver (4.3). Plot (b) is an enlargement of the marked interval in (a). Plot (d) is a magnification of the marked interval in (c). We note that the hierarchical structure is not fully developed.

map $S^1_{(x_0,e_0)}$ that is calculated when the driver is already switched off and the energy H_0 is constant. The plots in $(a)-(d)$ of fig. 4.6 display the results; we set $e_0 = 1$ and we choose $\nu = 1$ and $n = 360$ in (4.3). As above an orbit for v_0 in a regular interval is called hyperbolic and parabolic when $H_0 > h'$ and $H_0 = h'$ respectively.
$S^1_{(x_0,e_0)}$ displays structures that seem qualitatively similar to $S^2_{(x_0,e_0)}$; but note that the hierarchical structure does hold only partially. Between two N_c intervals there are no intervals with a number of crossings less than N_c. However some sets of orbits result to be lost: in particular they are orbits in the vicinity of parabolically escaping ones (see $N_c \geq 3$ orbits in (d) of fig. 4.6). These orbits have a very long return time and the number of their $x = 0$ crossings

depends on the duration of the driver in a more considerable way. This result is expected. A driver of infinite duration is needed so that the map structure can display a complete hierarchical pattern; a fractal generating mechanism needs an infinite iterative process.

3.2 The delay time function and scaling properties.

We now focus on the relation between the time of permanence in the interaction region and the regularity of the motion. The time interval spent by the particle in the interaction region is called delay time.

Given an ensemble of orbits (initial conditions) we determine the 'survival function' $N(t)$: it gives the number of orbits that have a delay time larger than t, i.e. the number of orbits that experience at least one crossing through $x = 0$ at $t_1 \geq t$. This definition is not exactly the same as that considered by some other authors [70, 26, 9] and which needs a bound region around $x = 0$ to be initially chosen and counts the number of orbits that still stay in the region at t.

In our case the set of initial conditions is defined by a uniform distribution of initial velocities in the interval $1.55 \leq \mathrm{v}_0 \leq 1.64$ and $x(0) = 0$. The line of initial conditions intersects the stable manifolds of the invariant set transversally. A scaling law is extracted by plotting $N(t)$ vs t in a log-log diagram shown in fig. 4.7. The plot is fitted by a straight line, i.e. $N(t)$ displays an algebraic behavior $N(t) \sim t^z$; the exponent is $z = 1.60 \pm 0.01$.

The power law in the long time tails of the delay time statistics is related to the non-hyperbolicity of the dynamics. We expect a behavior like $t^{-3/2}$ when KAM islands influence the scattering process (see Refs. [61], [20]) and t^{-2} when parabolic surfaces influence the scattering process, but KAM islands do not.

Another tool, that can be helpful to extract a statistical measure of the irregular dynamics in a scattering problem, is the distribution of the number of zeros. We consider the same ensemble of orbits as above; we determine the number $N(n)$ of orbits of the ensemble that perform at least n crossings through $x = 0$. We obtain again an algebraic law: $N(n) \sim n^{-z}$ for $z = 2.33 \pm 0.05$ (see fig. 4.7 - (b)). The power-law holds for $5 \leq n \leq 60$. For $n > 60$ $N(n)$ consists of a 'staircase' structure (see fig. 4.7 - (c)) where the jumps take place at an irregular sequence of points. In Ref. [9] it is obtained that $N(n)$ follows an exponential decay. The discrepancy is a consequence of a different choice of the parameters. We will come back to this point later.

4. The return map.

In this section we deal with a mapping that allows to reduce the analysis of the complete dynamical problem (4.5) to that of the states that either will still undergo at least a zero in the future or already underwent at least a zero in the past. Using this approach we can pick out

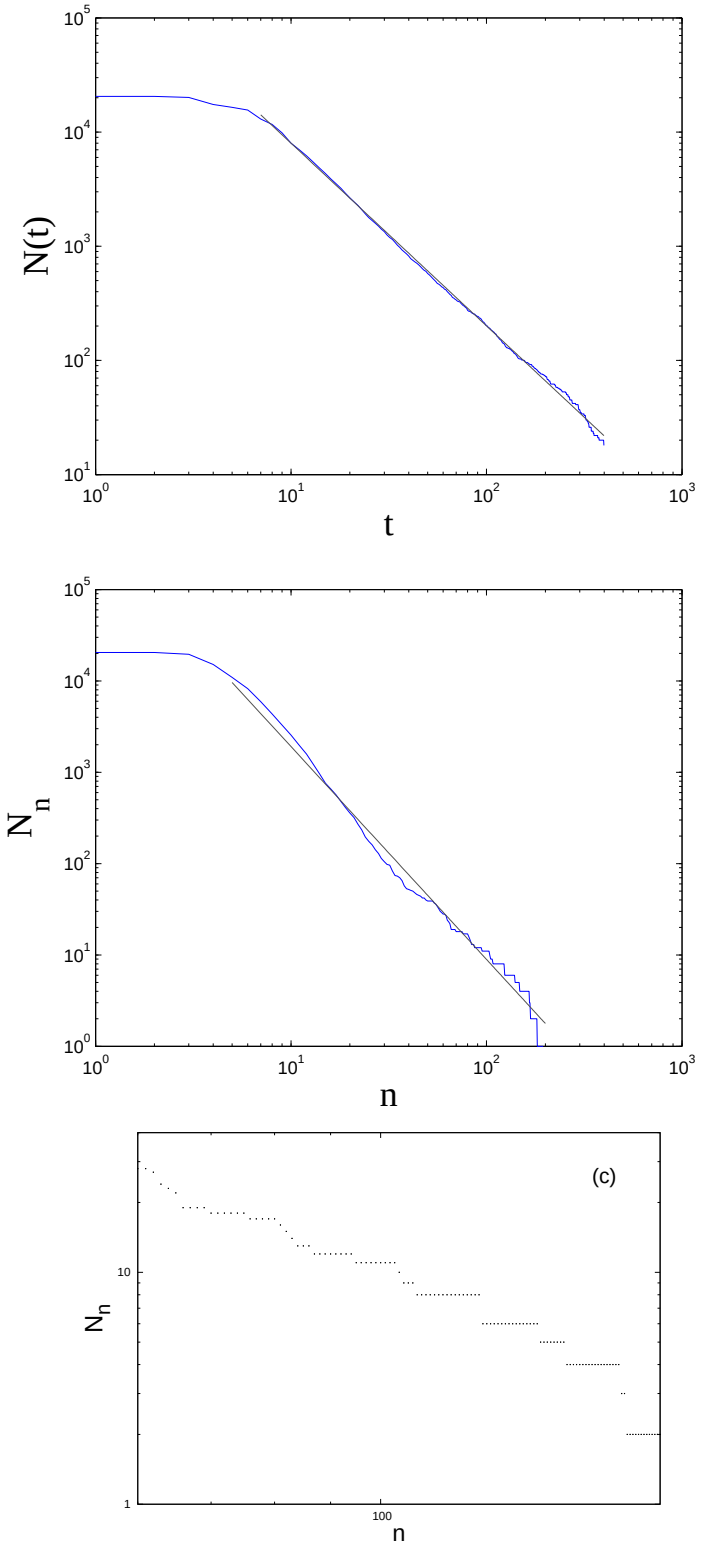

Figure 4.7: Log-log plots of $N(t)$ (plot (a)) and $N(n)$ (plot (b)) obtained from a sample of 2 10^4 orbits whose initial velocity is uniformly chosen in (1.55, 1.57). Plot (c) is an enlargement of the tail of the plot (b) from the marked point; it shows a 'stair-case' behavior of the distribution $N(n)$.

an arrangement of the states that provides an explanation of the scattering map structure. In this section we deal with the periodic driver f_2.

The considered map, called return map, is introduced in the Refs. [1, 28], where the authors investigate the irregular properties of the dynamics in periodically oscillating potential wells; they show that the map locally possesses the properties of the horseshoe. In our case we cannot conclude about the hyperbolicity of the invariant set because a better behavior of the potential $U(x,t)$, for $|x| \to +\infty$, is needed.

We define the return map D on the Poincaré section $x = 0$, that we denote by Γ. Consider a motion in which the particle crosses $x = 0$ at the instant t, with momentum p. The conditions $(x = 0, p, t)$ uniquely determine the solution $x(t'; p, t)$ of the problem (4.5). Whenever it exists consider the minimum time t_1, $t_1 > t$, such that $x(t_1; p, t) = 0$. The return map is defined by

$$D : (p,t) \longrightarrow (p_1, t_1) \tag{4.6}$$

where p_1 is the momentum at t_1.

Note that

$$x(t'; p, t) = x(-t'; -p, t) = x(t' + 2\pi/\nu; p, t + 2\pi/\nu) \tag{4.7}$$

since $H(p,x,t) = H(-p,x,-t) = H(p,x,\nu t + 2\pi)$. It follows that the zeros of the solutions of problem (4.5) can be marked by the 'polar' coordinates $p \geq 0$ and $\tau \equiv \nu t$. We denote by $R^+ \subset \Gamma$ the domain of D (see fig. 4.8). Let us consider $(p,\tau) \in R^+$ and $(p',\tau') = D(p,\tau)$. There exists the maximum (whenever $x \geq 0$) or minimum (whenever $x \leq 0$) $X^+(p,\tau)$ of $x(t; p, \tau)$ in the interval (τ, τ').

In our case the energy is not conserved, but one can, all the same, define an energy-like function. For all (p,τ) in R^+ it is given

$$h^+(p,\tau) = \mathcal{V}(X^+(p,\tau)) \tag{4.8}$$

where $\mathcal{V}$ is the time average

$$\mathcal{V}(x) = 1/(2\pi) \int_0^{2\pi} d\tau' \, U(x,\tau')$$

It is straightforward to show that $\mathcal{V} = V = V_i$, $i = 1, 2$. The function h^+ a composition of continuous applications; hence h^+ is a continuous function in R^+. We can extend by continuity the definition of h^+ at the boundary P^+ of R^+; P^+ consists of points $(\tilde{p}, \tilde{\tau})$ such that if $(p,\tau) \in R^+$ approaches $(\tilde{p}, \tilde{\tau})$ then $|X^+(p,\tau)| \to +\infty$ and

$$h^+(\tilde{p}, \tilde{\tau}) = \lim_{(p,\tau) \to (\tilde{p}, \tilde{\tau})} h^+(p,\tau) = V(+\infty)$$

A point (p,τ) in the set $H^+ = \Gamma \setminus (R^+ \cup P^+)$ is connected to an orbit $x(t; p, \tau)$ whose $X^+(p,\tau)$ is infinite; it follows that $\dot{x}(t; p, \tau)^2/2 + V(x(t; p, \tau)) \geq V(+\infty)$ for all t large enough. The orbit $x(t; p, \tau)$ is called hyperbolic for $t \to +\infty$.

We may introduce analogous quantities following the solutions backwards in time. We focus on the set of all zeros $(p,\tau) \in \Gamma$ for which there exists $x(t'; p, \tau) = 0$ at $t' < \tau/\nu$, i.e.

the particle returns to the origin if we follow the solution back to the past. We denote this set by R^- (see fig. 4.8); it is the imagine of R^+ under the return map. If $(p,\tau) \in R^-$ then it exists a finite last turning point $X^-(p,\tau)$. The function $h^-(p,\tau)$ is defined in R^-, analogously to (4.8); now substitute X^- for X^+. h^- is continuous in R^- and can be extended to the boundary P^- of R^-. We introduce $H^- = \Gamma \setminus (R^- \cup P^-)$, as well. The point (p,τ) is in H^- whenever $X^-(p,\tau)$ is infinite; the solution $x(t,\, p,\, \tau)$ is called hyperbolic for $t \to -\infty$.

If (p,τ) is in R^+ then

$$\lim_{(p,\tau)\to P^+} t' = +\infty \tag{4.9}$$

where t' is the time of the next following zero of the solution $x(t;\, p,\, \tau)$. Similarly,

$$\lim_{(p,\tau)\to P^-} t'' = -\infty \tag{4.10}$$

where t'' is the time of the last previous zero of $x(t;\, p\,, \tau)$ for $(p,\, \tau) \in R^-$. The properties (4.9) and (4.10) will play an important role.

If $e_0 = 0$ $D = I$ and $h^{\pm}$ coincide with the energy integral ($h^+ = h^- = H_0$). The set $R^+ = R^-$ is the circle $|p| \leq (2V(\infty))^{1/2}$.

The return map is derived from the Hamiltonian system (4.5). The integral $\oint \omega$ of the Poincaré-Cartan invariant $\omega = p\,dx - H(p,x,,t)\,dt$ assumes the form $\oint_c (-p^2/2)\,d\tau$ on the section Γ, c is the contour of a bounded area. It follows that D is area preserving in Γ (p and τ are polar coordinate in Γ).

Whenever $e_0 \neq 0$ the bounded regions R^+ and $R^- = D(R^+)$ have the origin in common and have the same area. Therefore the curve P^+ can lie neither wholly inside nor wholly outside P^-. It follows that $P^+ \cap P^-$ is non-empty.

We suppose there exists $A \in (P^+ \cap P^-)$ at which the tangents to P^+ and P^- are distinct; A is called 'regular' point.

The structure of the scattering function.

Following the Ref. [28], we catch the pattern of the scattering map through the map D. In the section Γ we give a construction of the sets of orbits with a determined number of crossings through $x = 0$. The structure of the sets shows the properties that we have pointed out in the analysis of the hierarchy in the scattering function.

We have already noted that the hierarchy of the regular intervals is established by the number of crossings of $x = 0$. This prompts to think that D and its iterates should play a role. Consider the sets

$$\begin{aligned} Q_n = \{(p,\tau) \,:\, & D^k(p,\tau) \in R^+ \quad k = 0, 1, \ldots\ n-1\,, \\ & D^n(p,\tau) \in (P^+ \cup H^+)\} \end{aligned} \tag{4.11}$$

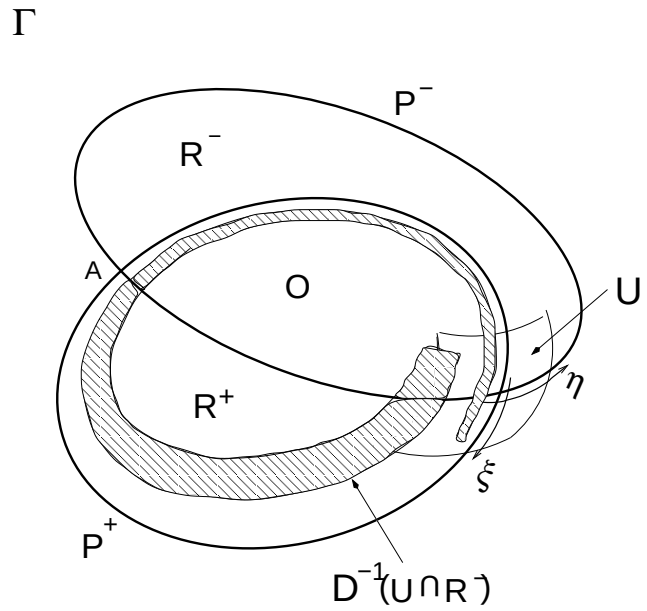

Figure 4.8: The panel shows the sets R^+ and R^- and their boundaries P^+ and P^- respectively. U is the neighborhood of a regular point where a system of local coordinates (ξ, η) is introduced. The pre-image of $U \cap R^-$ under the return map is shown.

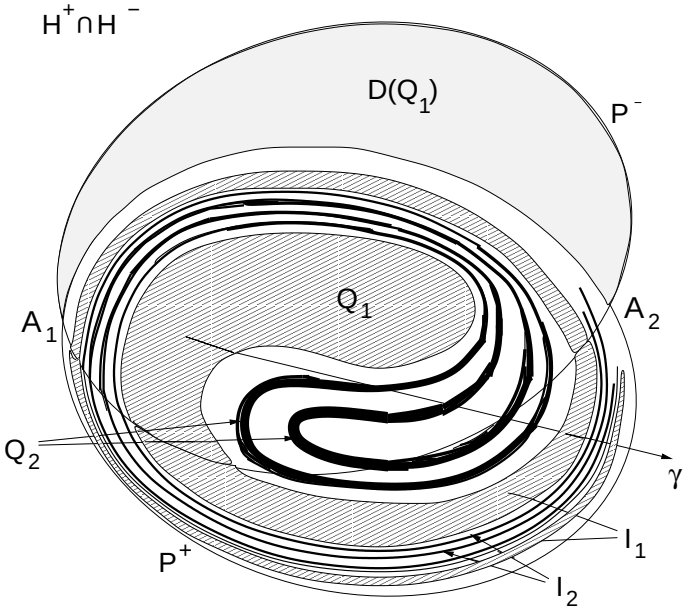

Figure 4.9: The set Q_1 is the pre-image of $R^- \cap (P^+ \cup H^+)$: it is a spiral winding on the boundary P^+. Q_2 is the pre-image of $R^- \cap Q_1$ and it consists of an infinite set of double spirals; two representatives are shown. The sets $I_i = Q_i \cap (P^- \cup H^-)$, $i = 1, 2$, are also displayed. The line γ represents a set of initial conditions ($x_0 = 0$, p_0) of orbits that get a map of type of fig. 4.1.

i.e. $x(t; p, \tau)$ escapes to a state of scattering after at least $n+1$ zeros. Q_n is non-empty. We want to understand the arrangement of the sets Q_n in the domain R^+

We start by noting that $D(Q_1) = R^- \cap (P^+ \cup H^+)$ (see fig. 4.9). The arc A_1A_2 of the

boundary of $R^- \cap (P^+ \cup H^+)$ intersects P^- transversally at the regular points A_1 and A_2; therefore its pre-image is a double spiral in R^+ as coming from P^+ as approaching to it. The double spiral separates $Q_1 \subset R^+$ from $R^+ \setminus Q_1$. It is straightforward to see that $D(Q_2) = Q_1 \cap R^- \subset (R^+ \cap R^-)$. It follows that $Q_2 \subset (R^+ \setminus Q_1)$. The set $Q_1 \cap R^-$ consists of an infinity of components that accumulate to P^+. Except, possibly, for a finite number, each of the components meet P^- transversally on both ends. As above, each stripe is mapped by D^{-1} to a loop spiraling twice against P^+ (from the property (4.10)) and that, again, crosses P^- transversally. Hence Q_2 is an infinity of double spirals (see fig. 4.9). The tail of Q_1 is located between the branches of each double spiral; the sequence of these double spirals accumulates to the boundary of Q_1.

This construction is repeated indefinitely. We find that $Q_n = D^{-1}(Q_{n-1} \cap R^-)$, $n \in \mathbb{N}$, is an infinite set of double spirals and each one of these is the image, under D^{-1}, of a strip in $R^- \cap R^+$, transversally met by P^-. Between the two tails of a double spiral of Q_{n-1} there is an infinity of double spirals of Q_n. In fact, we next show that $Q_n \subset R^+ \setminus (\cup_{m=1}^{n-1} Q_m)$. Let us assume $Q_n \cap Q_{n-k} \neq \emptyset$, $k = 1, 2, \ldots, n-1$. We take $D^{n-k}(Q_n)$ and $D^{n-k}(Q_{n-k})$ and we conclude that $(Q_k \cap R^-) \cap ((P^+ \cup H^+) \cap R^-) \neq \emptyset$. This conclusion is false because $Q_k \subset R^+$. Finally, Q_{n-1} and Q_n are dis-joined because they are images, under D^{-1}, of dis-joined set.

We focus on the set $I_n = Q_n \cap (P^- \cup H^-)$, i.e. we consider solutions with a finite number of zeros. They are parabolic or hyperbolic for $t \to +\infty$ and for $t \to -\infty$.
For all n, I_n is a subset of $R^+ \setminus R^-$. From the above construction for all $n \in \mathbb{N}$ between two stripes I_n there is an infinity of stripes I_{n+1}.

We are now able to explain the structure of the scattering maps (like fig. 4.1). We carry out the fig. 4.1 by fixing the initial position ($x(0) = 0$) and scanning an outgoing variable (the energy H_0) as a function of the initial velocity. In the plane Γ the organization of the scattering map (see figures 4.2-4.5) is connected to the pattern of the intersections of the set $\cup_n I_n$ with the radial line $\tau = 0$ (see fig. 4.10). In fig. 4.9 the radial line $\tau = 0$ is denoted by γ.

Note that the construction of fig. 4.10 is analogous to the construction of a Cantor set. In the first stage one removes a countable number of intervals I_1 that accumulate to P^+. In the second stage from each remaining interval a countable number of subintervals converging to both the ends of the interval are removed, and so on. The return map provides a construction

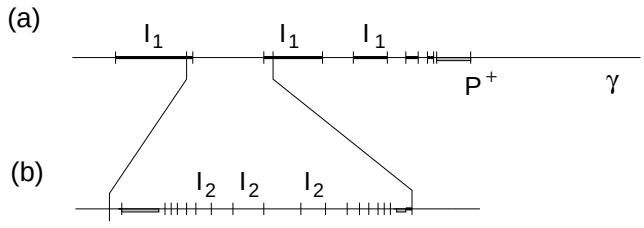

Figure 4.10: The structure of the intersections with a line γ, transversal to the boundary P^+. In (a) it is shown the set $\{I_1\}$ of intervals cut out on the spiral Q_1. The plot (b) displays the intervals I_2 cut out on the infinite number of double spirals between two branches of the tail of Q_1.

of an arrangement of sets in the phase space that strongly reminds us the hierarchical structure of the scattering function. The analysis is qualitative but effective.

The scattering map could play a more important role. In the Refs. [1] and [28] the authors analyze models with scattering by a one dimensional, periodically oscillating potential well. They construct a set Λ which is invariant under D and the dynamics of D in Λ is topologically conjugated to a symbolic dynamics; thus they conclude that their models show chaotic scattering. The potential is attractive with respect to the origin for all times; by means of this property they control the dynamics in the vicinity of the parabolically escaping orbits. This control is essential to establish that the return map is locally a horseshoe map and that Λ is a (non compact) Cantor set.

5. The fractal structure of the delay time function and the algebraic decay law.

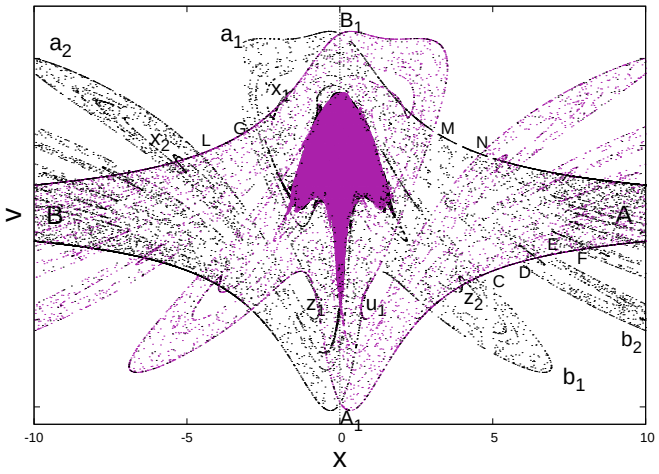

Figure 4.11: There are shown the stable manifolds (black) and the unstable ones (red) of the outermost fixed points A and B. They are determined through the method of sprinkler. The fundamental region $\mathcal{A}$ is the 'rectangle' AA_1BB_1. a_i and b_i $i = 1, 2$, are the stable tendrils of A and B, respectively. The points x_i, z_i, $i = 1, 2$ mark the tips of the stable gaps of first and second order. The point u_1 is the tip of the first order unstable gap.

5.1 The fundamental region and the invariant manifolds.

We are addressed to give a connection between the delay time of a trajectory and the number of steps that it performs in a given region of the phase space (in this section we deal with the periodic driver ($f = f_2 = \sin(\nu t)$). In order to do this we use some ideas of Ref. [57] and Ref. [33]. The considered region is a part of a phase space which contains the invariant set of the scattering process. Its boundaries are traced out by the segments of the invariant manifolds corresponding to the outermost fixed points in position space. Some non-hyperbolic areas may be found in the region.

We determine the invariant manifolds (the stable manifold W_s and the unstable one W_u)

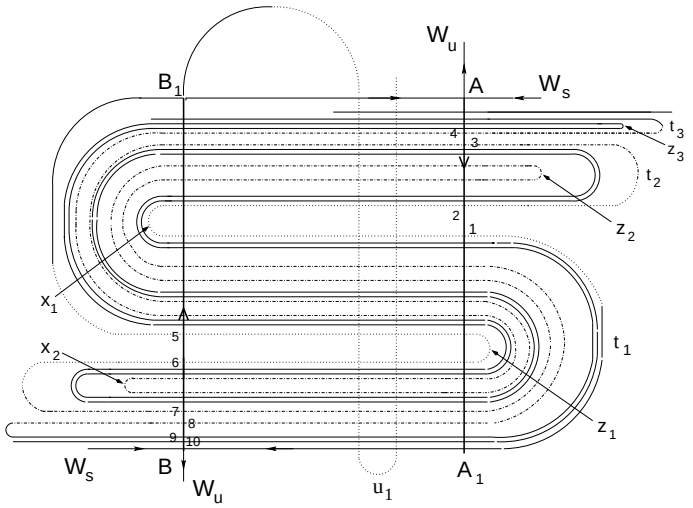

Figure 4.12: Schematic plot of a complete horseshoe. The outermost fixed points are labeled A and B. The rectangle AA_1BB_1 is the fundamental region $\mathcal{A}$. There are displayed gaps up to order three. The point x_i is the tip of the stable gap of B of $i-th$ order. The point t_i is the tip of the stable tendril of A of $i-th$ order. z_1 and u_1 label, respectively, the tip of stable and unstable first gap of A.

by means of the 'sprinkler algorithm' that was introduced in Ref. [60]. The method consists in considering a distribution of initial conditions from a region that contains the chaotic set. Each trajectory is followed until a given time t large enough. If the initial point is close enough to the stable manifold it spends a time larger than t to escape from the given region along the unstable manifold. Therefore the initial points, that still stay in the region at t, form the stable manifold and the set of points at time t forms the unstable manifold.

The fig. 4.11 gives the result of the numerical calculation; we use a grid of 20000×6000 initial points: the stable manifolds are shown in black and the unstable ones are shown in red. We focus on the diamond-shaped area AA_1BB_1 that we name fundamental region and denote by $\mathcal{A}$. The points A and B are the outermost saddle points respectively at $x > 0$ and $x < 0$. There is an elliptic fixed point close to the origin; it is encircled by KAM tori, secondary elliptic points and other possible invariant structures that are remnant of the quasi-periodic case. Altogether these structures determine a region of phase space where the dynamics is not hyperbolic.

The Hamiltonian (4.5) is not invariant under the transformation $x \to x' = -x$; therefore the underlying invariant structure seen by the particle is different when it comes from opposite directions. However the Hamiltonian is invariant under the composition of $t \to -t$ and $x \to -x$; it follows that, in the resultant pattern of fig. 4.11, we convert each stable manifold to an unstable one and vice versa by letting $x \to -x$.

The intertwined structure of fig. 4.11 is obtained by starting from the segments of the manifolds W_s and W_u that make up the boundaries of $\mathcal{A}$. The homoclinic/heteroclinic intersection points between W_s and W_u belong to the chaotic set and the topology of the intersections determines the structure of the outermost component of the set.

The fig. 4.12 gives a schematic plot of the intersections set of the invariant manifolds of

A and B (we do not consider chaotic structures owing to inner fixed points). It is the known construction of the Smale horseshoe: the fundamental region $\mathcal{A}$ (whose boundaries AA_1BB_1 are given by segments of the invariant manifolds of the outermost fixed points A and B) is stretched and folded back onto itself. We fold $\mathcal{A}$ two times because we have two fixed points.

We now describe in more detail the construction of fig. 4.12. The segments of the boundaries of the fundamental region (the unstable segments AA_1 and BB_1 and the stable ones AB_1 and BA_1) are called tendrils of zero order. We propagate the segments of the stable manifolds backward in time and the segments of the unstable manifolds forward. We focus on the stable manifold of the fixed point B and the local segment of the unstable manifold of A. The pre-images (images) of the stable (unstable) tendrils of zero order are tendrils of first order (the segment A_1t_11 of W_s is the tendril of order one); generally the tendril of order n is mapped to that of order $n+1$ (the arc $2t_23$ of W_s is the tendril of order two and it is the pre-image of A_1t_11).

In between these segments of W_s forming the tendrils there are other segments g_n^B of W_s going across the fundamental region; they are called gaps of order n. g_1^B is the arc $1x_12$. The points of g_1^B are mapped to the segment $3x_24$, i.e. the stable second order gap g_2^B. Generally the pre-image of g_n^B is the gap g_{n+1}^B. We may similarly proceed with the invariant manifolds of B; the segment $5z_16$ is the first gap g_1^A of W_s of the fixed point A; $7z_28$ and $9z_310$ are the gaps g_2^A and g_3^A, respectively, and so on.

In this construction we use the invariant manifolds of the fixed points on the corners of $\mathcal{A}$ (A and B). This choice implies a favorable property which does not hold in the case of the invariant manifolds of periodic points lying in the interior of $\mathcal{A}$. In fact the gaps which are cut into $\mathcal{A}$ by the manifolds of A and B are regions of $\mathcal{A}$ which do not cover the invariant set; no higher level segment of W_s will ever enter such gaps. Furthermore it holds: the topology of the intersections is determined by the intersection pattern between all the tendrils of the stable manifolds and the 'local' segments of the unstable manifolds, i.e. the branches AA_1 and BB_1 in the fig. 4.11. This fact can be easily understood if we think that each intersection (homoclinic, heteroclinic) point in $\mathcal{A}$ is the image-pre-image of an intersection point of W_s with the local segments.

The horseshoe construction is complete when the tip u_1 of the first order gap of the unstable manifold reaches the other side of the fundamental area (the schematic plot of fig. 4.12 shows a complete horseshoe). In this case a stable gap of order n reaches into all tendrils up to the order n. The fig. 4.13 shows a partial development of the pattern of gaps in a tendrils of order n. The innermost part is a gap of order n. Between this middle gap and the boundary of the tendril there are two gaps of order $n+1$. On the next level there are two gaps of order $n+2$ in between each pair of adjacent gaps of lower order or between the gaps of lower order and the boundary. This scheme continues to higher level. In a tendril of order n we find $2\times 3^{n_1-1}$ gaps of order $n+n_1$. Between any two adjacent gaps of the same order we find gaps of order arbitrarily high; hence in each neighborhood of a gap we find gaps of all orders high enough. In the area enclosed between a tendril and the local segment the gaps fill a subset of null measure. The resultant structure is a set of segments of W_s along the direction of the tendril whose sections in the transverse direction are Cantor sets. This structure is closely connected to the invariant set in the fundamental region.

The link between the gaps and the scattering problem is due to the following mechanism. The tendrils reach out into the incoming asymptotic region. We consider a particle that comes from far away and approaches the local segment and lies in a gap of a tendril of order n. Except for a fractal set of lines (resembling the invariant set) the particle is mapped to a point of a gap in $\mathcal{A}$. In fact, by the construction of the horseshoe, any point in the stable tendril of order n is mapped in the stable tendril of order $n-1$. The first order tendril of the stable manifold of A (t_1^s) is mapped in the first gap of the unstable manifold of B (u_1); more specifically, a point in a stable gap of order n (g_n^s) in t_1^s is brought into $u_1 \cap g_{n-1}^s$. Points of a gap are brought out of the fundamental region after a finite number of iterations of the dynamical map: the stable gap g_n^s is mapped to g_{n-1}^s and the image of g_1^s is the first order unstable tendril of B. At this point the particles leaves out of $\mathcal{A}$; in fact an unstable tendril of order n is mapped to an unstable tendril of order $n+1$, and so on. Finally, except for a set of zero measure, a scattering trajectory experiences a finite number of steps inside the fundamental area whenever it approaches the local segment of the unstable manifold along a gap in a stable tendril.

From these considerations we assert that the arrangement of singularities of a scattering function should be related to the structure of the chaotic invariant set and then to the sequence of tendrils along the local segment of the unstable manifold. In this sense we can reconstruct the structure of the horseshoe from the measure of the scattering functions, i.e. from asymptotic measurements.

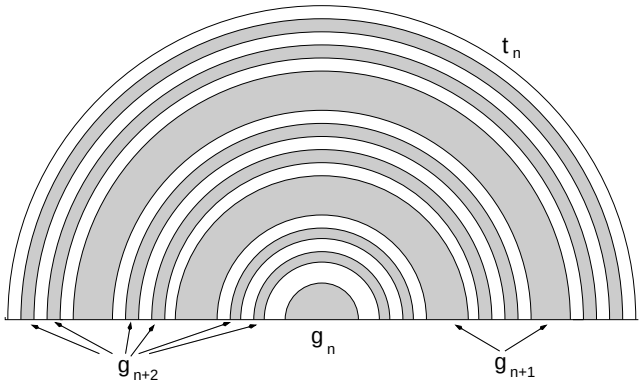

Figure 4.13: The plot displays the first few stages of the development of the pattern of gaps in a tendril of order n.

5.2 The scattering function and the structure of the invariant sets of the outermost fixed points.

We know that the set of singularities of a scattering function shows how the line of the incoming particle asymptotes pierces the bundle of stable manifolds of the chaotic invariant set. However we may state that the main properties of a scattering function are dominated by the component of the invariant set due to the outermost fixed points.
We focus on the delay time scattering function; we keep the initial position fixed and vary the initial velocity and for the corresponding trajectories we monitor the time interval τ between

the first and the last zero. The plot (a) of fig. 4.14 shows a typical pattern. The structure of the delay time closely corresponds to the structure of the N_c scattering function (compare (a) with (b)):

- an interval with a given number of zeros is related to a continuous branch of the delay time function;
- each regular interval of τ is accumulated by a sequence of regular intervals for τ going to arbitrary large values.

We are mainly interested in the singularity structure of the scattering functions. For this particular purpose the information provided by τ is the same as the time interval which the particle spends in the fundamental region. We have focused our attention on the features

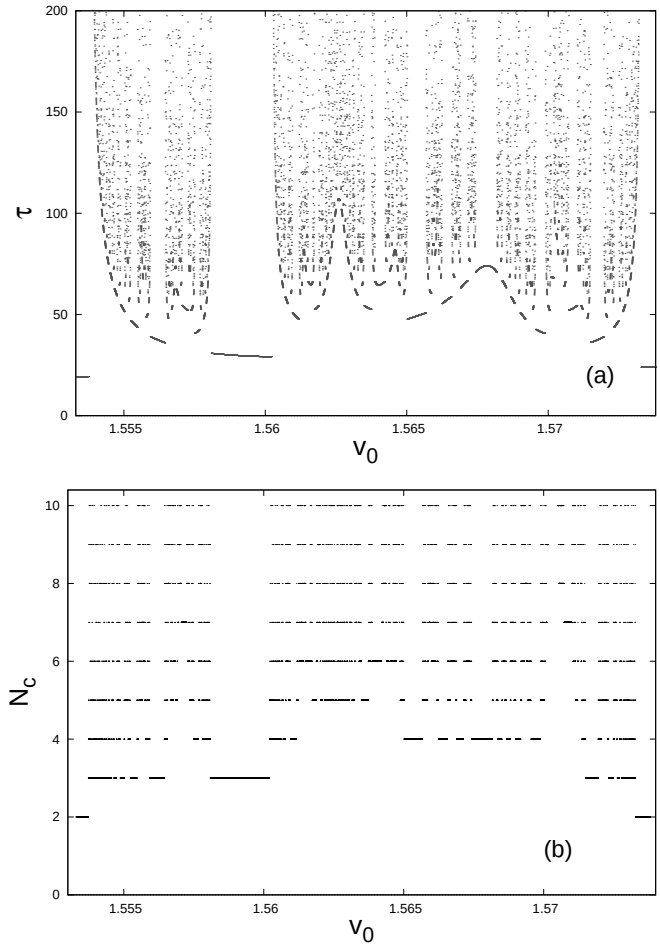

Figure 4.14: The plot (a) displays the delay time scattering function for the same line of initial conditions of (b) fig. 4.1. The plot (b) is the number of crossings of $x = 0$ in the same conditions of (a).

of the dynamics of particles approaching the fundamental region through the local unstable segment. Our considerations drive us to affirm that the singularities structure in τ is correlated

with the structure of intersections of W_s of a fixed point with the local branch of W_u of the other fixed point, i.e. the pattern of fig. 4.13.

On account of the structure of gaps in a tendril, we see that, except for a set of zero measure, the trajectories, coming from a line of initial conditions and intersecting the tendril, are mapped far away after they undergo a finite number of iterates inside the fundamental region. A trajectory that approaches the fundamental region along a gap belongs to a regular interval of the delay time function. On the other hand the set of singularities of the delay time function corresponds to the set of points in a tendril that do not belong to any gaps; the trajectory is confined forever inside the fundamental region.

The graph of τ possesses the following hierarchical organization. Consider the connection between τ and N_c. In the graph (b) of fig. 4.14 we remove all continuous branches corresponding to the intervals with the lowest N_c; the τ structure is separated into substructures that are similar to the parent one; each removed subinterval is surrounded by smaller subintervals with a higher value of τ ('castle-like' structure; see Ref. [92]). We may iterate the procedure and the number of zeros fixes the level of cutting out; at each step we get a generation of substructures similar to that of the previous generation. In this way we determine a hierarchical organization. It is important to observe that the pattern of gaps in a tendril (fig. 4.13) displays the same organization. In a tendril of order n, whenever we cut a gap of order $n+1$ away, the pattern is separated into substructures, with gaps of higher order, similar to each other. We may iterate the method for gaps of higher order; the hierarchy follows the order of the gap. In this way we establish a connection between the pattern of the delay time function and the structure of the N_c scattering function (compare (a) and (b) of fig. 4.2). Likewise the qualitative approach that refers the return map, in this section we have examined some features of the scattering function using global considerations on the dynamics (the invariant manifolds of the fixed points A and B). In addition we have not needed to take into account all the chaotic invariant set.

5.3 The algebraic decay.

In section 2, we have checked an algebraic law both for $N(t)$, the decay with time of the number of temporarily bound orbits, and for $N(n)$, the distribution of zeros. Hyperbolic systems usually exhibit $N(t)$ to have an exponential decay law [47, 64]. The algebraic decay would press to consider our system to be non-hyperbolic [71, 78] or, if it were hyperbolic, there should be a special mechanism that makes the decay slower than what is expected when the KAM tori structure is completely broken [74, 105]. Our problem should fall in with the non-hyperbolic situation. In fact the Poincaré map shows orbits that curl up tori, i.e. there is a mixture of motion close to the deformed tori and motion far away from them.

The presence of KAM surfaces affects the particle motion in the nearby chaotic regions; even if the particle starts in a chaotic region, sooner or later the particle approximates the surface and wanders close to it for a long time; it is the "stickiness effect". The motion in a KAM surface is quasi-periodic and hence, nearby the tori, the Lyapunov exponents in the directions along the surface are zero. Moreover, in our case, the Poincaré map is

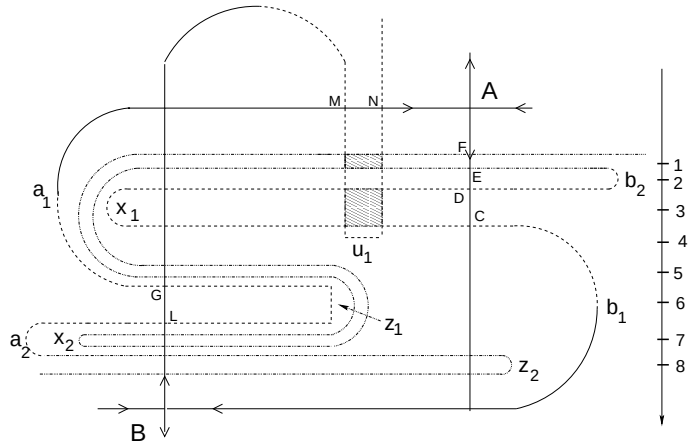

Figure 4.15: Schematic plot of the scenario in fig. 4.11. The horseshoe is incomplete and asymmetric; the first order unstable gap (tip u_1) does not reach the opposite side of the fundamental area. The numbers in the right column count all gaps up to order two. The horseshoe is characterized by the development parameters $\gamma_A = 1/3$ and $\gamma_B = 1$.

symplectic (the driver is periodic) and, because it is two-dimensional, the Lyapunov exponent perpendicular to the surface also has to be zero. The stickiness effect reduces the transport of orbits initialized in a chaotic region and explains the algebraic decay law instead of the exponential one. In the Ref. [71] it is established that the size of the decay depends on the complexity of the pattern of island chains: the more dominant the island chains in the chaotic region, the slower the escape process.

We have remarked that in the Ref. [9] an algebraic decay for the delay time function is obtained. Nevertheless in this case the effects of the KAM components are negligible. When we consider $V = V_2$, $V_2 \sim |x|^{-2}$ for $|x| \gg 1$, the explanation of Beeker et al., applied to our case, supplies a decay law slower than the law we observe. The reasoning of Beeker et al. attaches the most part of the importance to the orbits that spend the most part of time far away from the interaction region; they are trajectories which almost escape after e.g. the n-th zero, but are eventually recaptured, so that there is a long time elapsing between the n-th and the $(n+1)$-th zero. Because of the KAM surfaces, in our case we have to take into account the orbits that run inside the interactions region. Their 'life-time' is shorter than that of the temporarily bound orbits close to the parabolic one; in fact the energy absorptions mainly take place around the origin. On the basis of these considerations we expect the algebraic decay to be faster than the scaling determined by the class of orbits in the approximation of Ref. [9]. In order to give a quantitative characterization of the development stage of the horseshoe construction a parameter γ ('development parameter') was introduced in Ref. [92]. For the system under consideration there are three most effective fixed point: the outermost ones and the inner elliptic fixed points. The development parameter for the corresponding horseshoe is $\gamma = r_n\, 3^{-n}$; n is the highest order of the gap we consider and r_n is the order of gap, which the tip of the first unstable gap reaches, when we count the gaps from the fixed point (see Ref. [57]). Note, the value of γ does not depend on the choice of the order n we consider.

The parameter allows to evaluate how deep the first order gap penetrates into the fundamental area of the horseshoe compared to the complete case; in the development of a

horseshoe the parameter γ varies from 0 to 1. A horseshoe is complete whenever the unstable gap of order one reaches the opposite side of the fundamental area (see fig. 4.12); in this case $\gamma = 1$.

The parameter is used to qualitatively characterize the topology of the homoclinic/heteroclinic tangle of the outer fixed points. It remains the same when under variations of physical parameters the changes of the topology concern tangencies of branches of manifolds of level high enough. It is important to point out the relation of γ to the topological entropy K_0. In Ref. [92] it is obtained, by numerical computation, that K_0 is a monotonic function of γ. The parameter ignores the unique aspects of the KAM surfaces; it does not take into account the winding numbers of the elliptic points and neglects effects coming from the invariant manifolds that penetrate into the surroundings of the KAM islands. However the parameter considers the part of the invariant set which is the most important for the scattering function.

We focus on the fig. 4.11. We observe that the inner non-hyperbolic island obstructs the penetration of the unstable gap in the fundamental area and keeps from the complete growth of the saddle pattern. The fig. 4.15 is a schematic plot of fig. 4.11; the stable manifolds of A and B are plotted up to order two and W_u of the point B is plotted up to order one. The numbers in the right column count all gaps up to order two, consecutively from the top to the bottom. We note that the horseshoe is non-symmetric and hence it is incomplete. Actually the first unstable gap of A reaches the other side of the fundamental region (it is the mirror image of x_1) and the unstable gap u_1 does not. The horseshoe is thus described by two development parameters. The parameter value of W_u of B is $\gamma_B = 1$. On the other hand, when we consider gaps up to second order ($n = 2$) the u_1 ends in the third gap from the top ($r_2 = 3$), thus leading to $\gamma_A = 1/3$.

Concerning the scattering problem, the effects of KAM islands and their secondary structures should have little influence on the approximation of the horseshoe reconstruction: they are connected to the penetrations of the invariant manifolds of the outermost fixed points in the secondary structures around the KAM islands. In non-hyperbolic case the KAM component obstructs a full development of the horseshoe. In contrast to the complete horseshoe (fig. 4.13) in the incomplete case some inner gaps in a tendril can disappear (fig. 4.15). However the non transversal intersections between stable and unstable manifolds due to KAM tori have small effects on the scattering functions [92], i.e. on the structure of the intersections between the stable manifold and the local segment of the unstable manifold. For $\nu = 0.8$ and $e_0 = 1$ there are tangencies for gaps of order $n \geq 3$. The effects of the tangencies are visible on the scattering functions at the order $2n \geq 6$; in fact whenever the n-th order stable gap is tangent to the n-th unstable gap then the $(n+1)$-th order stable gap intersects the $(n-1)$-th unstable gap and, finally, the $(2n)$-th stable gap intersects the local segment at the $(2n)$-th tendril.

6. Scattering features as the driver amplitude is varied.

In this section we fix the initial conditions and vary the parameter e_0. We know (see Ref. [27]) that a scattering system can experience transitions from regular to chaotic scattering as a

parameter of the system is varied. The onset of chaotic scattering can be achieved through combination of bifurcation mechanisms: new periodic orbits are added and their stable and unstable manifolds intersect each other. These events cause changes in the chaotic set; as the parameter is varied the hyperbolic component increases and the formation of structures topologically equivalent to a horseshoe may occur.

We do not address the question of how the chaotic scattering arises as e_0 changes. We only discuss the qualitative behavior of the outgoing energy of a trajectory with given initial conditions. We argue that the main properties are connected to the invariant pattern caused by the outermost fixed points. We consider both the periodic case ($f = f_2$) and the finite duration driver ($f = f_1$). The initial conditions are set $x(0) = 0$ and $\mathrm{v}(0) = 1.049$ ($H_0 = 0.55$ at $e_0 = 0$).

In the case of $f = f_1$ the map links e_0 to the value of H_0 taken at t^*, after the driver is switched off (see fig. 4.16):

$$S^1_{(x_0,v_0)}: \;\; e_0 \;\mapsto\; H_0(p(t^*), x(t^*))$$

For the periodic driver we introduce the one-to-many values mapping:

$$S^2_{(x_0,v_0)}: \;\; e_0 \;\mapsto\; H_0(p(t_k), x(t_k))$$

$\mathrm{v}\, t_k = \pi/2 + k\,2\pi$, $k = 1, 2, \ldots$; the map links e_0 to the energies H_0, every driver period. In all cases we obtain patterns that display some of the features of the maps investigated above:

- There is a sequence of alternating regular and irregular intervals of e_0.
- A magnification of an irregular interval shows a pattern similar to the complete one (see (b) of fig. 4.16).
- Except for very few cases a regular interval corresponds to a determined number of crossings of $x = 0$ (or number of steps in the fundamental region. See (c) of fig. 4.16).

We should point out that, differently from sect. 3, the hierarchy of the regular intervals with respect to N_c, the number of crossings of $x = 0$, does not completely hold. In fact, there are some regular intervals where N_c changes value (see the jump from $N_c = 5$ to $N_c = 7$ of the regular interval at the left hand side of the plot (d) of fig. 4.16 and the jump from $N_c = 8$ and $N_c = 10$ of the regular interval $[4.954, 4.957]$).

We come back to the horseshoe construction that is traced out by the invariant manifolds of the outermost fixed points. We have stated that, for fixed e_0, the topology of homoclinic/heteroclinic intersections determines the structure of a scattering function corresponding to a line of initial conditions which cuts tendrils of the stable manifold close to the local branch. We want to explain what occurs when we fix the initial conditions and vary e_0. By changing e_0 the length of manifolds is affected and homoclinic bifurcations take place whenever the branches of two manifolds cross each other. Accordingly the invariant set changes its topology and some orbits may get lost.

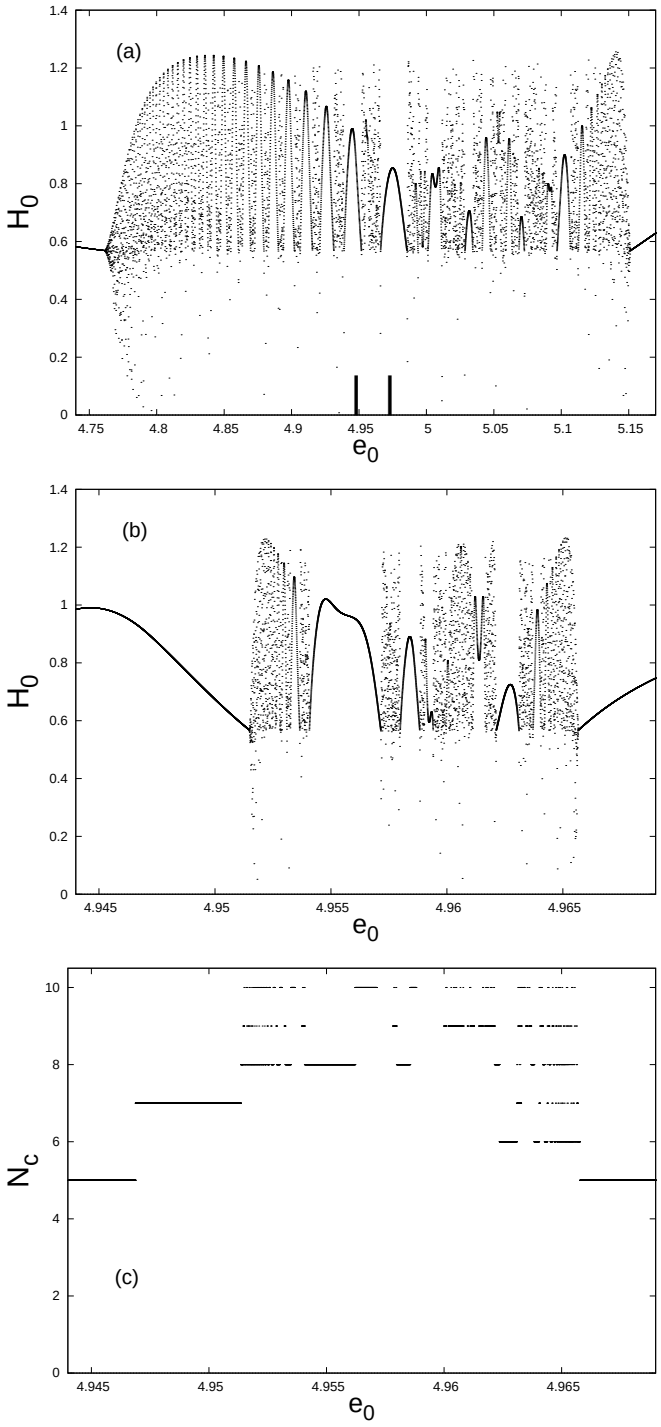

Figure 4.16: The plot (a) displays the asymptotic-out energy (H_0) vs the driver amplitude (e_0) for $f = f_1$. The plot (b) is a magnification of the marked interval of (a). The plot (d) shows N_c corresponding to the interval of e_0 in the plot (c)

Consider (a) of fig. 4.17: a tip u_1 reaches into a stable gap that, we know, is free of further gap of W_s, and the tips z_1 and x_2 lie in the areas of tendrils. In these situations stretching or compression of segments of manifolds do not cause any tangencies. If this is the case for the

tips of all gaps up to order n then, even if we vary e_0 over a suitable interval, the corresponding changes of the topology may affect only orbits with at least n iterates in the fundamental region. This implies a stability of a part of the structure of orbits against bifurcations. On the

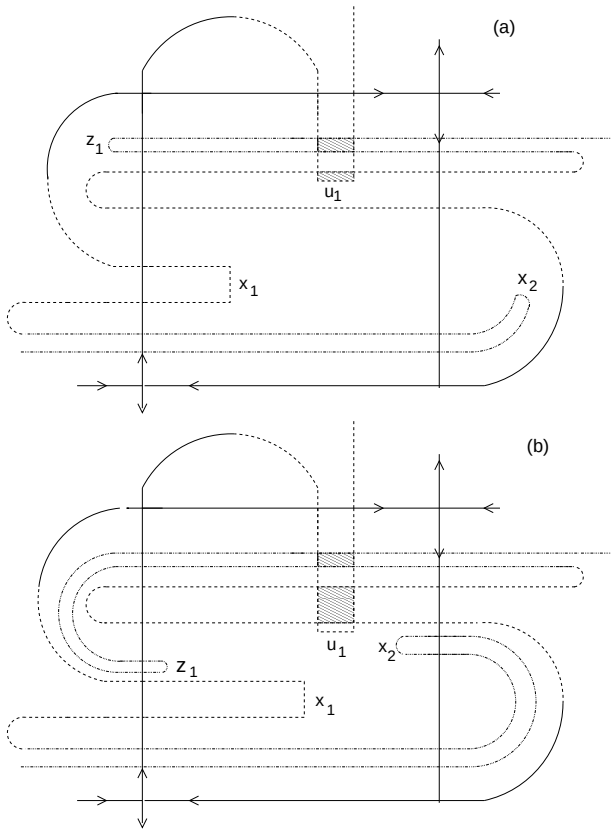

Figure 4.17: The plot (a) displays an incomplete horseshoe where the tips u_1, x_2 and z_1 enter areas where they cannot hit invariant manifolds. In the plot (b) the same tips can undergo tangencies under small changes of e_0.

other hand a tip that exits a gap can undergo a homoclinic tangency for small changes of e_0 (see (b) of fig. 4.17). In the fundamental region, the structure of the gaps, that is kept fixed over an interval of e_0, resembles the structure of homoclinic/heteroclinic intersections that is "seen" by a line of initial conditions, as long as we consider orbits with a number of steps in $\mathcal{A}$ not too large. The second structure is connected to the pattern of gaps in a tendril. We conclude that the structure of singularities of the maps $S^i_{(x_0,v_0)}$, $i = 1, 2$, should resemble to the scattering functions with respect to a line of initial conditions.

An essential observation is that there are parameter intervals in which the tips of the invariant manifolds do not create homoclinic bifurcations under small changes of the parameter. This occurs due to the gaps which are empty of invariant manifolds. It should be pointed out that the idea of the gaps may be helpful only if it is applied to a system with an open, infinite phase space (scattering systems). In fact in a bound Hamiltonian system the invariant manifolds are dense in a connected subset of the phase space not containing KAM tori.

Chapter 5

Conclusions.

The interaction between short, high-power laser beams and matter with charge densities large enough, as solid and liquid targets and clusters, is characterized by an energy absorption largely exceeding what a naive, linear, purely collisional description predicts, on account of the fact that in this contest electron-ion collisions are almost negligible, so that the electrons couple only to the laser field and the "collective field" generated by the plasma. Actually several, often overlapping mechanisms, dominated by nonlinear effects, have been proposed; each of them, in particular cases, is able to explain energy absorption since it allows the "adiabaticity" to be broken. However they do not satisfactorily capture the physics involved in the absorption, in particular, they do not provide any physical effect guaranteeing a finite phase shift between the current j and the driver field E. On the basis of the cycle-averaged Pointing theorem the shift is the condition of radiation absorption in extended media.

A physical phenomenon that can be assumed as a "paradigmatic", unifying principle able to describe collisionless absorption is the resonance in the collective plasma potential. In particular it can explain in a natural way

- the phase shift between current and driver,
- the "fast" (on fs time scale) transfer of energy to the electrons as it is observed in PIC simulations (see [87]).

For ultrashort laser pulses (about few tens of femtoseconds long), the interaction laser - solid matter cannot be modeled by a linear oscillator, with a proper frequency ω_0 usually of the order of the plasma frequency, driven by an exciting force $f(t) = a(t)\ \cos(\omega\ t)$. In fact, for the solid density matter it is $\omega_0 \gg \omega$ and in these circumstances the energy absorption by a harmonic oscillator is considerable whenever the exciting $a(t)$ has a support of length nearly ω_0^{-1}, whereas it is negligible for $a(t)$ of length ω^{-1} ($\gg \omega_0^{-1}$) (see [25]). Hence far from resonance the excitation is only "ballistic". Since even the shortest laser pulse contains several oscillations, ballistic excitation is not possible. Therefore a harmonic oscillator can absorb only if it meets the linear resonance $\omega_0 = \omega$. In order that this occurs a decreasing of the charge density has to lead to a sufficiently decreasing of ω_0; this can be given by the

fluidodynamics expansion of the plasma, but it usually needs laser pulse lengths at least in the picosecond regime.

Therefore, for very short pulses or during the early cycles of a long pulse, the driven non-linear oscillator can be assumed as the unifying process for the collisionless absorption in strongly overdense plasmas. That means that the system, originally out of resonance, moves in the anharmonic potential of the plasma. Under the influence of a driver large enough and with fixed period, the oscillator is excited to an amplitude such that it meets a non-linear resonance that couples an appreciable amount of energy by the adiabatic excitation into the system. Furthermore, the crossing of a resonance is the condition that makes the gain of energy to be "irreversible", i.e. when the driver is swichted off the absorbed energy is not turned back.

Our work consists in an investigation of the driven non-linear oscillator model, in which we pay prominent attention to the resonance issue. In order to characterize the dynamics in a resonance and the role of a resonance in the absorption issue we consider the following approaches:

- for small driver amplitude ε we refer to the methods of the Hamiltonian theory of perturbation, in particular to the techniques of the Nekhoroshev theorem. The analysis allows to determine, in a resonance, the nature (integrable or chaotic) of the dynamics and the significant time scales;
- without any restrictions on ε we perform a numerical study in which we compute the solutions of some discrete maps; in particular, for a periodic driver we determine the Poincaré map P. In this way we adopt a "geometric" approach. In fact, the graphical displays, generated by the solutions of P, allow to characterize some features, salient in the collisionless absorption, through a "qualitative" description of the topology of resonances in the phase space. In particular, we refer to the existence of a "threshold" in the amplitude driver for getting a resonance.

We assume that

- the driver is periodic with period T (frequency ν) and with amplitude ε;
- the oscillator (collective) potential V has a minimum. As regards the asymptotic behavior we admit two types of potential: (a) closed orbits can only occurs and (b) V possesses two heteroclinic orbits that connect the parabolic point at $+\infty$ to that at $-\infty$.

The one degree of freedom, forced oscillator is formulated as a Hamiltonian system with two degrees of freedoms, where the time t is a canonical angle. Because of the small number of the degrees of freedom the system has only "simple" resonances.

There is a general result for any integrable system that is weakly perturbed, i.e. for ε small enough: near a resonance the resonant angle can be always eliminated from the unperturbed Hamiltonian by a canonical transformation to a frame of reference that rotates with the resonant frequency. The resulting Hamiltonian, that governs the slow variables, is a

sum of the resonant normal form and a remainder, that is small with ε. The former describes the oscillations bounded by ε^{σ}, $\sigma > 0$, around the resonance up to a time scale that is long compared to $1/\varepsilon$, as far as the remainder does not appreciably move the actions. For a simple resonance the normal form describes a pendulum, with the two different types of periodic motions, rotation and libration, and the separatrix motion. The resonance is at the elliptic point; the hyperbolic point plays an important role on the time scales when the complete Hamiltonian has to be considered.

We obtain that the effect, which Mulser et al. invoked to explain the collisionless absorption, is just a "remnant", at large driver amplitude, of a "rational" torus that was broken. We deal with the invariant structures modified from the unperturbed ones, that are defined by the collective plasma potential. Even for ε not small enough, the phase portrait produced by P displays

- an elliptic point O, corresponding to the minimum of V. Around O there is a region $\mathcal{R}$ which is filled of quasi-periodic orbits encircling O, except for a domain which is reduced to a set with zero measure for ε small enough; we called $\mathcal{R}$ "KAM structure". The island $\mathcal{R}$ is the remnant of the elliptic structure of the critical point for $\varepsilon = 0$;
- some "pendulum-like" structures ("islands") at certain gaps between quasi-periodic orbits. This fact means the presence of a resonance at any gap; the number of islands depends on the order of the resonance. The resonances are located where the phase space topology is made quite different from that of the system for $\varepsilon = 0$.

Next, for determining the order of some resonances we refer to the "effective" frequency ω_{eff}, of the "free" oscillator, as a function of the energy E, i.e. for $\varepsilon = 0$, we determine the period $T(E)$ of the bounded motion with energy E. Put more explicitly, for $\varepsilon \neq 0$, along any orbit the function H takes all values on an interval; if we consider a set of orbits around a resonance we find that the spreading interval of H experiences a discontinuity at the resonance. The value $H = E$ at the discontinuity is an estimate of the energy of the resonant torus for $\varepsilon = 0$. Finally we are able to estimate the order of the resonance, namely the couple of entires $m,\ n$ such that $m\ \omega_{eff}(E) \simeq n\ \nu$. The method is rough; however the estimates agree with the number of islands.

The order of a resonance is helpful to draw attention to the following point. Mulser and al. suggest that the resonance condition in the plasma potential is met only if the oscillation period $T(E)$ and the driver period are nearly equal. Actually our investigation shows that, in general, it is not true that a considerable resonant absorption occurs at the resonance of order $1:1$. In fact the absorption is connected to how much the phase space topology close to a resonance is different from that of the free oscillator. This property is linked to the maximum escursion of the action at the resonance which depends on, besides the perturbation strength, a coefficient of the Fourier expansion of the reduced Hamiltonian H. In general the expansion does not imply that a sizable energy absorption occurs at the resonance of order $1:1$. However, the resonances of importance for modifying the action variable are always those with low harmonic number as the convergence properties of the expansion require the Fourier coefficients rapidly fall as the harmonic number increases.

Another point, worthy to be noted, is that the existence of an absorption threshold in ε

can be characterized in terms of invariant structures in the phase space. In fact, for ε small enough, an orbit, with initial data close to the unperturbed elliptic point, remains near the perturbed elliptic point, since it is confined by the almost periodic orbits of the island $\mathcal{R}$. Therefore the absorption of energy is negligible. Whereas, for ε large enough, the orbit leaves the region $\mathcal{R}$ and or it is constrained to the modified invariant manifolds at the resonance, if there exists, or it moves in regions of phase space where confining structures are lost. In any case the motion takes place in a region that is very larger than $\mathcal{R}$. Hence the absorbed energy is considerably more than above.

A resonance, besides being an area of the phase space where a perturbation can cause the most sizable changes in the invariant manifols geometry, is a place where the perturbation of an integrable system produces non-integrability. No matter how small ε is chosen, the non-integrability is closely related to the existence and unavoidability of resonances. We know that a Nekhoroshev-like perturbation theory is mainly helpful because it gives a general insight into the problem of stability for any system with at least three degrees of freedom. However, even for a system with only two degrees of freedom, it enables us to understand how chaotic motions can arise near a simple resonance; in particular it makes evident the existence of different time scales in which the motions show distinct behavior. More explicitly, through this approach it can be stated that, for ε small enough, a motion, with initial data closer to the resonance than ε^σ, $\sigma < 1/2$, is described up to a time $O(e^{\varepsilon^{-b}})$, $b > 0$, by the one dimensional pendulum Hamiltonian which implies, via energy conservation, the motion remains closer to the resonance than ε^σ. Therefore we can conclude that close to a simple resonance the motion remains integrable up to time exponentially large with $1/\varepsilon$. However, the Hamiltonian includes, besides the pendulum, a remainder, exponentially small with ε. Indeed this term can be given any preassigned form by a suitable choosing of the perturbation. Therefore the remainder, as it is a two degrees of freedom term, can exhibit chaotic motion. This motion appears as a homoclinic phenomenon which is confined to very thin strips, that are exponentially small with ε, around split separatrices of the pendulum-like structures of the resonance; one needs an exponentially large time scales so that the chaotic motion takes place in a area of order ε close to the hyperbolic points of the resonance. The homoclinic phenomenon requires the homoclinic point existence whose proof is obtained through the Melnikov integral technique.

We focus on the oscillator whose potential V has heteroclinic (parabolic) orbits connecting the critical points at the infinity. V is small outside some "interaction" region of finite spatial extent and the energy of the parabolic orbit is $V(\pm\infty) = h'$ as well. Moreover the oscillator is driven by a periodic force. The driver amplitude is large enough such that the ionization is "generic" with respect to any ensemble of initial data. In this driver regime the system can be approached as a potential scattering problem. By a numerical integration of the equations of motion we determine some suitable, discrete maps ("scattering maps") which display properties that occurr in a large class of driven oscillators and other systems. In our case the force experienced by the driven oscillator does not decay to zero with large distances. The system asymptotically undergoes "quiver" oscillations; therefore we can consider a suitable sequence $\mathcal{T}$ of asymptotic times at which some dynamical variables, like the velocity v_0 or the kinetic energy H_0, are almost constant and serve to label both the outgoing and the ingoing states. The "scattering map" defines the asymptotic out-variables as a function of the asymptotic in-variables. By numerical simulations, for a fixed initial position, we

determines some maps which connect v_0 to the oscillator energy H_0, measured at the times of the sequence $\mathcal{T}$. We can state that "similarity" property holds:

a. the dependence of H_0 on v_0 alternates between regular intervals, where H_0 shows a smooth behavior and gaps where H_0 jumps in a sensitive way;

b. a magnification of a gap shows the the irregular behavior of H_0 dissolves into a new series of intervals on which H_0 is still a smooth function of v_0; it is given a pattern qualitatively similar to the complete one. Whenever we continue in this way at each step we find a structure which looks similar to that of the previous step.

Furhermore when we marks an orbit by the number N of its zeros N as a function of v_0 displays the following properties which define the "hierarchy" of the structure of the scattering function:

1. N is constant in each regular interval of H_0;
2. in a gap between two intervals marked by the same N, each regular intervals has a number of zeros larger than N and a sequence of $N+1$ intervals accumulates as v_0 approaches a boundary of the gap.

Therefore N plays the role of an order parameter so that there is a hierarchy within the self-similar structure. Successive removal of all the smooth intervals with $N = 1, 2, 3, \ldots$ leads to a set of the singularities of the scattering function that appears to be Cantor-like.

For any orbit we consider the time interval τ between the first zero and the last one; τ is called "time delay". If, just as done above, we fix the initial position and we plot τ as a function of the initial velocity. We notice that the delay time map possesses the property of similarity a. - b. and displays the same pattern of discontinuities as the scattering map.

When the set of discontinuities of the scattering map is Cantor-like the scattering is called "chaotic" or "irregular". For the explanation of chaotic scattering Jung and Scholtz proposed the following line of argument (see [58, 59]). In the phase space of a system exhibiting chaotic scattering there is a hyperbolic invariant set consisting of an uncountable infinity of periodic and aperiodic orbits. Their stable and unstable manifolds extend to the asymptotic region by means of the Hamilton flow. If the projectile enters the interaction region along such a stable manifold it will be captured by the chaotic set on the corresponding orbit, thus leading to a singularity in the scattering map. The fractal structure of the discontinuities of the scattering data is an image of the dynamics of the hyperbolic set via the Hamiltonian flow.

We have said about the self-similar structure of the set of singularities; the following question is of interest. How is the rule of construction of the self-similar structure connected to the dynamics of the hyperbolic invariant set ? To this end it is introduced a map D ("return map") which is defined on a plane Γ. A point $z = (|p|, t \bmod 2\pi)) \in \Gamma$ corresponds to a crossing of the origin which occurs with momemtum p, at the time t; D maps z to the next solution zero z', if z' exists. There are defined the bounded subset R^+ and R^- in Γ of zeros of solutions which have at least one zero in the future and one zero in the past, respectively.

Through the map we can identify a pattern of subsets $I_n \subset (R^+ \cap \mathcal{C}(R^-))$, corresponding to solutions with just $n+1$ zeros. The map D is one to one; therefore the sets I_n's are disjointed because they are pre-images of disjointed sets. The following two properties are crucial:

- the spiral property of D (see (4.9) and (4.10)). Since I_n's are disjointed, it implies that the I_n's show an intertwined arrangement of tails of double spirals that accumulate near the boudary of R^+ and such that between two I_n strips there are an infinity of I_{n+1} strips;
- the set $(R^+ \cap \mathcal{C}(R^-))$ is in one-to-one correspondence with the initial states of a scattering map.

Therefore the structure in the interior of $(R^+ \cap \mathcal{C}(R^-))$ is a mirror of the structure of the singularities in the set of initial data of the scattering map.

We have seen that in our system, that is ionized due to the application of a external, periodic force, the time delay scattering, defined on a phase space set S, is singular on a set of points that we think to be Cantor-like. This is a consequence of an iterative application, repeated "ad infinitum", of a deplation rule due to the driver that removes a fraction of points in S, after each driver period. The law $N(t)$ of decay with time t of the Lebesgue measure of the set of points which are not removed after t depends on the process of depletion. In a Hamiltonian system without regular islands, i.e. phase space domains of stability which are surrounded by unbroken KAM surfaces, there are observed both an exponential decay of phase space population and an algebraic one. All cases result in a deplation of all phase space points except for the hyperbolic invariant set, which consists of all the trapped orbits of the system.

In our case, from numerical simulation we obtain an algebraic decay of the surviving population. Furthermore we notice the phase space is mixed, because there are KAM islands. In irregular scattering the impact of the presence of KAM tori on particles determines the following effect: if a particle, initialized in a chaotic region, enters a region near a KAM surface, the particle wanders close to the surface for a long time ("stickiness effect"). In fact the finite-time Lyapunov exponents of the motion close to a KAM surface are nearly zero; hence there is a slow divergence of the particle trajectory from the KAM torus. The main consequence of the stickiness effect is that the probabilty of escaping (ionizing) is asymptotically algebraic.

Appendices

1. The stochastic layer of a pendulum: the width.

Let us focus on the dynamics close to the separatrix of a perturbed pendulum.
We consider the Hamiltonian

$$H = 1/2\,\dot{x}^2 - \omega_0^2\,\cos x + \varepsilon\,\omega_0^2\cos(x+\nu t) \equiv H_0(\dot{x},x) + \varepsilon\,V(x,t) \tag{1}$$

where $x \in \mathbb{R}$.
We are going to compute the variation

$$\delta H_0 = H_0(t=\infty) - H_0(t=-\infty)$$

because of the perturbation. The equation of the unperturbed separatrix is given by ($x(t_0) = -\pi$ $\dot{x}(t_0) = \pm 2\,\omega_0$)

$$\dot{x}_{sx}(t) = \pm\frac{2\,\omega_0}{\cosh\omega_0\,(t-t_0)} \tag{2}$$

$$x_{sx}(t) = \pm 4\arctan(e^{\pm\omega_0\,(t-t_0)}) \tag{3}$$

Using $\dot{H}_0 = -\varepsilon\,\dot{x}\,\partial V/\partial x$ we may write

$$\delta H_0 \simeq -\varepsilon\int_{-\infty}^{+\infty} dt\,\dot{x}\,\frac{\partial V}{\partial x} = 2\,\varepsilon\,\omega_0^2\int_{-\infty}^{\infty} d\tau\,\frac{1}{\cosh\tau}\,\sin(x + \frac{\nu}{\omega_0}\,\tau + \nu t_0) \tag{4}$$

where $\tau = \omega_0\,(t-t_0)$ and we take into account that the particle spends the most part of its trajectory "close to the separatrix".
Let $x(\tau)$ the unperturbed separatrix solution. We note that $x(\tau) = -x(-\tau)$; as well from (2) we get $\cos(x/2) = (\cosh\tau)^{-1}$.
Hence we can write

$$\delta H_0 = 2\,\varepsilon\,\omega_0^2\int_{-\infty}^{\infty} d\tau\,e^{i\frac{x}{2}}\,e^{i\,(x+\frac{\nu}{\omega_0}\tau)}\,\sin(\nu t_0)$$

We should close the integration contour in the lower half-plane of the complex τ.
For the case of an high frequency perturbation $\nu \gg \omega_0$ the integral is approximated by

$$\delta H_0 \simeq \varepsilon\,\nu^2\,e^{-\frac{\pi\,\nu}{2\,\omega_0}}\sin(\nu\,t_0) \tag{5}$$

Let $\Delta E = E - \omega_0^2$ be the energy difference with respect to the unperturbed separatrix energy.
Let us know that the condition determining the border of the stochastic layer is

$$\frac{\nu}{\omega_0}\,\frac{\delta H_0}{\Delta E} \geq 1$$

and finally

$$\Delta E \leq \varepsilon\,\frac{\nu^3}{\omega_0}\,e^{-\frac{\pi\,\nu}{2\,\omega_0}} \tag{6}$$

For a high frequency perturbation the stochastic layer width exponentially decreases with respect to ν/ω_0.
We should point out that Namely

$$\delta H - \delta H_0 \approx \int_{-\infty}^{\infty} d\tau\,[(\varepsilon\,V(x_{sx},\tau), H] = 0$$

where

$$\delta H = \int_{-\infty}^{\infty} d\tau\,dH/d\tau = \varepsilon\int_{-\infty}^{\infty} d\tau\,\partial V/\partial\tau$$

is the change of the full Hamiltonian in a motion "close" to one branch of a separatrix.
Finally δH_0 represents the only change of the Hamiltonian which cumulates over many pendulum oscillations and may give rise to instability.

2. Classical perturbation theory.

2.1 The averaging principle and nearly integrable systems that satisfy it.

We consider a nearly integrable system, with n degrees of freedom, described in action-angle $(I, \varphi) \in \mathbb{R}^n \times \mathbb{T}^n$ coordinates by

$$H_\varepsilon(I, \varphi) = h(I) + \varepsilon\, f(I, \varepsilon) \tag{7}$$

The function has a Fourier series

$$f(I, \varphi) = \sum_\nu f_\nu(I)\, e^{i\nu\,\varphi} \tag{8}$$

The corresponding equations of motion have the form

$$\dot{I} = \varepsilon\, F(I, \varepsilon) \qquad\qquad \dot{\varphi} = \omega(I) + \varepsilon\, G(I, \varphi) \tag{9}$$

We consider the "averaged equation"

$$\dot{J} = \varepsilon\, \mathcal{F}(J) \tag{10}$$

where $\mathcal{F}(I) = \langle F(I, \cdot)\rangle_\varphi$ is the average on φ of F.
The system (9) satisfies the "averaging principle" if for any initial datum (I°, φ°)

$$|I(t) - J(t)| \longrightarrow 0$$

for $\varepsilon \to 0$ and $|t| \leq 1/\varepsilon$; $J(t)$ is the solution of (10) with $J(0) = I^\circ$.

An idea helpful to study (7) is to find a function $\mathcal{S}_\varepsilon(I, \varphi, \varepsilon)$, such that the family of canonical transformations $s_\varepsilon(I', \varphi') = (I, \varphi)$, with

$$s_\varepsilon(I', \varphi') = (I', \varphi') + \varepsilon\, \mathcal{S}_\varepsilon(I, \varphi, \varepsilon)\,, \tag{11}$$

brings to a new Hamiltonian $H' = H \circ s_\varepsilon$ whose form is

$$H'(I', \varphi') = h(I') + \varepsilon\, g(I') + \varepsilon^2\, f'(I', \varphi') + O(\varepsilon^3) \tag{12}$$

where the perturbation results to be a higher order than in H.

From the Hamilton equations we can estimate

$$|I'(t) - I'(0)| \leq c\,\varepsilon \quad |t| \leq 1/\varepsilon$$

$c \in \mathbb{R}^+$. We can conclude

$$|I(t) - I(0)| \leq c'\,\varepsilon \quad |t| \leq 1/\varepsilon \tag{13}$$

since (11) is $\varepsilon-$close to the identity. Therefore the averaging principle is satisfied whenever the transformation (11), i.e. the function $\mathcal{S}_\varepsilon$, exists.
The s_ε is called "$\varepsilon-$near the identity" transformation.

2.2 Generating the near the identity transformation.

Let us consider the phase space $\{(p,q) \in \mathbb{R}^{2n}\}$ and a function $\chi : \mathbb{R}^{2n} \to \mathbb{R}$. The flow Φ^t_χ generated by the "Hamiltonian" χ defines at any t a transformation

$$(p,q) = \Phi^t_\chi(p',q') \tag{14}$$

where the new variables are the initial data. In classical mechanics it is shown that (14) is canonical. For a small $t = \varepsilon$ (14) is a $\varepsilon-$near to the identity canonical transformation. It is straightforward to check that

$$(p,q) = \Phi^\varepsilon_\chi(p',q') \;=\; \Phi^1_{\varepsilon\chi}(p',q') \tag{15}$$

i.e. an infinitesimal transformation (14) is given by the flow determined by the small Hamiltonian $\varepsilon\chi$. We note that a generic near the identity transformation does not have the form of a flow generated by a small hamiltonian. [1]. However through this method sufficiently many near the identity transformations are available. The method defined by (15) is based on the Lie series. It is used in the perturbation theory; the transformed functions are given as truncated expansions of the Lie series[2].

For any function g we write

$$g \circ \Phi^1_{\varepsilon\chi} = g + \varepsilon\{g,\chi\}, + \frac{\varepsilon^2}{2}\{\chi,\{\chi,g\}\} \circ \Phi^{t'}_{\varepsilon\chi} = g + \varepsilon\{g,\chi\}, + \frac{\varepsilon^2}{2}\{\chi,\{\chi,g\}\} \;+\; O(\varepsilon^3) \tag{19}$$

with a suitable $t' \in (0,1)$.

2.3 The fundamental equation of the perturbation theory.

We are going to establish an equation for the generating function χ of the flow $\Phi^1_{\varepsilon\chi}$ such that $H \circ \Phi^1_{\varepsilon\chi}$ takes the form (12).

Using (19) to transform $H(I,\varphi) = h(I) + \varepsilon\, f(I,\varphi)$ we then straightforwardly find

$$H' \equiv H \circ \Phi^1_{\varepsilon\chi} = h + \varepsilon\,(\{h,\chi\} \;+\; f) \;+ O(\varepsilon^2) \tag{20}$$

This is the same equation as (12) after the identification

$$\omega(I)\,\frac{\partial\chi}{\partial\varphi}(I,\varphi) \;+\; f(I,\varphi) \;=\; g(I) \tag{21}$$

[1] Given any near the identity canonical transformation (11) a function $\mathcal{S}(p',q,\varepsilon)$ exists such that (11) admits a generating function

$$S_\varepsilon(p',q) = p'q + \varepsilon\,\mathcal{S}(p',q,\varepsilon) \tag{16}$$

i.e. the transformation is implicitly defined by the equations

$$\begin{aligned} p &= \frac{\partial S_\varepsilon}{\partial q}(p',q) = p' + \varepsilon\,\frac{\partial\mathcal{S}}{\partial q}(p',q,\varepsilon) \\ q' &= \frac{\partial S_\varepsilon}{\partial p'}(p',q) = q + \varepsilon\,\frac{\partial\mathcal{S}}{\partial q}(p',q,\varepsilon) \end{aligned} \tag{17}$$

[2] The function $f \circ \Phi^t_\chi$ which is transformed by the flow generated by a Hamiltonian χ is formally expressed in a Lie series

$$g \circ \Phi^t_\chi = \sum_n^\infty \frac{t^k}{k!}\, L^k_\chi g \tag{18}$$

where $L_\chi g = \{g,\chi\}$

since $\{h, \chi\} = -\omega\, \partial\chi/\partial\varphi$.

We observe that $\langle\{h, \chi\}\rangle = \langle dh/dt\rangle = 0$, where $\langle\cdot\rangle$ denotes the average on φ, since for small ε the angles run much faster than the actions. It follows that $\langle\partial\chi/\partial\varphi\rangle = 0$. Hence the average in the angles of (21) gets $\langle f\rangle = g$ and the equation for χ turns out to be

$$\omega(I)\,\frac{\partial\chi}{\partial\varphi}(I,\varphi) = f(I,\varphi) - \langle f\rangle \tag{22}$$

It is called the "fundamental equation" of the perturbation theory (it is also called "first order Hamilton-Jacobi equation"). If the equation (22) admits a solution then in the new variables (I', φ') ($(I, \varphi) = \Phi^1_{\varepsilon\chi}(I', \varphi')$)

$$H'(I', \varphi') = h(I') + \varepsilon\,\langle f\rangle + O(\varepsilon^2)$$

Later on we drop the primes of the variables.

The preliminary problem is that of understanding whether the equation (22) admits a solution.

We formally expand $\chi(I, \varphi) = \sum_\nu \chi_\nu(I)\, e^{i\nu\varphi}$; hence

$$\omega(I)\,\frac{\partial\chi}{\partial\varphi}(I,\varphi) = \sum_\nu i\,\nu\,\omega(I)\,\chi_\nu(I)\,e^{i\nu\varphi}$$

In order χ to satisfy (22) in a set B it is necessary that for all $I \in B$ and all the equations

$$i\,(\nu\,\omega(I))\chi_\nu(I) = f_\nu(I) \tag{23}$$

for $0 \neq \nu \in \mathbb{Z}^2$. If it exists the solution is clearly given by

$$\chi(I,\varphi) = \sum_{\nu\neq 0} \frac{f_\nu(I)}{i\nu\,\omega(I)}\, e^{i\nu\,\varphi} \tag{24}$$

It is easy to show that the function $\mathcal{S}$ of a generic transformation close to the identity (see (16)) satisfies the same equation as before[3].

If we try to solve the equations (23) we could deal with the problem of the "small divisors". The resonance $\omega(I)\,\nu = 0$ prevents reaching arbitrary precision even if the expansion parameters are small, or, equivalently, the fundamental equation cannot "generically" be solved. In fact the following theorem of Poincaré holds: a system with Hamiltonian $h(I) + \varepsilon\, f(I,\varphi)$, $(I,\varphi) \in B \times \mathbb{T}^n$, $n \geq 2$, is not integrable by a completely canonical map s_ε analytic in ε, I, φ if (i) $det(\partial h/\partial I \partial I) \neq 0$ and (ii) f has essentially full Fourier series, i.e. for any $\nu \in \mathbb{Z}^n$ there exists ν' parallel to ν such $f_{\nu'} \neq 0$.

[3]The inversion of (17) gives

$$\varphi = \varphi' + O(\varepsilon)$$
$$I = I' + \varepsilon\,\frac{\partial\mathcal{S}}{\partial\varphi} + O(\varepsilon)$$

Then we substitute the primed variables for (I, φ) in (7) and we find

$$H'(I', \varphi') = h(I') + \varepsilon\,(\omega(I')\,\frac{\partial\mathcal{S}}{\partial\varphi}(I', \varphi') + f(I', \varphi')) + O(\varepsilon^2))$$

H' can be rearranged into the form (12) if there exists $\mathcal{S}$ that solves (21); $g = \langle f\rangle$ since the average over φ of $\frac{\partial\mathcal{S}}{\partial\varphi}$ vanishes.

In fact from the assumption (i) we can assert that there are a dense $B' \subset B$ and ν such that $\omega(I)\,\nu = 0$ for $I\,in B'$; from (ii) we find $f_{\nu'} \neq 0$ for some ν' parallel to ν. It follows that a function χ, the first order in ε of s_ε, that solves (24), does not exist.

This proposition is called "Poincaré difficulty". Its meaning is the explanation of the fact that, whenever a resonance occurs, the averaging principle cannot be proved by naively solving the fundamental equation. However it is possible to escape the difficulties raised by the proposition and establish some results on the stability of the actions. The idea is to understand which assumption on h are necessary to prove that the system obeys the averaging principle.

3. Quasi-convexity. Energy conservation provides confinement.

Let $\mathcal{L}$ be a one dimensional subgroup of $\mathbb{Z}^2$.

The confinement of the motion $I(t)$, $I(0) = I_0$inside the drift line $l_{\mathcal{L}}(I_0)$ (see section (2.3)) is provided by a geometric assumption on the unperturbed Hamiltonian.

We consider a function

$$h : \mathcal{B} \longrightarrow \mathbb{R}$$

$\mathcal{B} \subset \mathbb{R}^2$. Let us denote by $h' = \frac{\partial h}{\partial I}$ and $h'' = \frac{\partial^2}{\partial I \partial I}$, $I \in \mathcal{B}$.

The function h is call quasi-convex in $\mathcal{B}$ if for any $I \in \mathcal{B}$ and $w \in \mathcal{B}$

$$h'(I)\, w = 0$$
$$h''(I)\, w \cdot w = 0$$

holds if and only if $w = 0$.

Quasi convexity of h implies the following two facts

1. *the line of fast drift $l_{\mathcal{L}}$ and the resonance line $\Sigma_{\mathcal{L}}$ are transversal.*

Let $\{\nu\}$ be a basis of $\mathcal{L}$. We assume that a $w \in l_{\mathcal{L}}((I_0)$

$$w = a\,\nu \ ,$$

$a \in \mathbb{R}$, is tangent to $\Sigma_{\mathcal{L}}$ in some point $I^* \in \Sigma_{\mathcal{L}}$. Since w is parallel to $\mathcal{L}$

$$u(I) \equiv h'(I)\, w = 0 \tag{25}$$

for all $I \in \Sigma_{\mathcal{L}}$. Hence the vector $u'(I)$ is orthogonal to $\Sigma_{\mathcal{L}}$ in I and consequently, according to the assumption on w, $u'(I^*)\, w = 0$. Furthermore, according to (25) it is $u(I^*) = 0$. Together, these two conclusions are against the quasi convexity.

2. The function h, restricted to $l_{\mathcal{L}}(I_0)$, has a quadratic extremal in the unique intersection point $I = I^*$ between $\Sigma_{\mathcal{L}}$ and $l_{\mathcal{L}}$.

In fact, for any $\zeta \in l_{\mathcal{L}}$ we have

$$h(I^* + \zeta) = h(I^*) + h'(I^*)\, \zeta + h''(I^*)\, \zeta \cdot \zeta + O(\|\zeta\|^3) \tag{26}$$

We note that since ζ is parallel to $\mathcal{L}$ and $I^* \in \Sigma_{\mathcal{L}}$ the second term vanishes and for the quasi-convexity the quadratic term has a definite sign.

4. Cauchy estimates.

A Cauchy's estimate, also called "dimensional estimate", is an application of the Cauchy's theorem. For a function g, analytic in D, it leads to an estimate of a derivative of g in a reduced domain $D' \subset D$. In particular let B be a compact and ρ and σ positive. Let $D_{\alpha,\beta} = D_{(\rho-\alpha\delta,\sigma-\beta\,\xi)}(B^{-\alpha\delta})$, where the number $\delta < \rho$, $\xi < \sigma$, $\alpha \leq 1$, $\beta \leq 1$ are positive. We have the following dimensional estimates:

$$\left\| \frac{\partial g}{\partial I} \right\|_{D_{1,0}} \leq \frac{\|g\|_{W_{0,0}}}{\delta} \qquad \left\| \frac{\partial g}{\partial \varphi} \right\|_{D_{0,1}} \leq \frac{\|g\|_{W_{0,0}}}{\xi} \tag{27}$$

5. A property of the Fourier series of a analytic function

The following lemma contains some estimates on Fourier series of an analytic function which are helpful to determine the "ultraviolet part" of the perturbation and suited to handle some basic equation for the generating function.

Lemma 5..1 ([42]) *If $g(I,\varphi)$ is analytic in $D_{0,0} \equiv D_{(\rho,\sigma)}(B)$ (see 3.4), in which $B \subset \mathbb{R}^2$ is compact and ρ and σ are positive parameters, and $\|g\|_{D_{0,0}} < \infty$ then the amplitude of the Fourier components g_ν decreases exponentially with $|\nu|$*

$$\|g_\nu\|_{D_{0,0}} \leq C\, e^{-\sigma\,|\nu|} \tag{28}$$

where $C = \|g\|_{D_{0,0}}$. Conversely, if the condition (28) holds for any ν then the series with Fourier components g_ν is analytic in $D_{0,0}$.

We consider the "ultraviolet part" of g

$$g^{>N}(I,\varphi) = \sum_{|\nu|>N} g_\nu(I)\; e^{i\nu\,\varphi}$$

On the basis of the inequality (28), for $\xi < \sigma$, we can deduce

$$\|g^{>N}\|_{D_{0,1}} \leq\; M\,\xi^{-2}\, e^{-\frac{1}{2}\xi\,N}\; \|g\|_{D_{0,0}} \tag{29}$$

where M is a positive constant depending on the number of degrees of freedom $l = 2$ of the system. The inequality (29) yields the estimate for the ultraviolet part of g.

6. Elementary estimates on Fourier series of an analytic function. An application of Cauchy estimates to a Fourier polynomial.

Lemma 6..1 ([42]) *If it is defined in $D_{0,0}$*

$$\chi(I,\varphi) = \sum_{|\nu|\leq N} x_\nu(I)\; e^{i\varphi\,\nu} \tag{30}$$

whose coefficients x_ν satisfy the condition (28) then

$$\|\chi\|_{D_{0,\frac{1}{2}}} \leq C\,\xi^{-2} \tag{31}$$

and

$$\left\|\frac{\partial\chi}{\partial I}\right\|_{D_{\frac{1}{2},\frac{1}{2}}} \leq 2\ \frac{\|\chi\|_{D_{0,\frac{1}{2}}}}{\delta} \qquad \left\|\frac{\partial\chi}{\partial\varphi}\right\|_{D_{0,\frac{1}{2}}} \leq 2\ \frac{\|\chi\|_{D_{0,\frac{1}{2}}}}{\xi} \tag{32}$$

where $D_{0,1/2} = D_{(\rho,\sigma-\xi/2)}(B)$ and $D_{1/2,1/2} = D_{(\rho-\delta/2,\sigma-\xi/2)}(B-\delta/2)$.

7. A sufficient condition for the existence of a canonical transformation.

Lemma 7..1 ([42]) *The parameters ρ and σ are positive and $B \subset \mathbb{R}^2$ is compact. Let χ be an analytic function in $\mathcal{B} = D_{(\rho,\sigma)}(B)$. We assume*

$$\left\|\frac{\partial\chi}{\partial I}\right\|_{\mathcal{B}_{\frac{1}{2}}} \leq\ a_1\,\xi \qquad \left\|\frac{\partial\chi}{\partial\varphi}\right\|_{\mathcal{B}_{\frac{1}{2}}} \leq\ a_2\,\delta \tag{33}$$

for positive $\delta < \rho$ and $\xi < \sigma$ and $\mathcal{B}_{\frac{1}{2}} = D_{(\rho-\delta/2,\sigma-\xi/2)}(B)$; $a_1 \leq 1/2$, $a_2 \leq 1/2$.

Then there exists a canonical transformation

$$\Phi_\chi = (\Phi^I_\chi, \Phi^\varphi_\chi)\ :\ \mathcal{B}_1 \longrightarrow \mathcal{B}$$

whose generating function is χ and defined in a domain

$$\mathcal{B}_1 = D_{(\rho-\delta,\sigma-\xi)}(B')$$

with

$$D^{-\delta} \subset B' \subset D^{-\delta/2} \qquad D^{-\delta} \subset \Phi^I_\chi(B') \subset D^{-\delta/2}$$

The distance between Φ_χ and the identity $I = (I^I, I^\varphi)$ can be arranged to be arbitrarily small:

$$\|\Phi^I_\chi - I^I\|_{\mathcal{B}_1} \leq \frac{\delta}{2} \qquad \|\Phi^\varphi_\chi - I^\varphi\|_{\mathcal{B}_1} \leq \frac{\xi}{2}$$

For any function g, analytic in $\mathcal{B}$, the transformed function $g' = g \circ \Phi_\chi$ is analytic in $\mathcal{B}_1$ and satify

$$\|g'\|_{\mathcal{B}_1} \leq \|g\|_{\mathcal{B}} \tag{34}$$

and

$$\|g' - g - \{g,\chi\}\|_{\mathcal{B}_1} \leq \frac{1}{2}\,\|\chi,\{\chi,g\}\|_{\mathcal{B}} \tag{35}$$

8. Poisson backets estimates.

In order to obtain estimates of the terms of the transformed Hamiltonian (3.36), chapter 2, we have to yield the estimates of Poisson brackets $\{g,\chi\}$ and $\{\{g,\chi\},\chi\}$, between a Fourier polynomial (30) in $D_{0,0}$, which satisfies (28), and a function g, analytic in $D_{0,0}$.

In order to do this we need:

- to determine estimates of the first and second derivatives of g using the Cauchy's inequalities (see appendix 4.);
- to consider the inequalities (33) for the first derivatives of χ and analogous ones for the second derivatives of χ:

$$\left\| \frac{\partial^2 \chi}{\partial I_i \partial \varphi_j} \right\|_{D_{\frac{1}{2},\frac{1}{2}}} \leq a\, \delta^{-1}\, \xi^{-1}\, \|\chi\|_{D_{0,\frac{1}{2}}}$$

$$\left\| \frac{\partial^2 \chi}{\partial I_i \partial I_j} \right\|_{D_{\frac{1}{2},\frac{1}{2}}} \leq b\, \delta^{-2}\, \|\chi\|_{D_{0,\frac{1}{2}}}$$

$$\left\| \frac{\partial^2 \chi}{\partial \varphi_i \partial \varphi_j} \right\|_{D_{0,\frac{1}{2}}} \leq c\, \xi^{-2}\, \|\chi\|_{D_{0,\frac{1}{2}}}$$

  a, b, c are constant. The first two are deduced from suitable dimensional inequalities applied to the first of (32) and the third (that is different in nature from the others) is obtained from the second of (32) via some algebraic manipolations (see appendix C of [42]);
- to count the number of terms of the brackets.

We conclude that the estimates on the Poisson brackets take the form:

$$\|\{g,\chi\}\|_{D_{\frac{1}{2},\frac{1}{2}}} \leq C_2\, \delta^{-1}\, \xi^{-1}\, \|\chi\|_{D_{0,\frac{1}{2}}}\, \|g\|_{D_{0,0}} \tag{36}$$

$$\|\{\{g,\chi\},\chi\}\|_{D_{\frac{1}{2},\frac{1}{2}}} \leq C_3\, \delta^{-2}\, \xi^{-2}\, \|\chi\|^2_{D_{0,\frac{1}{2}}}\, \|g\|_{D_{0,0}} \tag{37}$$

Bibliography

[1] V.M. Alekseev. *Math. USSR Sbornik*, 6(4):505, 1968.

[2] V.M. Alekseev. *Math. USSR Sbornik*, 7(1):1, 1969.

[3] V.M. Alekseev and M.V. Yakobson. *Phys. Report*, 75(5):287, 1981.

[4] H. Aref, J. B. Kadtke, I. Zawadski, L. J. Campbell, and B. Eckhardt. *Fluid. Dyn. Res.*, 3:63, 1988.

[5] V.I. Arnold. Proof of a.n. kolmogorov's theorem on the preservation of quasiperiodic motions under small perturbations of the hamiltonian. *Russ. Math. Surv.*, 18:9, 1963.

[6] V.I. Arnold. Small divisor problems in classical and celestial mechanics. *Russ. Math. Surv.*, 18:85, 1963.

[7] V.I. Arnold. *Geometrical methods in the theory of ordinary differential eqution*s. Springer, 1978.

[8] D. Bauer and P. Mulser. *Phys. Plasmas*, 14:023301, 2007.

[9] A. Beeker and P. Eckelt. *Chaos*, 3:490, 1993.

[10] A. Bergmann. *Europhys. Lett.*, 14:661, 1991.

[11] M. Born and E. Wolf. *Principles of Optics*. Pergamon Press, Oxford, fourth edition edition, 1970.

[12] R. Bowen. *Equilibrium States and the Ergodic Theory of Anosov Diffeomorphims*. Springer-Verlag, Berlin, 1975.

[13] F. Brunel. Not so resonant. *Phys. Rev. Lett.*, 59:52, 1987.

[14] F. Brunel. *Phys. Fluids*, 31:2714, 1988.

[15] Chirikov B.V. A universal instability of many-dimensional oscillator systems. *Physics Reports*, 52(5):263, 1979.

[16] Rose-Petruck C., Schafer K.J., Wilson K.R., and Barty C.P.J. *Phys. Rev. A*, 55:1182, 1997.

[17] Siedschlag C. and Rost J.M. *Phys. Rev. Lett.*, 93:43402, 2004.

[18] J. Zanghellini C. Jungreuthmayer, L. Ramunno and T. Brabec. *T. Mol. Opt. Phys.*, 38:3029, 2005.

[19] P.J. Catto and R.M. More. *Phys. Fluids*, 20:704, 1977.

[20] B. V. Chirikov and D. L. Shepelyanski. *Physica D*, 13:394, 1984.

[21] B.V. Chirikov. *Plasma Physics*, 1:253, 1960.

[22] G. Cicogna and M. Santoprete. *Regular and Chaotic Dynamics*, 6:377, 2001.

[23] Bauer D. *J. Phys. B*, 37:3085, 2004.

[24] H. Dankowicz and P. Holmes. *J. Diff. Eq.*, 116:468, 1995.

[25] D.Bauer and P.Mulser. Irreversible energy gain by linear and nonlinear oscillators. *J. Phys.: Conf. Ser*, 11:169, Jan 2005.

[26] M. Ding, T. Boundis, and E. Ott. *Phys. Lett. A*, 151:395, 1990.

[27] M. Ding, C. Grebogi, E. Ott, , and J. A. Yorke. *Phys. Rev. A*, 42:7025, 1990.

[28] P. Eckelt and E. Zienicke. *J. Phys. A*, 24:153, 1991.

[29] B. Eckhardt. *J. of Phys. A*, 20:5971, 1987.

[30] B. Eckhardt. *Physica D*, 33:89, 1988.

[31] B. Eckhardt and H. Aref. *Philos. Trans. Roy. Soc. A*, 326:655, 1988.

[32] B. Eckhardt and C.Jung. *J. Phys. A*, 19:L829, 1986.

[33] A. Emmanouilidou, C. Jung, and L. E. Reichl. *Phys. Rev. E*, 68:46207, 2003.

[34] A. Macchi et al. *Phys. Rev. Lett.*, 87:205004, 2001.

[35] A. Macchi et al. Laser acceleration of ion bounches at the front surface of overdense plasmas. *Phys. Rev. Lett.*, 94:165003, 2005.

[36] L. M. Chen et al. *Phys. Plasmas*, 8:2925, 2001.

[37] M. Cerchez et al. *Phys. Rev. Lett.*, 100:245001, 2008.

[38] P. Mulser et al. *Laser interactions with matter*. Word Scientific, Singapore, 1989.

[39] R. Sauerbrey et al. *Phys. Plasmas*, 1:1635, 1994.

[40] T.Y. Brian Yang et al. *Phys. Plasmas*, 3:2702, 1996.

[41] Megi F., Belkacem M., Bouchene M.A., Suraud E., and Zwicknagel G. *J. Phys. B*, 36, 2003.

[42] Benettin G., Galgani G., and Giorgilli A. A proof of nekhoroshev's theorem for the stability times in nearly integrable hamiltonian systems. *Celestial Mechanics*, 37:1, 1985.

[43] Benettin G., Galgani G., Giorgilli A., and Strelcyn J.M. *Nuovo Cim.*, 79B:201, 1984.

[44] Benettin G. and Gallavotti G. Stability of motions near resonances in quasi-integrable hamiltonian systems. *J. Stat. Phys.*, 44:293, 1986.

[45] Freidberg G.P., Mitchell R.W., Morse R.L., and Rudsinski L.I. *Phys. Rev. Lett.*, 28:795, 1972.

[46] I.S. Gradshteyn and I.M. Ryzhik. *Table of integrals, series and Products*. Alan Jeffrey Editor.

[47] C. Grebogi, E. Ott, and J.A. Yorke. *Phys. Rev. Lett.*, 57:1284, 1986.

[48] J. Guckenheimer and P. Holmes. *Nonlinear oscillations, Dynamical Systems, and Bifurcations of Vector Fields*. Springer, New York, 1983.

[49] Ruhl H., Macchi A., and Mulser P. *Phys. Rev. Lett.*, 82:2095, 1999.

[50] G. Haller. *Chaos near resonance*. Springer-Verlag, New York, 1999.

[51] C. T. Hansen and S. C. Wilks. *Phys. Rev. Lett.*, 83:5019, 1999.

[52] C. F. Hillermeier, R. Blümel, and U. Smilansky. *Phys. Rev. A*, 45:3486, 1992.

[53] Chen L.M.and Zhang J., Dong Q.L., Teng H., Liang T.J., Zhao L.Z., and Wei Z.Y. *Phys. Plasmas*, 8:2925, 2001.

[54] Moser J. *Stable and Random Motions in dynamical system*. Princeton University Press, Princeton, 1973.

[55] C. Jung. *J. Phys. A*, 19:1345, 1986.

[56] C. Jung. *J. Phys. A*, 20:1719, 1987.

[57] C. Jung, C. Lipp, and T.H. Seligman. *Ann. Phys.*, 275:151, 1999.

[58] C. Jung and H.J. Scholz. *J. of Phys. A: Math. Gen.*, 20:3607, 1987.

[59] C. Jung and H.J. Scholz. *J. of Phys. A: Math. Gen.*, 21:2301, 1988.

[60] H. Kantz and P. Grassberger. *Physica D*, 17:75, 1985.

[61] C. F. F. Karney. *Physica D*, 8:360, 1983.

[62] B. P. Koch and B. Bruhn. *J. Phys. A*, 25:3945, 1992.

[63] A.N. Kolmogorov. On conservation of conditionally periodic motions under small perturbations of the hamiltonian. *Dokl. Akad. Nauk. SSSR*, 98:527, 1954.

[64] Z. Kovacs and T. Tél. *Phys. Rev. Lett.*, 64:1617, 1990.

[65] W. L. Kruer. *The Physics of Laser Plasma Interactions*. Westview Press, Oxford, 2003.

[66] W.L. Kruer and K. Estabrook. *Phys. Fluids*, 28:430, 1985.

[67] H.J. Kull. *Phys. Plasmas*, 26:1881, 1983.

[68] M. Kundu and D. Bauer. Collisionless energy absorption in the short-pulse intense laser-cluster interaction. *Phys. Rev. A*, 74(6):063202, Dec 2006.

[69] M. Kundu and D. Bauer. Nonlinear resonance absorption in the laser-cluster interaction. *Phys. Rev. Lett.*, 96(12):123401, Mar 2006.

[70] Y. C. Lai, R. Blumel, E. Ott, and C. Grebogi. *Phys. Rev. Lett.*, 68:3491, 1992.

[71] Y. C. Lai, M. Ding, C. Grebogi, and R. Blümel. *Phys. Rev. A*, 46:4661, 1992.

[72] Y. C. Lai, K. Zyczkowski, and C. Grebogi. *Phys. Rev. E*, 59:5261, 1999.

[73] L.J. Laslett. *In Focusing of charged particles*, 2:355, 1967.

[74] K. C. Lee. *Phys. Rev. Lett.*, 60:1991, 1988.

[75] Lichtenberg A.J.and Lieberman M.A. *Regular and chaotic dynamics*. Springer, 1992.

[76] A. Macchi, F.Cornolti, and F.Pegoraro. *Phys. Plasmas*, 9(5):1704, 2002.

[77] C.J. McKinstrie and D.F. DuBois. *Phys. Fluids*, 31:278, 1988.

[78] J. D. Meiss and E. Ott. *Phys. Rev. Lett.*, 55:2741, 1985.

[79] J. Moser. On invariant curves of area-preserving mappings of an annulus. *Nachr. Akad. Wiss. Göttingen Math. Phys. Kl.*, 2:1, 1962.

[80] P. Mulser and D. Bauer. *High Power Laser-Matter Interaction*. Springer, 2010.

[81] N.N. Nekhoroshev. An exponential estimate of the time of stability of nearly integrable hamiltonian systems. *Russ. Math. Surv.*, 32:1, 1977.

[82] Denisov N.G. *Sov. Phys. Tech. Phys. JETP*, 4:544, 1957.

[83] Gibbon P. and Bell A.R. *Phys. Rev. Lett.*, 68:1535, 1992.

[84] Mulser P., Cornolti F., and Bauer D. *Phys. Plasmas*, 5:4466, 1998.

[85] Mulser P. and Kanapathipillai M. Collisionless absorption in cluster out of linear resonance. *Phys. Rev. A*, 71:63201, 2005.

[86] Mulser P., Kanapathipillai M., and Hoffmann D.H.H. Two very efficient nonlinear absorption mechanisms in cluster. *Phys. Rev. Lett.*, 95:103401, 2005.

[87] D. Bauer P. Mulser and H. Ruhl. Collisionless laser-energy conversion by anharmonic resonance. *Phys. Rev. Lett.*, 101(22):225002, Nov 2008.

[88] J.M. Petit and M. Hénon. *Icarus*, 66:536, 1986.

[89] A.D. Piliya. *Sov. Phys. Tech. Phys.*, 11:609, 1966.

[90] H. Poincaré. *Méthodes nouvelles de la mecánique celèste*. Gauthier-Villars, Paris, 1987.

[91] E. Pollack and P. Pechukas. *J. Chem. Phys.*, 69:1218, 1978.

[92] B. R*ü*ckerl and C. Jung. *J. Phys. A*, 27:55, 1994.

[93] Godwin R.P. *Phys. Rev. Lett.*, 28:85, 1972.

[94] D. Ruelle. *Elements of Differentiable Dynamics and Bifurcation Theory*. Academic Press, 1989.

[95] Kato S. *J. Plasma Fusion Res. Series*, 6:658, 2004.

[96] M. Seidl. *Plasma Physics*, 6:597, 1964.

[97] K. Sitnikov. *Sov. Phys. Dokl.*, 5:647.

[98] R. T. Skodje and M. J. Davis. *J. Chem. Phys.*, 95:2429, 1988.

[99] S. Smale. *Bull. Amer. Math. Soc.*, 73:747, 1967.

[100] S. Smale. *The Mathematics of Time*. Springer, 1980.

[101] P. Sprangle, E. Esary, and A. Ting. *Phys. Rev. lett.*, 64:2011, 1990.

[102] Ditmire T., Smith R.A., Tish J.W.G., and Hutchinson M.H.R. *Phys. Rev. Lett.*, 78:3121, 1997.

[103] G. Troll and U.Smilansky. *Physica D*, 35:34, 1988.

[104] A. Avez V.I. Arnold. *Ergodic problems of classical mechanics*. Addison-Wesley, New York, 1989.

[105] F. Vivaldi, G. Casati, , and I. Guarnieri. *Phys. Rev. Lett.*, 51:727, 1983.

[106] Melnikov V.K. *Trans. Moscow Math. Soc.*, 12:1, 1963.

[107] Rozmus W. and Tikhonchuk V.T. *Phys. Rev. A*, 42:7401, 1990.

[108] E.S. Weibel. *Phys. Fluids*, 10:741, 1967.